Developing Tools to Investigate Protein Sulfenylation in Living Cells

by

Stephen E. Leonard

A dissertation submitted in partial fulfillment
Of the requirements for the degree of
Doctor of Philosophy
(Chemical Biology)
In The University of Michigan
2011

Doctoral Committee:

Professor Kate S. Carroll, co-Chair
Professor Anna K. Mapp, co-Chair
Professor Mark A. Saper
Professor Raymond C. Trievel

Stephen E. Leonard

2011

To my wife Jolie, my support and happiness.

Acknowledgements

First, I would like to thank my mentor, Dr. Kate Carroll, for the opportunity to work in her lab and for her knowledge, guidance, and support. I would like to acknowledge and thank all of the Carroll lab members. I have enjoyed working with everyone in the lab. They have always provided great feedback in experimental design, preparing for talks, and editing my writing. Specifically I would like to thank my fellow graduate students Candie Paulsen, Devayani Bhave, Jiyoung Hong, Thu Ha Truong, and Francisco Garcia for the good times and the science. I would like to thank Dr. Young Ho Seo and Dr. Khalilah Reddie for always being willing to discuss our work and helping me troubleshoot problem experiments. Also, I would like to thank Jesse Song for being the hardest working undergraduate scientist I have ever come across.

Outside of the lab I would like to thank Dr. Anna Mapp, Dr. Mark Saper, and Dr. Ray Trievel for meeting with me as my thesis committee over the past three years. They have all given me valuable input on my research and been good sounding boards when determining my future directions. Matthieu Depuydt and Dr. Jean-Francois Collet collaborated with me on a very successful project and showed me that other people could use the tools that I developed. Dr. Jason Gestwicki and all of the Gestwicki lab members deserve special thanks for providing me with space to work and camaraderie when I was separated from my lab.

Finally, I would like to thank my family for their support and encouragement over the last five years. Jolie, thank you for making it through graduate school with me and keeping me motivated and always encouraging me every day. Also, thanks for getting us cats.

Preface

This thesis is the compilation of published and unpublished work on the development of sulfenic acid-specific probes to monitor protein cysteine oxidation in living cells. Sulfenic acid is the oxidation product that forms when a cysteine thiolate reacts with hydrogen peroxide. Protein sulfenic acid formation is a reversible process that has emerged as a central mechanism for dynamic post-translational modification in all major protein classes and correlates with disease states.

In Chapter 1, we discuss chemical and biological features of sulfenic acids while placing them in the larger context of protein cysteine modifications and review current methods for their study. This work has been published as a review for which the citation is Leonard S.E. and Carroll, K.S., "Chemical 'omics' approaches for understanding protein cysteine oxidation in biology," (2011) *Curr Opin Chem Biol* (2011) Feb;15(1):88-102.

Chapter 2 focuses on the synthesis and evaluation of DAz-1, the first cell-permeable probe capable of trapping and tagging sulfenic acid modifications directly in cells. The citation for this article is Reddie, K.G., Seo, Y.H., Muse, W.B. Leonard, S.E. and Carroll, K.S., "A chemical approach for detecting sulfenic acid-modified proteins in living cells.," Mol Biosyst. (2008) Jun;4(6):521-31.

In Chapter 3, we present the development and application of a second generation probe for sulfenic acids, DAz-2. This analogue exhibits significantly improved potency for detecting sulfenic acids both *in vitro* and in cells. DAz-2 was used to conduct a proteomic investigation of the sulfenome in the HeLa human tumor cell line. This study identified approximately two hundred proteins that undergo sulfenic acid formation, which are distributed throughout the cell and function in a diverse array of biological processes. These data are published as Leonard, S.E., Reddie, K.G., and Carroll, K.S., "Mining the thiol proteome for sulfenic acid modifications reveals new targets for oxidation in cells," ACS Chem Biol. (2009) Sep 18;4(9):783-99.

In Chapter 4, DAz-2 was used to examine oxidation of single cysteine-containing proteins in the *Escherichia coli* periplasm, an oxidizing environment in which most thiols are involved in disulfide bonds. Experiments with the DAz-2 probe led to the discovery of two thioredoxin-related proteins that protect single cysteines from irreversible oxidation to sulfinic and sulfonic acid, with functional homologues in eukaryotic cells. This work was published as Depuydt, M., Leonard, S.E., Vertommen D., Denoncin K., Morsomme P., Wahni K., Messens J., Carroll K.S., and Collet J.F. "A periplasmic reducing system protects single cysteine residues from oxidation," Science (2009) Nov 20;326(5956):1109-11.

Chapter 5 details how chemical probes for detecting sulfenic acids were further refined through the addition of a binding module to target the protein tyrosine phosphatase (PTP) family of

enzymes. These probes exhibit significantly improved sensitivity for detecting cysteine oxidation in this important class of signaling enzymes. This work has been published as Leonard S.E., Garcia F.J., Goodsell D.S., Carroll K.S. "Redox-Based Probes for Protein Tyrosine Phosphatases." Angew Chem Int Ed Engl. (2011) May 2;50(19):4423-7.

Finally, Chapter 6 is a discussion of future directions for developing and applying cell-permeable small molecule probes for detecting protein sulfenic acid formation in cells.

Table of Contents

Dedication ii

Acknowledgements iii

Preface v

List of Figures xvi

List of Schemes xix

List of Tables xx

List of Appendices xxi

List of Abbreviations xxii

Abstract xxvii

Chapter

1. Omics approaches for understanding protein cysteine oxidation in biology

1.1. Abstract 1

1.2. Introduction 2

1.3. Indirect versus direct detection of oxidative cysteine modifications 5

1.4. Lysate versus Cellular analysis of oxidative cysteine modifications 7

1.5. Chemical approaches to detect reactive cysteines 7

1.6. General chemical approaches to detect cysteine oxidation 9

1.7. Direct detection of protein disulfide formation 11

1.8. Chemical approaches to detect protein glutathionylation 12

1.9. Chemical approaches to detect protein nitrosylation 14

1.10. Chemical and immunochemical approaches to detect protein sulfenylation 18

1.11. Conclusions and future directions 24

1.12. References and recommended reading 26

2. A chemical approach for detecting sulfenic acid-modified proteins in living cells 33

2.1. Abstract 33

2.2. Introduction 34

2.3. Results 39

2.3.1.DAz-1 irreversibly labels sulfenic acid-containing proteins 39

2.3.2.DAz-1 detects sulfenic acid-modified proteins in cell lysate 47

2.3.3.Incorporation of DAz-1 into proteins in cultured human cells 50

2.4. Discussion 56

2.5. Experimental Procedures 57

2.5.1. Preparation, enzymatic assay and chemical modifications of papain 57

2.5.2. NBD-Cl assay and chemical modification of HAS 58

2.5.3. P-biotin labeling of papain and HSA 59

2.5.4. Immunoblotting 59

2.5.5. Cell culture 60

2.5.6. DAz-1 labeling of Jurkat lysate 60

2.5.7. DAz-1 labeling of Jurkat cells 61

2.5.8. DAz-1 labeling of Jurkat cells post-oxidant challenge 61

2.5.9. Chemical Methods 62

2.6. Appendix of ^{1}H and ^{13}C NMR 65

2.7. References 67

3. Mining the thiol proteome for sulfenic acid modifications reveals new targets 72

For oxidation in cells

3.1. Abstract 72

3.2. Introduction 73

3.3. Results 76

3.3.1. Synthesis of DAz-2 76

3.3.2. Comparative analysis o sulfenic acid labeling by DAz-1 and DAz-2 in 78
Recombinant protein and whole cell lysate

3.3.3. Specific labeling of sulfenic acid-modified proteins in cells using DAz-2 80

3.3.4. Global detection and proteomic analysis of sulfenic acid-modified 83
proteins in cells

3.3.5. *In vitro* validation of selected candidate proteins 85

3.4. Discussion 89

3.4.1. Comparative analysis of related modifications and proteomic studies 91

3.4.2. Protein candidates for sulfenic acid modification 94

3.4.2.1. Signal transduction 94

3.4.2.2. DNA repair and replication 95

3.4.2.3. Metabolism 95

3.4.2.4. Redox homeostasis 96

3.4.2.5. Nuclear transport 97

3.4.2.6. Vesicle trafficking 97

3.4.2.7. Chaperone-mediated protein folding 98

3.5. Conclusion 99

3.6. Experimental procedures 100

3.6.1. Chemical methods 100

3.6.2. Cloning, expression, and purification of Rab1a 102

3.6.3. Cloning of FLAG and HA-tagged GAPDH Prx1 103

3.6.4. Transfection of GAPDH and Prx1 104

3.6.5. Sulfenic acid detection in HeLa cells treated with hydrogen peroxide 104

3.6.6. Measuring intracellular ROS concentrations in HeLa cells 105

3.6.7.Quantification of total, reduced, and oxidized glutathione in HeLa cells 105

3.6.8. Trypan blue evaluation of cell viability 106

3.6.9. LogP determination 106

3.6.10. Staudinger ligation 106

3.6.11. Western blot 107

3.6.12. Cell culture 107

3.6.13. Preparation of HeLa cell lysates 108

3.6.14. Enrichment of biotinylated proteins 108

3.6.15. Isolation of DAz-2 labeled proteins for MS analysis 108

3.6.16. Detection of sulfenic acid modifications in Rab1a and calreticulin 109

3.7. Appendices 110

3.7.1. Appendix Table of proteins identified in proteomic study 110

3.8. References 118

4. A periplasmic reducing system protects single cysteine residues from oxidation 125

4.1. Abstract 125

4.2. Introduction 125

4.3. Results 126

4.3.1. DsbG substrate identification 126

4.3.2. DsbG reduces the oxidized cysteine of YbiS *in vitro* 128

4.3.3. DsbG reduces the oxidized cysteine of YbiS *in vivo* 128

4.3.4. YbiS is sulfenylated *in vitro* 130

4.3.5. YbiS is sulfenylated *in vivo* 132

4.3.6. DsbG and DsbC control the level of sulfenylation in the periplasm 133

4.4. Discussion 133

4.5. Experimental Procedures 135

4.5.1. Strains and microbial techniques 135

4.5.2. Media and growth conditions 136

4.5.3. Plasmid construction 136

4.5.4. Proteomic analysis of periplasmic extracts 137

4.5.5. Overexpression and purification of DsbC, DsbG, and YbiS 138

4.5.6. Purification and separation of DsbG-substrate complexes 139

4.5.7.Determination of the *in vivo* redox state of YbiS 139

4.5.8. Identification of the substrates of DsbG by mass spectrometry 140

4.5.9. YbiS-TNB reduction analysis 140

4.5.10. DAz-1 labeling of purified YbiS 141

4.5.11. Identification of YbiS-dimedone adduct 141

4.5.12. Pull down experiments of biotinylated YbiS with DAz-2 142

4.5.13. *In vivo* DAz-2 labeling of periplasmic extracts 143

4.5.14. Purification of DAz-2 labeled YbiS on His SpinTrap columns 143

4.6. Appendices 144

4.6.1. Periplasmic proteins identified by 2D-LC-MS/MS in WT, and *dsbG* strains 144

4.6.2. Strains used in this study 147

4.6.3.Plasmids used in this study 148

4.6.4. Primers used in this study 149

4.7. References 149

5. Redox-based probes for protein tyrosine phosphates 152

5.1. Introduction 152

5.1.1. Redox signaling 152

5.1.2. Protein tyrosine phosphatase oxidation 153

5.1.3. Methods to detect protein tyrosine phosphatase oxidation 154

5.2. Results 157

5.2.1.The protein tyrosine phosphatase YopH forms a sulfenic acid 157

5.2.2. PTP active site is targeted by the RBP binding element 158

5.2.3. RBPs detect YopH sulfenic acid 160

5.2.4. RBPs demonstrate increased sensitivity for PTP sulfenic acids 161

5.2.5. Molecular modeling of RBP 6 in the YopH active site 162

5.3. Discussion 163

5.4. Experimental procedures 163

5.4.1. Materials 164

5.4.2. Chemical methods 164

5.4.3. Chemical synthesis 164

5.4.4. General procedures for PTP activity assay 181

5.4.5. LC/MS analysis of dimedone-tagged YopH 182

5.4.6. Determination of the dissociation constant for inhibitor binding (K_i) 182

5.4.7. Detecting reversible PTP oxidation with azido-probes 182

5.4.8. Probing sulfenic acid modification of GAPDH 183

5.4.9.Western blot 183

5.4.10. Computational method for Autodock calculations 184

5.5. Appendices 184

5.5.1.Representative plot measuring K_i of RBP **6** 184

5.5.2. Long exposure of Figure 5.5a 185

5.5.3. ^{1}H NMR and ^{13}C NMR 186

5.6. References 192

6. **Conclusions and future directions** 196

6.1. Abstract 196

6.2. Conclusions: Developing tools to detect cysteine sulfenylation 196

6.3. Future directions 197

6.3.1. Proteomic quantification of protein sulfenylation 197

6.3.1.1. Isotope-coded and iodo-DAz-2 198

6.3.1.2. Alkyne-functionalized probes for sulfenic acid detection 200

6.3.2. Investigating the relevant oxidation targets that mediate ROS-dependent endothelial cell migration 200

6.4. Concluding remarks 203

6.5. References 205

Appendix A. Experimental procedures for the synthesis of DYn-2 206

Appendix B. ^{1}H and ^{13}C NMR for the synthesis of DYn-2 209

List of Figures

1.1 Oxidation fates of protein cysteines 3

1.2 Indirect and direct chemical techniques to monitor cysteine oxidation 6

1.3 Chemical approaches to detect cysteine oxidation 10

1.4 Chemical approaches to detect protein glutathionylation 13

1.5 Chemical approaches to detect protein *S*-nitrosylation 17

1.6 Chemical approaches to detect protein sulfenylation 19

1.7 Chemical approaches for direct detection of protein sulfenylation 21

1.8 High throughput immunochemical detection of dimedone-modified sulfenic acid epitope using arrays. 23

2.1 Chemoselective probe for labeling proteins with sulfenic acid modifications in living cells 36

2.2 DAz-1 modifies sulfenic acid-modified papain *in vitro* 41

2.3 Covalent papain adducts are not reduced by DTT 43

2.4 DAz-1 labels sulfenic acid-modified HSA *in vitro* 46

2.5 DAz-1 labels sulfenic acid-modified HSA and additional proteins in cell lysates 48

2.6 β-actin is labeled in vivo by DAz-1 50

2.7 DAz-1 labels sulfenic acid-modified proteins in living cells 52

2.8 DAz-1 detects an increase in thiol oxidation in living cells 54

2.9 Jurkat cells remain viable after H_2O_2 challenge 55

2.10 Peroxiredoxin thiols are oxidized to sulfinic and sulfonic acids after FCCP 56

challenge

3.1 Trapping and tagging proteins that undergo sulfenic acid modification 74

3.2 DAz-2 exhibits increased sensitivity for sulfenic acids *in vitro* 79

3.3 Expression, DAz-2 sulfenic acid labeling, and enrichment is performed with human Prx1 and GAPDH in HeLa cells 80

3.4 DAz-2 protein labeling is dose dependent and can respond to changes in protein sulfenic acid formation within cells 81

3.5 DAz-2 exhibits increased sensitivity for sulfenic acids in living cells 82

3.6 DAz-2 treatment does not trigger endogenous oxidative stress or cell death 84

3.7 Analysis of candidates identified in our proteomic experiments with HeLa cells 85

3.8 *In vitro* validation of DAz-2 labeling in selected candidates 101

3.9 Venn diagram of proteins sensitive to sulfenic acid formation in HeLa cells 103

4.1 Identification of DsbG substrates 127

4.2 Multiple sequence alignment of ErfK, YbiS, and YnhG 128

4.3 DsbG interacts with YbiS *in vitro* and *in vivo* 129

4.4 DsbG substrates are not glutathionylated 130

4.5 YbiS forms a stable sulfenic acid *in vitro* and *in vivo* 131

4.6 Mass spectrometry analysis of oxidized YbiS 132

4.7 Protein sulfenic acids accumulate in the periplasm of *dsbCdsbG* strains. 133

4.8 A model for sulfenic acid reduction in the periplasm 135

5.1 Proposed model for redox-dependent signal transduction 152

5.2 Redox-based probes (RBPs) for detecting reversible PTP oxidation 155

5.3 Analysis of YopH PTP oxidation by H_2O_2 157

5.4 YopH forms a covalent adduct with dimedone with 1:1 stoichiometry 158

5.5 Analysis of RBP selectivity for oxidized YopH 160

5.6 Compound **6** selectively modifies sulfenic acid-modified YopH 161

5.7 Analysis of RBP selectivity for oxidized PTP1B 162

5.8 The binding conformation of RBP **6** with YopH predicted by AutoDock 163

6.1 Modified ICDID to quantify sulfenic acid modification in cells 198

6.2 DAz-2 and alkyne derivative, DYn-2 200

6.3 Proposed model for redox-dependent signal transduction in cell migration 201

List of Schemes

1.1 Reaction of thiol-specific alkylating agents N-ethylmaleimide (NEM) **1** and Iodoacetamide (IAM) **2** with cysteine thiols 8

2.1 Selective reaction of dimedone with a sulfenic acid affords a new thioether bond 37

2.2 Synthesis of DAz-1, a sulfenic acid-specific chemical probe 39

3.1 Synthesis of new cell-permeable probe for identifying sulfenic acid protein modifications in cells, DAz-2 77

5.1 Selective reaction between a protein sulfenic acid and dimedone 1 156

List of Tables

3.1 Abbreviated list of identified proteins with sulfenic acid modifications in HeLa cells 86

5.1 Inhibition constants for DAz-1 **2** and compounds **3-8** with YopH 159

List of Appendices

Appendix 2.6 Appendix of ^{1}H and ^{13}C NMR 65

Appendix 3.7.1 Table of proteins identified in proteomic study 110

Appendix 4.6.1 Periplasmic proteins identified by 2D-LC-MS/MS in WT, and *dsbG* strains 144

Appendix 4.6.2 Strains used in this study 147

Appendix 4.6.3 Plasmids used in this study 148

Appendix 4.6.4 Primers used in this study 149

Appendix 5.5.1 Representative plot measuring K_i of RBP **6** 184

Appendix 5.5.2 Long exposure of Figure 5.5a 185

Appendix 5.5.3 ^{1}H NMR and ^{13}C NMR 186

Appendix A. Experimental procedures for the synthesis of DYn-2 206

Appendix B. ^{1}H and ^{13}C NMR for the synthesis of DYn-2 209

List of Abbreviations

4-HNE	4-hydoxynonenal
4-MUP	4-methylumbelliferyl phosphate
ADH	Alcohol Dehydrogenase
AhpCF	alkyl hydroperoxidase
BAPNA	N_{α}-benzoyl-L-arginine 4-nitroanilide hydrochloride
BIAM	biotinylated iodoacetamide
BioGEE	biotinylated glutathione ethyl ester
BSA	bovine serum albumin
BST	biotin switch technique
CAN	ceric (IV) ammonium nitrate
Cys	cysteine
DAz-1	*N*-(3-Azidopropyl)-3,5-dioxocyclohexanecarboxamide
DAz-2	4-(3-azidopropyl)cyclohexane-1,3-dione
DCF-DA	2',7'-dichlorofluorescin diacetate
DCM	dichloromethane
DIC	N,N'-Diisopropylcarbodiimide
DMF	dimethylformamide
DMSO	dimethyl sulfoxide
DSP	dual-specificity phosphatases
DTT	dithiothreitol

EDC	1-ethyl-3-(3-dimethylaminopropyl) carbodiimide)
ER	endoplasmic reticulum
ESI	electrospray ionization
EtOAc	ethyl acetate
FCCP	trifluormethoxy carbonylcyanide phenylhydrazone
FBS	fetal bovine serum
GAPDH	glyceraldehyde-3-phosphate dehydrogenase
Glu	glutathione
Gly	glycine
Grx	glutaredoxin
GSH	glutathione
GshA	gamma-glutamylcysteine synthase
GSSG	glutathione disulfide
GST	glutathione S-transferase
H_2O_2	hydrogen peroxide
HMPA	hexamethylphosphoramide
hnRNP	heterogeneous nuclear ribonucleoprotein
HPDP	N-[6-(biotinamido)hexyl]-3'-(2'-pyridyldithio)-propionamide
HRP	horseradish peroxidase
HSA	human serum albumin
HOBt	N-Hydroxybenzotriazole

IAM	iodoacetamide
ICAT	Isotope-coded affinity tag
ICDID	2-iododimedone
K_i	inhibition constant
KatE	catalase
LC-MS	liquid chromatography mass spectrometry
LDA	lithium diisopropylamide
LMW	low molecular weight
MCM	mini-chromosome maintenance
MMTS	methylmethane thiosulfonate
mPEG	maleimide-polyethylene glycol
MS	mass spectrometry
NADPH	nicotinamide adenine dinucleotide phosphate
NBD-Cl	4-chloro-7-nitrobenzo-2-oxa-1,3-diazole
n-BuLi	*n*-butyl lithium
NEM	*N*-ethylmaleimide
NMR	nuclear magnetic resonance
NO	nitric oxide
NO_2	nitrogen dioxide
$O_2^{\cdot -}$	superoxide
$OH^{\cdot}$	hydroxyl radical

p-biotin	phosphine biotin
PBS	phosphate buffered saline
PI	protease inhibitor
PI3K	phosphoinositide-3-kinase
Phox	phagocytic NADPH oxidase
PP1	serine/threonine-protein phosphatase
ppm	parts per million
Prx1	peroxiredoxin I
PSG	penicillin-streptomycin-L-glutamate
PTM	posttranslational modification
PTP	protein tyrosine phosphatase
PTP1B	protein tyrosine phosphatase 1B
RBP	redox-based probe
RCK	mitogen-activated protein kinase protein kinase
RNS	reactive nitrogen species
ROS	reactive oxygen species
RTK	receptor tyrosine kinase
SDS	sodium dodecyl sulfate
Ser	serine
SOH	sulfenic acid
SO_2H	sulfinic acid

SO_3H	sulfonic acid
Strep-HRP	streptavidin-conjugated horseradish peroxidase
TBAF	tetrabutylammonium fluoride
t-BOOH	*t*-butyl hydroperoxide
TBST	tris buffered saline with tween
TCEP	tris[2-carboxyethyl] phosphine
TEA	triethylamine
THF	tetrahydrofuran
Thr	threonine
TLC	thin layer chromatography
TNB	2-nitro-5-thiobenzoate
Trx	thioredoxin
Tyr	tyrosine
WT	wild-type

ABSTRACT

Developing Tools to Investigate Protein Sulfenylation in Living Cells

by

Stephen E. Leonard

Co-Chair: Kate S. Carroll and Anna Mapp

Oxidation of cysteine to sulfenic acid has emerged as a biologically relevant post-translational modification with particular importance in redox-mediated signal transduction; however, the identity of modified proteins remains largely unknown. In the present study we report the development of DAz-1, a cell-permeable chemical probe capable of detecting sulfenic acid-modified proteins directly in living cells. We then describe DAz-2, an analog of DAz-1 that exhibits significantly improved potency *in vitro* and in cells. Application of this new probe for global analysis of the sulfenome in a tumor cell line identifies most known sulfenic acid-modified proteins – 14 in total, plus more than 175 new candidates, with further testing confirming oxidation in several candidates. The newly identified proteins have roles in signal transduction, DNA repair, metabolism, protein synthesis, redox homeostasis, nuclear transport, vesicle trafficking, and ER quality control. Next we employ DAz-2 to discover two thioredoxin-related proteins that protect single cysteines from irreversible oxidation to sulfinic and sulfonic acid in

Escherichia coli, which have functional homologues in eukaryotic cells. Finally we further refine these sulfenic acid probes to develop redox based probes of protein tyrosine phosphatases

(PTPs) which show greatly increased sensitivity towards PTP sulfenic acid modification over previous probes. The combination of selective chemical enrichment and live-cell compatibility makes these sulfenic acid probes powerful new tools with the potential to reveal new regulatory mechanisms in signaling pathways, and identify new therapeutic targets.

Chapter 1

Omics approaches for understanding protein cysteine oxidation in biology

1.1 Abstract

Oxidative cysteine modifications have emerged as a central mechanism for dynamic post-translational regulation of all major protein classes and correlate with many disease states. Elucidating the precise roles of cysteine oxidation in physiology and pathology presents a major challenge. This Chapter reviews the current, targeted proteomic strategies that are available to detect and quantify cysteine oxidation. A number of indirect methods have been developed to monitor changes in the redox state of cysteines, with the majority relying on the loss of reactivity with thiol-modifying reagents or restoration of labeling by reducing agents. Recent advances in chemical biology allow for the direct detection of specific cysteine oxoforms based on their distinct chemical attributes. In addition, new chemical reporters of cysteine oxidation have enabled *in situ* detection of labile modifications and improved proteomic analysis of redox-regulated proteins. Progress in the field of redox proteomics should advance our knowledge of regulatory mechanisms that involve oxidation of cysteine residues and lead to a better understanding of oxidative biochemistry in health and disease.

1.2 Introduction

The discovery of thiol-mediated regulatory switches in both prokaryotic and eukaryotic organisms has established a fundamental role for cysteine oxidation in biology.[1,2] The ability of cysteine residues to function as reversible redox switches in proteins relies upon the unique redox chemistry of this amino acid.[3] It is also well known that oxidative stress correlates with many common diseases and conditions, and serves either as the initiating factor for these disorders (*e.g.,* atherosclerosis, hypertension, diabetes) or as the basis for their complications (*e.g.,* stroke, cancer, and neurodegenerative disease).[4-7] Elucidation of the exact function of cysteine oxidation in physiological and pathological events has been hampered by the inability to detect distinct thiol modifications with selectivity in complex biological environments. Consequently, much remains to be learned about signaling pathways that involve cysteine oxidation and the pathophysiologic role of redox-based thiol modification. For example, the mechanisms that dictate selectivity of cysteine oxidation in proteins are still not well understood. Moreover, the molecular details for the majority of these modifications, including a comprehensive inventory of proteins containing oxidative cysteine modifications *in vivo* and the specific sites of modification remain largely unknown. The extent of thiol oxidation within the cell remains another open topic of investigation. These questions have vital implications for assessing redox-based modifications relevant to cell signaling pathways in healthy cells and under oxidative stress-related conditions.

In the present review, we briefly outline the most prevalent forms of oxidative cysteine modifications found in proteins and summarize recent progress in chemical biology that is enabling more cellular studies of cysteine oxidation and improved approaches for proteomic

analysis of oxidized proteins. For a more comprehensive treatment of sulfur redox reactions, thiol-based regulatory switches, redox-mediated signal transduction, and pathological states related to oxidative stress, the interested reader is referred to additional reviews.[1-3,8-11]

The thiol side chain of cysteines can be modified in biological systems by reactive oxygen species (ROS) and reactive nitrogen species (RNS) such as hydrogen peroxide (H_2O_2) and nitrogen dioxide (NO_2) (Figure 1.1). Selective fluorescent probes of ROS and RNS are available to detect these species in cellular systems.[12,13] Upon cell-surface receptor activation (*e.g.,* tyrosine kinase), controlled bursts of ROS and RNS can function as second messengers to modulate signal transduction pathways. By contrast, constitutively elevated levels of ROS and RNS are associated with oxidative stress. The propensity for a particular cysteine residue to undergo

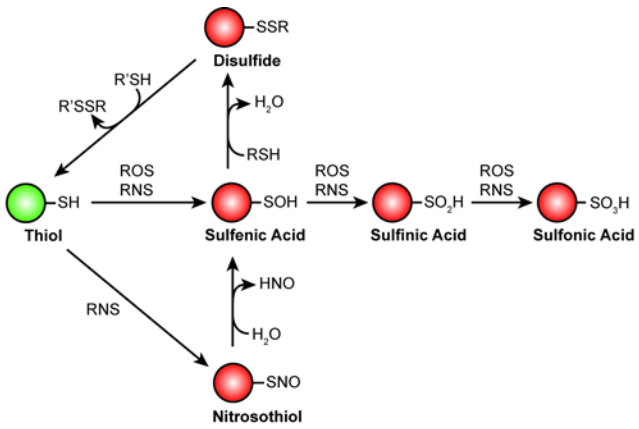

Figure 1.1 Oxidation fates of protein cysteines. Protein thiols, particularly low pKa thiols, react with ROS/RNS. The initial oxidation product of this reaction is sulfenic acid. This transient modification may be stabilized by the protein micro environment or condense with a second cysteine resulting in glutathionylation or intra- or inter-molecular protein disulfides. Alternatively, sulfenic acids may be oxidized to sulfinic acid and under severe oxidizing conditions, sulfonic acid. Reaction of thiols with RNS also generate nitrosothiols. This modification may be stabilized, hydrolyzed to form a sulfenic acid, or condense with a second cysteine to form a disulfide (not shown).

oxidation is dictated by a number of factors including low p*K*a, protein microenvironment (*i.e.,* adjacent residues and metal ions), and proximity to the oxidant source.[3,11]

The initial oxidation product of cysteine is sulfenic acid and this post-translational modification has been implicated in the redox modulation of a growing number of proteins.[10,14] *In vitro* studies indicate that second-order rate constants for sulfenic acid formation in proteins by H_2O_2 range from 1-10^7 $M^{-1}s^{-1}$.[11] Sulfenic acids may be stabilized by the protein microenvironment or serve as a central intermediate to other reversible and largely irreversible species. Condensation with the tripeptide glutathione (γ-L-Glu-L-Cys-Gly, GSH) or a protein thiol results in glutathione-protein mixed disulfides or intra- and inter-molecular protein disulfides. In some cases, the cysteine sulfenate can also react with an amide group of the protein backbone to generate the cyclic sulfenyl amide.[15] Disulfides and glutathione conjugates are reversible modifications and can be restored to free thiols by the thioredoxin or the glutaredoxin systems. A protein that reduces sulfenic acids directly back to the thiol form has also recently been discovered in bacteria.[16] Alternatively, sulfenic acids can be oxidized to sulfinic acid and, under more severe oxidizing conditions, to sulfonic acid. Second-order rate constants for H_2O_2-mediated formation of sulfinic acid from sulfenic acid have been obtained for a handful of proteins and vary between 0.1-100 $M^{-1}s^{-1}$.[17-21] Nitrosothiols are formed by reaction of thiols with RNS or through transnitrosylation from another nitrosothiol derivative. *In vitro* rates of thiol nitrosylation in human and bovine serum albumin proteins are on the order of 10^3-10^4 $M^{-1}s^{-1}$.[22]

Although not depicted in Figure 1.1, it is important to note that reactive cysteines also undergo redox reactions with biological electrophiles such as acrolein or 4-hydroxynonenal (4-HNE).[23] Analogous to ROS/RNS-mediated oxidation, thiol-electrophile adducts can also modulate cell signaling pathways and methods for detecting protein adduction by electrophiles have recently been reviewed.[23] Whether induced by ROS/RNS or electrophiles, redox-dependent modification of cysteine residues can have a profound effect on catalytic activity, biomolecular interactions, subcellular localization, and the stability of target proteins.[3,10,24] Given the significance of these modifications to human health and disease, investigating the role of cysteine oxidation has emerged as an important area of research. Accordingly, a variety of chemical proteomic strategies have been developed to monitor changes in the redox state of cysteine residues in proteins.

1.3 Indirect versus direct detection of oxidative cysteine modifications

Both indirect and direct methods have been developed to investigate oxidative cysteine modifications (Figure 1.2). These approaches are complementary, and each has its own advantages and disadvantages. The majority of indirect methods to monitor changes in the redox state of cysteines rely on the loss of reactivity with thiol-modifying reagents (Figure 1.2a) or restoration of labeling by reducing agents (Figure 1.2b). These approaches require that free thiols are completely blocked by alkylating agents prior to the reduction step and, for this reason, are restricted to analysis of cell lysates or purified proteins. Recent advances in chemical biology allow for the direct detection of specific cysteine oxoforms based on their distinct chemical attributes (Figure 1.2c). Such methods are based on small-molecule probes that will selectively react with one class of oxidative cysteine modification. Thus, a key

challenge for this strategy lies in designing a probe that modifies only the desired target among all other competing functional groups.

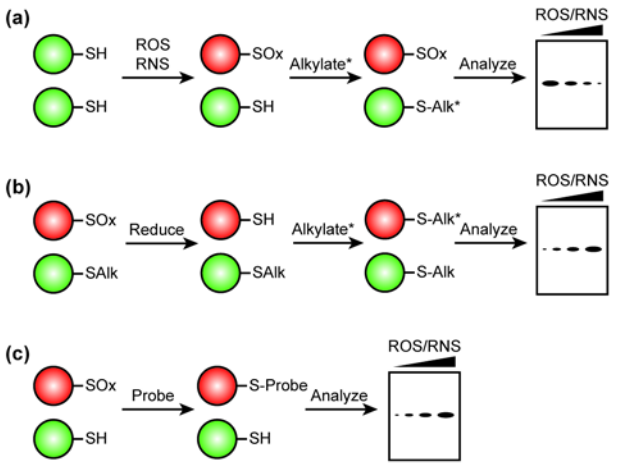

Figure 1.2 Indirect and direct chemical techniques to monitor cysteine oxidation. (a) Loss of reactivity with thiol-modifying reagents indirectly monitors cysteine oxidation. ROS and RNS oxidize reactive protein thiols (red protein). Addition of a thiol-specific alkylating agent such as NEM or IAM derivatized with a detection handle covalently modifies free thiols. Increased cysteine oxidation exhibits a decrease in probe signal. (b) Restoration of thiol-labeling by reducing agents indirectly monitors cysteine oxidation. Initially samples are incubated with NEM or IAM to irreversibly alkylate free thiols. Next a reducing agent returns oxidized cysteines to free thiols. Addition of NEM or IAM derivatized with a detection handle covalently modifies nascent thiols. Increased cysteine oxidation exhibits an increase in probe signal. (c) Direct detection of specific cysteine oxoforms. Samples are incubated with a chemoselective alkylating agent for a specific cysteine oxoform (i.e. nitrosothiols and sulfenic acids) derivatized with a detection handle. Visualization of probe incorporation results in an increase in signal with increased oxidation.

1.4 Lysate versus cellular analysis of oxidative cysteine modifications

Provided that the small-molecule is membrane permeable, direct chemoselective detection methods enable the investigator to probe cysteine oxidation directly in cells. This is an important consideration since the principle redox couples are not in equilibrium with each other and are maintained at distinct potentials in the cytoplasm, mitochondria, nuclei, the secretory pathway, and the extracellular space.[25] Mitochondria, nuclei and the cytoplasm are characterized by more reduced redox potentials, whereas the secretory pathway and extracellular space are oxidizing environments. When the finely tuned redox balance of the cell is disrupted by the lysis procedure, proteins are likely to undergo artifactual oxidation, which increases the challenges associated with identifying low abundance sites of modification and for interpreting the biological significance. Methods to decrease oxidation artifacts in lysates have been reported and rely on the addition of trichloroacetic acid or oxidant-metabolizing enzymes to the cell lysis buffer.[26,27] However, additional limitations inherent to studies in lysates, such as protein denaturation with concomitant loss of labile modifications, are not addressed by this approach. On the other hand, a charge that can be levied against any cellular probe is that it may alter the biological processes under investigation. Analogous to studies of nonredox phenomena, this issue can be addressed in a number of ways including the addition of probe at discrete time points after triggering the process of interest and by profiling relevant biological markers in probed and unprobed cells. In aggregate, lysate and cellular analysis of cysteine oxidation are complementary approaches; each can be used to accelerate discovery efforts and our understanding of these protein modifications.

1.5 Chemical approaches to detect reactive cysteines

Because of the fundamental importance of reactive cysteines in many protein functions, development of tools to probe these residues is an active field of research. In its reduced or thiol form, cysteine is typically the most potent nucleophile in a protein. The reactivity of cysteine is largely dependent on ionization to the thiolate anion.[28] Although the average p*K*a of thiol group in proteins is ~8.5, this value can range from 2.5 to 12.[29,30] Functionally important cysteine thiol groups, such as those found in enzyme active sites, are often characterized by lower p*K*a values. Since thiolate anions are more reactive than thiols, they are also prone to oxidation by ROS/RNS.[31] Thus, identifying reactive cysteines within the proteome is a strategic approach to map key residues and candidates for redox regulation.

Existing methods to identify reactive cysteines involve alkylating the free thiol followed by various detection methods to monitor labeled proteins. *N*-ethylmaleimide (NEM) **1** and iodoacetamide (IAM) **2** (Scheme 1.1) are both thiol-specific alkylating agents that react with cysteine thiolate anions more readily than with free thiols.[32] NEM and IAM undergo nucleophilic attack by a thiolate anion *via* Michael addition or S_N2 displacement, respectively. The reaction of NEM with thiols is more rapid as compared to IAM; however, in some cases it may also be less specific. For example, NEM has been reported to react slowly with lysine, histidine, and tyrosine residues when used in large excess.[33] Both reagents form covalent bonds with reactive cysteines and can be derivatized with biotin, fluorophores, stable and radioactive isotopes. Biotin can be used as a handle to facilitate Western blot detection or enrichment using streptavidin-conjugated

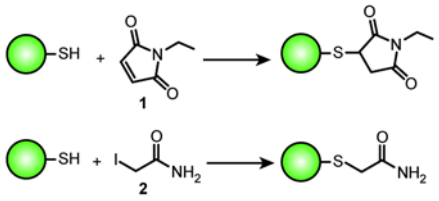

Scheme 1.1 Reaction of thiol-specific alkylating agents N-ethylmaleimide (NEM) 1 and iodoacetamide (IAM) 2 with cysteine thiols.

reagents, while radiolabels or fluorophores enable the detection of modified cysteines by one- or two-dimensional gel electrophoresis.

1.6 General chemical approaches to detect cysteine oxidation

Biotinylated iodoacetamide (BIAM) is one of the most commonly used reagents to detect protein oxidation by differential labeling of cysteine residues under both normal and oxidative stress conditions followed by streptavidin blotting or enrichment (Figure 1.3a). In these experiments, cysteines that become oxidized after exposure to oxidant stress exhibit a decrease in BIAM-labeling, owing to the diminished nucleophilicity of the sulfur atom. A variation on the BIAM approach is the use of acid-cleavable, IAM-based isotope-coded affinity tag (ICAT) reagents.[34,35] In this strategy, the extent of cysteine oxidation is quantified from the ratio of light (^{12}C) to heavy (^{13}C) ICAT label by liquid chromatography-mass spectrometry (LC-MS) (Figure 1.3b). By definition, both BIAM and ICAT-based methods for detecting oxidized cysteine residues are indirect since they rely on loss of reactivity with thiol-alkyating reagents. Although these reagents do not reveal the exact nature of the oxidative cysteine modification and can give rise to false positives they have, nonetheless, shown wide utility in redox proteomics. For example, BIAM and ICAT approaches were recently utilized in a detailed and elegant study of surface exposed, reactive cysteine residues in *Saccharomyces cerevisiae.*[36]

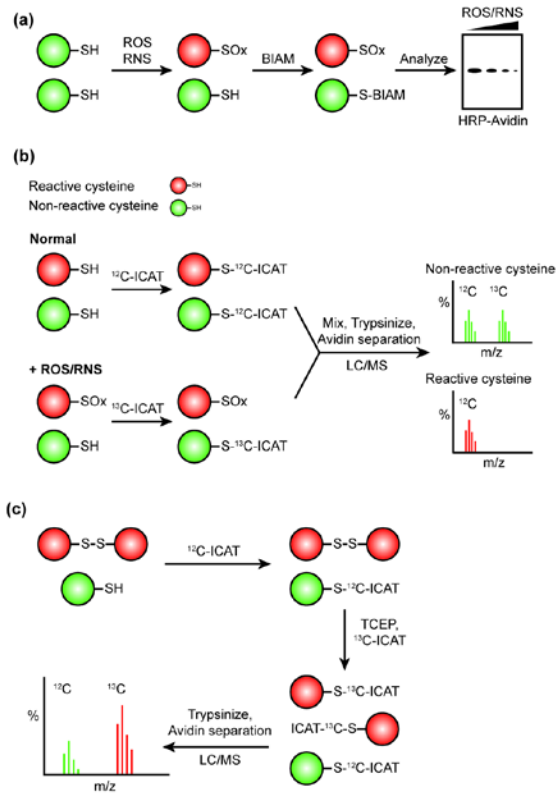

Figure 1.3 Chemical approaches to detect cysteine oxidation. (a) Reactive cysteines are detected using biotinylated iodoacetamide (BIAM). Exposure to ROS/RNS oxidizes reactive protein thiols. Samples are next incubated with BIAM to covalently modify remaining free thiols. Oxidized cysteines exhibit a decrease in BIAM labeling. (b) Isotope-coded affinity tag (ICAT) reagents determine the ratio of oxidized cysteines. Samples are subjected to normal and oxidative stress conditions. Following protein oxidation, free thiols are labeled using the IAM-based light (12C) ICAT reagent in the normal condition and the heavy (13C) ICAT reagent in the oxidant stress condition. These reagents biotinylate free thiols. Next, samples are mixed and trypsinized generating chemically identical, labeled peptides which differ in mass by 9 Da when alkylated with the heavy reagent. Labeled peptides are purified by avidin separation and analyzed by LC-MS. Protein cysteines which are not oxidized (green protein) show two peaks with identical mass intensities. Oxidized protein cysteines in the oxidant stress condition (red protein) show a decrease shifted mass. From the relative peak intensities of the MS of light and heavy ICAT-labeled peptides, the percent oxidation of thiols in the samples can be determined with loss of signal for the heavy peptide indicating cysteine oxidation. (c) OxICAT method couples ICAT with differential thiol trapping to quantify reversible cysteine oxidation. Cell lysates are generated in the presence of trichloroacetic acid and denaturants to fully expose all cysteine side chains while inhibiting thiol/disulfide exchange. Labeling with the light (12C) ICAT reagent irreversibly modifies all reduced cysteines (green protein). Next, all reversibly oxidized cysteines (RSSR, RSNO, RSOH, and RSSG; red protein) are reduced with Tris(2-carboxyethyl)phosphine (TCEP). The resulting free thiols are subsequently modified with the heavy (13C) ICAT reagent. Then all proteins are trypsinized, avidin purified to generate chemically identical peptides which differ in mass by 9 Da due to incorporation of either light or heavy ICAT reagents, and analyzed by LC-MS. From the relative peak intensities of the MS of light and heavy ICAT-labeled peptides, the ratio of reversible oxidation of thiols in the samples can be determined.

More recently, Leichert *et al.* have developed the OxICAT method to quantify reversible oxidation of cysteine residues.[27] The OxICAT approach couples ICAT with differential thiol trapping in five key steps (Figure 1.3c): (1) cell lysis in the presence trichloroacetic acid to inhibit thiol/disulfide exchange; (2) protein denaturation and alkylation with the light (^{12}C) ICAT reagent; (3) treatment with tris[2-carboxyethyl] phosphine (TCEP), which returns reversibly oxidized cysteine residues (*i.e.,* disulfides, nitrosothiols, sulfenic acids) to their thiol form; (4) alkylation of nascent free thiols with the heavy (^{13}C) ICAT reagent; and (5) the ratio of light to heavy-isotope labeled cysteines is quantified by LC-MS. Since sulfenyl and nitrosyl thiol modifications are often sensitive to changes in pH and protein microenvironment [37,38] this technique is ideally suited for disulfide analysis.

1.7 Direct detection of protein disulfide formation

Under non-stressed conditions, disulfide bond formation occurs primarily in oxidizing compartments such as the periplasm in bacteria and the endoplasmic reticulum of eukaryotic cells.[39] In general, disulfide bonds make significant contributions to protein stability and are formed during the folding process with assistance from protein disulfide isomerases.[39] Once they are properly folded, proteins can undergo disulfide bond formation during a catalytic cycle, thiol/disulfide exchange, or by condensation of a thiol with a sulfenic acid (Figure 1.1) or nitrosothiol. Disulfide bond formation, a major mechanism of transcription factor regulation in bacteria and yeast, allows cells to respond rapidly to changes in redox balance.[40,41] In higher eukaryotes, well known disulfide-mediated redox switches include the Trx1/Ask-1 signalosome and the Nrf2/Keap1 couple.[42,43]

The ability to identify regulatory disulfides is central to our understanding of cysteine-based redox regulation. However, the only direct and high-throughput method to identify proteins that undergo oxidant-induced disulfide formation is sequential nonreducing/reducing two-dimensional sodium dodecyl sulfate polyacrylamide gel electrophoresis, also known as Redox 2D-PAGE.[44] In this procedure, proteins are first electrophoresed under nonreducing conditions. In subsequent steps, proteins are reduced in gel, excised, layered onto a second gel and electrophoresed at 90° to the original direction. Proteins that do not contain disulfide bonds will migrate on the diagonal across the gel in this system, whereas proteins with inter- or intramolecular disulfide bonds migrate below or above the diagonal, respectively. After separation by 2D-PAGE, oxidized proteins can be cut from the gel and identified by LC-MS. The greatest limitation of this technique is that it cannot reliably visualize or produce analytical quantities of proteins that are present in less than 1000 copies per cell. Nonetheless, this strategy has successfully identified cysteines in more abundant proteins that are susceptible to inter- and intra-molecular disulfide formation in both bacteria and mammalian cells.[44]

1.8 Chemical approaches to detect protein glutathionylation

Glutathione (GSH) is a low-molecular weight thiol that is maintained at millimolar concentrations in the cell. Oxidative stress can lead to accumulation of its oxidized form, glutathione disulfide (GSSG). However, during normal conditions, greater than 98% of the cellular GSH is present in the reduced form. A decrease in the cellular GSH/GSSG ratio is indicative of oxidative stress and correlates with many disease states, including cancer.[45] If GSSG accumulates within the cell it can generate protein-GSH adducts through thiol-disulfide exchange (Figure 1.1) or when GSH reacts with sulfenic acids or nitrosothiols. Protein

glutathionylation is reversible through the action of two enzymes, glutaredoxin (Grx) and sulfiredoxin.[46] Identifying protein targets of GSH is of high interest and has led to the development of several methods to examine this modification. The section below is intended only as a brief introduction to detecting protein cysteine GSH modifications. The interested reader may refer to [47] for a more complete discussion of this topic.

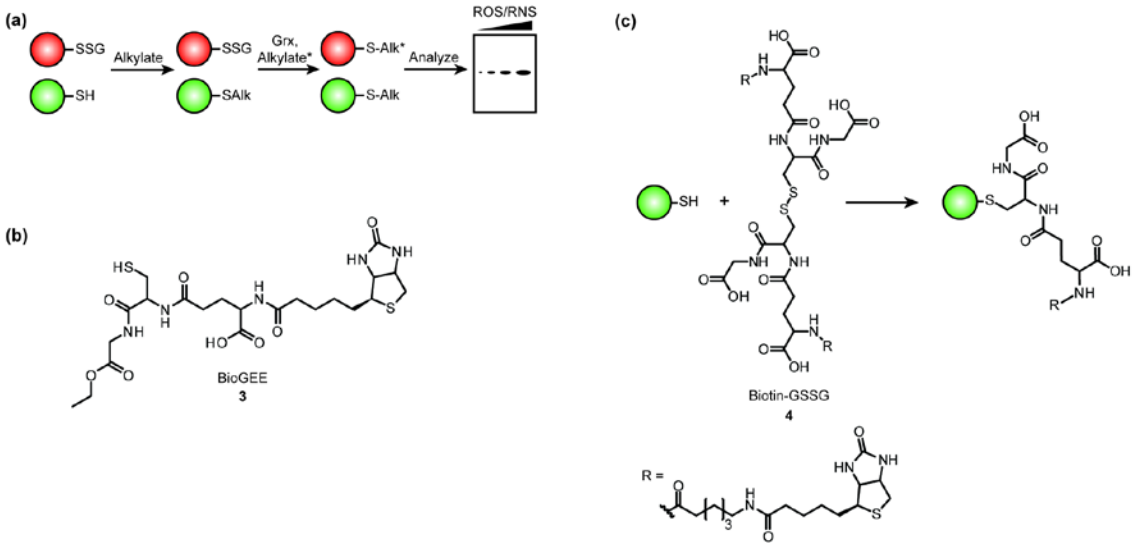

Figure 1.4 Chemical approaches to detect protein glutathionylation. (a) Restoration of thiol-labeling by glutaredoxin indirectly monitors S-glutathionylation. First, samples are incubated with NEM or IAM to irreversibly alkylate free thiols. Next glutaredoxin selectively reduces protein-GSH adducts to free thiols leaving all other cysteine oxoforms intact. Addition of NEM or IAM derivatized with a detection handle covalently modifies nascent thiols. Increased cysteine glutathionylation exhibits an increase in probe signal. (b) Biotinylated glutathione ethyl ester (BioGEE) enables in situ detection of S-glutathionylated proteins. (c) N,N-biotinyl glutathione disulfide (Biotin-GSSG) identifies proteins which become S-glutathionylated through disulfide exchange.

Protein *S*-glutathionylation can be monitored by an indirect method comprised of three principle steps (Figure 1.4a) [48]: (1) alkylation of free thiols with NEM or IAM, (2) reduction of protein-GSH adducts by Grx, which does not affect other reversible cysteine modifications such as inter- or intramolecular proteins disulfides, sulfenic acids, or nitrosothiols; and (3) tagging of nascent protein thiols with thiol-reactive biotinylated or fluorescent reagents. In future studies,

it may be possible to quantify the extent of *S*-glutathionylation by combining Grx-mediated reduction of protein-GSH adducts with the OxICAT approach described above.

Direct detection of protein-GSH adducts was originally achieved with radiolabeled ^{35}S-GSH.[49] However, this technology is prone to artifacts arising from the need to inhibit protein synthesis while labeling the intracellular GSH pool. Biotinylated glutathione ethyl ester (BioGEE) **3 (**Figure 1.4b**)** was subsequently developed and enables *in situ* detection and purification of *S*-glutathionylated proteins.[50] *N*,*N*-biotinyl glutathione disulfide (Biotin-GSSG) **4** (Figure 1.4c) has also shown utility in affinity purification and proteomic analysis of *S*-glutathionylation.[51] General limitations of these approaches are steric occlusion and poor cellular trafficking of biotinylated probes.[52,53]

1.9 Chemical approaches to detect protein nitrosylation

Nitric oxide (NO) is an important second messenger in cellular signal transduction and accumulating evidence indicates that modification of redox-sensitive protein thiols plays a central role in these pathways.[54] Many proteins have been identified as *S*-nitrosylation targets and the functional effect of the modification have been characterized.[34,55,56] However, *S*-nitrosylated proteins are often identified in studies that utilize exceptionally high, unphysiological concentrations of NO-donors. Specialized methods required to generate and identify nitrosylated protein cysteine residues in complex biological systems are still evolving. In the last few years, however, there has been significant progress among *in vitro* methods for the direct detection of *S*-nitrosothiols. We outline these new chemical approaches below and refer

the interested reader to [57,58] for additional discussion of the biology, generation and detection of *S*-nitrosothiols.

The most popular approach to identify nitrosothiols is known as the biotin switch technique (BST).[55] The BST is an indirect method consisting of three major steps (Figure 1.5a): (1) blocking of free cysteine thiols by *S*-methylthiolation with methylmethane thiosulfonate (MMTS; a reactive thiosulfonate); (2) reduction of *S*-nitrosothiols with ascorbate; and (3) labeling nascent thiols with biotin–HPDP (*i.e.,* biotin-N-[6-(biotinamido)hexyl]-3'-(2'-pyridyldithio)-propionamide), a reactive mixed disulfide analog of biotin. Analogous to other indirect methods of detection, the success of this approach relies on quantitative alkylation of free thiols in the first step and specificity of the reducing agent. Indeed, the selectivity of ascorbate as a cleaving agent for the S-N bond has recently been called into question.[57,59] Even so, this technique has found wide utility in identification of *S*-nitrosothiol protein modifications when performed alongside appropriate controls.[60,61]

The BST approach has also been successfully adapted to protein microarrays.[62] This technique shows a small percentage of false positives and does not cover the entire proteome; however, this high throughput method allows for rapid screening of candidates for *S*-nitrosylation and a comparison between different chemical classes of various NO-donor compounds. More recently, Sinha *et al.* have combined BST with isotope-labeled NEM (d5-NEM) to afford a quantitative method for *S*-nitrosothiol detection, termed d-Switch (Figure 1.5b).[63] Future renditions of this approach might include a biotin affinity handle, analogous to the ICAT technology.

An attractive alternative to the strategies outlined above is the application of chemoselective reactions to directly target *S*-nitrosothiol modifications. In this regard, triarylphosphine reagents have shown particular promise as probes for *S*-nitrosylation.[64] Phosphine reagent **5** has been employed as a covalent nitrosothiol ligating agent in THF-PBS systems (Figure 1.5c) [65] to form a disulfide linkage with biotin. A coumarin-based fluorescent compound **6** has also been developed (Figure 1.5d).[66] King *et al.* have also reported on a water soluble triarylphosphine **7** (Figure 1.5e).[67] This compound generates a stable *S*-alkylphosphonium adduct and enables ^{31}P NMR spectroscopic analysis. At present time, however, this reagent lacks an affinity tag. Future studies are needed to investigate the utility of all phosphine-based reagents for *in situ* detection of protein *S*-nitrosothiol modifications. In addition, their specificity for *S*-nitrosothiols must be rigorously addressed since similar phosphine reagents have been shown to react with disulfides and cross-reactivity with sulfenic acids has not been ruled out.[67]

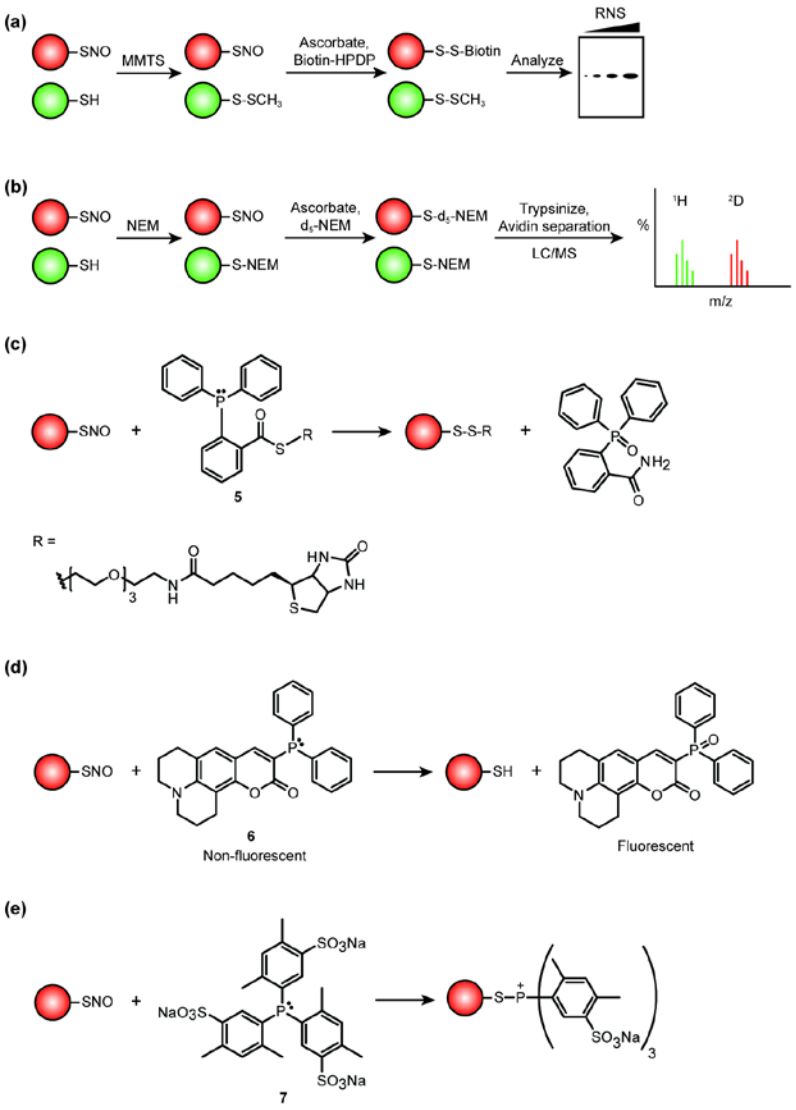

Figure 1.5 Chemical approaches to detect protein S-nitrosylation. (a) The biotin switch technique (BST) indirectly monitors S-nitrosylation. Proteins are incubated with methylmethane thiosulfonate (MMTS), an S-methylthiolating agent to block free thiols (green protein). Secondly, ascorbate reduction returns nitrosothiols (red protein) to free thiols. Nascent thiols are labeled with biotin-HPDP appending a biotin moiety. Increased protein S-nitrosylation exhibits an increase in probe signal. (b) The d-Switch combines the BST with isotope labeled NEM (d5-NEM) to quantify cysteine nitrosylation. Proteins are labeled with NEM to covalently modify all free thiols (green protein). Next ascorbate reduction reduces nitrosylated cysteines to free thiols (red protein). Nascent thiols are labeled with d5-NEM. Proteins are trypsinized generating chemically identical peptides which differ in mass by 5 Da due to incorporation of either light or heavy NEM and analyzed by LC-MS. Relative peak intensities can determine the ratio of S-nitrosylation. (c) Triarylphosphine reagent 5 reacts directly with nitrosothiols to form a disulfide linkage with biotin. (d) Compound 6 fluorescently detects nitrosothiols. (e) Water soluble triarylphosphine 7 generates a stable S-alkylphosphonium adduct.

1.10 Chemical and immunochemical approaches to detect protein sulfenylation

The initial oxidation product of a protein cysteine residue is sulfenic acid (Figure 1.1). Like many other oxidative cysteine modifications, sulfenic acid formation is reversible (either directly or indirectly by disulfide formation) and affords a mechanism in which changes in cellular redox state can be exploited to regulate protein function. The stability of a sulfenic acid modification is largely dependent upon the protein microenvironment and proximity to other thiols. In the presence of excess ROS, protein sulfenic acids can be further oxidized to sulfinic and sulfonic oxyacids. These hyperoxidized forms of cysteine are generally considered to be irreversible. One notable exception, however, is sulfiredoxin-catalyzed reduction of cysteine sulfinic acid in peroxiredoxins.[68]

Sulfenic acids have been identified in the catalytic cycle of multiple enzymes, including peroxiredoxin, NADH peroxidase, and methionine sulfoxide- and formylglycine-generating enzymes.[10,18,40,41] Formation of sulfenic acid has also been linked to oxidative stress-induced transcriptional changes in bacteria due to altered DNA binding of OxyR and OhrR and changes in the activity of the yeast peroxiredoxin and Yap1 protein.[2,40,41] Less is known about the mechanisms that underlie sulfenic acid-mediated regulation of mammalian protein function and signal transduction pathways; however, cysteine residues of several transcription factors (*i.e.,* NF-κB, Fos, and Jun), or proteins involved in cell signaling or metabolism (*i.e.,* glyceraldehyde-3-phosphate dehydrogenase, GSH reductase, tyrosine phosphatases, kinases, and proteases) can be converted to sulfenic acid *in vitro*. Sulfenic acid formation has also been proposed to regulate tumor necrosis factor-induced JNK (c-Jun NH_2-terminal kinase) activation,

inactivation of protein tyrosine phosphatase 1B by epidermal growth factor, and CD8+ T cell proliferation.[69-71]

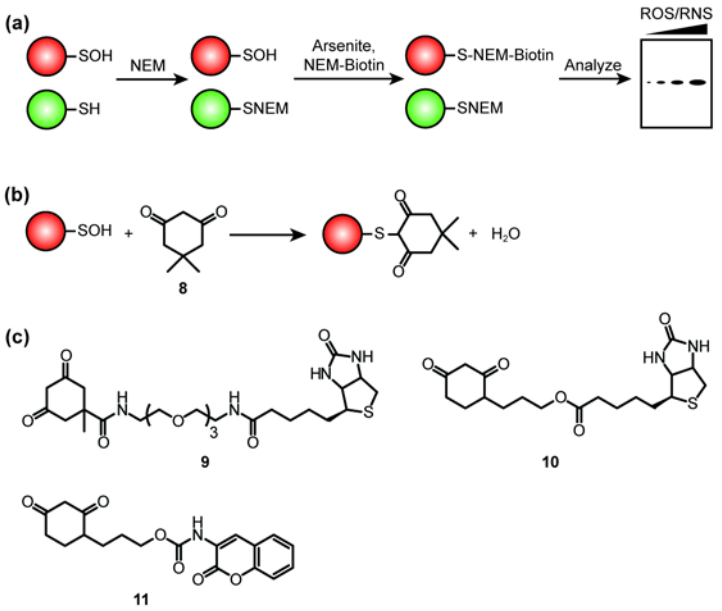

Figure 1.6 Chemical approaches to detect protein sulfenylation. (a) Arsenite modification of the BST indirectly monitors sulfenylation. . Proteins are labeled with NEM to covalently modify all free thiols (green protein). Next arsenite reduction selectively reduces sulfenic acids to free thiols (red protein). Nascent thiols are labeled with a biotinylated NEM. Increased protein sulfenylation exhibits an increase in probe signal. (b) Selective reaction of 5,5-dimethyl-1,3-cyclohexanedione with sulfenic acids. (c) Direct conjugation of dimedone derivatives to biotin or fluorophores for sulfenic acid detection.

Owing to the central role of sulfenic acid in the oxidation pathway of cysteine, several methods have been developed for its detection. One major advantage of detecting sulfenic acids in proteins is that this modifications represents the initial product of oxidation and functions as a marker for ROS/RNS-sensitive cysteine residues, while a potential disadvantage is the often transient nature of this modification.[14] Arsenite-mediated reduction of sulfenic acids has led to a variation on the BST method to detect protein sulfenylation in three steps (Figure 1.6a): (1)

alkylation of free thiols; (2) reduction of sulfenic acids by arsenite; and (3) biotin-maleimide labeling of nascent free thiols.[72] Proteomic analyses of protein sulfenic acid formation in rat kidney cell extracts have been performed using this technique.[73] However, the same limitations discussed above regarding indirect detection and the selectivity/efficiency of arsenite reduction of sulfenic acids apply.[59]

Methods that allow for direct detection of protein sulfenic acid modifications are based on the electrophilic character of the oxidized sulfur atom. The selective reaction between 5,5-dimethyl-1,3-cyclohexanedione (dimedone) **8** and protein sulfenic acids was first reported by Benitez and Allison in 1974 (Figure 1.6b).[74] This chemistry has been exploited to detect protein sulfenic acids by MS or through direct conjugation to biotin **9-10** or fluorophores such as **11** (Figure 1.6c)**.**[26,70,75-78] Recently, membrane-permeable azide- and alkyne-based analogs of dimedone, termed DAz-1 **12** [53,79], DAz-2 **13** [80], DYn-1 and DYn-2 **14-15** (Unpublished) (Figure 1.7a), have been developed that enable trapping and tagging of sulfenic acid-modified proteins directly in cells. DAz and DYn probes are comprised of two key elements: a dimedone warhead that reacts selectively with sulfenic acids and an azide or alkyne reporter group suitable for bioorthogonal Staudinger and Huisgen [3+2] cycloaddition coupling reactions (Figure 1.7b) for analysis of labeled proteins. Using DAz-2, our laboratory has reported on the global analysis of the sulfenome in a human tumor cell line (Figure 1.7c). This study identified the majority of known sulfenic acid-modified proteins and revealed more than 175 new targets of oxidation.[80] Cross-comparison of our findings with those from disulfide and glutathionylation proteomes revealed a modest amount of overlap, suggesting that many

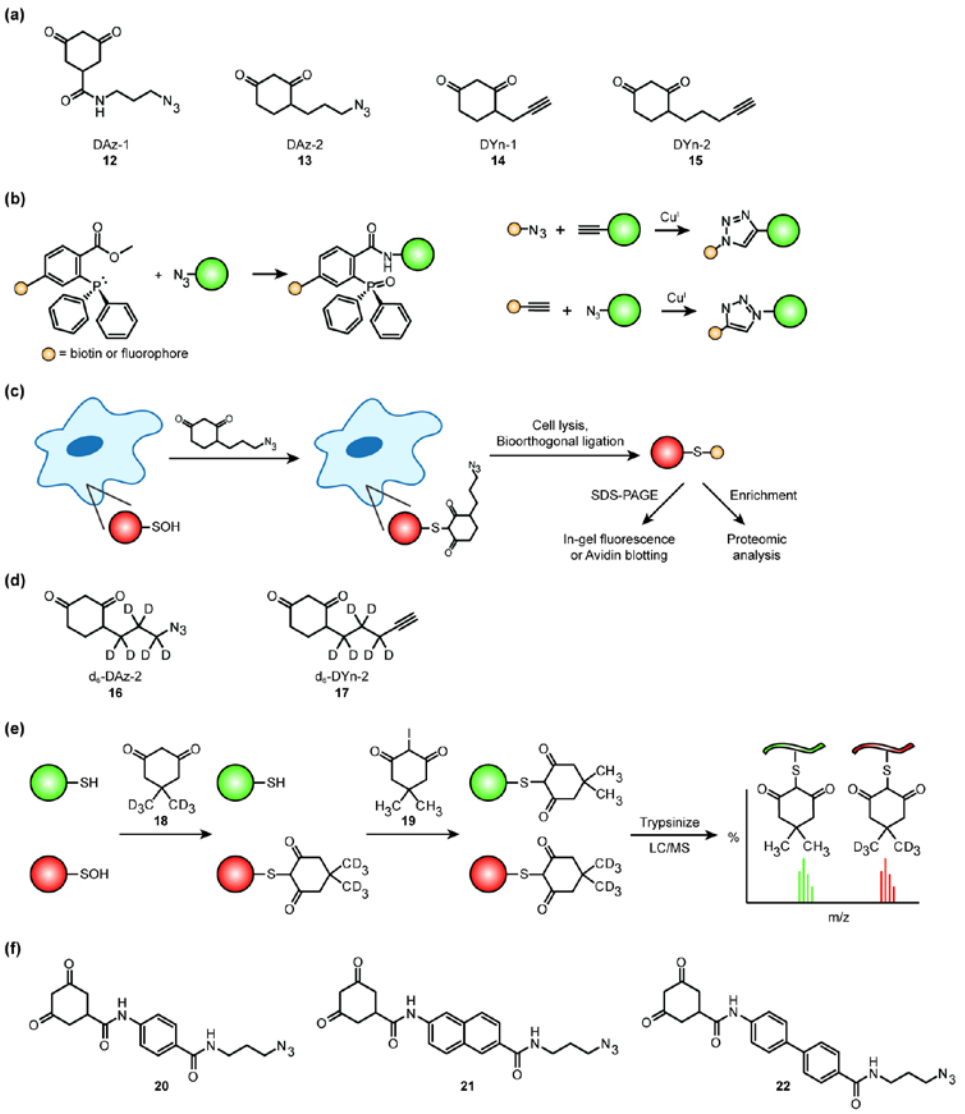

Figure 1.7 Chemical approaches for direct detection of protein sulfenylation. (a) Membrane-permeable azide- and alkyne-based analogs of dimedone. (b) Bioorthogonal Staudinger ligation appends a detection tag to an azide-modified protein. Bioorthogonal Huisgen [3+2] cycloaddition couples azide- or alkyne-modified proteins with detection tags. (c) In situ detection of protein sulfenylation using DAz-2. Sulfenylated proteins are labeled in situ using the cell permeable DAz-2. Following alkylation, cells are lysed and bioorthogonal ligation of labeled proteins to biotin or fluorophores allows detection through SDS-PAGE or enrichment for proteomic analysis. (d) Isotopically heavy derivatives of DAz-2 and DYn-2. (e) Isotope-coded dimedone and 2-iododimedone (ICDID) allows quantitation of protein sulfenylation. Proteins are labeled with isotope-coded dimedone (d6-dimedone) to covalently modify all sulfenic acids (red protein). Next, excess reagent is removed and 2-iododimedone covalently alkylates all free thiols (green protein) resulting in a dimedone-labeled cysteine which differs in mass by 6 Da due to incorporation of dimedone or d6-dimedone. Proteins are trypsinized generating chemically identical peptides and analyzed by LC-MS. Relative peak intensities can determine the ratio of sulfenylation on a particular cysteine. (f) Chemical probes that target the redox-sensitive catalytic cysteine in protein tyrosine phosphatases through incorporation of a chemical scaffold with high affinity for the enzyme active site.

sulfenic acid modifications may be more stable than previously recognized and/or go on to form sulfinic and sulfonic acid.

An alternative method that we have developed to monitor protein sulfenic acid modifications is immunochemical detection.[81] In this strategy, the sulfenic acid is derivatized with dimedone to generate a unique epitope for recognition (Figure 1.8). The antibody elicited against this hapten is exquisitely specific, context-independent, and capable of visualizing sulfenic acid formation in cells. Application of this immunochemical approach to protein lysate arrays (Figure 1.8a) and cancer cell lines allowed us to monitor changes in the redox status of protein thiols and revealed diversity in sulfenic acid modifications among different subtypes of breast tumors. In a subsequent study, Maller *et al.* also report an antibody that detects a protein sulfenic acid derivatized by dimedone adduct and use this reagent to investigate the role of glyceraldehyde 3-phosphate dehydrogenase oxidation in H_2O_2-treated cells.[82] A future application for this immunochemical method will be in using antibody arrays to analyze protein sulfenylation within specific signaling pathways (Figure 1.8b).

Beyond simple detection of sulfenic acids, the next step to providing insight into their physiological and pathological significance is to quantify redox-dependent changes in the extent of this modification. To this end, we have recently developed two complementary strategies: (1) isotopically light and heavy derivatives of DAz-2 (**16**) or DYn (**17**) (Figure 1.7d); and (2) isotope-coded dimedone (**18**) and 2-iododimedone (**19**, ICDID) (Figure 1.7e).[84] The first method permits relative quantitation of sulfenic acid modification between different cellular states, whereas the second approach factors out changes in protein abundance and enables

estimation of absolute sulfenylation site occupancy. ICDID consists of two key tagging steps: (1) deuterium-labeled dimedone (d6-dimedone) selectively labels sites of sulfenic acid modification; and (2) free thiols are alkylated with 2-iododimedone. The products of these reactions are chemically identical, but differ in mass by 6 Da. Accordingly, the extent of sulfenic acid modification at any given cysteine residue can be determined from the ratio of heavy/light isotope-labeled peak intensities in the mass spectrum.

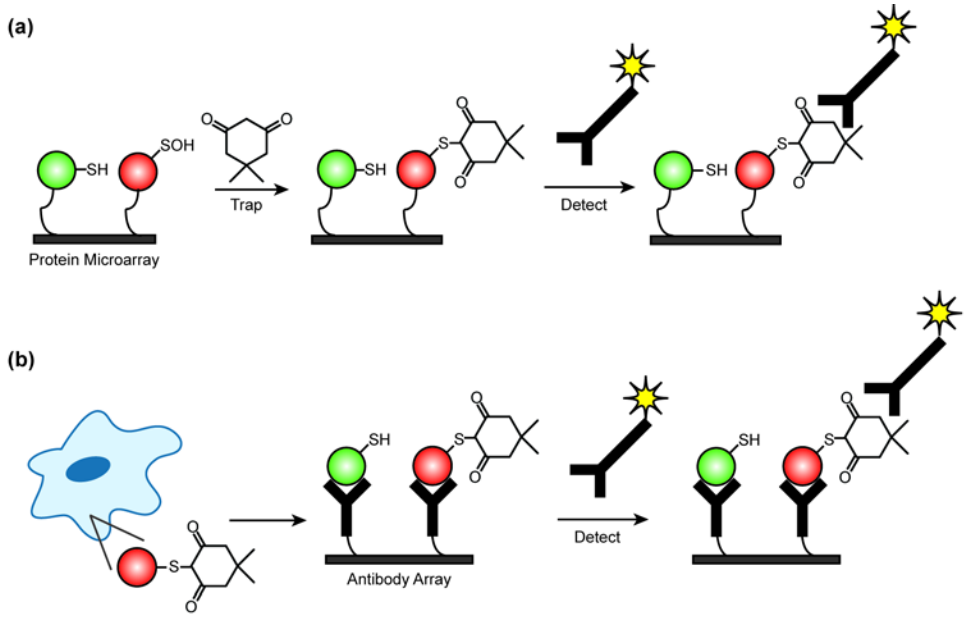

Figure 1.8 High throughput immunochemical detection of dimedone-modified sulfenic acid epitope using arrays. (a) Protein microarrays can be used to identify sulfenylated proteins. Sulfenylated proteins on the microarray are alkylated with dimedone to form an epitope for antibody recognition. Addition of the antibody allows identification of the modified proteins. (b) Antibody arrays can probe specific signaling events for protein sulfenylation. Cells are incubated with dimedone to modify sulfenylated proteins. Antibody arrays are used to capture signaling proteins from cell lysates. Probing with antibody to detect dimedone modification allows identification of sulfenylated proteins within a specific signaling pathway.

Analogous to irreversible inhibitors that modify conserved cysteine residues in growth factor receptors [83], dimedone-based probes can be further specialized to target sulfenic acid modifications in a specific class of signaling proteins. The design strategy for these probes is to couple a portion of a high affinity ligand that is proximal to the targeted cysteine and install the dimedone functionality at a position that is compatible with the formation of the covalent bond. As proof of concept, we have developed probes that target the redox-sensitive catalytic cysteine in protein tyrosine phosphatases (PTP).[85] These reagents are comprised of the dimedone nucleophile, a chemical scaffold that uniquely enhances its capacity for target binding, and an azide chemical reporter group (Figure 1.7f; **20-22**). These reagents demonstrate significantly increased potency for detecting sulfenic acid modification of the catalytic cysteine in the *Yersinia pestis* PTP. These probes should serve as useful chemical tools to investigate redox-regulation of PTPs and can be further modified to target individual members of the cysteine phosphatase superfamily.

1.11 Conclusions and future directions

The field of cysteine-based redox proteomics is an active and exciting area of research stimulated by recent discoveries and increasing interest in the role of ROS/RNS as second messengers. The repertoire of methods for detecting oxidative cysteine modifications has been greatly expanded in the last decade, including selective probes, chemical reporters and reagents that target a specific class of proteins. Even so, reagents for irreversible modifications have yet to be developed and the biocompatibility of probes for cellular detection must be further assessed in order that experiments in tissue and animals can be considered. We expect that *in vitro* and *in situ* analysis of cysteine oxidation will yield highly complementary sets of data. Both

strategies have been deployed successfully to discover the identity of oxidized proteins, which is a necessary first step toward understanding the biology of protein cysteine oxidation. As the technical hurdles toward discovery are overcome, where the rubber will meet the road in this exciting field is in gaining insight into the functional consequences of these modifications in human health and disease.

Acknowledgements

We apologize to those authors whose work we could not cite due to space limitations. We thank the American Heart Association (0835419N) and The Camille and Henry Dreyfus Foundation for support of research from our laboratory that was covered in this review.

Notes

This work has been published as “Chemical 'omics' approaches for understanding protein cysteine oxidation in biology.” in Curr Opin Chem Biol. 2011 Feb;15(1):88-102.

1.12 References and recommended reading

Papers of particular interest, published within the period of review have been highlighted as:

• of special interest

•• of outstanding interest

1. Kumsta C, Thamsen M, Jakob U: **Effects of Oxidative Stress on Behavior, Physiology, and the Redox Thiol Proteome of Caenorhabditis elegans**. *Antioxid Redox Signal* 2010.

2. Antelmann H, Helmann JD: **Thiol-based redox switches and gene regulation**. *Antioxid Redox Signal* 2010.

3. •• Reddie KG, Carroll KS: **Expanding the functional diversity of proteins through cysteine oxidation**. *Curr Opin Chem Biol* 2008, **12**:746-754.

This review details the chemical reactivity of cysteine posttranslational modifications.

4. Hirooka Y, Sagara Y, Kishi T, Sunagawa K: **Oxidative stress and central cardiovascular regulation. - Pathogenesis of hypertension and therapeutic aspects**. *Circ J* 2010, **74**:827-835.

5. Koh CH, Whiteman M, Li QX, Halliwell B, Jenner AM, Wong BS, Laughton KM, Wenk M, Masters CL, Beart PM, et al.: **Chronic exposure to U18666A is associated with oxidative stress in cultured murine cortical neurons**. *J Neurochem* 2006, **98**:1278-1289.

6. Visconti R, Grieco D: **New insights on oxidative stress in cancer**. *Curr Opin Drug Discov Devel* 2009, **12**:240-245.

7. Wei W, Liu Q, Tan Y, Liu L, Li X, Cai L: **Oxidative stress, diabetes, and diabetic complications**. *Hemoglobin* 2009, **33**:370-377.

8. Giustarini D, Dalle-Donne I, Tsikas D, Rossi R: **Oxidative stress and human diseases: Origin, link, measurement, mechanisms, and biomarkers**. *Crit Rev Clin Lab Sci* 2009, **46**:241-281.

9. Janssen-Heininger YM, Mossman BT, Heintz NH, Forman HJ, Kalyanaraman B, Finkel T, Stamler JS, Rhee SG, van der Vliet A: **Redox-based regulation of signal transduction: principles, pitfalls, and promises**. *Free Radic Biol Med* 2008, **45**:1-17.

10. •• Paulsen CE, Carroll KS: **Orchestrating redox signaling networks through regulatory cysteine switches**. *ACS Chem Biol* 2010, **5**:47-62.

This review details examples in which cysteine oxidation is used to regulate protein function.

11. Winterbourn CC, Hampton MB: **Thiol chemistry and specificity in redox signaling**. *Free Radic Biol Med* 2008, **45**:549-561.

12. Miller EW, Chang CJ: **Fluorescent probes for nitric oxide and hydrogen peroxide in cell signaling**. *Curr Opin Chem Biol* 2007, **11**:620-625.

13. McQuade LE, Lippard SJ: **Fluorescent probes to investigate nitric oxide and other reactive nitrogen species in biology (truncated form: fluorescent probes of reactive nitrogen species)**. *Curr Opin Chem Biol* 2010, **14**:43-49.

14. Poole LB, Nelson KJ: **Discovering mechanisms of signaling-mediated cysteine oxidation**. *Curr Opin Chem Biol* 2008, **12**:18-24.

15. Sivaramakrishnan S, Cummings AH, Gates KS: **Protection of a single-cysteine redox switch from oxidative destruction: On the functional role of sulfenyl amide formation in the redox-regulated enzyme PTP1B**. *Bioorg Med Chem Lett* 2010, **20**:444-447.

16. • Depuydt M, Leonard SE, Vertommen D, Denoncin K, Morsomme P, Wahni K, Messens J, Carroll KS, Collet JF: **A periplasmic reducing system protects single cysteine residues from oxidation**. *Science* 2009, **326**:1109-1111.

This report identifies the first cellular reducing system to protect sulfenylated cystienes from over-oxidation.

17. Crane EJ, 3rd, Parsonage D, Poole LB, Claiborne A: **Analysis of the kinetic mechanism of enterococcal NADH peroxidase reveals catalytic roles for NADH complexes with both oxidized and two-electron-reduced enzyme forms**. *Biochemistry* 1995, **34**:14114-14124.

18. Hugo M, Turell L, Manta B, Botti H, Monteiro G, Netto LE, Alvarez B, Radi R, Trujillo M: **Thiol and sulfenic acid oxidation of AhpE, the one-cysteine peroxiredoxin from Mycobacterium tuberculosis: kinetics, acidity constants, and conformational dynamics**. *Biochemistry* 2009, **48**:9416-9426.

19. Peskin AV, Low FM, Paton LN, Maghzal GJ, Hampton MB, Winterbourn CC: **The high reactivity of peroxiredoxin 2 with H(2)O(2) is not reflected in its reaction with other oxidants and thiol reagents**. *J Biol Chem* 2007, **282**:11885-11892.

20. Sohn J, Rudolph J: **Catalytic and chemical competence of regulation of cdc25 phosphatase by oxidation/reduction**. *Biochemistry* 2003, **42**:10060-10070.

21. Turell L, Botti H, Carballal S, Ferrer-Sueta G, Souza JM, Duran R, Freeman BA, Radi R, Alvarez B: **Reactivity of sulfenic acid in human serum albumin**. *Biochemistry* 2008, **47**:358-367.

22. Kharitonov VG, Sundquist AR, Sharma VS: **Kinetics of nitrosation of thiols by nitric oxide in the presence of oxygen**. *J Biol Chem* 1995, **270**:28158-28164.

23. Rudolph TK, Freeman BA: **Transduction of redox signaling by electrophile-protein reactions**. *Sci Signal* 2009, **2**:re7.

24. Klomsiri C, Karplus PA, Poole LB: **Cysteine-Based Redox Switches in Enzymes**. *Antioxid Redox Signal* 2010.

25. • Go YM, Jones DP: **Redox compartmentalization in eukaryotic cells**. *Biochim Biophys Acta* 2008, **1780**:1273-1290.

This study highlights the delicate redox balance that is maintained through compartmentalization in the cell.

26. Klomsiri C, Nelson KJ, Bechtold E, Soito L, Johnson LC, Lowther WT, Ryu SE, King SB, Furdui CM, Poole LB: **Use of dimedone-based chemical probes for sulfenic acid detection evaluation of conditions affecting probe incorporation into redox-sensitive proteins**. *Methods Enzymol* 2010, **473**:77-94.

27. • Leichert LI, Gehrke F, Gudiseva HV, Blackwell T, Ilbert M, Walker AK, Strahler JR, Andrews PC, Jakob U: **Quantifying changes in the thiol redox proteome upon oxidative stress in vivo**. *Proc Natl Acad Sci U S A* 2008, **105**:8197-8202.

This report describe the OxICAT technique to ratiometrically determine reversible cysteine oxidation.

28. Dahl KH, McKinley-McKee JS: **The reactivity of affinity labels: A kinetic study of the reaction of alkyl halides with thiolate anions--a model reaction for protein alkylation**. *Bioorganic Chemistry* 1981, **10**:329-341.

29. Berti PJ, Storer AC: **Alignment/phylogeny of the papain superfamily of cysteine proteases**. *J Mol Biol* 1995, **246**:273-283.

30. Mavridou DA, Stevens JM, Ferguson SJ, Redfield C: **Active-site properties of the oxidized and reduced C-terminal domain of DsbD obtained by NMR spectroscopy**. *J Mol Biol* 2007, **370**:643-658.

31. • Winterbourn CC, Metodiewa D: **Reactivity of biologically important thiol compounds with superoxide and hydrogen peroxide**. *Free Radic Biol Med* 1999, **27**:322-328.

This study measures the reaction rates of biologically relevant thiols with hydrogen peroxide and superoxide.

32. Ying J, Clavreul N, Sethuraman M, Adachi T, Cohen RA: **Thiol oxidation in signaling and response to stress: detection and quantification of physiological and pathophysiological thiol modifications**. *Free Radic Biol Med* 2007, **43**:1099-1108.

33. Hill BG, Reily C, Oh JY, Johnson MS, Landar A: **Methods for the determination and quantification of the reactive thiol proteome**. *Free Radic Biol Med* 2009, **47**:675-683.

34. Sethuraman M, Clavreul N, Huang H, McComb ME, Costello CE, Cohen RA: **Quantification of oxidative posttranslational modifications of cysteine thiols of p21ras associated with redox modulation of activity using isotope-coded affinity tags and mass spectrometry**. *Free Radic Biol Med* 2007, **42**:823-829.

35. Sethuraman M, McComb ME, Huang H, Huang S, Heibeck T, Costello CE, Cohen RA: **Isotope-coded affinity tag (ICAT) approach to redox proteomics: identification and quantitation of oxidant-sensitive cysteine thiols in complex protein mixtures**. *J Proteome Res* 2004, **3**:1228-1233.

36. Marino SM, Li Y, Fomenko DE, Agisheva N, Cerny RL, Gladyshev VN: **Characterization of surface-exposed reactive cysteine residues in Saccharomyces cerevisiae**. *Biochemistry* 2010, **49**:7709-7721.

37. Claiborne A, Miller H, Parsonage D, Ross RP: **Protein-sulfenic acid stabilization and function in enzyme catalysis and gene regulation**. *FASEB J* 1993, **7**:1483-1490.

38. Gu J, Lewis RS: **Effect of pH and metal ions on the decomposition rate of S-nitrosocysteine**. *Ann Biomed Eng* 2007, **35**:1554-1560.

39. Depuydt M, Messens J, Collet JF: **How Proteins Form Disulfide Bonds**. *Antioxid Redox Signal* 2010.

40. Chen H, Xu G, Zhao Y, Tian B, Lu H, Yu X, Xu Z, Ying N, Hu S, Hua Y: **A novel OxyR sensor and regulator of hydrogen peroxide stress with one cysteine residue in Deinococcus radiodurans**. *PLoS One* 2008, **3**:e1602.

41.• Paulsen CE, Carroll KS: **Chemical dissection of an essential redox switch in yeast**. *Chem Biol* 2009, **16**:217-225.

This study demonstrates that sulfenic acid modification of Gpx3 is required for activation of the transcription factor Yap1 in cells.

42. Holland R, Fishbein JC: **Chemistry of the cysteine sensors in Kelch-like ECH-associated protein 1**. *Antioxid Redox Signal* 2010, **13**:1749-1761.

43. Katagiri K, Matsuzawa A, Ichijo H: **Regulation of apoptosis signal-regulating kinase 1 in redox signaling**. *Methods Enzymol* 2010, **474**:277-288.

44. Cumming RC: **Analysis of global and specific changes in the disulfide proteome using redox two-dimensional polyacrylamide gel electrophoresis**. *Methods Mol Biol* 2008, **476**:165-179.

45. Owen JB, Butterfield DA: **Measurement of oxidized/reduced glutathione ratio**. *Methods Mol Biol* 2010, **648**:269-277.

46. Dalle-Donne I, Milzani A, Gagliano N, Colombo R, Giustarini D, Rossi R: **Molecular mechanisms and potential clinical significance of S-glutathionylation**. *Antioxid Redox Signal* 2008, **10**:445-473.

47. Tew KD, Townsend DJ: *Curr Opin Chem Biol* 2010.

48. Lind C, Gerdes R, Hamnell Y, Schuppe-Koistinen I, von Lowenhielm HB, Holmgren A, Cotgreave IA: **Identification of S-glutathionylated cellular proteins during oxidative stress and constitutive metabolism by affinity purification and proteomic analysis**. *Arch Biochem Biophys* 2002, **406**:229-240.

49. Fratelli M, Demol H, Puype M, Casagrande S, Eberini I, Salmona M, Bonetto V, Mengozzi M, Duffieux F, Miclet E, et al.: **Identification by redox proteomics of glutathionylated proteins in oxidatively stressed human T lymphocytes**. *Proc Natl Acad Sci U S A* 2002, **99**:3505-3510.

50. Sullivan DM, Wehr NB, Fergusson MM, Levine RL, Finkel T: **Identification of oxidant-sensitive proteins: TNF-alpha induces protein glutathiolation**. *Biochemistry* 2000, **39**:11121-11128.

51. Brennan JP, Miller JI, Fuller W, Wait R, Begum S, Dunn MJ, Eaton P: **The utility of N,N-biotinyl glutathione disulfide in the study of protein S-glutathiolation**. *Mol Cell Proteomics* 2006, **5**:215-225.

52. Cohen MS, Hadjivassiliou H, Taunton J: **A clickable inhibitor reveals context-dependent autoactivation of p90 RSK**. *Nature Chemical Biology* 2007, **3**:156-160.

53. Seo YH, Carroll KS: **Facile synthesis and biological evaluation of a cell-permeable probe to detect redox-regulated proteins**. *Bioorg Med Chem Lett* 2009, **19**:356-359.

54. Jaffrey SR, Erdjument-Bromage H, Ferris CD, Tempst P, Snyder SH: **Protein S-nitrosylation: a physiological signal for neuronal nitric oxide**. *Nat Cell Biol* 2001, **3**:193-197.

55. •• Jaffrey SR, Snyder SH: **The biotin switch method for the detection of S-nitrosylated proteins**. *Sci STKE* 2001, **2001**:pl1.

This study details the biotin switch technique to identify *S*-nitrosylation.

56. Foster MW, Hess DT, Stamler JS: **Protein S-nitrosylation in health and disease: a current perspective**. *Trends Mol Med* 2009, **15**:391-404.

57. Wang H, Xian M: **Chemical methods to detect S-nitrosation**. *Curr Opin Chem Biol* 2010.

58. Stamler JS: *Curr Opin Chem Biol* 2010.

59. Giustarini D, Dalle-Donne I, Colombo R, Milzani A, Rossi R: **Is ascorbate able to reduce disulfide bridges? A cautionary note**. *Nitric Oxide* 2008, **19**:252-258.

60. Forrester MT, Thompson JW, Foster MW, Nogueira L, Moseley MA, Stamler JS: **Proteomic analysis of S-nitrosylation and denitrosylation by resin-assisted capture**. *Nat Biotechnol* 2009, **27**:557-559.

61. Forrester MT, Foster MW, Benhar M, Stamler JS: **Detection of protein S-nitrosylation with the biotin-switch technique**. *Free Radic Biol Med* 2009, **46**:119-126.

62. Foster MW, Forrester MT, Stamler JS: **A protein microarray-based analysis of S-nitrosylation**. *Proc Natl Acad Sci U S A* 2009, **106**:18948-18953.

63. Sinha V, Wijewickrama GT, Chandrasena RE, Xu H, Edirisinghe PD, Schiefer IT, Thatcher GR: **Proteomic and mass spectroscopic quantitation of protein S-nitrosation differentiates NO-donors**. *ACS Chem Biol* 2010, **5**:667-680.

64. • Wang H, Xian M: **Fast reductive ligation of S-nitrosothiols**. *Angew Chem Int Ed Engl* 2008, **47**:6598-6601.

This study first reports the reaction of triarylphosphines with nitrosothiols.

65. Zhang J, Li S, Zhang D, Wang H, Whorton AR, Xian M: **Reductive ligation mediated one-step disulfide formation of S-nitrosothiols**. *Org Lett* 2010, **12**:4208-4211.

66. Pan J, Downing JA, McHale JL, Xian M: **A fluorogenic dye activated by S-nitrosothiols**. *Mol Biosyst* 2009, **5**:918-920.

67. •• Bechtold E, Reisz JA, Klomsiri C, Tsang AW, Wright MW, Poole LB, Furdui CM, King SB: **Water-soluble triarylphosphines as biomarkers for protein S-nitrosation**. *ACS Chem Biol* 2010, **5**:405-414.

This study develops the first water soluble triarylphosphine to directly modify nitrosothiols, and additionally observes low triarylphosphine reactivity with disulfides cautioning thorough investigation of the specificity of novel reagents.

68. Biteau B, Labarre J, Toledano MB: **ATP-dependent reduction of cysteine-sulphinic acid by S. cerevisiae sulphiredoxin**. *Nature* 2003, **425**:980-984.

69. Pantano C, Reynaert NL, van der Vliet A, Janssen-Heininger YM: **Redox-sensitive kinases of the nuclear factor-kappaB signaling pathway**. *Antioxid Redox Signal* 2006, **8**:1791-1806.

70. Michalek RD, Nelson KJ, Holbrook BC, Yi JS, Stridiron D, Daniel LW, Fetrow JS, King SB, Poole LB, Grayson JM: **The requirement of reversible cysteine sulfenic acid formation for T cell activation and function**. *J Immunol* 2007, **179**:6456-6467.

71. Lee SR, Kwon KS, Kim SR, Rhee SG: **Reversible inactivation of protein-tyrosine phosphatase 1B in A431 cells stimulated with epidermal growth factor**. *J Biol Chem* 1998, **273**:15366-15372.

72. Saurin AT, Neubert H, Brennan JP, Eaton P: **Widespread sulfenic acid formation in tissues in response to hydrogen peroxide**. *Proc Natl Acad Sci U S A* 2004, **101**:17982-17987.

73. Tyther R, Ahmeda A, Johns E, McDonagh B, Sheehan D: **Proteomic profiling of perturbed protein sulfenation in renal medulla of the spontaneously hypertensive rat**. *J Proteome Res* 2010, **9**:2678-2687.

74. • Benitez LV, Allison WS: **The inactivation of the acyl phosphatase activity catalyzed by the sulfenic acid form of glyceraldehyde 3-phosphate dehydrogenase by dimedone and olefins**. *J Biol Chem* 1974, **249**:6234-6243.

This study is the first to identify the chemoselective reaction of dimedone with sulfenic acids.

75. Charles RL, Schroder E, May G, Free P, Gaffney PR, Wait R, Begum S, Heads RJ, Eaton P: **Protein sulfenation as a redox sensor: proteomics studies using a novel biotinylated dimedone analogue**. *Mol Cell Proteomics* 2007, **6**:1473-1484.

76. Poole LB, Klomsiri C, Knaggs SA, Furdui CM, Nelson KJ, Thomas MJ, Fetrow JS, Daniel LW, King SB: **Fluorescent and affinity-based tools to detect cysteine sulfenic acid formation in proteins**. *Bioconjug Chem* 2007, **18**:2004-2017.

77. Poole LB, Zeng BB, Knaggs SA, Yakubu M, King SB: **Synthesis of chemical probes to map sulfenic acid modifications on proteins**. *Bioconjug Chem* 2005, **16**:1624-1628.

78. Carballal S, Radi R, Kirk MC, Barnes S, Freeman BA, Alvarez B: **Sulfenic acid formation in human serum albumin by hydrogen peroxide and peroxynitrite**. *Biochemistry* 2003, **42**:9906-9914.

79. • Reddie KG, Seo YH, Muse Iii WB, Leonard SE, Carroll KS: **A chemical approach for detecting sulfenic acid-modified proteins in living cells**. *Mol Biosyst* 2008, **4**:521-531.

This study employs the first probe demonstrating an ability to trap and detect sulfenic acid

formation on proteins within living cells allowing *in situ* detection of protein sulfenylation.

80. •• Leonard SE, Reddie KG, Carroll KS: **Mining the thiol proteome for sulfenic acid modifications reveals new targets for oxidation in cells**. *ACS Chem Biol* 2009, **4**:783-799.

This study identifies over 175 novel targets of protein sulfenylation.

81. • Seo YH, Carroll KS: **Profiling protein thiol oxidation in tumor cells using sulfenic acid-specific antibodies**. *Proc Natl Acad Sci U S A* 2009, **106**:16163-16168.

This report describes the first immunochemical detection of sulfenic acids using a dimedone modified epitope.

82. Maller C, Schroder E, Eaton P: **Glyceraldehyde 3-Phosphate Dehydrogenase is Unlikely to Mediate Hydrogen Peroxide Signaling: Studies with a Novel Anti-Dimedone Sulfenic Acid Antibody**. *Antioxid Redox Signal* 2010.

83. Zhou W, Ercan D, Chen L, Yun CH, Li D, Capelletti M, Cortot AB, Chirieac L, Iacob RE, Padera R, et al.: **Novel mutant-selective EGFR kinase inhibitors against EGFR T790M**. *Nature* 2009, **462**:1070-1074.

84. Seo YH, Carroll KS: **Quantification of protein sulfenic acid modifications using isotope-coded dimedone and iododimedone**. *Angew Chem Int Ed Engl* 2011, **50**:1342-1345.

85. Leonard SE, Garcia FJ, Goodsell, DG, Carroll KS: **Redox-Based Probes for Protein Tyrosine Phosphatases.** Angewandte Chemie Int'l Ed. 2011 May 2;50(19):4423-7.

Chapter 2

A chemical approach for detecting sulfenic acid-modified proteins in living cells

2.1 Abstract

Oxidation of the thiol functional group in cysteine (Cys–SH) to sulfenic (Cys–SOH), sulfinic (Cys–SO_2H) and sulfonic acid (Cys–SO_3H) is emerging as an important post-translational modification that can activate or deactivate the function of many proteins. Changes in thiol oxidation state have been implicated in a wide variety of cellular processes and correlate with disease states but are difficult to monitor in a physiological setting because of a lack of experimental tools. Here, we describe a method that enables live cell labeling of sulfenic acid-modified proteins. For this approach, we have synthesized the probe DAz-1, which is chemically selective for sulfenic acids and cell permeable. In addition, DAz-1 contains an azide chemical handle that can be selectively detected with phosphine reagents *via* the Staudinger ligation for identification, enrichment and visualization of modified proteins. Through a combination of biochemical, mass spectrometry and immunoblot approaches we characterize the reactivity of DAz-1 and highlight its utility for detecting protein sulfenic acids directly in mammalian cells. This novel method to isolate and identify sulfenic acid-modified proteins should be of widespread utility for elucidating signaling pathways and regulatory mechanisms that involve oxidation of cysteine residues.

2.2 Introduction

The generation of reactive oxygen species (ROS) is an unavoidable consequence of life in an aerobic environment. ROS are distinguished by their high chemical reactivity and include both free radicals, such as superoxide ($O_2^{\cdot -}$) and hydroxyl radicals ($OH^{\cdot}$), and non-radical species such as hydrogen peroxide (H_2O_2). One of the earliest recognized consequences of ROS in biology is the generation of oxidative stress, a condition characterized by an excess of free radicals, a decrease in antioxidant levels or both. Oxidative stress has been implicated in the initiation and progression of many human diseases including atherosclerosis, cancer, diabetes, neurodegenerative diseases and aging.[1] In addition, immune cells capitalize on the toxic effects of ROS and generate high levels of these oxidants for the sole purpose of microbial killing.[2,3] More recently, it has been established that ROS also play important roles in eukaryotic signal transduction, regulating normal cellular events such as cell proliferation, differentiation, and migration.[4-6] To this end, cellular ROS production is spatially and temporally controlled to modulate the biological activity of signaling proteins.[7]

It is well known that many amino acid residues in proteins are susceptible to oxidation (electron removal) by various forms of ROS, and that oxidatively modified proteins accumulate during aging[8], oxidative stress[9], and in neurodegenerative diseases.[10] Cysteine residues, with a polarizable sulfur atom, are particularly sensitive to oxidation by ROS.[11] However, unlike other amino acid residues, oxidation of this sulfur-containing amino acid can be reversed

through the action of dedicated enzymes such as thioredoxin. Proteins employ cysteine residues extensively as nucleophiles in catalysis, metal-binding and to facilitate large-scale structural rearrangements. The strong nucleophilic character of the cysteine residue derives from thiol deprotonation to the thiolate anion, the pK_a of which may range from ~ 4 - 9 depending on the local protein environment and solvent accessibility. Since many proteins rely on the unique properties of the thiol functional group for their biological activity, oxidation of specific cysteines residues can operate like a switch, activating or deactivating its cellular function in a manner analogous to more widely studied modifications, such as phosphorylation and dephosphorylation.[12,13]

Despite studies implicating cysteine oxidation as a modulator of cellular processes, the molecular details of the majority of these modifications, including the complete repertoire of proteins containing thiol post-translational modifications (PTMs) and the specific sites of modification remain largely unknown. Furthermore, since thiol-modified proteins are studied in purified proteins and cell extracts the response to oxidative challenge *in vitro* and the importance of these modifications in a cellular context remain a hotly debated issue.[6,7,14-16] For these reasons, cell permeable chemical probes that selectively recognize specific cysteine oxidation states or 'oxoforms' will be required to identify modifications and elucidate signaling pathways that are mediated by thiol oxidation *in vivo*.

One such key 'oxoform' is the sulfenic acid moiety (Cys–SOH), which is formed upon reaction of the thiol side chain with mild oxidizing agents.[17] Molecular oxygen can oxidize protein thiols

to sulfenic acids in the presence of a metal catalyst. However, the most biologically significant oxidizing agents are thought to include peroxides such as H_2O_2, organic hydroperoxides, peroxynitrite, nitric oxide and its derivatives. Each of these agents can convert a thiol side chain to a sulfenic acid and elevated levels of these oxidants have been detected in association with activation of many cell surface receptors, which support a role for these oxidants in cell signaling.[13]

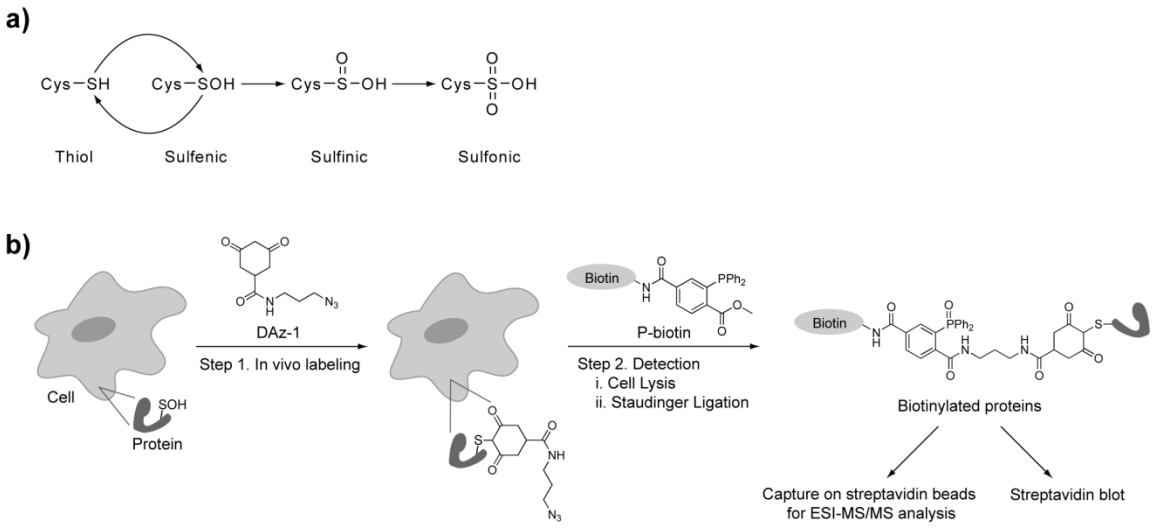

Figure 2.1 Chemoselective probe for labeling proteins with sulfenic acid modifications in living cells. a) Oxidation states of protein cysteines that are implicated in biological function. b) Strategy for detecting sulfenic acid-modified proteins directly in living cells.

Cysteine sulfenic acids are the simplest oxy-acid of organic sulfur and are inherently reactive moieties.[18] Consequently, sulfenic acids are often intermediates *en route* to more stable oxidation states such as sulfinic ($Cys–SO_2H$) and sulfonic acid ($Cys–SO_3H$) (Figure 2.1a). Alternatively, since the sulfur atom is sufficiently electrophilic in the sulfenic oxidation state, this group can react with a neighboring cysteine thiolate to form a disulfide bond. In spite of their high reactivity, sulfenic acids can also be isolated and stabilized within protein

microenvironments by proximity to favorable electrostatic interactions.[19-23] Indeed, the first chemical evidence supporting the existence of stable sulfenic acids in proteins was reported over forty years ago[24] and, more recently, these moieties have been observed by X-ray crystallography and NMR spectroscopy in a wide variety of proteins[21] including tyrosine phosphatases[25], which are intimately involved in signal transduction cascades. Thus, sulfenic acids are unique protein functional groups that are proposed to play pivotal roles in enzyme catalysis, redox homeostasis and regulation of cell signaling events.[13,17,19-21]

Investigating the role of sulfenic acids in proteins requires reagents for their detection. To this end, in 1974, Benitez and Allison presented the first evidence that adduct formation with 5,5-dimethyl-1,3-cyclohexadione (dimedone) (Scheme 2.1) could be used as a diagnostic tool to detect sulfenic acids in proteins.[24] Another reagent widely employed for the detection of protein sulfenic acids is 4-chloro-7-nitrobenzo-2-oxa-1,3-diazole (NBD-Cl).[26] Though NBD-Cl can also react with other amino acid residues including cysteine, the product that forms with sulfenic acid is distinguished from other functional groups by its characteristic spectral property (λ_{max} = 347 nm). More recently, Poole and colleagues reported the synthesis of 1,3-cyclohexadione derivatives linked to isatoic acid and coumarin-based fluorophores.[27] Though the spectral properties of these probes were unchanged upon reaction with the cysteine sulfenic acid, these reagents were demonstrated to modify the sulfenic acid form of a bacterial peroxidase, Cys165Ser AphC, based on ESI-MS detectable adduct formation.

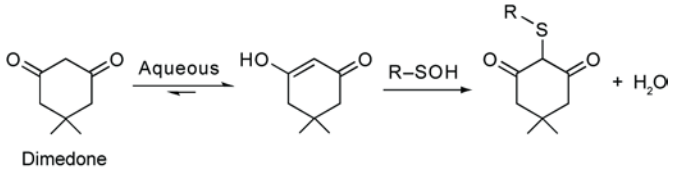

Scheme 2.1 Selective reaction of dimedone with a sulfenic acid affords a new thioether bond.

Though useful in biochemical studies, the reagents described above are not ideally suited for proteomic analysis. In particular, NBD-Cl is not specific for sulfenic acids and all reported compounds lacked an affinity handle for isolating modified proteins. For these reasons, Saurin *et al.* developed a new method to detect sulfenic acid-modified proteins based on the arsenite-specific reduction of protein sulfenic acids under denaturing conditions and subsequent labeling with biotin-maleimide.[28] This method, however, has not been widely employed since the use of denaturants results in loss of protein structure, which is an essential requirement for sulfenic acid stabilization. In addition, the thiol-reactive reagent used to covalently modify cysteine residues prior to arsenite reduction also reacts with sulfenic acids[29], further diminishing the sensitivity of this technique. Dimedone-biotin conjugates were subsequently reported for detection and enrichment of sulfenic acid-modified proteins.[30,31] Despite their reactivity with sulfenic acids, dimedone-biotin conjugates are large and have poor trafficking properties. Hence, their range of applications is limited and does not include intact cells. The ability to investigate protein thiol modifications with cell permeable probes is an especially important consideration since cell lysis alters redox homeostasis.[6,16,32]

Here, we describe a method that enables live cell labeling of sulfenic acid-modified proteins (Figure 2.1b). For this approach, we have designed and synthesized the probe DAz-1, which is chemically selective for sulfenic acids and cell permeable. DAz-1 also contains an azide chemical handle that can be selectively detected with phosphine reagents *via* the Staudinger ligation for identification, enrichment and visualization. Through a combination of biochemical, ESI-mass

spectrometry and immunoblot analyses we demonstrate that DAz-1 selectively detects sulfenic acids in purified proteins, complex protein mixtures and mammalian cells. Furthermore, we observe distinct protein labeling patterns in living cells as compared to lysates, which confirms that when removed from their cellular context, proteins are prone to oxidation.

2.3 Results

2.3.1 DAz-1 irreversibly labels sulfenic acid-containing proteins

Sulfenic acids exhibit both nucleophilic and electrophilic reactivity.[18] Electrophilic groups in proteins are rare and thus, this unique property of sulfenic acids can be exploited for their selective detection. To this end, we designed and synthesized a bi-functional chemical probe *N*-(3-Azidopropyl)-3,5-dioxocyclohexanecarboxamide referred to as DAz-1 (Figure 2.1b and Scheme 2.2). DAz-1 includes the nucleophilic reagent 1,3-cyclohexanedione, a dimedone analog that reacts specifically with sulfenic acids in aqueous media to form a stable thioether adduct (Scheme 2.1).[19,23,27] In addition, DAz-1 is functionalized with an azide group, installed onto the cyclohexyl framework *via* an amide bond linkage. The azide moiety is a unique chemical handle that permits selective coupling with bioorthogonal phosphine or alkyne-derivatized reagents for detection and isolation by affinity purification for subsequent proteomic analysis.[33-38] The advantage of DAz-1 over existing probes for sulfenic acid detection is its small size, which contributes to its favorable uptake in cells and facilitates protein labeling.

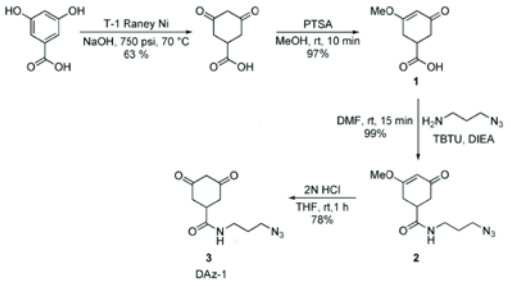

Scheme 2.2 Synthesis of DAz-1, a sulfenic acid-specific chemical probe

Moreover, once introduced into proteins the azide group can be tagged by a wide variety of affinity and fluorescent reagents *ex vivo*.[33]

While the synthesis of 1,3-cyclohexanedione analogs linked to fluorophores or biotin has been reported,[27,30,31] the specificity of these reagents for sulfenic acids has not been rigorously evaluated. In order to test the effects of functionalizing 1,3-cyclohexanedione on its overall reactivity, two model proteins were examined *in vitro*.

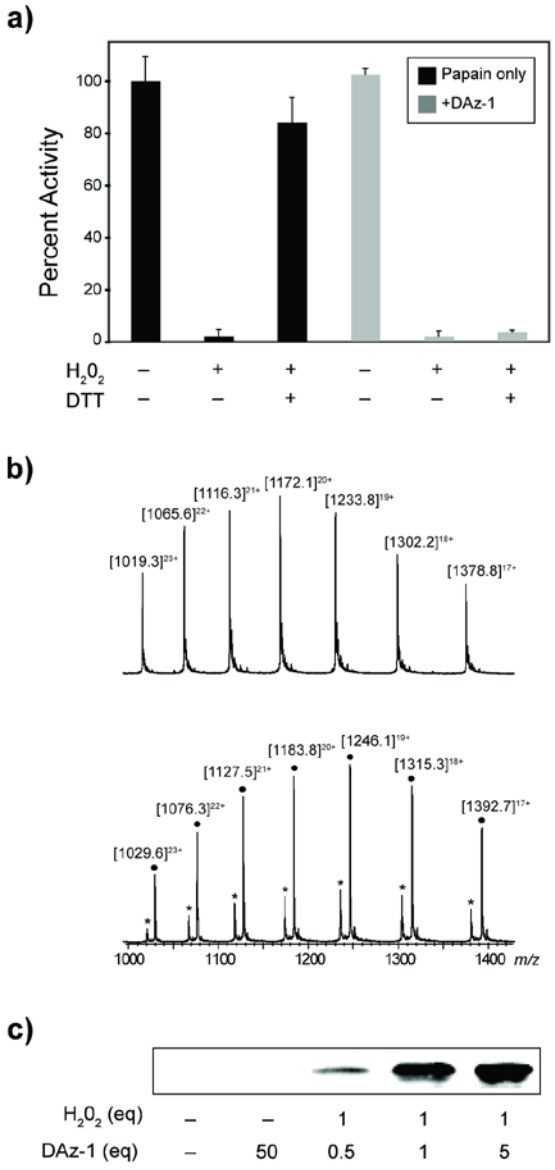

Figure 2.2 DAz-1 modifies sulfenic acid-modified papain in vitro. a) Papain activity as monitored by cleavage of a colorimetric substrate, L-BAPNA. Black bars: Untreated papain was fully active. Papain treated with a single equivalent of H2O2 for 30 min was completely inactivated. Treatment of oxidized papain with DTT restored activity. Grey bars: Active papain was not inhibited by 20 mM DAz-1 alone. When reacted with DAz-1, the activity of oxidized papain was not restored by DTT treatment. Data represent the average of three independent experiments. b) ESI mass spectra of papain showing the charge state distribution. Top: Mass spectra of active papain (23,422.4 Da expected; 23,422.7 Da observed). No adduct is observed between DAz-1 and unoxidized papain. Bottom: Mass spectra of peroxide-treated papain reacted with DAz-1 (•; 23,658.4 Da expected; 23,658.3 Da observed). Papain sulfinic acid (*), which was also present in the oxidized sample, did not react with DAz-1. c) Visualization of DAz-1 papain labeling. Sulfenic acid-modified papain was selectively labeled by DAz-1.

The ability of DAz-1 to site-specifically alkylate protein sulfenic acids was first evaluated using papain from *Carica papaya*. Papain is the prototype cysteine endopeptidase and it has been extensively studied because of its homology with mammalian cysteine proteases involved in several diseases related to tissue degeneration.[39] Chemical modification of the active site Cys25 of papain (*e.g.,* alkylation, oxidation) induces the loss of its enzymatic activity.[22,40] Therefore, we could assess modification at Cys25 by monitoring cleavage of the chromogenic substrate N_{α}-benzoyl-L-arginine 4-nitroanilide hydrochloride (BAPNA) (Figure 2.2a). Papain exhibited robust catalytic activity with BAPNA as a substrate (47 U mg^{-1}). However, when treated with a stoichiometric concentration of hydrogen peroxide (H_2O_2) protease activity was abolished. Treatment of the oxidized papain sample with the reducing agent dithiothreitol (DTT) led to reactivation of enzymatic activity, demonstrating that the Cys25 sulfenic acid was reduced back to the thiol form. Control experiments with the thiol-reactive reagent *N*-ethyl maleimide show that alkylated papain could not be reactivated by DTT, as expected (Figure 2.3). Having established that papain activity could be reversibly modulated by H_2O_2 and DTT, we investigated the effect of DAz-1 in this assay. In the absence of oxidant, inclusion of 20 mM DAz-1 in the reaction mixture had no affect on protease activity. However, when DAz-1 was incubated with oxidized papain no DTT-recoverable activity was detected. These data suggest that treatment of the sulfenic acid form of papain with DAz-1 leads to covalent modification of Cys25. Analogous results were obtained when dimedone was employed in place of DAz-1 (Figure 2.3).

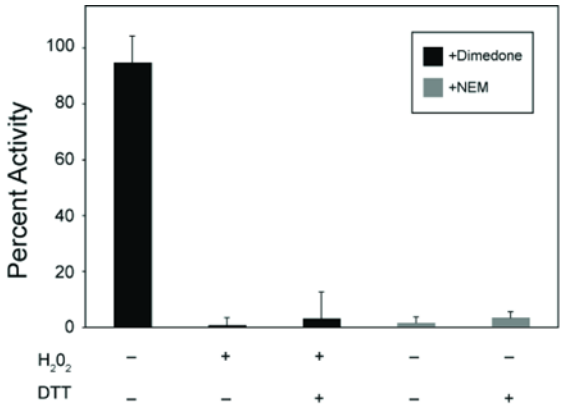

Figure 2.3 Covalent papain adducts are not reduced by DTT. Black bars: Active papain was not inhibited by 10 mM dimedone alone. Papain was inactivated by the addition of stoichiometric H2O2. When oxidized papain was reacted with dimedone, protease activity was not recovered by DTT treatment. Light grey bars: Active papain was inhibited by treatment with the thiol-reactive probe, NEM. The activity of NEM-modified papain was not restored by DTT.

Samples of modified papain and the starting material were further analyzed by ESI-MS. The molecular mass of reduced papain was consistent with the calculated value (Figure 2.2b top spectrum, 23422.7 ± 2 Da found, 23422.4 Da calc). When papain was oxidized with H_2O_2 and immediately infused into the ESI-MS instrument we observed a mass increase consistent with Cys25 sulfenic acid in the intact papain enzyme (23437.0 ± 2 Da found, 23438.4 Da calc). Though sulfenic acids are considered to be labile moieties, ESI-MS evidence for a protein sulfenic acid has also been observed with the redox-regulated Ohr repressor.[41] The molecular mass of the adduct that resulted from reaction of DAz-1 with papain sulfenic acid (Figure 2.2b bottom spectrum, •) was equal to the calculated mass of a conjugate with 1:1 stoichiometry (23658.3 ± 2 Da found, 23658.4 Da calc). The small fraction of papain sulfinic acid that formed during H_2O_2 treatment (Figure 2.2b bottom spectrum, *) did not react with DAz-1, as expected.

The selectivity of DAz-1 labeling was also probed by Western blot (Figure 2.2c). Reduced or oxidized papain was incubated with DAz-1 and then subjected to bioorthogonal labeling with phosphine-biotin (p-biotin) *via* the Staudinger ligation[42] (Figure 2.1b). The reactions were then separated by gel electrophoresis and analyzed by streptavidin blotting. Treatment of oxidized papain with DAz-1 afforded selective protein labeling that was dependent on the stoichiometry of oxidant to protein and the concentration of DAz-1. In the absence of oxidant, papain was not detected by streptavidin blotting, demonstrating the specificity of our bioorthogonal labeling conditions. The labeling of protein sulfenic acids with DAz-1 followed by reaction with p-biotin affords a sensitive method to detect sulfenic acid-modified proteins, as labeled proteins can be easily visualized by streptavidin blotting. Furthermore, using alkyne or phosphine-based fluorescent reagents, we anticipate that this approach can be extended to a solution or gel-based assay to determine the concentration of sulfenic acids in purified proteins *in vitro*.[43-45]

To evaluate the specificity of the DAz-1 probe in the context of a different protein, we used human serum albumin. HSA is the most abundant protein in plasma and is proposed to have an antioxidant role in biological systems.[46] Out of 585 amino acids, HSA contains 17 disulfide bridges and one free cysteine, Cys34. The ability of HSA to function as a 'sacrificial' antioxidant is attributed to the thiol in Cys34, which accounts for ~80% of total free thiol content in plasma. Like papain, the free thiol residue of HSA reacts preferentially with reactive oxygen species[47,48] and detailed mass spectrometry and biochemical studies by Carballal and colleagues demonstrate that Cys34 in HSA oxidizes to form a stable sulfenic acid.[49]

In our own experiments, we assessed the thiol and sulfenic acid content of native HSA under aerobic conditions using NBD-Cl (Figure 2.4a).[26] HSA reaction with NBD-Cl yielded an absorbance spectrum with a major peak at 347 nm, indicating the formation of HSA-SO-NBD adducts. An additional peak at 400 nm was also identified in the spectrum, consistent with the formation of HSA-S-NBD adducts. To probe the reactivity of DAz-1 with HSA, we pre-incubated albumin protein with DAz-1 prior to the addition of NBD-Cl (Figure 2.4a). Based on the reactivity observed with papain sulfenic acid, we predicted that DAz-1 would covalently modify sulfenic acid-containing HSA and would therefore, preclude the formation of HSA-SO-NBD adducts. As predicted, when DAz-1 modified HSA was reacted with NDB-Cl the sulfenic acid peak at 347 nm disappeared, leaving a distinct thiol peak at 400 nm. DAz-1 labeling of oxidized HSA was also analyzed by Western blot (Figure 2.4b). HSA, incubated with DAz-1 and ligated to p-biotin, gave a robust chemiluminescent signal, which could be blocked by incubating HSA with dimedone prior to azido-probe addition. In the absence of DAz-1, a faint signal was observed with HSA. This background could result from p-biotin, HRP-streptavidin or the combination of these detection reagents. Control experiments indicated that the HRP-streptavidin secondary detection reagent was the source of the low background signal (data not shown).

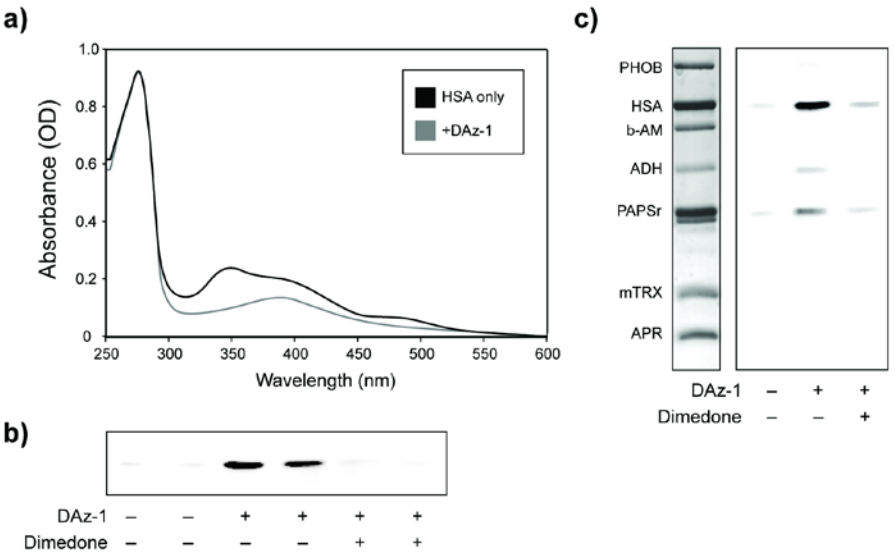

Figure 2.4 DAz-1 labels sulfenic acid-modified HSA in vitro. a) UV-vis spectra of the NBD adducts of native and DAz-1 treated HSA. Protein (50 µM) in phosphate buffer (pH 7.4, EDTA 1 mM), either native (black line) or treated with 1 mM DAz-1 for 1 h (grey line). Samples were separated from small molecules by ultrafiltration and incubated with NBD-Cl for 1 h followed by ultrafiltration to remove unreacted NBD-Cl. b) Visualization of HSA-sulfenic acid labeled with DAz-1 in vitro. After DAz-1 treatment the samples were labeled with p-biotin and then analyzed by Western blot using streptavidin-HRP. To block DAz-1 labeling, samples were incubated with dimedone prior to DAz-1 treatment. Reactions were carried out in duplicate and each lane contains 200 ng total HSA. c) HSA-sulfenic acid detected in a complex protein mixture in vitro. Reactions included aprotinin (APR, 6 KDa), thioredoxin Cys35Ala (mTRX, 14 KDa), PAPS reductase (PAPSr, 28.5 KDa), alcohol dehydrogenase (ADH, 37.5 KDa), ß-amylase (ß-AM, 50 KDa), HSA (HSA, 66 KDa) and phosphorylase B (PHOB, 90 KDa) were each present at 1mg mL^{-1}. Left panel: Coomassie-stained gel of protein mixture. Right panel: After DAz-1 treatment, the samples were labeled with p-biotin and then analyzed by Western blot using streptavidin-HRP. To block DAz-1 labeling, samples were incubated with dimedone prior to DAz-1 treatment. Each lane contains 200 ng of each protein present in the mixture.

We next performed an experiment to determine whether sulfenic acid-modified HSA could be detected under controlled conditions within a mixture of other purified proteins. To this end, we added sulfenic acid-containing HSA to a large excess of standard proteins that included aprotinin, thioredoxin Cys35Ala, alcohol dehydrogenase, PAPS reductase, B-amylase, and

phosphorylase B. The protein mixture was probed with DAz-1 and cysteine sulfenic acids were detected by Western blot, as described above. Figure 2.4c shows DAz-1 dependent detection of sulfenic acid-modified HSA within the protein mixture. Moreover, this signal could be effectively blocked by incubating the reaction with dimedone, prior to the addition of DAz-1. In this experiment, DAz-1 labeling also reveals a low amount of sulfenic acid-modified cysteine in two other proteins, PAPS reductase and alcohol dehydrogenase. Consistent with the observed labeling, PAPS reductase possesses a catalytic cysteine residue that can undergo reversible S-glutathionylation (*e.g.,* Cys-S-GSH) *via* a sulfenic acid intermediate.[50] Alcohol dehydrogenase coordinates two zinc ions through multiple cysteine residues, which are readily oxidized to higher oxidation states, resulting in the loss of metal ion with concomitant enzyme inactivation.[51]

2.3.2 DAz-1 detects sulfenic acid-modified Proteins in Cell Lysate

Having established the specificity of DAz-1 labeling for sulfenic acids in homogenous protein solutions, we next investigated whether the azido-probe could be exploited for detection of sulfenic acid-modified proteins in a complex, unfractionated cell lysate. To this end, we carried out our optimized chemistry (Figures 2.2 and 2.4) in whole Jurkat cell extract that was doped with a known concentration (50 nM - 5 μM) of DAz-1-tagged HSA (Figure 2.5a) or sulfenic acid-modified HSA (Figure 2.5b). Figure 2.5a shows an HRP-streptavidin Western blot, which indicates that ~100 nM azide-tagged protein (arrowhead) can be detected under the conditions employed (*e.g.,* concentration of p-biotin, incubation times, μg protein loaded on the gel). **Figure 2.5b** shows the HRP-streptavidin Western blot analysis of sulfenic acid-modified HSA added to Jurkat cell lysate and then probed with DAz-1. In this case, signal from DAz-1 labeled HSA was also observed at 100 nM and greater concentrations. Thus, even with a highly complex

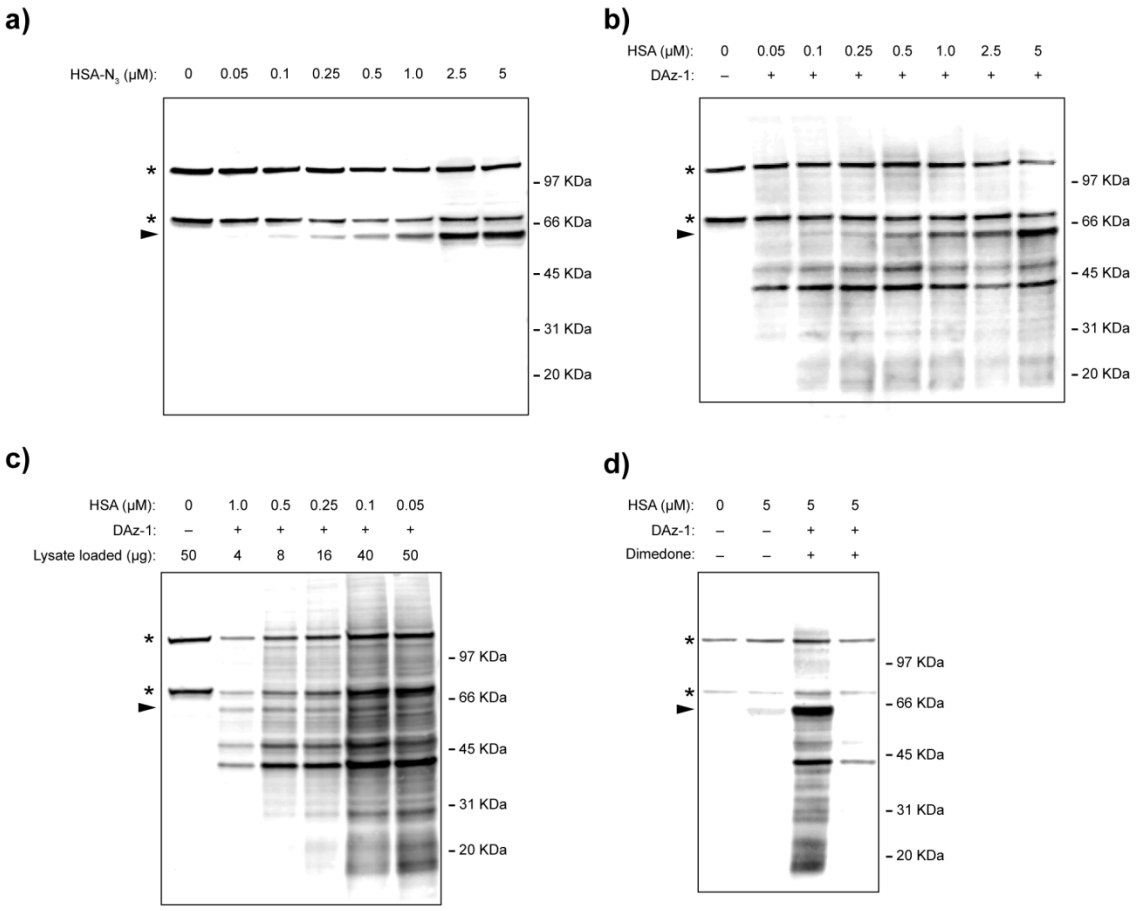

Figure 2.5. DAz-1 labels sulfenic acid-modified HSA and additional proteins in cell lysate. a) DAz-1 modified HSA (HSA-N_3) is detected in cell lysate. HSA-N_3 (0-5 μM) in the presence of 1 mg mL^{-1} of Jurkat cell lysate was labeled with p-biotin (100 μM) and DTT (5 mM) for 2 h at 37 °C. Reactions were terminated by acetone precipitation, and proteins were analyzed by Western blot using streptavidin-HRP. Each lane contains 25 μg total protein. Highlighted bands in Figure 4a-d represent HSA modified by DAz-1 (arrowhead) and endogenously biotinylated proteins (*). b) Sulfenic acid-modified HSA is labeled by DAz-1 in Jurkat cell lysate. HSA (0-5 μM) in the presence of Jurkat cell lysate (1 mg mL^{-1}) was incubated with DAz-1 (1 mM) for 1 h at 37 °C and analyzed as described above. Each lane contains 25 μg total protein. c) DAz-1 modifies sulfenic acid-containing HSA and additional oxidized proteins in cell lysate. HSA (0-1 μM) in the presence of Jurkat cell lysate (1 mg mL^{-1}) was labeled with DAz-1 (1 mM) and analyzed as described above. Each lane contains 250 ng total HSA. d) Dimedone blocks DAz-1 modification of HSA and additional sulfenic acid-modified proteins in lysate. HSA (5 μM) was incubated in the presence of Jurkat cell lysate (1 mg mL^{-1}) in the presence or absence of dimedone (10 mM) for 1 h at rt. In a subsequent step, DAz-1 (1 mM) was incubated with each reaction for 1 h at 37 °C and analyzed as described above. Each lane contains 50 μg total protein.

starting material the sulfenic acid moiety present on HSA can be detected with DAz-1, affirming its selectivity. Furthermore, the combination of enrichment *via* an affinity tag and the increasing sensitivity of mass spectrometers[52-55] should yield a substantial increase in the limit of detection for protein sulfenic acids.

Though the complete repertoire of proteins that form sulfenic acids *in vivo* are not yet known, proteins that have been identified typically possess a cysteine residue with a low ionization constant, whose thiolate is stabilized by electrostatic interactions within a protein cavity or enzyme active site. Since DAz-1 has a small molecular footprint, access to sulfenic acids should be possible and we anticipated that other proteins in the Jurkat cell lysate should be labeled by DAz-1 in addition to HSA. This expectation was born out and a number of discrete protein bands were observed in the Western blot analysis of DAz-1 labeled Jurkat lysate (Figure 2.5b). To further highlight the spectrum of proteins that were labeled by DAz-1 in these experiments, we repeated DAz-1 labeling of HSA-spiked cell lysate such that in the subsequent Western blot analyses, protein loading was normalized to afford a constant amount of HSA per lane. Consequently, as the concentration of HSA in the reaction decreased, the amount of cell lysate loaded in each lane was increased (Figure 2.5c). As expected, the signal obtained from DAz-1 labeled HSA remained constant, while the signal from other DAz-1 modified proteins became more pronounced. Of particular note, a very prominent band is observed that migrates at ~41 kDa. Using antibodies, the identity of the ~41 kDa band was identified as the cytoskeletal protein, β-actin (Figure 2.6). Actin is the most abundant protein in most eukaryotic cells[56] and possesses a reactive cysteine residue that forms disulfide bonds under conditions of oxidative stress.[57] Moreover, a recent study investigating actin modifications demonstrates that this

protein is glutathionylated in cells in response to oxidative stress.[58] In these experiments, glutathionylation of actin is blocked by the addition of dimedone to cells prior to oxidative challenge, suggesting that protein modification occurs *via* a sulfenic acid intermediate. Consistent with these observations, we have directly identified actin as a sulfenic acid-modified protein in Jurkat cell lysate with our azido-probe, DAz-1. Since dimedone and DAz-1 both react similarly with protein sulfenic acids we anticipated that incubating Jurkat cell lysate with dimedone, prior to the addition of DAz-1, would preclude azido-probe binding and thus, decrease the signal in our HRP-streptavidin Western blot. As predicted, minimal labeling was observed when cell lysate was first challenged with dimedone and then treated with DAz-1 (Figure 2.5d). Collectively, the studies above demonstrate the selectivity of DAz-1 for sulfenic acids in purified proteins, protein mixtures and cell extracts.

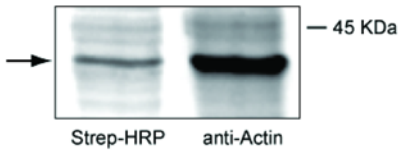

Figure 2.6 β-actin is labeled in vivo by DAz-1. β-actin antibody probe shows a DAz-1 labeled biotinlyated band at ~41 kDa in the Strep-HRP blot to be actin (arrow). A streptavidin-HRP blot (left lane) from live cell labeling of Jurkats with DAz-1 (10 mM) was reprobed with anti-β-actin antibody (right lane). In brief, the blot was incubated in 15% H_2O_2 for 1 h at rt to deactivate the Strep-HRP reagent, blocked in 5% non fat dry milk, then reprobed with anti-β actin for 1 h at rt (1:10,000). After secondary antibody incubation for 1 h (rabbit anti-mouse HRP, 1:40:000), the blot was washed and developed with chemiluminescence reagents.

2.3.3 Incorporation of DAz-1 into proteins in cultured human cells

Post-translational modification of cysteine residues is vital for cell signaling and also has significant potential as a biomarker for specific disease states.[13,59,60] While chemical methods to identify sulfenic acid-modified proteins have been reported, their range of applications is limited and does not include intact cells.[28,61,62] To address this issue, we have developed a new method to detect sulfenic acid-modified proteins directly in living cells (Figure

2.1b). In this approach, treatment of cells with the membrane permeable probe DAz-1 enables covalent modification of sulfenic acid-containing proteins. Reaction of the azide chemical handle on DAz-1 with a bioorthogonal phosphine-based detection reagent, such as p-biotin, allows visualization of sulfenic acid-modified proteins by streptavidin Western blot and also enables proteomic analysis of DAz-1 labeled proteins by mass spectrometry after affinity enrichment with streptavidin beads. Two-step labeling methods analogous to this approach have been successfully employed to profile protein glycosylation[38], farnesylation[63] and protease activity.[34]

Once the specificity of DAz-1 was validated *in vitro* we proceeded to test the azido-probe, and our overall strategy, in cultured human cells. In these experiments we employed the human T lymphoma cell line Jurkat, which are well characterized and resemble naive primary T-cells in their response to stimulation.[64] To detect the basal level of sulfenic acid-modified proteins Jurkat cells were incubated with increasing concentrations of DAz-1. After labeling, the media was exchanged to remove excess probe and cell viability was assessed. In subsequent steps, cells were lysed and DAz-1 labeled proteins were detected after ligation with p-biotin. Figure 2.7a depicts a representative Western blot from these experiments, which shows that the intensity of DAz-1 labeling increases in a dose-dependent manner. At the highest concentration of DAz-1 employed, ~30 discrete protein bands could be identified in the HRP-streptavidin Western blot. Figure 2.7b shows that cells retained similar viability as those treated with vehicle DMSO at the highest concentration of DAz-1 employed for these experiments. In addition, cells exhibited normal morphology throughout treatment (K.G.R., unpublished observations). DAz-1 labeling was also time-dependent, as signal was observable at 15 min and increased in intensity

over the duration of the experiment (Figure 2.7c). Time and dose-dependent protein labeling by DAz-1 demonstrates that probe incorporation in polypeptides analyzed by this approach are not the result of post-lysis activity.

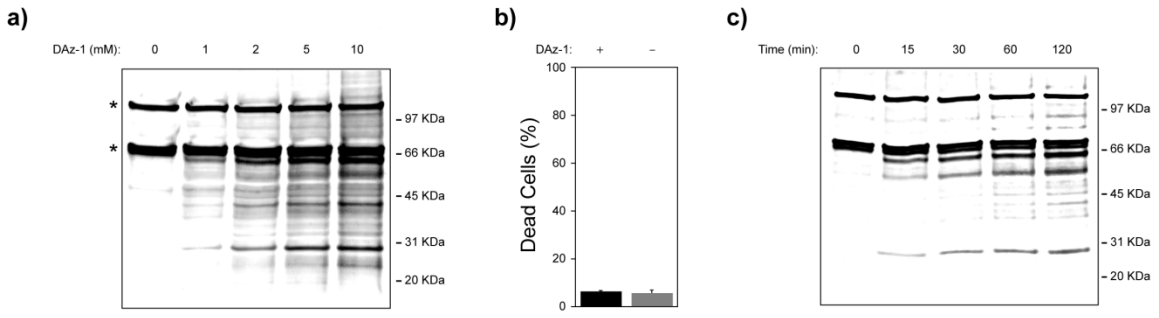

Figure 2.7 DAz-1 labels sulfenic acid-modified proteins in living cells. a) Dose-dependence of DAz-1 labeling. DAz-1 was incubated with Jurkat cells at the indicated concentrations for 2 h at 37 °C. In subsequent steps, cells were washed to remove excess DAz-1 and a cell lysate fraction was prepared. The lysate was labeled with p-biotin (100 µM) for 2 h at 37 °C. Reactions were terminated by acetone precipitation, and proteins were analyzed by Western blot using streptavidin-HRP. Each lane contains 50 ug total protein. Highlighted bands in Figure 5a represent endogenously biotinylated proteins (*). b) Effect of DAz-1 on viability of Jurkat cells. Cells were exposed to DMSO (grey bar) or DAz-1 (10 mM, black bar) for 1 h at 37 °C. After incubation, cell viability was quantified by trypan blue exclusion. Data represent the average of three independent cell viability counts. c) Time-dependence of DAz-1 labeling. Jurkat cells were incubated with DMSO only (0 min) or DAz-1 (2 mM) for 15 min, 30 min, 1 or 2 h at 37 °C. Reactions were then analyzed as described above. Each lane contains 25 µg total protein.

Prior to this method, protein sulfenic acids have not been directly detected in unmanipulated, intact cells. Hence, at the outset of these experiments the number of proteins that would contain this cysteine 'oxform' was an open question. Notably, in our Western blot analysis the number of DAz-1 labeled proteins observed in living cells is considerably fewer than those found in cell lysates (*e.g.,* Figure 2.5c, lane 6 vs. Figure 2.7a, lane 2). It is possible that the difference in cell labeling relative to lysate results from differences in DAz-1 concentration. However, significant differences in labeling persisted when 10-fold more DAz-1 was employed in cell-

labeling experiments as compared to lysate analysis (Figure 2.7a, lane 5). Furthermore, the pattern and intensity of DAz-1 labeling between live cells and lysates is distinct. For example, when lysate is probed with DAz-1, actin is the most intensely labeled protein. By contrast, actin does not appear as the most prominent protein in DAz-1 labeled cells. Instead proteins between 25-30 KDa and 55-65 KDa emerge in intensity. One possible explanation for these observations is that disrupting the cell membrane and other cellular compartments during extract preparation artificially increases the level of oxidized actin. Since actin is the most abundant protein in eukaryotic cells, a high percentage of oxidized actin in cell extract may diminish the ability to detect other protein sulfenic acids that are less abundant. These data highlight differences between lysates and live cells in protein sulfenic acid labeling.

Experiments performed on purified proteins *in vitro* demonstrate that numerous proteins containing reactive thiolates, including peroxiredoxins[65], GAPDH (glyceraldehyde-3-phosphate dehydrogenase)[66] and PTP1B (protein-tyrosine phosphatase 1B)[67] are converted to sulfenic acids and higher oxidation states when treated with oxidants such as hydrogen peroxide. In addition, many proteins have been identified as forming disulfide bonds in response to hydrogen peroxide treatment in Jurkat cell lysates.[68] To determine whether our own approach could detect increases in protein thiol oxidation in human cell culture, we treated Jurkat cells with 20 or 200 μM H_2O_2, t-butyl hydroperoxide (*t*-BOOH) or a mitochondrial membrane potential depolarizing agent, trifluormethoxy carbonylcyanide phenylhydrazone (FCCP), and monitored for an increase of protein sulfenic acids in these cells, as judged by DAz-1 labeling (Figure 2.8). To maximize our chances of detecting an increase in protein oxidation we employed a concentration of DAz-1 and incubation time that produced little detectable labeling

in the absence of oxidant stimulation. Figure 2.8 shows the HRP-streptavidin Western blot analysis of Jurkat cells that were probed with DAz-1 with or without exogenously added oxidant. As expected, in the absence of oxidant, only minor signal from DAz-1 labeled proteins is observed (Figure 2.8). By contrast, robust protein labeling is observed when 200 µM H_2O_2 or *t*-BOOH was applied to the cells; maximal DAz-1 labeling with FCCP is observed at 20 µM. Control experiments demonstrated that the observed increase in protein labeling was not due to compromised cell membrane integrity in the presence of oxidant (Figure 2.9). Collectively, these experiments establish that the chemoselective probe DAz-1 can detect protein sulfenic acids directly in mammalian cells and is selectively installed on sites of protein oxidation.

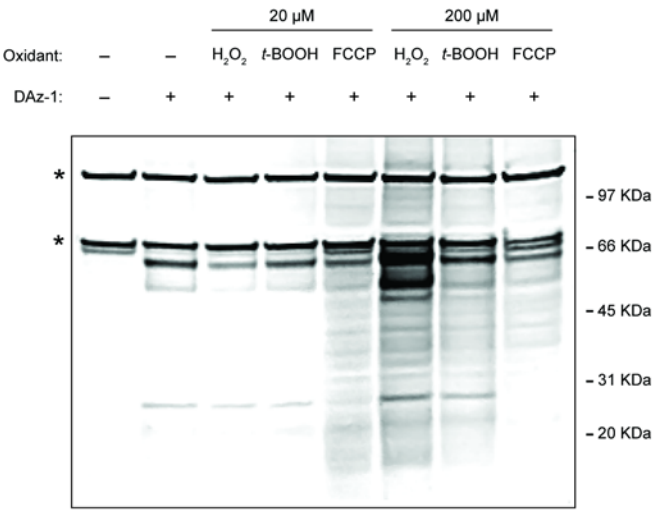

Figure 2.8 DAz-1 detects an increase in thiol oxidation in living cells. Oxidants (H2O2, t-BOOH, or FCCP) were added to the cell suspensions at final concentration of 20 or 200 µM and incubated at 37 ⊠C for 15 min. Daz-1 (2 mM) or DMSO was added and the cells incubated for 1 h at 37 ⊠C. In subsequent steps, samples were prepared and analyzed by HRP-streptavidin Western blot as previously described. Each lane contains 25 ug total protein. Highlighted bands in Figure 6 represent endogenously biotinylated proteins (*).

Of the three oxidants that were tested in our panel, FCCP was the most potent. Following treatment with 20 µM FCCP, an increase in protein labeling with DAz-1 relative to untreated cells was consistently observed. When 200 µM FCCP was employed in these experiments, protein labeling by DAz-1 diminished relative to cells treated with 10-fold less reagent. The loss

of signal observed at high FCCP concentrations may result from oxidation of protein sulfenic to sulfinic and sulfonic acids, which are not targets for DAz-1. This hypothesis was confirmed using an antibody that detects the sulfinic and sulfonic acid forms of peroxiredoxin[69], regarded as a hallmark of protein 'hyperoxidation' (Figure 2.10). In these experiments, we also observed a robust increase in DAz-1 detectable protein sulfenic acids in cells treated with H_2O_2 and *t*-BOOH, though higher concentrations were necessary to observe this effect relative to FCCP. In contrast to the FCCP protonophore, which concentrates in the mitochondria, H_2O_2 or *t*-BOOH are freely diffusible through cell membranes. As a consequence, a rapid equilibrium is established in which the intracellular concentration of these oxidants is ~10-fold less than their applied extracellular concentration.[70,71] Hence, the intracellular concentration of H_2O_2 or *t*-BOOH in these experiments is estimated to be 2 - 20 µM.

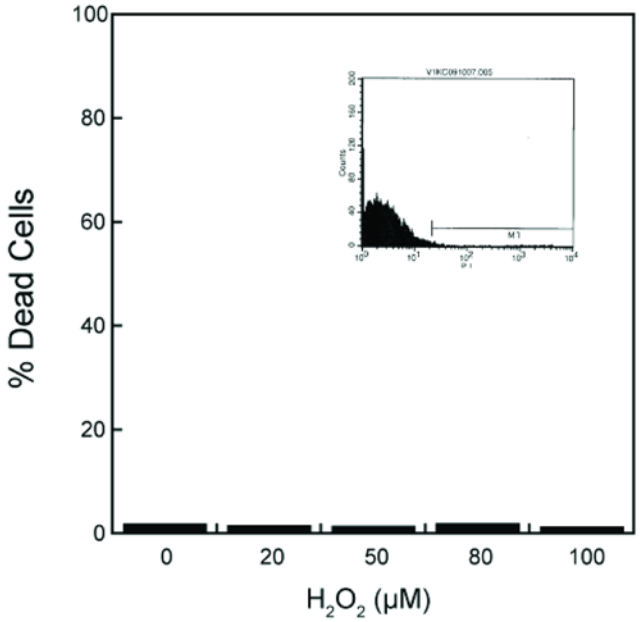

Figure 2.9 Jurkat cells remain viable after H_2O_2 challenge. Jurkat cell viability after 10 min H_2O_2 challenge as assessed by propidium iodide (PI) and flow cytometry. Cells were incubated in 2% FBS RPMI with H_2O_2 for 10 min at rt, washed with PBS, incubated in 250 µL PI (3 µM) for 15 min at rt then analyzed for uptake of the fluorescent PI compound. Cells showed no difference in viability compared to the control (no uptake of PI, and hence fluorescent signal is equivalent to control). Inset shows typical histogram obtained for Jurkat cells on viability analysis.

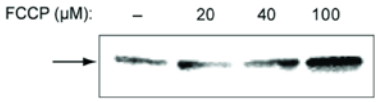

Figure 2.10 Peroxiredoxin thiols are oxidized to sulfinic and sulfonic acids after FCCP challenge. Western blot obtained from FCCP challenge of live Jurkat cells was probed with anti-peroxiredoxin-SO_3 antibody (1:2000) for 1 h at rt, incubated with secondary (1:200,000) for 1 h, then developed with chemiluminescence reagents. Blot shows increased oxidation of peroxiredoxin thiols with increased concentration of FCCP oxidant.

2.4.1 Discussion

New tools are needed to further our understanding of post-translational protein thiol modifications. To this end, we have designed and synthesized the azido-probe DAz-1, which is chemically selective for sulfenic acids and cell permeable. Using model sulfenic acid-containing proteins, in their purified form or doped in cell extract, we showed that DAz-1 is selective for sulfenic acids *in vitro*. Once the reactivity of the probe was characterized, we demonstrated that sulfenic acid-modified proteins could be detected in living cells. Furthermore, DAz-1 could detect the global increase in protein thiol modification under oxidizing cellular conditions. During these studies we also observed distinct protein labeling patterns in living cells as compared to lysates. These findings confirm that when removed from their cellular context proteins are prone to oxidation and highlight the importance of probing intact cells to investigate redox regulation of protein function. A major strength of this approach is that protein labeling *in vivo* is decoupled from subsequent analytical steps. This feature allows the sulfenic acid-specific probe to be small, which facilitates protein labeling and diffusion across cell membranes. In addition, the ability to 'tag' proteins with biotin or a range of other affinity and fluorescent reagents *via* the azide chemical reporter on DAz-1 provides an opportunity for enrichment and proteomic analysis of oxidized proteins.[33,34] These studies are currently

underway and will be reported in due course. This new method to detect sulfenic acid-modified proteins provides a powerful means to detect changes in cysteine oxidation *in vivo* and should find a wide variety of applications for the study of biological processes that are central to human health and disease.

2.5 Experimental procedures

2.5.1 Preparation, enzymatic assay and chemical modification of papain

Papain from papaya latex (EC 3.4.22.2) was obtained as a powder (Sigma, P4762) and further purified by affinity chromatography following the method of Funk *et al.*[72], with Gly-Gly-Tyr-Arg (Sigma, G5386) as the immobilized inhibitor on Sepharose 4 Fast Flow resin (GE Healthcare). The concentration of the resulting papain solution was determined by absorbance at 280 nm (E^{mM} = 57.6). A kinetic, spectrophotometric amidase assay with N_{α}-Benzoyl-L-arginine 4-nitroanilide hydrochloride (L-BAPNA, B3279, Sigma) as substrate was used to measure papain activity.[73,74] Assays contained papain (2 - 5 µM), 50 mM Tris pH 7.1, 1 mM EDTA and were initiated by the addition of L-BAPNA (2 mM). The absorbance increase at 410 nm was recorded on a Uvikon XS spectrophotometer (Research Instruments International). Freshly prepared papain had an enzymatic activity of 47 U mg^{-1} at 25 $^{\circ}$C. To inactivate the enzyme, papain was incubated with 1 eq of H_2O_2 (Sigma, 516813) for 15 min at rt. In some experiments, active or peroxide-inactivated papain (40 µM) was incubated with DAz-1, dimedone or N-ethylmaleimide (NEM) in PBS for 30 min at rt. DAz-1 and dimedone stocks were made up in DMSO with 0.1M Bis-Tris HCl pH 7.5. To quantify recoverable enzyme activity after these treatments, papain was incubated with 1 mM dithiothreitol (DTT) for 5 min at rt and assayed as described above. The

ESI-MS spectra of native and modified papain were acquired using a Nanoacuity Q TOF LC-MS/MS system (Waters) in positive-ion mode. Samples for mass spectrometric analysis (20 μM protein) were separated by C18 reverse phase HPLC with a gradient of 3% to 75% B in 45 min (buffer A: 0.1% formic acid in water; buffer B: 0.1 % formic acid in acetonitrile) at a flow rate of 0.5 μL/min.

2.5.2 NBD-Cl assay and chemical modification of HSA

Human serum albumin (HSA, A-9511, Sigma) was obtained as a powder and resuspended to 50 μM in PBS supplemented with 1 mM EDTA. Stocks of 7-chloro-4-nitro-benzo-2-oxadiazole (NBD-Cl, 163260, Aldrich) solutions were prepared in DMSO. To quantify the thiols and sulfenic acid content of HSA, a two-fold excess (100 μM) of NBD-Cl[26] was incubated with HSA for 1 h at rt. Unbound NBD-Cl was removed from the labeled protein using a Microcon YM-50 centrifugal filter unit (Millipore). In some experiments, HSA was pretreated with DTT (1 eq) or DAz-1 (1 mM). Excess small molecules were then removed by ultrafiltration prior to NBD-Cl treatment. To obtain azide-tagged HSA (HSA-N_3) for use in lysate titration experiments, protein (50 μM) was reacted with DAz-1 (2 mM) for 12 h at rt. Excess DAz-1 was removed from the labeled protein using an Amicon Ultra-4 10KDa MWCO centrifugal filter unit (Millipore) followed by gel filtration using a PD-10 Sephadex column (GE Healthcare). To detect sulfenic acid-modified HSA, protein (10uM) was reacted with DAz-1 (1 mM) for 1 h at 37 $^{\circ}$C. To detect sulfenic acid-modified HSA in a more complex protein mixture, aprotinin (Sigma, A-3886), *Escherichia coli* thioredoxin Cys35Ala, alcohol dehydrogenase (Sigma, A-8656), *E. coli* PAPS reductase, B-amylase (Sigma, A-8781), and phosphorylase B (Sigma, P-6635) were each included in the reaction mixture at 1mg mL^{-1}. *E. coli* thioredoxin and PAPS reductase were prepared as previously described.[75] In

dimedone blocking experiments, reactions were incubated with dimedone (10 mM) for 1 h at rt, prior to treatment with DAz-1.

2.5.3 P-biotin labeling of papain and HSA

Phosphine-biotin (p-biotin) was synthesized as previously described.[38] Staudinger ligation labeling of azide-modified proteins[42] was performed by incubation of papain or HSA with phosphine-biotin (100 μM) for 2 h at 37 °C. The reactions were terminated by the addition of cold acetone, and the products were incubated at -30 °C for 20 min and centrifuged at 4 °C for 10 min at 20,000*g* to precipitate proteins. The supernatant was decanted, and the protein pellet was resuspended in PBS or TS buffer (50mM Tris, 0.2% SDS, pH 7.4).

2.5.4 Immunoblotting

P-biotin labeled proteins were separated by SDS-PAGE using Criterion XT 4-12 % Bis-Tris gels (BioRad) in XT MES running buffer, transferred to a PVDF membrane (BioRad), and the membrane was blocked with 5% nonfat dried milk in TBST overnight at 4 °C or 1 h at rt. The membrane was washed in TBST (2 × 10 min) and then incubated with 1:5,000-1:100,000 streptavidin-HRP (GE Healthcare) in TBST for 1h at rt, washed (1 × 5 min then 1×10 min) with TBST and developed with chemiluminescence (Amersham ECL Plus Western Blotting Detection Reagents). To assess the quality of protein transfer and loading in each lane, membranes were stained with Ponceau S staining prior to the blocking step.

2.5.5 Cell culture

Jurkat cells were cultured in RPMI media supplemented with 10% fetal bovine serum (FBS) and 1% penicillin-streptomycin-L-glutamate (PSG). Cells were incubated in a 5% CO_2 humidified incubator at 37 °C and were typically seeded at 0.5×10^6/mL and grown to a density of 2×10^6/mL.

2.5.6 DAz-1 labeling of Jurkat lysate

Jurkat cells (6×10^6) were collected by centrifugation (1000*g* for 5 min) and washed three times with sterile PBS. The media free cell pellet was then suspended in 100 μL of cold lysis buffer (1.0% NP-40, 50 mM Tris-HCl, 150 mM NaCl, and 2X Complete Mini Protease Inhibitor Cocktail, pH 8.0) and incubated on ice for 30 min with frequent mixing. The supernatant was collected by centrifugation at 20,000g and 4 °C for 20 min. The lysate was the transferred to a second tube and subjected to the same centrifugation protocol. Protein concentration of the lysate was determined by Bradford assay (BioRad). Cell lysate, 50 μg or 100 μg in 50 or 100 μL total reaction volume was labeled by incubation with DAz-1 (1 mM) for 1 h at 37 °C followed by incubation with p-biotin (100 μM) and DTT (5 mM) for 2 h at 37 °C. Ligation reactions were terminated by the addition of 1 mL cold acetone and light vortexing. The suspension was incubated at -80 °C for 1 h then centrifuged at 4 °C for 20 min at 20,000g to pellet precipitated proteins. Pellets were then dissolved in TS buffer (50 μL) and precipitated a second time, as described above. The resulting pellet was suspended in SDS-protein loading buffer containing 10% 2-βME. For DAz-1 labeling of sulfenic acid HSA in Jurkat lysate, HSA (0-5.0 μM final concentration) was added to lysate (50 μg) and the protein mixture labeled with DAz-1 (1 mM) for 1 h at 37 °C. In dimedone blocking experiments, HSA (5 μM) was added to Jurkat lysate (50

μg) and the mixture incubated with dimedone (10 mM) for 1h at rt, prior to DAz-1 treatment. After the labeling step, reactions were ligated, processed and analyzed as described above. For detection of HSA-N_3, lysate (50 μg) was combined with HSA-N_3 at a final concentration of 0-5 μM. The HSA-N_3 doped lysate was then ligated, processed and analyzed as described above.

2.5.7 DAz-1 labeling of Jurkat cells

DAz-1 (1, 2, 5, and 10 mM) was incubated with Jurkat cells in RPMI with 2% FBS for 1-2 h at 37 °C. In subsequent steps, cells were washed three times with sterile PBS to remove excess DAz-1 and a cell lysate fraction was prepared. The lysate was labeled with p-biotin as described above. Reactions were terminated by acetone precipitation, and proteins were analyzed by streptavidin blotting. In time course experiments, Jurkat cells were incubated with DMSO or DAz-1 (2 mM) for 15, 30 min, 1 or 2 h at 37 °C. At the end of each time point, cells were harvested, washed and processed as described above. To quantify the number of viable cells after DAz-1 treatment Jurkat cells were treated with DMSO or DAz-1 and cell viability was quantified by trypan blue exclusion.

2.5.8 DAz-1 Labeling of Jurkat Cells Post-Oxidant Challenge

Jurkat cells (1×10^6) were washed three times with sterile PBS and resuspended in 2 % FBS RPMI. Oxidants (H_2O_2, *t*-BOOH, or FCCP) were added to the cell suspensions at final concentration of 20 or 200 μM and the suspension was incubated at 37 °C for 15 min. Daz-1 (2 mM) or DMSO was added and the cells incubated for an additional hour at 37 °C. Following incubation, the

cells were spun at 1000 rpm for 5 min, washed three times with PBS to remove the media. Subsequently, cell lysate was prepared and the samples were processed as previously described.

2.5.9 Chemical Methods

Unless otherwise noted, all reactions were performed under an argon atmosphere in oven-dried glassware. Methylene chloride and triethyl amine were distilled over calcium hydride prior to use. Additional reagents and solvents were purchased from Sigma or other commercial sources and were used without further purification. Thin layer chromatography (TLC) was carried out using Analtech Uniplate silica gel plates. TLC plates were visualized using a combination of UV, *p*-anisaldehyde, ceric ammonium molybdate, ninhydrin, and potassium permanganate staining. Flash chromatography was performed using silica gel (32-63 μM, 60Å pore size) from Sorbent Technologies Incorporated. NMR spectra were obtained on a Varian Inova 400 (400 MHz for ^{1}H; 100 MHz for ^{13}C), or a Varian Mercury 300 (300 MHz for ^{1}H; 75 MHz for ^{13}C NMR) spectrometer. ^{1}H and ^{13}C NMR chemical shifts are reported in parts per million (ppm) relative to TMS, with the residual solvent peak used as an internal reference. Low-resolution electrospray ionization (ESI) mass spectra were obtained with Water-Micromass LCT at the University of Michigan Mass Spectrometry Laboratory. Reversed phase HPLC purification was performed on a Beckman Coulter System Gold 126p equipped with System Gold 166p detector (λ= 220) using a C18 (21.2×150 mm) Beckman Coulter Ultraprep column.

3-Methoxy-5-oxocyclohex-3-enecarboxylic acid (1). To an oven-dried round bottom flask purged with argon was added to 3,5-diketohexahydrobenzoic acid (0.209 g, 1.34 mmol), PTSA

(0.0130g, 0.0669 mmol), and 10 mL of methanol. The solution was stirred at RT for 10 min. The reaction mixture was concentrated *in vacuo* and purified by silica gel chromatography, eluting with 1:1 ethyl acetate: methanol to provide the title compound (0.221 g, 1.30 mmol) in 97% yield as a white solid. R_f: 0.55 (1:1 ethyl acetate: methanol). ^{1}H NMR (CD_3OD, 400 MHz): δ 5.36 (s, 1H), 3.72 (s, 3H), 3.04-2.94 (m, 1H), 2.70-2.66 (m, 2H), 2.54 (d, *J* = 10.0, 2H). ^{13}C NMR (CD_3OD, 100 MHz): δ 201.19, 180.63, 129.93, 102.55, 56.93, 40.62, 40.15, 32.64. ESI-LRMS calcd. for $C_8H_{10}NaO_4$ ($M+Na^+$) 193.0, found 193.0.

***N*-(3-Azidopropyl)-3-methoxy-5-oxocyclohex-3-enecarboxamide (2).** To a solution of (**1**) (0.0290 g, 0.171 mmol) in 2 mL of DMF was added TBTU (0.0660 g, 0.205 mmol) followed by diisopropylethylamine (0.0360 mL, 0.205 mmol). To the stirring solution was added a solution of 3-aminopropylazide (0.0190 g, 0.188 mmol) in 1 mL of DMF. The reaction mixture was stirred at RT for 15 min. The solution was concentrated *in vacuo* and purified by silica gel chromatography, eluting with ethyl acetate to provide the title compound (0.425 g, 0.168 mmol) in 99% yield. R_f: 0.38 (ethyl acetate). ^{1}H NMR ($CDCl_3$, 300 MHz): δ 6.13 (s, 1H), 5.37 (s, 1H), 3.71 (s, 3H), 3.36 (q, *J* = 6.3 Hz, 4H), 2.89-2.79 (m, 2H), 2.62-2.45 (m, 2H), 1.86-1.75 (m, 2H). ^{13}C NMR ($CDCl_3$, 75 MHz): δ 197.27, 177.30, 172.20, 101.80, 56.03, 49.43, 40.72, 39.83, 37.43, 31.43, 28.60. ESI-LRMS calcd. for $C_{11}H_{16}N_4NaO_3$ ($M+Na^+$) 275.1, found 275.2.

***N*-(3-Azidopropyl)-3,5-dioxocyclohexanecarboxamide (3).** To a solution of (**2**) (0.0360 g, 0.143 mmol) in 5 mL of THF was added 2 mL of 2N HCl. The solution was stirred at RT for 1 h. To the solution was added 0.3 g of silica gel and concentrated *in vacuo*. The residue powder was subjected to flash chromatography, eluting with 3:1 – 1:1 ethyl acetate:methanol to provide the

title compound (0.0270 g, 0.112 mmol) in 78% yield as a white solid. The compound was further purified by C18 reversed phase HPLC (10 m, 21.2×150 mm, Beckman coulter) with a gradient of 0% to 30 % B in 30 min (buffer A: 0.1% TFA in water; buffer B: 0.1% TFA in acetonitrile) at a flow rate of 15 mL/min. R_f: 0.14 (3:1 ethyl acetate: methanol). ^{1}H NMR (DMSO-d_6, 300 MHz): δ 7.99 (t, *J* = 5.1 Hz, 1H), 5.19 (s, 1H), 3.34 (t, *J* = 6.6 Hz, 2H), 3.11 (q, *J* = 6.3 Hz, 2H), 2.91-2.80 (m, 1H), 2.43 (dd, *J* = 16.8 Hz, 11.1 Hz, 2H), 2.29 (dd, *J* = 16.8 Hz, 4.5 Hz, 2H), 1.69-1.60 (m, 2H). ^{13}C NMR (D_2O, 100 MHz): δ 191.11, 175.07, 48.55, 39.52, 36.64, 34.02, 27.44. ESI-LRMS calcd. for $C_{10}H_{14}N_4NaO_3$ ($M+Na^+$) 261.1, found 261.0.

Acknowledgements

This work was supported by the Life Sciences Institute at the University of Michigan and a Special Fellows Award to K.S.C. from the Leukemia & Lymphoma Society. We also thank Professor Howard Hang for many useful discussions and Professor Anna Mapp for comments on the manuscript.

Notes

This work has been published as “A chemical approach for detecting sulfenic acid-modified proteins in living cells.” Mol Biosyst**. 2008** Jun; 4(6):521-31. Stephen E. Leonard, Khalilah G. Reddie, Wilson B. Muse, Young Ho Seo, and Kate S Carroll designed the experiments. Wilson B. Muse purified papain. Stephen E. Leonard and Wilson B. Muse conducted *in vitro* experiments. Khalilah G. Reddie and Stephen E. Leonard conducted live cell experiments. Young Ho Seo performed organic synthesis.

2.6 Appendix of ^{1}H and ^{13}C NMR

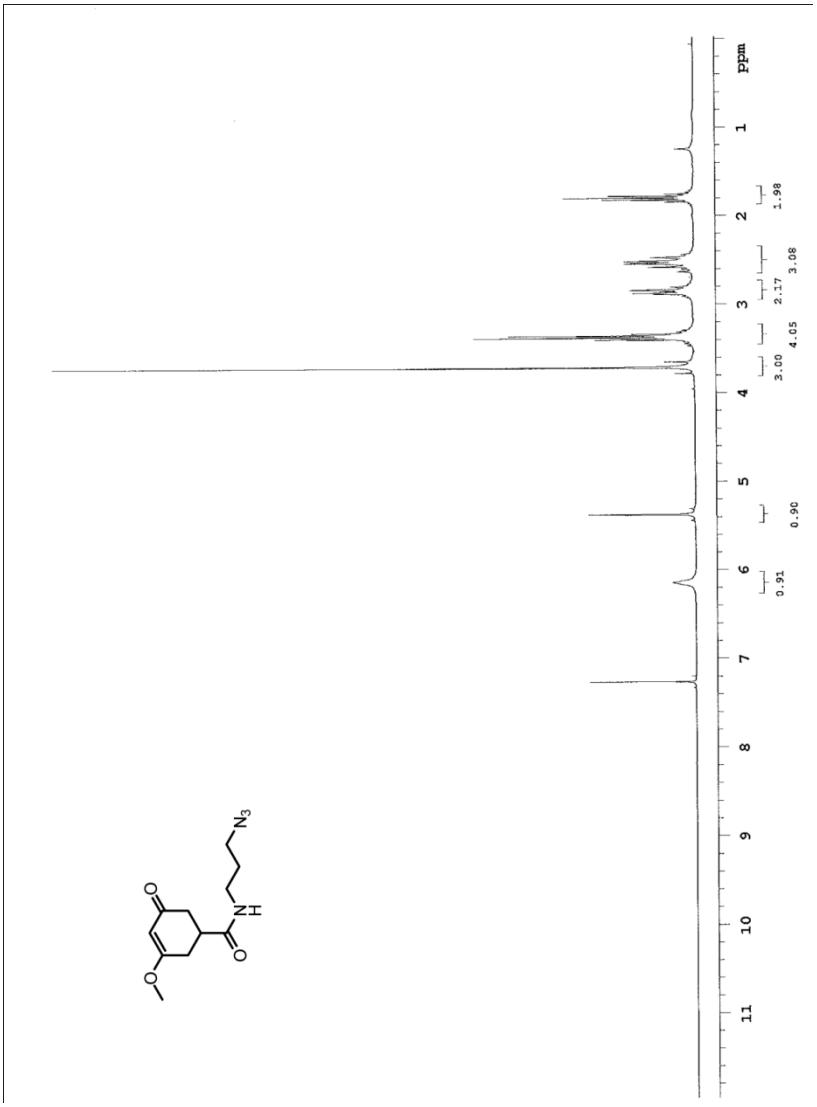

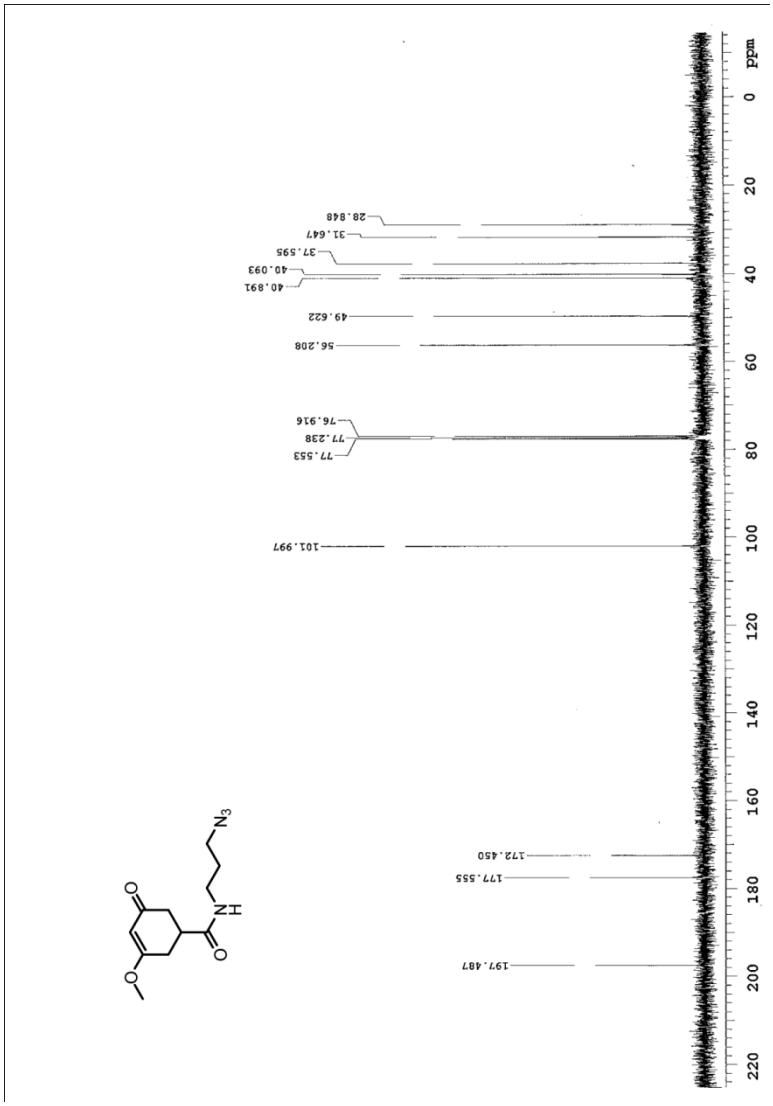
197.487
177.555
172.450
101.997
76.916
77.553
77.238
56.208
49.622
40.891
40.093
37.595
31.647
28.848
ppm
0
20
40
60
80
100
120
140
160
180
200
220
O
O
O
N
H
N3

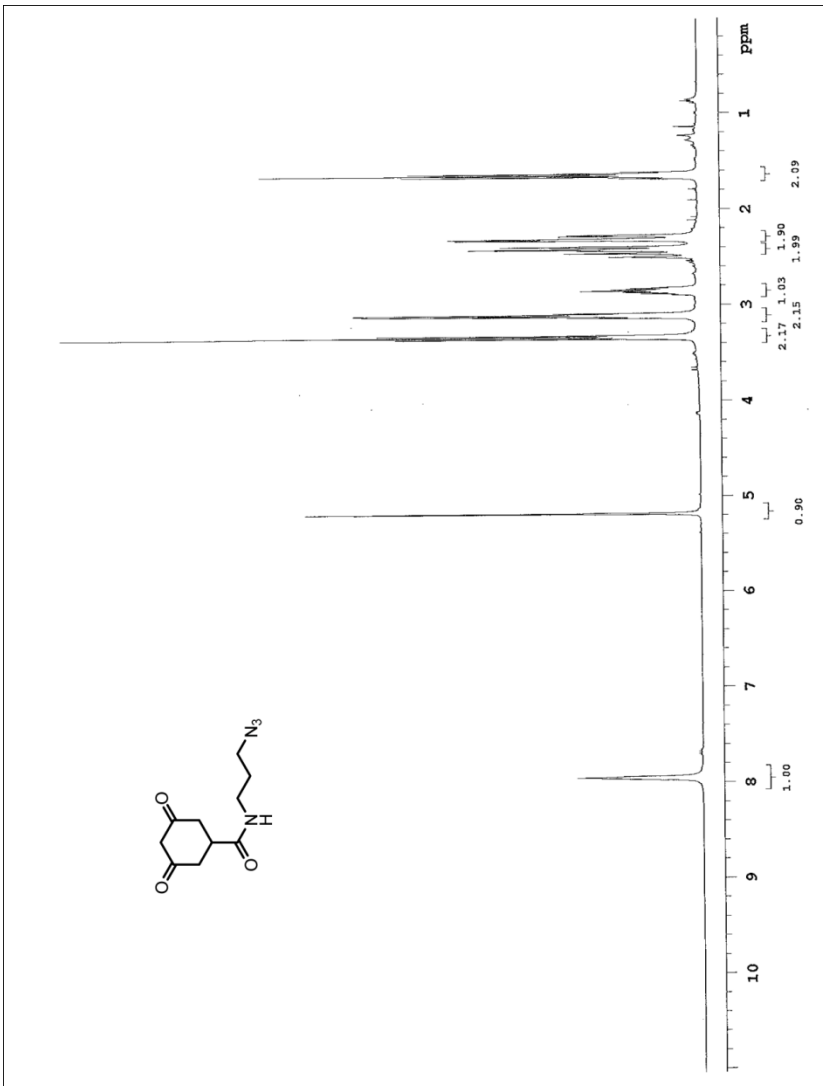

2.7 References

1. Halliwell B, Gutteridge JMC: *Free radicals in biology and medicine* edn 4. Oxford: Oxford Univeristy Press; 2007.
2. Segal AW, Abo A: **The biochemical basis of the NADPH oxidase of phagocytes**. *Trends Biochem. Sci.* 1993, **18**:43-47.
3. Woodman RC, Ruedi JM, Jesaitis AJ, Okamura N, Quinn MT, Smith RM, Curnutte JT, Babior BM: **Respiratory burst oxidase and three of four oxidase-related polypeptides are associated with the cytoskeleton of human neutrophils**. *J. Clin. Invest.* 1991, **87**:1345-1351.
4. D'Autreaux B, Toledano MB: **ROS as signalling molecules: mechanisms that generate specificity in ROS homeostasis**. *Nat. Rev. Mol. Cell Biol.* 2007, **8**:813-824.
5. Rhee SG: **Cell signaling. H2O2, a necessary evil for cell signaling**. *Science* 2006, **312**:1882-1883.

6. Stone JR, Yang S: **Hydrogen peroxide: a signaling messenger**. *Antioxid. Redox Signal.* 2006, **8**:243-270.
7. Terada LS: **Specificity in reactive oxidant signaling: think globally, act locally**. *J. Cell. Biol.* 2006, **174**:615-623.
8. Stadtman ER: **Protein oxidation and aging**. *Science* 1992, **257**:1220-1224.
9. Friguet B: **Oxidized protein degradation and repair in ageing and oxidative stress**. *FEBS Letters* 2006, **580**:2910-2916.
10. Reynolds A, Laurie C, Lee Mosley R, Gendelman HE, Giacinto Bagetta MTCaSAL: **Oxidative Stress and the Pathogenesis of Neurodegenerative Disorders**. In *International Review of Neurobiology*. Edited by: Academic Press; 2007:297-325. vol Volume 82.]
11. Di Simplicio P, Franconi F, Frosali S, Di Giuseppe D: **Thiolation and nitrosation of cysteines in biological fluids and cells**. *Amino Acids* 2003, **25**:323-339.
12. Jacob C, Holme AL, Fry FH: **The sulfinic acid switch in proteins**. *Org. Biomol. Chem.* 2004, **2**:1953-1956.
13. Poole LB, Karplus PA, Claiborne A: **Protein sulfenic acids in redox signaling**. *Annu. Rev. Pharmacol. Toxicol.* 2004, **44**:325-347.
14. Giorgio M, Trinei M, Migliaccio E, Pelicci PG: **Hydrogen peroxide: a metabolic by-product or a common mediator of ageing signals?** *Nat. Rev. Mol. Cell Biol.* 2007, **8**:722-728.
15. Hensley K, Floyd RA: **Oxidative modification of proteins in cell signaling**. *Antioxid. Redox Signal.* 2005, **7**:523-525.
16. Stone JR: **An assessment of proposed mechanisms for sensing hydrogen peroxide in mammalian systems**. *Arch. Biochem. Biophys.* 2004, **422**:119-124.
17. Claiborne A, Yeh JI, Mallett TC, Luba J, Crane EJ, 3rd, Charrier V, Parsonage D: **Protein-sulfenic acids: diverse roles for an unlikely player in enzyme catalysis and redox regulation**. *Biochemistry* 1999, **38**:15407-15416.
18. Aversa MC, Barattucci A, Bonaccorsi P, Giannetto: **Recent advances and perspectives in the chemistry of sulfenic acids**. *Curr. Org. Chem.* 2007, **11**:1034-1052.
19. Allison WS: **Formation and reactions of sulfenic acids in proteins**. *Acc. Chem. Res.* 1976, **9**:293.
20. Claiborne A, Mallett TC, Yeh JI, Luba J, Parsonage D: **Structural, redox, and mechanistic parameters for cysteine-sulfenic acid function in catalysis and regulation**. *Adv. Protein Chem.* 2001, **58**:215-276.
21. Claiborne A, Miller H, Parsonage D, Ross RP: **Protein-sulfenic acid stabilization and function in enzyme catalysis and gene regulation**. *FASEB J.* 1993, **7**:1483-1490.
22. Lin WS, Armstrong DA, Gaucher GM: **Formation and repair of papain sulfenic acid**. *Can. J. Biochem.* 1975, **53**:298-307.
23. Willett WS, Copley SD: **Identification and localization of a stable sulfenic acid in peroxide-treated tetrachlorohydroquinone dehalogenase using electrospray mass spectrometry**. *Chem. Biol.* 1996, **3**:851-857.
24. Benitez LV, Allison WS: **The inactivation of the acyl phosphatase activity catalyzed by the sulfenic acid form of glyceraldehyde 3-phosphate dehydrogenase by dimedone and olefins**. *J Biol Chem* 1974, **249**:6234-6243.
25. van Montfort RL, Congreve M, Tisi D, Carr R, Jhoti H: **Oxidation state of the active-site cysteine in protein tyrosine phosphatase 1B**. *Nature* 2003, **423**:773-777.
26. Ellis HR, Poole LB: **Novel application of 7-chloro-4-nitrobenzo-2-oxa-1,3-diazole to identify cysteine sulfenic acid in the AhpC component of alkyl hydroperoxide reductase**. *Biochemistry* 1997, **36**:15013-15018.

27. Poole LB, Zeng BB, Knaggs SA, Yakubu M, King SB: **Synthesis of Chemical Probes to Map Sulfenic Acid Modifications on Proteins**. *Bioconjugate Chem.* 2005, **16**:1624.
28. Saurin AT, Neubert H, Brennan JP, Eaton P: **Widespread sulfenic acid formation in tissues in response to hydrogen peroxide**. *Proc. Natl. Acad. Sci. U. S. A.* 2004, **101**:17982-17987.
29. Poole LB, Ellis HR: **Identification of cysteine sulfenic acid in AhpC of alkyl hydroperoxide reductase**. *Methods Enzymol* 2002, **348**:122-136.
30. Charles RL, Schroder E, May G, Free P, Gaffney PRJ, Wait R, Begum S, Heads RJ, Eaton P: **Protein sulfenation as a redox sensor: Proteomics studies using a novel biotinylated dimedone analogue**. *Mol. Cell. Proteomics* 2007, **6**:1473-1484.
31. Poole LB, Klomsiri C, Knaggs SA, Furdui CM, Nelson KJ, Thomas MJ, Fetrow JS, Daniel LW, King SB: **Fluorescent and Affinity-Based Tools To Detect Cysteine Sulfenic Acid Formation in Proteins**. *Bioconjugate Chem.* 2007, **18**:2004-2017.
32. Leopz-Mirabal HR, Winter JR: **Redox characteristics of the eukaryotic cytosol**. *Biochim. Biophys. Acta* 2007, **In press**.
33. Agard NJ, Baskin JM, Prescher JA, Lo A, Bertozzi CR: **A comparative study of bioorthogonal reactions with azides**. *ACS Chem. Biol.* 2006, **1**:644-648.
34. Hang HC, Loureiro J, Spooner E, van der Velden AW, Kim YM, Pollington AM, Maehr R, Starnbach MN, Ploegh HL: **Mechanism-based probe for the analysis of cathepsin cysteine proteases in living cells**. *ACS Chem. Biol.* 2006, **1**:713-723.
35. Prescher JA, Bertozzi CR: **Chemistry in living systems**. *Nat. Chem. Biol.* 2005, **1**:13-21.
36. Prescher JA, Dube DH, Bertozzi CR: **Chemical remodelling of cell surfaces in living animals**. *Nature* 2004, **430**:873-877.
37. Speers AE, Cravatt BF: **A tandem orthogonal proteolysis strategy for high-content chemical proteomics**. *J. Am. Chem. Soc.* 2005, **127**:10018-10019.
38. Vocadlo DJ, Hang HC, Kim EJ, Hanover JA, Bertozzi CR: **A chemical approach for identifying O-GlcNAc-modified proteins in cells**. *Proc. Natl. Acad. Sci. U. S. A.* 2003, **100**:9116-9121.
39. Otto HH, Schirmeister T: **Cysteine Proteases and Their Inhibitors**. *Chem. Rev.* 1997, **97**:133-172.
40. Drenth J, Jansonius JN, Koekoek R, Wolthers BG: **The structure of papain.** *Adv. Protein Chem.* 1971, **25**:79-115.
41. Fuangthong M, Helmann JD: **The OhrR repressor senses organic hydroperoxides by reversible formation of a cysteine-sulfenic acid derivative**. *Proc. Natl. Acad. Sci. U. S. A.* 2002, **99**:6690-6695.
42. Saxon E, Bertozzi CR: **Cell surface engineering by a modified Staudinger reaction**. *Science* 2000, **287**:2007-2010.
43. Laughlin ST, Agard NJ, Baskin JM, Carrico IS, Chang PV, Ganguli AS, Hangauer MJ, Lo A, Prescher JA, Bertozzi CR: **Metabolic labeling of glycans with azido sugars for visualization and glycoproteomics**. *Methods Enzymol.* 2006, **415**:230-250.
44. Sawa M, Hsu T-L, Itoh T, Sugiyama M, Hanson SR, Vogt PK, Wong C-H: **Glycoproteomic probes for fluorescent imaging of fucosylated glycans in vivo**. *Proceedings of the National Academy of Sciences* 2006, **103**:12371-12376.
45. Speers AE, Adam GC, Cravatt BF: **Activity-based protein profiling in vivo using a copper(i)-catalyzed azide-alkyne [3 + 2] cycloaddition**. *J Am Chem Soc* 2003, **125**:4686-4687.
46. Halliwell B: **Albumin--an important extracellular antioxidant?** *Biochem. Pharmacol.* 1988, **37**:569-571.
47. Radi R, Beckman JS, Bush KM, Freeman BA: **Peroxynitrite oxidation of sulfhydryls. The cytotoxic potential of superoxide and nitric oxide**. *J. Biol. Chem.* 1991, **266**:4244-4250.

48. Radi R, Bush KM, Cosgrove TP, Freeman BA: **Reaction of xanthine oxidase-derived oxidants with lipid and protein of human plasma**. *Arch. Biochem. Biophys.* 1991, **286**:117-125.
49. Carballal S, Radi R, Kirk MC, Barnes S, Freeman BA, Alvarez B: **Sulfenic acid formation in human serum albumin by hydrogen peroxide and peroxynitrite**. *Biochemistry* 2003, **42**:9906-9914.
50. Lillig CH, Potamitou A, Schwenn JD, Vlamis-Gardikas A, Holmgren A: **Redox regulation of 3'-phosphoadenylylsulfate reductase from Escherichia coli by glutathione and glutaredoxins**. *J. Biol. Chem.* 2003, **278**:22325-22330.
51. Men L, Wang Y: **The oxidation of yeast alcohol dehydrogenase-1 by hydrogen peroxide in vitro**. *J. Proteome Res.* 2007, **6**:216-225.
52. Ahn NG, Shabb JB, Old WM, Resing KA: **Achieving in-depth proteomics profiling by mass spectrometry**. *ACS Chem. Biol.* 2007, **2**:39-52.
53. Guerrera IC, Kleiner O: **Application of mass spectrometry in proteomics**. *Biosci. Rep.* 2005, **25**:71-93.
54. Ong SE, Mann M: **Mass spectrometry-based proteomics turns quantitative**. *Nat. Chem. Biol.* 2005, **1**:252-262.
55. Shen Y, Smith RD: **Advanced nanoscale separations and mass spectrometry for sensitive high-throughput proteomics**. *Expert Rev. Proteomics* 2005, **2**:431-447.
56. Bulinski JC: **CELL BIOLOGY: Actin Discrimination**. *Science* 2006, **313**:180-181.
57. Brennan JP, Wait R, Begum S, Bell JR, Dunn MJ, Eaton P: **Detection and Mapping of Widespread Intermolecular Protein Disulfide Formation during Cardiac Oxidative Stress Using Proteomics with Diagonal Electrophoresis**. *J. Biol. Chem.* 2004, **279**:41352-41360.
58. Johansson M, Lundberg M: **Glutathionylation of beta-actin via a cysteinyl sulfenic acid intermediary**. *BMC Biochem.* 2007, **8**:26.
59. Frein D, Schildknecht S, Bachschmid M, Ullrich V: **Redox regulation: A new challenge for pharmacology**. *Biochem. Pharmacol.* 2005, **70**:811-823.
60. Stadtman ER, Berlett BS: **Reactive oxygen-mediated protein oxidation in aging and disease**. *Drug Metab. Rev.* 1998, **30**:225-243.
61. Dalle-Donne I, Scaloni A, Butterfield DA, Desiderio DM, Nibbering NM (Ed): *Redox proteomics: From protein modifications to cellular dysfuncgtion and diseases*: Wiley; 2006.
62. Michalek RD, Nelson KJ, Holbrook BC, Yi JS, Stridiron D, Daniel LW, Fetrow JS, King SB, Poole LB, Grayson JM: **The requirement of reversible cysteine sulfenic acid formation for T cell activation and function**. *J. Immunol.* 2007, **179**:6456-6467.
63. Kho Y, Kim SC, Jiang C, Barma D, Kwon SW, Cheng J, Jaunbergs J, Weinbaum C, Tamanoi F, Falck J, et al.: **A tagging-via-substrate technology for detection and proteomics of farnesylated proteins**. *Proc Natl Acad Sci U S A* 2004, **101**:12479-12484.
64. Wiskocil R, Weiss A, Imboden J, Kamin-Lewis R, Stobo J: **Activation of a human T cell line: a two-stimulus requirement in the pretranslational events involved in the coordinate expression of interleukin 2 and gamma-interferon genes**. *J Immunol* 1985, **134**:1599-1603.
65. Yang K-S, Kang SW, Woo HA, Hwang SC, Chae HZ, Kim K, Rhee SG: **Inactivation of Human Peroxiredoxin I during Catalysis as the Result of the Oxidation of the Catalytic Site Cysteine to Cysteine-sulfinic Acid**. *J. Biol. Chem.* 2002, **277**:38029-38036.

66. Schuppe-Koistinen I, Moldeus P, Bergman T, Cotgreave IA: **S-thiolation of human endothelial cell glyceraldehyde-3-phosphate dehydrogenase after hydrogen peroxide treatment**. *Eur. J. Biochem.* 1994, **221**:1033-1037.
67. Cho S-H, Lee C-H, Ahn Y, Kim H, Kim H, Ahn C-Y, Yang K-S, Lee S-R: **Redox regulation of PTEN and protein tyrosine phosphatases in H2O2-mediated cell signaling**. *FEBS Lett.* 2004, **560**:7-13.
68. Baty JW, Hampton MB, Winterbourn CC: **Proteomic detection of hydrogen peroxide-sensitive thiol proteins in Jurkat cells**. *Biochem. J.* 2005, **389**:785-795.
69. Woo HA, Kang SW, Kim HK, Yang KS, Chae HZ, Rhee SG: **Reversible oxidation of the active site cysteine of peroxiredoxins to cysteine sulfinic acid. Immunoblot detection with antibodies specific for the hyperoxidized cysteine-containing sequence**. *J. Biol. Chem.* 2003, **278**:47361-47364.
70. Antunes F, Cadenas E: **Estimation of H2O2 gradients across biomembranes**. *FEBS Lett.* 2000, **475**:121-126.
71. Makino N, Sasaki K, Hashida K, Sakakura Y: **A metabolic model describing the H2O2 elimination by mammalian cells including H2O2 permeation through cytoplasmic and peroxisomal membranes: comparison with experimental data**. *Biochim. Biophys. Acta.* 2004, **1673**:149-159.
72. Funk MO, Nakagawa Y, Skochdopole J, Kaiser ET: **Affinity chromatographic purification of papain**. *Int. J. Pept. Protein Res.* 1979, **3**:296-303.
73. Singh R, Blattler WA, Collinson AR: **An amplified assay for thiols based on reactivation of papain**. *Anal. Biochem.* 1993, **213**:49-56.
74. Singh R, Blattler WA, Collinson AR: **Assay for thiols based on reactivation of papain**. *Methods Enzymol.* 1995, **251**:229-237.
75. Chartron J, Shiau C, Stout CD, Carroll KS: **3'-Phosphoadenosine-5'-phosphosulfate reductase in complex with thioredoxin: a structural snapshot in the catalytic cycle**. *Biochemistry* 2007, **46**:3942-3951.

Chapter 3

Mining the thiol proteome for sulfenic acid modifications reveals new targets for oxidation in cells

3.1 Abstract

Oxidation of cysteine to sulfenic acid has emerged as a biologically relevant post-translational modification with particular importance in redox-mediated signal transduction; however, the identity of modified proteins remains largely unknown. We recently reported DAz-1, a cell-permeable chemical probe capable of detecting sulfenic acid-modified proteins directly in living cells. Here we describe DAz-2, an analog of DAz-1 that exhibits significantly improved potency *in vitro* and in cells. Application of this new probe for global analysis of the sulfenome in a tumor cell line identifies most known sulfenic acid-modified proteins – 14 in total, plus more than 175 new candidates, with further testing confirming oxidation in several candidates. The newly identified proteins have roles in signal transduction, DNA repair, metabolism, protein synthesis, redox homeostasis, nuclear transport, vesicle trafficking, and ER quality control. Cross-comparison of these results with those from disulfide, *S*-glutathionylation, and *S*-nitrosylation proteomes reveals moderate overlap, suggesting fundamental differences in the chemical and biological basis for target specificity. The combination of selective chemical enrichment and live-cell compatibility makes DAz-2 a powerful new tool with the potential to reveal new regulatory mechanisms in signaling pathways, and identify new therapeutic targets.

3.2 Introduction

Historically, reactive oxygen species (ROS) have been considered solely as toxic byproducts of metabolism. However, a growing body of work suggests that oxidants can also act as a second messenger in signal transduction pathways that regulate normal cellular processes such as cell growth, differentiation, and migration [1-3]. Early studies by Sundaresan *et al.* showed that hydrogen peroxide (H_2O_2) generation was required for platelet-derived growth factor signal transduction [4]. Later, Lee *et al.* reported that peptide growth factors stimulate H_2O_2 production in epithelial cells and that ROS transiently inactivate protein tyrosine phosphatase 1B (PTP1B), implicating oxidants in post-translational modification (PTM) of proteins in a manner analogous to regulatory *O*-phosphorylation [5]. The subsequent finding of superoxide-generating homologues of the phagocytic NADPH oxidase (Phox) by Suh *et al.* revealed the enzymatic source of ligand-stimulated ROS production [6]. From these seminal discoveries, the field of redox signaling in mammalian cells emerged.

The signaling roles and sources of ROS are well established, however, the specific intracellular protein targets of oxidation remain largely unknown. Emerging evidence suggests that redox-sensitive cysteine residues in proteins may function as oxidant sensors [7-9]. Oxidation of sulfur alters its chemical reactivity and metal binding properties, which can serve as a molecular switch to control protein structure and function [10,11]. In addition, thiols exhibit a wide range of reactivity with H_2O_2 (1-10^7 M^{-1} s^{-1}), which may account in part for target selectivity [1]. The initial oxidation product of cysteine and H_2O_2 is sulfenic acid. This cysteine oxoform resides at a hub and can be reduced back to the thiol or converted to sulfinic and sulfonic acid, which are interesting oxidation states in their own right [12] (Figure 3.1a). Stable sulfenic acids have been

observed in a growing number of proteins [13-18]. Furthermore, essential functions for sulfenic acid have been demonstrated for redox signaling in yeast and T-cell activation, providing strong support for the growing roles of this modification in biology [9,19].

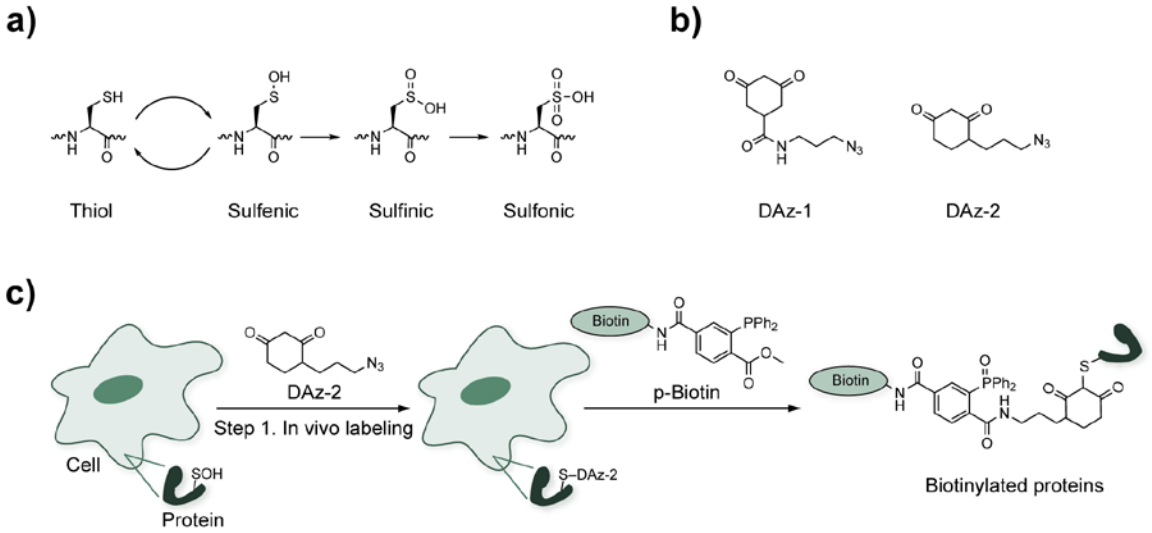

Figure 3.1 Trapping and tagging proteins that undergo sulfenic acid modification, directly in living cells. (a) Oxidation states of protein cysteines that are implicated in biological function. (b) Azido-probes for detecting and identifying sulfenic acid-modified proteins, depicted in their keto form. (c) Two-step strategy for detecting cellular sulfenic acid modifications.

The chemical reactivity of sulfenic acids has been well studied in the last several decades [20-22]. The sulfur atom in sulfenic acid has both electrophilic and nucleophilic characteristics. This is underscored by the facile reaction that occurs between sulfenic acids to form a thiosulfinate. Sulfenic acids also undergo nucleophilic conjugate addition reactions. The chemoselective reaction between 5,5-dimethyl-1,3-cyclohexadione (dimedone) and protein sulfenic acids was first reported by Benitez and Allison in 1974 [17]. Since then, this reaction has been exploited to detect protein sulfenic acids using mass spectrometry (MS) [23,24] and, more recently, through direct conjugation to fluorophores or biotin [25-27]. Nonetheless, these previous approaches have limited utility in live-cell proteomic labeling for a variety of reasons. These include (i)

membrane impermeability, (ii) the presence of endogenously biotinylated proteins, and/or (iii) lack of a chemical handle for affinity enrichment.

In particular, live-cell investigation is vital to expand our understanding of the role that sulfenic acids and other oxidative cysteine modifications play in biological systems. In large part this is due to redox compartmentalization in cells, consisting of highly oxidizing organelles such as the endoplasmic reticulum and peroxisomes amidst the cytoplasm and nucleus, which represent very reducing compartments [28,29]. Cell lysis destroys this delicate redox balance, producing hyperoxidized proteins and making it difficult to decipher modifications that occur under biologically relevant conditions [28,29]. To address these issues, we recently reported on the development of DAz-1 (Figure 3.1b), a bi-functional chemical probe that is cell-permeable and chemoselective for sulfenic acids [30,31]. In addition, DAz-1 incorporates the azide chemical reporter group that permits selective coupling with bioorthogonal phosphine or alkyne-derivatized reagents for subsequent detection of oxidized proteins [32,33].

In the present study, we report a new probe for sulfenic acid detection, 4-(3-azidopropyl)cyclohexane-1,3-dione (**1**) or DAz-2 (Figure 3.1b), an analog of DAz-1 with improved potency *in vitro* and in living cells. Application of this new probe for global analysis of the "sulfenome" in a tumor cell line, using the strategy outlined in Figure 3.1c, identifies most known sulfenic acid-modified proteins – 14 in total, plus more than 175 new candidates, with further testing confirming oxidative modifications in vesicle-targeting GTPase and ER glycoprotein chaperone candidate proteins. The newly identified proteins have roles in signal transduction, DNA repair, metabolism, protein synthesis, redox homeostasis, nuclear transport,

vesicle trafficking, and ER quality control, demonstrating broad cellular manifestations of this oxidative modification. Cross-comparison of these results with those from disulfide, *S*-glutathionylation, and *S*-nitrosylation proteomes reveals moderate overlap, suggesting fundamental differences in the chemical and biological basis for target specificity.

3.3 Results

We previously designed and synthesized DAz-1 (Figure 3.1b), the first chemical probe capable of trapping and tagging sulfenic acid-modified proteins directly in living cells [30,31]. DAz-1 is composed of two key components: (i) the 1,3-cyclohexadione scaffold, which is chemically selective for sulfenic acids [17,25-27,30,31,34] and, (ii) an azide chemical handle that allows selective conjugation to phosphine or alkyne-derivatized reagents for subsequent analysis of labeled proteins [32,33]. DAz-1 selectively tags sulfenic acid-modified proteins *in vitro* and in living cells, however, this probe is less well suited for global proteomic studies because its reactivity is decreased relative to dimedone (not shown). In addition, the polar amide group attached to the C5 position of DAz-1 could reduce cell permeability or accessibility to partially buried sulfenic acids. To extend the utility of our two-step labeling approach to detect cellular sulfenic acids, we sought an analog of DAz-1 with increased potency. Such a probe would allow us to more comprehensively profile and define the cellular sulfenome. To address these issues, we envisioned an analog of DAz-1 – 4-(3-azidopropyl)cyclohexane-1,3-dione or DAz-2 (**1**) – with a propyl azide linker installed directly at the C4 position of the 1,3-cyclohexadione scaffold (Figure 3.1b).

3.3.1 Synthesis of DAz-2

We explored the synthesis of DAz-2 *via* two routes (Scheme 3.1). The synthesis of DAz-2 *via* route A began with protection of the reactive diketone of 1,3-cyclohexadione (**6**). The protected 3-ethoxycyclohex-2-enone (**5**) was generated with iodine in ethanol in 73% yield. A lithium diisopropylamide (LDA) solution was then used to activate **5** for alkylation with 3-iodo-tert-butyldimethylsilyloxypropane (**9**) to give **4** in 37% yield. Compound **4** was then deprotected with tetrabutylammonium fluoride (TBAF) to give the primary alcohol **3** in 92% yield [27]. The azide chemical handle was installed *via* mesylation of 6-(3-hydroxypropyl)-3-ethoxycyclohex-2-enone (**3**) and subsequent nucleophilic displacement of the mesyl alcohol by sodium azide in 70% yield, over two steps. The resulting 6-(3-azidopropyl)-3-ethoxycyclohex-2-enone (**2**) was deprotected using ceric (IV) ammonium nitrate (CAN) in water/acetonitrile in 90% yield. The overall yield of DAz-2 over 6 steps was 16%. In an attempt to reduce the number of synthetic steps we synthesized DAz-2 by the alternative route B (Scheme 3.1). A lithium diisopropylamide (LDA) solution was used to activate **5** for alkylation with 3-iodo-propylazide (**11**) [35] to give **2** in 14% yield. Compound **2** was then deprotected to give the final product DAz-2 in 9% overall yield over 3 steps.

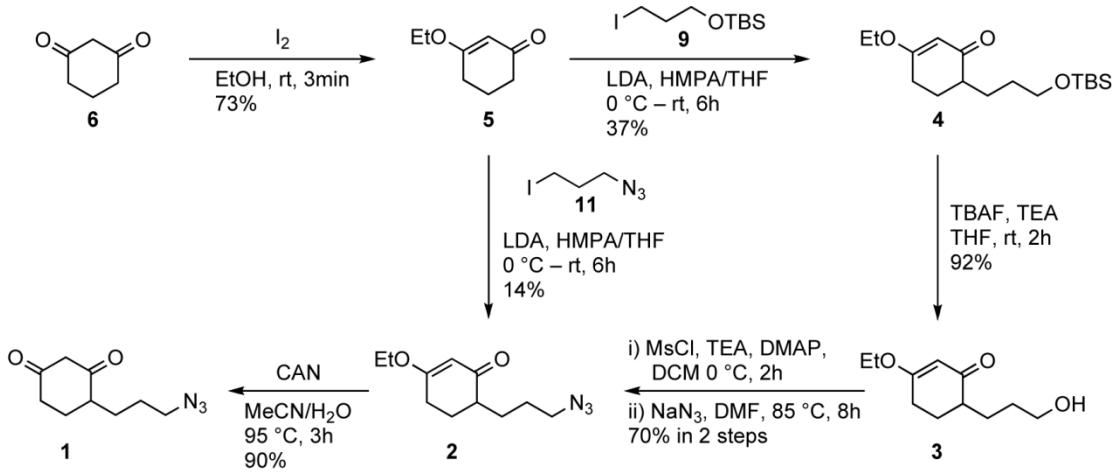

Scheme 3.1 Synthesis of new cell-permeable probe for identifying sulfenic acid protein modifications in cells, DAz-2.

3.3.2 Comparative analysis of sulfenic acid labeling by DAz-1 and DAz-2 in recombinant protein and whole cell lysate

The chemical selectivity of DAz-1 and C4-functionalized 1,3-cyclohexadione analogs for sulfenic acid has been well established [17,25-27,30,31,34]. To test the hypothesis that DAz-2 would be more effective at sulfenic acid detection than DAz-1, we compared their reactivity using glyceraldehyde 3-phosphate dehydrogenase (GAPDH), a glycolytic enzyme with an active site cysteine, Cys149, that is readily oxidized [17,36]. For these experiments untreated or H_2O_2-treated GAPDH was reacted with DAz-1 or DAz-2. In subsequent steps, excess probe was removed; azide-tagged proteins were conjugated to phosphine-biotin (p-Biotin) and analyzed by HRP-streptavidin Western blot (Figure 3.2a). In reactions without H_2O_2, faint labeling of GAPDH by DAz-1 and DAz-2 was observed and is consistent with the high reactivity of Cys149, which oxidizes in the presence of trace metal ions under aerobic conditions [17,36]. Control reactions carried out in the absence of DAz-1 or DAz-2 demonstrated no detectable protein labeling. Addition of H_2O_2, and concomitant oxidation of GAPDH, resulted in a marked increase in protein labeling, as expected. Notably, protein labeling of GAPDH with DAz-2 is more intense relative to DAz-1. Next, we compared the reactivity of DAz-1 and DAz-2 in HeLa whole cell lysates using the procedure outlined for GAPDH. Sulfenic acid detection by the azido-sulfenic acid probes was time (Figure 3.2b) and dose-dependent (not shown); protein-labeling patterns were also similar. Analogous to the results obtained with GAPDH, DAz-2 proved more effective at sulfenic acid detection in lysates, as indicated by the prominent increase in signal relative to DAz-1.

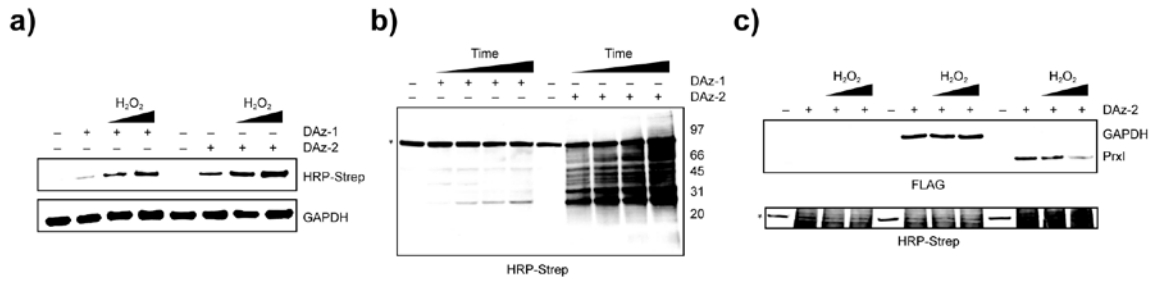

Figure 3.2 DAz-2 exhibits increased sensitivity for sulfenic acids in vitro. (a) Comparison of sulfenic acid detection by DAz-1 and DAz-2 in the glycolytic enzyme, GAPDH. Protein (10 µM) was reacted with or without H2O2 (10 or 50 µM) for 20 min at rt and then with DAz-1 (1 mM), DAz-2 (1 mM), or DMSO (5% v/v) for 15 min at rt. Reactions were quenched with DTT (5 mM) and excess reagent removed by gel-filtration. After Staudinger ligation (see Methods), proteins were resolved by 4-12% SDS-PAGE, transferred to PVDF membrane and detected by HRP-streptavidin Western blot (see Methods). (b) Comparison of sulfenic acid detection by DAz-1 and DAz-2 in HeLa whole cell lysates. Protein lysate (50 µg) was labeled with DAz-1 (0.5 mM), DAz-2 (0.5 mM), or DMSO (5% v/v) for 0.5, 1, 1.5, and 2 h at 37 °C. After labeling, excess reagent was removed by gel-filtration and samples were analyzed as described above. (c) DAz-2 detects sulfenic acid modifications in lysate from cells expressing FLAG and HA epitope-tagged GAPDH and PrxI. Protein lysate (200 µg) was treated with or without H_2O_2 (50 or 100 µM) for 15 min and then with DAz-2 (1 mM) or DMSO (2% v/v) for 1 h at 37 °C. After Staudinger ligation, biotinylated proteins were captured on NeutrAvidin beads, processed and analyzed by Western blot using anti-FLAG antibody and HRP-streptavidin (see Methods). The asterisk marks proteins that are endogenously biotinylated.

Having demonstrated that DAz-2 was more effective at detecting sulfenic acids *in vitro*, we next tested our strategy to enrich labeled proteins from lysate prepared from cells expressing N-terminally FLAG and HA epitope-tagged GAPDH and Peroxiredoxin I (PrxI), an antioxidant protein with a redox-active cysteine that is oxidized to sulfenic acid by its peroxide substrate [37] (Figure 3.3). Untreated or H_2O_2-treated lysates were probed with DAz-2 and azide-tagged proteins conjugated to p-Biotin. Biotinylated proteins were then captured on immobilized NeutrAvidin, a modified avidin derivative [38]. After extensive washing, bound proteins were eluted and analyzed by Western blot using a monoclonal anti-FLAG antibody and HRP-streptavidin (Figure 3.2c). The extent of GAPDH enrichment did not parallel the increase in exogenously added H_2O_2 and confirmed that complete oxidation of GAPDH occurred during cell lysis [28]. On the other hand, PrxI enrichment decreased concomitantly with elevated H_2O_2, suggesting that in the absence of a functional reducing system, the active site cysteine formed

an intramolecular disulfide or was overoxidized to sulfinic acid, precluding reaction with DAz-2 [37]. These data confirm DAz-2-dependent capture of oxidized GAPDH and PrxI, as compared to cells expressing an empty vector control, and underscore the importance of probing labile cysteine modifications directly in cells.

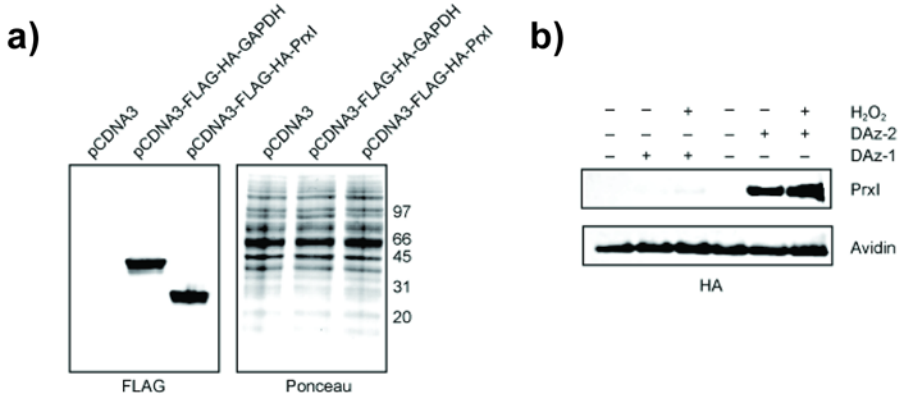

Figure 3.3 Expression, DAz-2 sulfenic acid labeling, and enrichment is performed with human PrxI and GAPDH in HeLa cells. (a) Expression levels of GAPDH and PrxI in HeLa cells determined. HeLa cells were transfected with empty vector, GAPDH, or PrxI. After 24 h lysates were collected and analyzed for protein levels by SDS-PAGE and Western Blot analysis. Membrane was probed with anti-FLAG antibodies (1:10,000). Ponceau S staining was used to verify equal protein loading. (b) DAz-2 is more effective than DAz-1 for detecting sulfenic acid formation in cellular PrxI C173A. HeLa cells were transfected with a plasmid encoding HA and FLAG-tagged PrxI C173A. After 24 h, cells were untreated or treated with H_2O_2 (200 μM) for 15 min at rt followed by labeling with DAz-1 (5 mM), DAz-2 (5 mM), or DMSO (2% v/v) for 2 h at 37 °C. Cells were washed, a cell lysate was generated, ligated with p-Biotin, and enriched as described in the main text. Proteins were eluted and analyzed by Western blot with anti-HA antibodies (1:1,000).

3.3.3 Specific labeling of sulfenic acid-modified proteins in cells using DAz-2

DAz-2 was then evaluated for detecting sulfenic acid modifications in living cells. In these studies, the extent and selectivity of covalent modification of sulfenic acid-modified proteins was examined by performing the Staudinger ligation in lysates from cells treated with azido-

probe. Protein labeling by DAz-2 was time (Figure 3.3a) and dose-dependent (Figure 3.4a). Cells probed using DAz-1 or DAz-2 exhibited similar protein-labeling patterns with higher signal intensity obtained with cells treated with DAz-2, as anticipated based on *in vitro* observations.

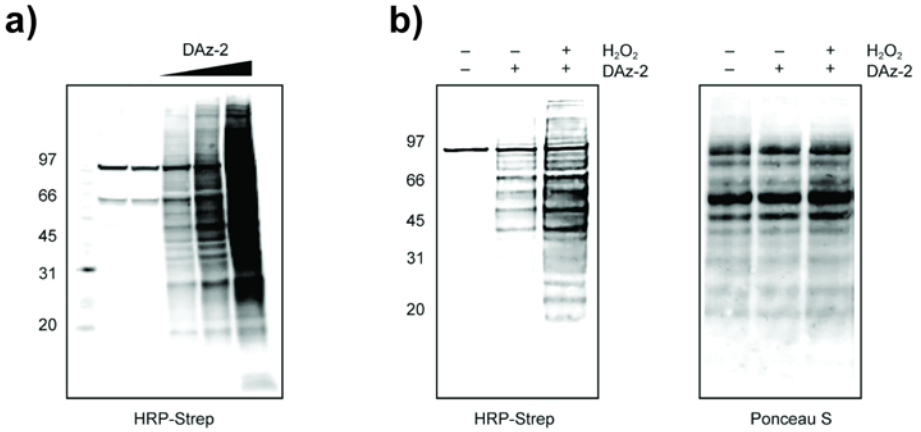

Figure 3.4 DAz-2 protein labeling is dose-dependent and can respond to changes in protein sulfenic acid formation within cells. (a) Dose-dependent labeling of sulfenic acids by DAz-2 in living cells. HeLa cells were treated with 2.5, 5, 10 mM DAz-2 or DMSO (2% v/v) for 2 h at 37 °C, harvested in lysis buffer, and ligated with p-Biotin. Protein samples (25 µg protein/lane) were resolved by SDS-PAGE and analyzed by HRP-streptavidin Western blot. (b) DAz-2 detects peroxide-mediated changes in sulfenic acid content of HeLa cells. HeLa cells were untreated or treated with H_2O_2 (200 µM) for 15 min at rt followed by incubation with DAz-2 (5 mM) or DMSO (1% v/v) for 2 h at 37 °C. Cells were harvested in lysis buffer and ligated with p-Biotin. Protein samples (13 µg protein/lane) were resolved by SDS-PAGE and analyzed by HRP-streptavidin Western blot. Ponceau S was used to verify equal protein loading.

Upon addition of a moderate concentration of H_2O_2 to cells (200 µM, Figure 3.4b), we observed an increase in protein labeling by DAz-2. Mock-treated cells displayed only low levels of background labeling from HRP-streptavidin binding to endogenous biotinylated proteins (Figures 3.4 and 3.5). These data establish that DAz-2 is membrane-permeable and can respond to changes in protein sulfenic acid formation within cells. Control experiments performed with the cell-permeable oxidant-sensitive probe, 2',7'-dichlorofluorescin diacetate (DCF-DA) showed that

DAz-2 treatment does not increase intracellular ROS levels (Figure 3.6a). In addition, no difference in the ratio of reduced to oxidized glutathione (GSH/GSSG) was found between untreated and DAz-2 treated cells (Figure 3.6b). Moreover, no increase in the inactive forms of PrxI-IV, detected using anti-Prx-SO3 antibodies that recognize both sulfinic and sulfonic forms of over-oxidized Prx *[39]*, was observed over the course of DAz-2 treatment (Figure 3.5a). Lastly, trypan blue exclusion studies confirm that cell viability was not significantly affected by incubation with 5 mM DAz-2 in the time frame analyzed at 37 °C (Figure 3.6c). Taken together, the data indicate that DAz-2 treatment does not trigger endogenous oxidative stress or cell death.

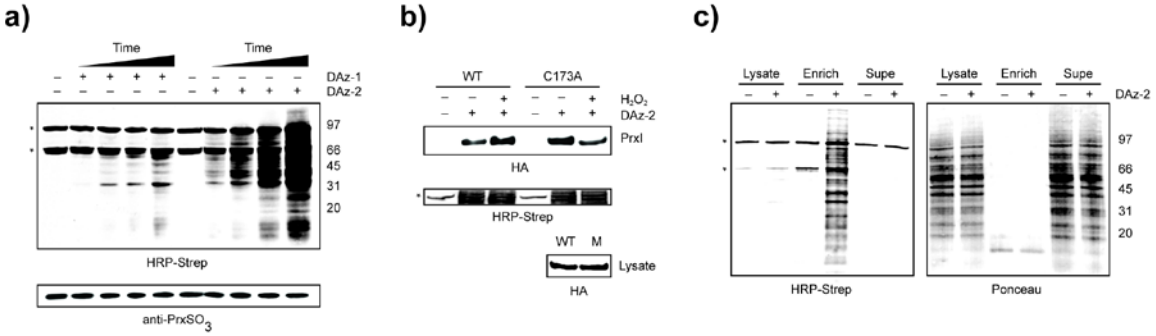

Figure 3.5 DAz-2 exhibits increased sensitivity for sulfenic acids in living cells. (a) Comparison of cellular sulfenic acid detection by DAz-1 and DAz-2. HeLa cells were treated with DAz-1 (5 mM), DAz-2 (5 mM), or DMSO (2% v/v) for 0.5, 1, 1.5, and 2 h at 37 °C, harvested in lysis buffer (see Methods) and processed as described for Figure 3.2a above. In order to examine endogenous oxidative stress, the Western blot was reprobed using an antibody that recognizes the sulfinic and sulfonic acid forms of Prxs I-IV (see Methods). (b) DAz-2 detects sulfenic acid modification of wild-type and C173A PrxI directly in cells. HeLa cells expressing FLAG and HA epitope-tagged wild-type or C173A PrxI were treated with or without H_2O_2 (400 μM) for 15 min at rt and then with DAz-2 (5 mM) or DMSO (1% v/v) for 2 h at 37 °C. Cells were harvested in lysis buffer and processed as described in Figure 2c above, except that anti- FLAG was replaced by anti-HA antibody. (c) Representative example of enrichment of proteins labeled by DAz-2 in cells. HeLa cells were treated with DAz-2 (5 mM) or DMSO (1% v/v), processed as described in Figure 3.2c above and detected by HRP-streptavidin Western blot. The asterisk marks proteins that are endogenously biotinylated.

Next, we investigated whether DAz-2 could monitor changes in the cellular oxidation state of the thiol peroxidase, PrxI. Cells expressing epitope-tagged PrxI or a C173A variant (predicted to

stabilize the sulfenic acid intermediate at the peroxidatic cysteine [37]) were untreated or exposed to H_2O_2, probed with DAz-1 or DAz-2 and subjected to the enrichment procedure outlined above. Immobilized proteins were then analyzed by Western blot using a monoclonal anti-HA antibody and HRP-streptavidin (Figure 3.3 and Figure 3.5b). In DAz-2-treated cells, the

amount of wild-type PrxI isolated on solid phase paralleled the increase in H_2O_2 concentration, as expected (Figure 3.5b). This trend was reversed in PrxI C173A, which exhibited a more intense labeling relative to the wild-type enzyme in the absence of exogenous oxidant, consistent with an increase in basal oxidation level in the variant protein (Figure 3.5b). DAz-2 incorporation in PrxI C173A decreased in cells exposed to H_2O_2 (Figure 3.5b). These findings suggest that in the absence of a resolving cysteine the peroxidatic cysteine overoxidizes to the sulfinic and sulfonic acid forms, which are not detected with dimedone-based probes. Collectively, these results establish that DAz-2 is capable of detecting changes in the oxidation state of PrxI in cells.

3.3.4 Global detection and proteomic analysis of sulfenic acid-modified proteins in cells

Having demonstrated the improved potency of DAz-2 labeling *in vitro* and in cells, we proceeded to use the reagent for global detection and proteomic analysis of sulfenic acid-modified proteins. HeLa human tumor cells were chosen for these studies owing to their routine use in culture and high intrinsic level of oxidative stress, which is thought to drive cell proliferation and immortalization [40]. To identify sulfenic acid-modified proteins, cells were treated with DAz-2 and azide-tagged proteins were subjected to Staudinger ligation using p-Biotin and subsequently purified by NeutrAvidin beads. Labeled proteins were separated by SDS-PAGE, digested in-gel with trypsin, extracted and the resulting peptides were subjected to LC-MS/MS analysis for

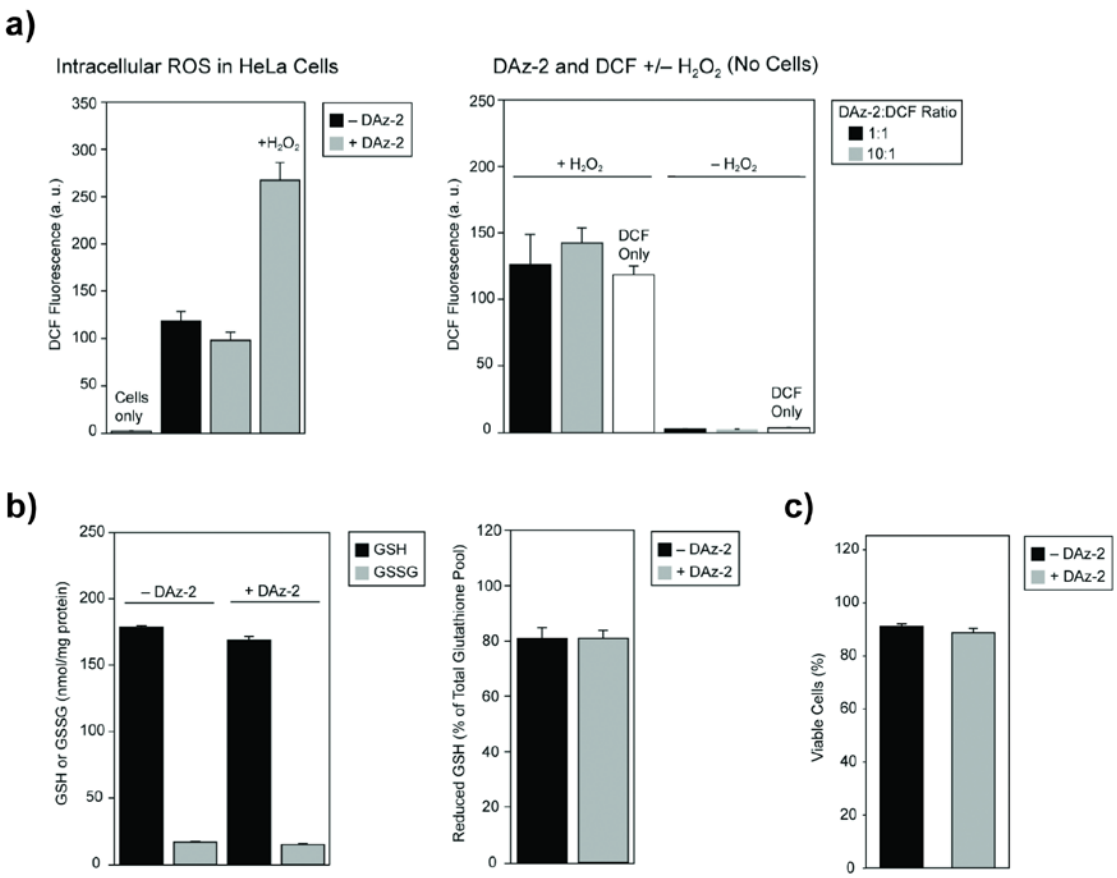

Figure 3.6 DAz-2 treatment does not trigger endogenous oxidative stress or cell death. (a) DAz-2 treatment does not increase intracellular ROS in HeLa cells. Left Panel: HeLa cells were treated with DAz-2 (5 mM) or DMSO (1% v/v) for 2 h at 37 °C. Additionally, HeLa cells were treated with DAz-2 (5 mM) for 2 h at 37 °C and then exposed to H_2O_2 (400 μM). In subsequent steps, cells were washed and loaded with DCF-DA (10 μM in PBS). Fluorescence emission was monitored at 525 nm after excitation at 488 nm over the course of 30 min. Bars represent fluorescence intensity and are the means +/−SEM of three determinations. Right Panel: Fluorescence intensity of DCF (10 μM in PBS), DCF (10 μM in PBS) with 400 μM H_2O_2, DCF (10 μM in PBS) with DAz-2 (10 μM or 100 μM), and DCF (10 μM in PBS) with DAz-2 (10 μM or 100 μM) and 400 μM H_2O_2. Bars represent fluorescence intensity and are the means +/−SEM of three determinations. (b) DAz-2 treatment does not change the GSH/GSSG ratio in HeLa cells. Cells were treated with DAz-2 (5 mM) or DMSO (1% v/v) for 2 h at 37 °C. Lysates were prepared and levels of reduced and oxidized glutathione were measured using the Glutathione Assay kit (cat. no. 703002, Cayman Chemicals) according to the manufacturer's instructions. Bars represent nmoles of GSH or GSSG per mg of protein (left panel), or the percentage of the total glutathione present in the reduced form (right panel) and are the means +/−SEM of two determinations. The GSH/GSSG ratios for DAz-2 and DMSO-treated samples were 8.7 +/− 1.6 and 8.8 +/− 2.2, respectively. (c) DAz-2 treatment does not decrease HeLa cell viability. HeLa cells were treated with DAz-2 (5 mM) or DMSO (1% v/v) for 2 h at 37 °C and then analyzed for trypan blue exclusion. Bars represent the percentage of trypan blue negative (viable) cells and are the means +/−SEM of three determinations.

protein identification. Figure 3.5c shows a representative example of affinity-purified proteins obtained from DAz-2 versus mock-treated cells. A protein sequence database search using the MS/MS data led to the identification of 193 proteins (Table 3.1 and Appendix 3.6.1) with a diverse range of biological functions (Figure 3.7a), cellular distribution and abundance. Of these candidate proteins 44% (85 of 193) are known to harbor redox-active cysteine residues subject to disulfide, glutathionyl, nitrosyl, or sulfenic acid modification (or some combination thereof) (Figure 3.7b) [25,41-52]. Among the 44% known redox-active proteins, 16% (14 of 85) have been confirmed to undergo sulfenic acid modification, including PrxI and GAPDH (Figure 3.7b) [17,37]. The identification of proteins previously known to have redox-active cysteines confirms the ability of DAz-2 for efficient isolation and identification of sulfenic acid modifications. To the best of our knowledge, the remaining 56% (108 of 193) of candidates identified in our study have not been previously established as having redox-active cysteines. Finally, 93% (179 of 193) were previously unknown to undergo sulfenic acid modification (Figure 3.7b).

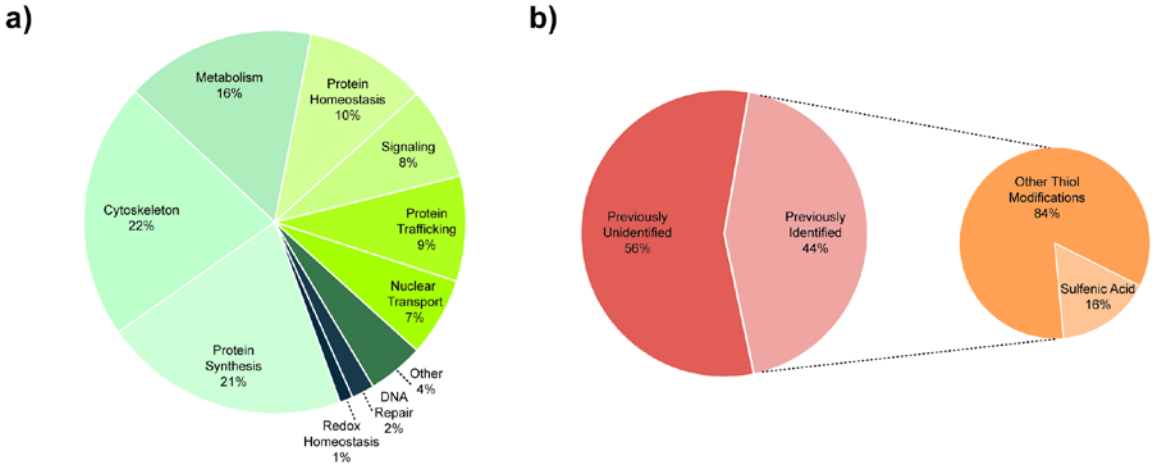

Figure 3.7 Analysis of candidates identified in our proteomic experiments with HeLa cells. (a) Percentage of candidates previously identified as having redox-active cysteines that undergo oxidation to sulfenic acid or other oxidative cysteine modifications including disulfide, S-glutathionylation and S-nitrosylation. (b) All candidates grouped on the basis of protein function. Because some proteins are involved in multiple processes, some generalizations were necessary.

3.3.5 *In vitro* validation of selected candidate proteins

Table 3.1 Abbreviated list of identified proteins with sulfenic acid modifications in HeLa cells. [a]

Protein	Location[b]	Function	Previous Identification[c]	Reference
		DNA Repair		
Ku80	N	Double-stranded DNA damage repair, helicase		
MCM6	N	DNA replication initiation		
80 kDa MCM3-associated protein	C,N	DNA replication, acetyltransferase		
		Metabolism		
Amino acid transporter E16	C,PM	Cationic amino acid transporter		
Catechol-O-methyltransferase	C,PM	Transfers methyl group from SAM to catecholamines		
C1-tetrahydrofolate synthase	C,M	One-carbon metabolism		
Glyceraldehyde-3-phosphate dehydrogenase	C	Glycolysis	X	(*17, 46, 50, 52, 62*)
Glucosidase alpha	ER,G	N-glycan biosynthesis		
Iron-sulfur protein assembly 1 homolog	C,N	Iron-sulfur cluster assembly, transcription regulator	X	(*52*)
Neutral amino acid transporter B	PM	Neutral amino acid transporter		
		Nuclear Transport		
Importin 9	C,N	Regulates nuclear transport and interacts with PP2A		
Karyopherin beta 1	C,N	Interacts with protein nuclear localization signals		
Ran	C,N	Regulates nuclear transport and DNA synthesis	X	(*52, 113*)
		Protein Homeostasis		
Calnexin	ER	Ca^{2+} binding, ER chaperone		
Calreticulin	C,ER,N	Ca^{2+} binding, ER chaperone, regulator of transcription	X	(*43*)
ER-Golgi intermediate compartment protein 1	ER,G	Upregulates protein turnover		
Hsp75 (TRAP1)	M	Mitochondrial chaperone		
Hsp90-Alpha	C	Stress-inducible chaperone	X	(*61*)
Ubiquitin-activating enzyme E1	C,N	Catalyzes the first step in ubiquitin conjugation	X	(*114*)
		Protein synthesis		
Gln-tRNA synthetase	C	Protein synthesis and biogenesis of rRNA	X	(*46*)
hnRNP U protein	N	mRNA splicing		
Met-tRNA synthetase	C,NU,PM	Protein synthesis and biogenesis of rRNA		
Ribosomal protein S3	C,N	Protein synthesis and regulator of DNA repair		
Ribosomal protein S6	C,N,NU	Protein synthesis and TOR signaling		
Thr-tRNA synthetase	C	Protein synthesis and biogenesis of rRNA		
U2 small nuclear RNA auxiliary factor 1	N	mRNA splicing		
		Redox Homeostasis		
Glutathione transferase Mu 3	C	Detoxification of electrophiles by conjugation to glutathione	X	(*48*)
Peroxiredoxin I	C,N	Peroxide catabolism and regulator of cell proliferation	X	(*37, 43, 48*)

To further confirm that our methodology targets sulfenic acid-modified proteins labeled by DAz-2 in cells, we examined the ability of the azido-probe to detect oxidation in two candidates – Rab1a and calreticulin. Rab1a is a small GTPase that regulates protein transport between the Golgi and endoplasmic reticulum (ER) [53]. The primary sequence of Rab1a contains four

Table 3.1 Abbreviated list of identified proteins with sulfenic acid modifications in HeLa cells.

Protein	Location[b]	Function	Previous Identification[c]	Reference
		Signaling		
Aspartyl beta-hydroxylase	ER	Hydroxylates aspartic acid residues in EGF-like domains		
Cardiotrophin-like cytokine factor 1	S	Cytokine-mediated signaling		
IQGAP1	C,PM	Regulates small GTPase activity		
G protein, beta polypeptide 2	C,PM	Regulatory heterotrimeric G protein subunit		
PI-3-kinase, catalytic subunit	C,M	Phosphorylates 3'-hydroxyl of inositol		
Protein GPR107	PM	G-protein coupled receptor		
Protein phosphatase PP1, catalytic subunit	C	Dephosphorylates serine and threonine residues		
SH2 domain-containing adapter protein F	C	Phosphotyrosine recognition		
		Vesicle Transport		
Rab1a	C,ER,G	Regulates ER to Golgi vesicle transport		
Rab10	C,G,PM	Regulates vesicle traffic through early endosomes		
Rab33b	C,G	Modulates autophagosome formation		

[a] Peptides from proteins with probability values of $P \leq 0.05$ were considered statistically significant.
[b] C, cytoplasm; ER, endoplasmic reticulum; G, golgi; M, mitochondria; N, nucleus; NU, nucleolus; PM, plasma membrane; S, secreted.
[c] Previous identification as redox-active whether oxidized or S-thiolated (with corresponding references).

cysteine residues (Cys26, Cys126, Cys204 and Cys205). Of these, two are constitutively geranylgeranylated in cells (Cys204 and Cys205) [54], which leaves the remaining two residues, Cys26 and Cys126, as potential targets for oxidation. Experiments were performed with a variant form of Rab1a lacking the -XXCC prenylation motif, which was produced in bacteria and purified to homogeneity (hereafter referred to as wild-type Rab1a). When oxidized protein was reacted with DAz-2, an intense signal was observed by HRP-streptavidin Western blot analysis (WT, Figure 3.8a), which establishes that Rab1a undergoes sulfenic acid modification. To identify the site or sites of modification, we explored a panel of Rab1a variants – C26A, C126A and the C26A, C126A double mutant (DM) – in further detail (Figure 3.8a). Oxidized Rab1a proteins were treated with DAz-2 and probe incorporation was assessed, as described above (Fig 3.8a). Protein labeling was observed for C26A and C126A Rab1a. However, the C126A variant showed a substantial decrease in labeling relative to wild-type and C26A Rab1a. Removal of Cys26 and Cys126 abolished DAz-2 incorporation and control reactions with protein

minus DAz-2 gave no background signal, as expected. Together, these data show that Rab1a undergoes sulfenic acid modification at Cys126 and, to a lesser extent, at Cys26. Next, we investigated sulfenic acid formation in the candidate protein calreticulin, a multi-functional calcium-binding chaperone in the ER that functions in quality control and folding of newly-synthesized (glyco)proteins [55]. The primary sequence of calreticulin contains three conserved cysteines, two of which form a disulfide bridge. Based on homology modeling with a related chaperone, calnexin [56], the remaining cysteine resides in the globular N-terminal domain, which interacts with newly synthesized protein substrates. Experiments were performed with commercially available calreticulin owing to the difficulty of production in bacteria. Labeling of calreticulin by DAz-2 in the absence of exogenously added peroxide was observed (Figure 3.8b), indicating the redox-sensitive cysteine was already modified to sulfenic acid. Exposure to high concentrations of H_2O_2 abolished

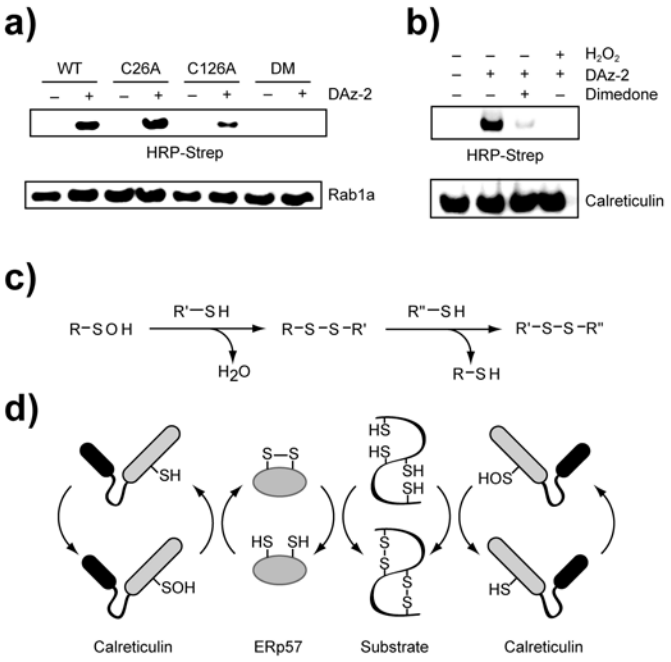

Figure 3.8 In vitro validation of DAz-2 labeling in selected candidates, Rab1a and calreticulin, and hypothetical role for oxidizied calreticulin in protein folding. (a) Rab1a undergoes sulfenic acid modification at C26 and C126. Oxidized wild-type and cysteine variants of Rab1a (10 μM) were treated with DAz-2 (1 mM) or DMSO (10% v/v) for 15 min at rt and processed as described for Figure 2a above. (b) DAz-2 detects sulfenic acid modification of calreticulin. Protein (1 μM) was treated with dimedone (10 mM), H_2O_2 (1 mM), or buffer for 0.5 h at rt and then with DAz-2 (1 mM) or DMSO (10% v/v) for 15 min at rt. Reactions were processed as described for Figure 2a above. (c) Sulfenic acids can condense with a nearby cysteine thiolate to generate a disulfide, which is then subject to thiol-disulfide exchange. (d) Oxidized calreticulin may drive protein folding by promoting disulfide formation in ERp57 (left). Alternatively, oxidized calreticulin could directly promote disulfide formation in target proteins (right).

labeling of calreticulin (presumably due to overoxidation to sulfinic and sulfonic acid) and pre-treatment with dimedone, prior to the addition of azido-probe, produced a significant reduction in signal. Taken together, these results establish that Rab1a and calreticulin undergo sulfenic acid modifications that can be detected by DAz-2 *in vitro* and further confirm our findings in living cells.

3.4 Discussion

Redox-active cysteine residues are highly conserved in protein sequences and are present in all three domains of life: eukaryotes, prokaryotes and archaea. A recent and particularly elegant computational study predicts redox-active cysteines in 10,412 unique sequences among all completed genomes, which can be further organized into 40 protein families and superfamilies with significant functional diversity [57]. A small amount of these proteins are known to undergo sulfenic acid modification *in vitro*, which raises a fundamental question: can all redox-active cysteines in proteins be modified to sulfenic acid? Most certainly, the answer to this question depends on contextual factors such as environment as well as the nature of the oxidant and its concentration. An important follow-up question is: of the cysteines that undergo sulfenic acid modification, which of these modifications have functional relevance in cells? Pivotal roles for sulfenic acid modification in redox-regulated signal transduction have been proposed by many [2,7,8], however, progress in this area, and the investigation of other cysteine oxoforms, has been limited due in large part to the lack of chemical tools to trap and tag labile, oxidative modifications directly in cells. Clearly, then, addressing the questions posed above requires us to devise new methods for sulfenic acid detection. Recent technological advances in detection of cellular ROS underscores the promise of selective and live cell-compatible reagents to broaden our understanding of redox-signaling pathways [58].

Inspired by earlier chemical approaches [17,27,59,60], the development of DAz-1 represented an important step forward in cellular sulfenic acid detection [30,31]. However, the modest reactivity of DAz-1 made the reagent less suited for global proteomic studies. For this reason we designed and synthesized DAz-2, a cell-permeable probe that detects sulfenic acids more effectively *in vitro* (Figure 3.2) and in living cells (Figure 3.5). Differences in reactivity between DAz-1 and DAz-2 could be due to several factors including polarity, nucleophilicity, and stability of the probes. The logP values of DAz-1 and DAz-2 are 0.02 and 0.5, respectively (see Methods) and thus, the increased hydrophobicity of DAz-2 could enhance its membrane permeability. It is also possible that the decreased polarity and size of DAz-2 could facilitate access to partially buried protein sulfenic acids. The nucleophilic carbons in DAz-1 and DAz-2 have almost identical ^{13}C NMR chemical shifts (103.5 and 103.4 ppm, respectively), indicating similar electronic environments. Lastly, the amide bond of DAz-1 could be cleaved by cellular amidases and thus, preclude Staudinger ligation. Additional experiments, including a detailed analysis of the reaction mechanism, will be required to identify the precise factors that underlie the observed differences in reactivity.

Using DAz-2 and the strategy outlined in Figure 3.1, we conducted global proteomic analysis of the sulfenome in the HeLa tumor cell line. This study resulted in the identification of 193 proteins (Table 3.1 and Appendix 3.6.1, Figure 3.9a) including the majority of known sulfenic acid-modified proteins – 14 in total, with more than 175 new candidates (Table 3.1 and Appendix 3.6.1), with further verification in Rab1a and calreticulin candidate proteins (Figure 3.8a and b). The newly identified proteins have roles in signal transduction, DNA repair,

metabolism, protein synthesis, redox homeostasis, nuclear transport, vesicle trafficking, and ER quality control (Figure 3.7a), which suggest broad cellular manifestations of this oxidative modification. The implications of these findings will be discussed in turn.

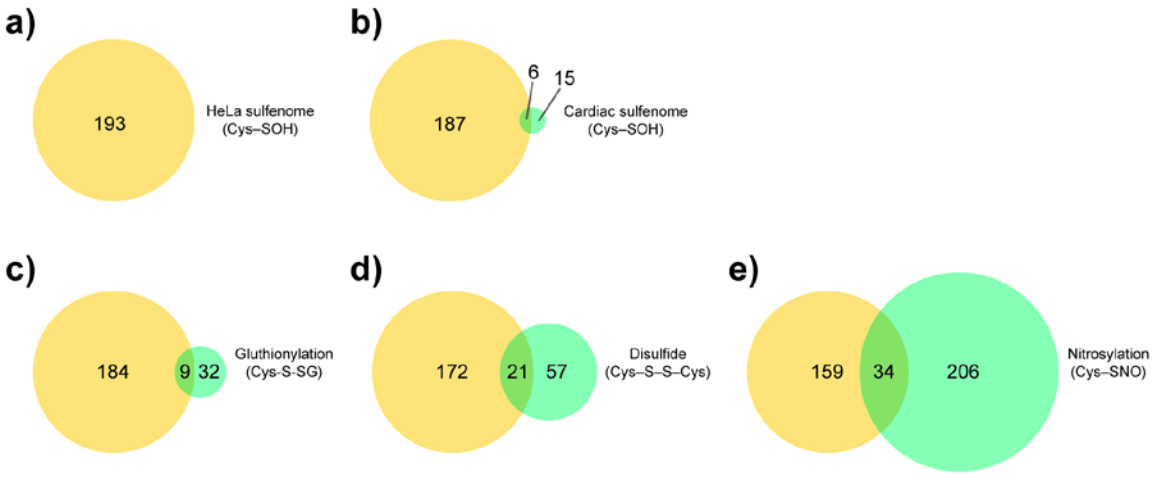

Figure 3.9 Venn diagram of proteins sensitive to sulfenic acid formation in HeLa cells (a) compared to prior sulfenic acid (25) (b), disulfide (45) (c), S-glutathionylation (46) (d), and S-nitrosylation (48) (e) proteomic studies. The circle area is proportional to the number of proteins identified in each study.

3.4.1 Comparative analysis of related modifications and proteomic studies

The Venn diagrams in Figure 3.9 provide a comparative analysis of overlap among candidate proteins identified in the current study to those reported in previous redox thiol proteomic studies [25,42,44,46].[1] Using a biotinylated derivative of dimedone, Charles *et al.* identified a

[1] For the sake of comparison, mammalian studies reporting the largest compendium of proteins in each category of modification are included in Figure 3.9. Many other excellent thiol redox proteomic studies have been reported [25. Charles RL, Schroder E, May G, Free P, Gaffney PR, Wait R, Begum S, Heads RJ, Eaton P: **Protein sulfenation as a redox sensor: proteomics studies using a novel biotinylated dimedone analogue**. *Mol Cell Proteomics* 2007, **6**:1473-1484, 41. Brennan JP, Miller JI, Fuller W, Wait R, Begum S, Dunn MJ, Eaton P: **The utility of N,N-biotinyl glutathione disulfide in the study of protein *S*-glutathiolation**. *Mol Cell Proteomics* 2006, **5**:215-225, 42. Brennan JP, Wait R, Begum S, Bell JR, Dunn MJ, Eaton P: **Detection and mapping of widespread intermolecular protein disulfide formation during cardiac oxidative stress using proteomics with diagonal electrophoresis**. *J Biol Chem* 2004, **279**:41352-41360, 43. Cumming RC, Andon NL, Haynes PA, Park M, Fischer WH, Schubert D: **Protein disulfide bond formation in the cytoplasm during oxidative stress**. *J Biol Chem* 2004, **279**:21749-21758, 44. Fratelli M, Demol H, Puype M, Casagrande S, Eberini I, Salmona M, Bonetto V, Mengozzi M, Duffieux F, Miclet E, et al.: **Identification by redox proteomics of glutathionylated proteins in oxidatively stressed human T lymphocytes**. *Proc Natl Acad Sci U S A* 2002, **99**:3505-3510, 45. Greco TM, Hodara R, Parastatidis I, Heijnen HF, Dennehy MK, Liebler DC, Ischiropoulos H: **Identification of *S*-nitrosylation motifs by site-specific mapping of the *S*-nitrosocysteine proteome in human vascular smooth muscle cells**. *Proc Natl Acad Sci U S A* 2006, **103**:7420-7425, 46. Lefievre L, Chen Y, Conner SJ, Scott JL, Publicover SJ, Ford WC, Barratt CL: **Human spermatozoa contain**

collection of 21 cytoskeletal and metabolic proteins in peroxide-treated rat ventricular myocytes that undergo sulfenic acid modification [25]. Of these proteins, six out of the 19 whose expression is not confined to cardiac tissue were also identified by our study, providing independent verification and validation for these candidates (Figure 3.9b). Addition of a biotin tag to dimedone precludes membrane permeability [31,59,60] and may account for the relatively modest number of proteins identified in this prior study [25].

Many redox-active cysteines undergo more than one kind of oxidative modification [61]. We therefore compared candidates identified in this study with *S*-glutathionyl [44] (Figure 3.9c), disulfide [42] (Figure 3.9d), and *S*-nitrosyl [46] (Figure 3.9e) proteomes in eukaryotic cells. *S*-glutathionylation is another physiological, reversible modification of protein cysteine residues defined by the addition of the tripeptide glutathione (GSH) to form a mixed disulfide (Cys-S-SG) [66]. *S*-glutathione adducts are hypothesized to protect cysteine residues from overoxidation and can be formed *via* many routes including attack of a redox-active cysteine on oxidized glutathione (GSSG) or condensation of a protein sulfenic acid with GSH [67]. Assessment in human T lymphocytes using ^{35}S-labeled glutathione revealed 41 proteins with *S*-glutathione modifications [44] and 9 of these proteins overlapped with candidates identified in the current

---

multiple targets for protein *S*-nitrosylation: an alternative mechanism of the modulation of sperm function by nitric oxide? *Proteomics* 2007, **7**:3066-3084, 48. Baty JW, Hampton MB, Winterbourn CC: **Proteomic detection of hydrogen peroxide-sensitive thiol proteins in Jurkat cells**. *Biochem J* 2005, **389**:785-795, 50. Eaton P, Byers HL, Leeds N, Ward MA, Shattock MJ: **Detection, quantitation, purification, and identification of cardiac proteins *S*-thiolated during ischemia and reperfusion**. *J Biol Chem* 2002, **277**:9806-9811, 51. Gao C, Guo H, Wei J, Mi Z, Wai PY, Kuo PC: **Identification of *S*-nitrosylated proteins in endotoxin-stimulated RAW264.7 murine macrophages**. *Nitric Oxide* 2005, **12**:121-126, 52. Le Moan N, Clement G, Le Maout S, Tacnet F, Toledano MB: **The Saccharomyces cerevisiae proteome of oxidized protein thiols: contrasted functions for the thioredoxin and glutathione pathways**. *J Biol Chem* 2006, **281**:10420-10430, 61. Ghezzi P, Bonetto V, Fratelli M: **Thiol-disulfide balance: from the concept of oxidative stress to that of redox regulation**. *Antioxid. Redox Signal.* 2005, **7**:964-972, 62. Hao G, Derakhshan B, Shi L, Campagne F, Gross SS: **SNOSID, a proteomic method for identification of cysteine *S*-nitrosylation sites in complex protein mixtures**. *Proc Natl Acad Sci U S A* 2006, **103**:1012-1017, 63. Leichert LI, Gehrke F, Gudiseva HV, Blackwell T, Ilbert M, Walker AK, Strahler JR, Andrews PC, Jakob U: **Quantifying changes in the thiol redox proteome upon oxidative stress in vivo**. *Proc Natl Acad Sci U S A* 2008, **105**:8197-8202, 64. McDonagh B, Ogueta S, Lasarte G, Padilla CA, Barcena JA: **Shotgun redox proteomics identifies specifically modified cysteines in key metabolic enzymes under oxidative stress in Saccharomyces cerevisiae**. *J. Proteomics* 2009, **72**:677-689, 65. Saurin AT, Neubert H, Brennan JP, Eaton P: **Widespread sulfenic acid formation in tissues in response to hydrogen peroxide**. *Proc Natl Acad Sci U S A* 2004, **101**:17982-17987.] and are included, as appropriate, in Table 3.1 and Appendix 3.6.1.

study (Figure 3.9c). Disulfide bonds are formed from the oxidation of two thiol groups (Cys–S–S–Cys) and play an important role in folding and stability of proteins that reside in oxidizing environments [61]. In addition, reversible disulfide bond formation serves a regulatory function in many proteins, including transcription factors [9,68]. Proteomic analysis of intermolecular disulfide formation in rat ventricular myocytes *via* two-dimensional PAGE analysis identified 78 candidates [42], 21 of which are present in the current study (Figure 3.9d). A complementary study reported by Cumming *et al.* looking at both intra- and inter-molecular disulfide formation in HT22 cells identified 47 candidate proteins [43], 19 of which were also found in the current study. Finally, *S*-nitrosylated proteins (Cys–SNO) form when cysteine reacts with nitric oxide in the presence of an electron acceptor and in transnitrosylation reactions [69,70]. Similar to H_2O_2, nitric oxide has been identified as second messenger in signal transduction cascades and modulates many biological processes [71,72]. A recent investigation of *S*-nitrosylation in human spermatozoa using the ascorbate-mediated biotin switch technique identified 240 candidate proteins [46], 34 of which were also identified in the present study (Figure 3.9e).

As illustrated by the comparisons above, a subset of the proteins identified in our study undergo an array of oxidative cysteine modifications. For example, the glycolytic enzyme GAPDH has been found in virtually all redox proteomic studies reported to date (Table 3.1), which indicates a high level of promiscuity in oxidative cysteine modification for this protein. However, it is also important to emphasize that not all cysteine residues in proteins are readily oxidized and not all low pK_a thiols undergo multiple modifications [73]. Indeed, the majority of proteins in the current study have not been identified in *S*-glutathionyl, disulfide, or *S*-nitrosyl proteomic studies (Table 3.1 and Appendix 3.6.1, Figure 3.7b). Although much remains to be understood

about the features of a cysteine residue that favor oxidation by H_2O_2, our data suggest that some proteins preferentially undergo sulfenic acid modification in cells. To this end, protein structure and cellular environment are likely to play a critical role in defining target specificity.

3.4.2 Protein candidates for sulfenic acid modification

The protein targets of sulfenic acid modification identified in this study are found in many cellular locations and have diverse roles in signal transduction, DNA repair, metabolism, protein synthesis, redox homeostasis, nuclear transport, vesicle trafficking, and ER quality control (Table 3.1 and Appendix 3.6.1, Figure 3.7a).

3.4.2.1 Signal transduction

Although considerable evidence implicates ROS as mediators of cellular signaling, the molecular mechanisms by which ROS alter these pathways are not well known. In receptor tyrosine kinase (RTK)-mediated signal transduction pathways, reversible inactivation of protein tyrosine phosphatases (PTPs) [7] and changes in the activity of kinases such as Src [74,75] have been accredited to tightly regulated growth factor and cytokine-stimulated ROS generation. In the present study, a number of proteins with pivotal roles in signal transduction have been identified as new candidates for redox-regulation (Table 3.1 and Appendix 3.6.1) such as phosphoinositide-3-kinase (PI3K) and IQGAP1, both of which are intimately connected to RTK signaling [76]. IQGAP1 is proposed to interact with the NADPH oxidase Nox2 to enhance ROS production in endothelial cells and, under conditions of oxidative stress, IQGAP1 localizes to the cell membrane where it regulates Src activity [77]. We have also identified serine/threonine-protein phosphatase (PP1), a regulatory protein downstream of PI3K in insulin signaling [78].

While oxidation of the active site cysteine in the family of PTPs has been well established [5,79], redox-regulation of serine/threonine phosphatases is not well understood [80].

3.4.2.2 DNA repair and replication

Recent studies estimate that ~2×10^4 ROS-related DNA damaging events occur in a typical human cell every day [81]. Given this statistic, it is perhaps not surprising that DNA repair proteins Ku80 and MCM6 were identified in this study (Table 3.1). *In vitro* studies have shown that Ku-DNA binding activity is redox-sensitive and requires reduced thiols [82,83]. However, no disulfide bonds have been observed in the crystal structure of free Ku or the Ku-DNA complex *[84]*. It light of our findings, it is possible that oxidation of key cysteine(s) in Ku80 to sulfenic acid, and possibly higher states, may regulate DNA binding activity. To our knowledge, oxidative modification of mini-chromosome maintenance (MCM) proteins has not been previously reported and additional studies will be required to elucidate the potential role of cysteine oxidation in these proteins.

3.4.2.3 Metabolism

Glycolytic enzymes such as aldolase, enolase, pyruvate kinase, and GAPDH were identified in the present study (Table 3.1 and Appendix 3.6.1). GAPDH, pyruvate kinase and other glycolytic enzymes have also been identified in a proteomic study of low pK_a cysteines [64]. Oxidative inactivation of GAPDH is proposed to function as a cellular switch to redirect carbohydrate flux and promote generation of the reduced electron carrier nicotinamide adenine dinucleotide phosphate (NADPH), an important cofactor for cellular antioxidant enzymes [85].

3.4.2.4 Protein synthesis

Studies in yeast show that oxidative stress causes the dissociation of actively translating ribosomes and that this response is mediated, in part, by the mitogen-activated protein kinase protein kinase, Rck2 [86]. On the other hand, i*n vitro* translation studies show that direct exposure of translational machinery to oxidants such as H_2O_2 increases the rate of protein synthesis [87]. In the present study, we have identified a subset of ribosomal proteins and aminoacyl tRNA synthetases as candidates for sulfenic acid modification (Table 3.1 and Appendix 3.6.1). Ribosomal proteins of the 40S and 60S subunits and heterogeneous nuclear ribonucleoproteins (hnRNPs) are predicted to harbor redox-active cysteines in their RNA recognition motifs [49]. However, oxidation of these residues has not been verified experimentally. Another recent study of reversibly oxidized proteins in yeast uncovered redox-active cysteines in elongations factors and components of the 60S ribosomal complex [64]. These data provide independent confirmation for the candidates in the current study and suggest that cysteine oxidation may play an important regulatory role in protein synthesis.

3.4.2.5 Redox homeostasis

Two proteins with known roles in redox homeostasis were identified in our study: the antioxidant enzyme PrxI and glutathione S-transferase (GST), a detoxifying protein that catalyzes the conjugation of reduced glutathione to electrophilic agents in the cell (Table 3.1) [88]. GST is known to form intermolecular disulfides in response to oxidative stress inactivating its normal maintenance functions [89]. Disulfide formation in GST might be accelerated by condensation

of the sulfenic acid or this modification may serve a different function altogether. By contrast, the ubiquitous thioredoxin (Trx) and glutaredoxin (Grx) antioxidant enzymes, which also harbor reactive cysteines, were not identified in this study. It is possible that intramolecular disulfide formation between the cysteines in their CXXC redox active site motifs outcompetes reaction of DAz-2 with the sulfenic acid form of these proteins.

3.4.2.6 Nuclear transport

Numerous *in vitro* and cellular studies show that oxidative stress disrupts nuclear transport [90-93] and Ran, a regulatory GTPase, has two redox-active cysteine residues (C85 and C120) that undergo nitrosylation *in vitro* [91]. In support of these prior observations we have identified Ran as a protein that undergoes sulfenic acid modification in cells (Table 3.1). Additional candidate proteins with roles in nuclear import and export were identified (Table 3.1 and Appendix 3.6.1) including transportin 1, a member of the importin-β family, previously found in a disulfide proteomic study [43].

3.4.2.7 Vesicle trafficking

In this study we also identified a subset of Rab GTPase proteins, which function as key regulators of vesicle transport in eukaryotes (Table 3.1 and Appendix 3.6.1) [94]. The Rab family of proteins (~60 in encoded the human genome) is part of the Ras superfamily of small GTPases. Previous work shows Ras can be *S*-nitrosylated and *S*-glutathionylated within a conserved NKCD motif, leading to an increase in Ras activity and to downstream signaling [95,96]. Another sequence motif – GXXXXGK(S/T)C – is subject to oxidation in the related Rho GTPase [97]. In our

study, we identified a total of ten Rab GTPases. Among these, five possessed the NKCD motif and nine contained the GXXXXGK(S/T)C motif. Additional experiments performed with recombinant Rab1a, which harbors both sequence motifs above, confirmed sulfenic acid modification of both cysteines, Cys26 and Cys126 in the GXXXXGK(S/T)C and NKCD motifs, respectively (Figure 3.8a). While both single variants exhibited DAz-2 labeling, C126A exhibited the greatest decrease in modification (Figure 3.8a). It is possible that cysteine oxidation in Rab GTPases might regulate membrane association by modulating their catalytic cycle and/or protein-protein interactions *via* modification-associated conformational changes.

3.4.2.8 Chaperone-mediated protein folding

Chaperone proteins belonging to the major 90, 70, and 60 kDa families were also identified as targets of DAz-2 in cells (Table 3.1 and Appendix 3.6.1). No prior evidence of sulfenic acid modifications of these proteins exists, however, and a subset of these proteins have been reported to undergo *S*-nitrosylation [46]. Overexpression of Hsp75 is associated with a decrease in ROS production and helps maintain mitochondrial membrane potential during glucose deprivation of astrocytes [98]. Hsp70 and Hsp90 possess a redox-sensitive cysteine in close proximity to their ATP binding pockets [99] and, under conditions of oxidative stress, peptide binding to Hsp70 and complex stability are enhanced [100].

The molecular chaperones calnexin and calreticulin were also identified in our study. Additional experiments performed with calreticulin show that this chaperone contains a highly redox-active cysteine that undergoes sulfenic acid modification (Figure 3.8b). Although the precise site

of oxidation was not explored in the current study, the most likely candidate is the free cysteine C146 [101], located within the substrate-interacting N-terminal domain. Calreticulin interacts with the protein-disulfide isomerase homologue, ERp57 to promote oxidative folding of nascent glycoproteins in the ER lumen [102-104]. To date, however, the role of calreticulin in glycoprotein folding has been relegated solely to binding target proteins [55,105]. The presence of a redox-active cysteine in calreticulin suggests that this chaperone may play additional roles in protein folding and in promoting the formation of protein disulfides (Figure 3.8c and d). Sulfenic acids can condense with a nearby cysteine thiolate to generate a disulfide, which is then subject to thiol-disulfide exchange (Figure 3.8c). By extension, oxidized calreticulin might drive protein folding by promoting disulfide formation in ERp57, (Figure 3.8d, left). In support of this hypothesis, the yeast homologue of calreticulin, Cne1p enhances the activity of a yeast oxireductase Mpd1p *in vitro* [106]. Alternatively, oxidized calreticulin could directly promote disulfide formation in target proteins (Figure 5d, right). To this end, small angle X-ray studies show that calreticulin can dimerize to form an additional binding site capable of interacting with peptides [107]. We also note that calreticulin is also found in the nucleus, where it interacts with the DNA-binding domain of various nuclear receptors and modulates gene transcription [55]. Thus, it is possible that oxidation of redox-active cysteine residues in calreticulin might also modulate this particular cellular function.

3.5 Conclusion

In summary, we have described DAz-2, a new chemical tool for selective detection of protein sulfenic acids in cells. Using this reagent, we have conducted the first global proteomic study of proteins that harbor sulfenic acid modifications in cells. Candidates identified from this study are distributed in locations throughout the cell and function in a diverse array of biological

processes. These findings suggest that sulfenic acid modifications may play broader biological roles than previously thought and highlight the need for future research in this emerging field. The ability to detect protein sulfenic acid modifications in living cells provides a powerful strategy for mapping redox-regulated signaling networks in normal physiological functions and disease.

3.6 Experimental Procedures

3.6.1 Chemical Methods

All reactions were performed under an argon atmosphere in oven-dried glassware. Reagents and solvents were purchased from Sigma or other commercial sources and were used without further purification. Analytical thin layer chromatography (TLC) was carried out using Analtech Uniplate silica gel plates and visualized using a combination of UV and potassium permanganate staining. Flash chromatography was performed using silica gel (32–63 μM, 60Å pore size) from Sorbent Technologies Incorporated. NMR spectra were obtained on a Varian Inova 400 (400 MHz for ^{1}H; 100 MHz for ^{13}C). ^{1}H and ^{13}C NMR chemical shifts are reported in parts per million (ppm) referenced to the residual solvent peak. High-resolution electrospray ionization (ESI) mass spectra were obtained with a Micromass AutoSpec Ultima Magnetic sector mass spectrometer at the University of Michigan Mass Spectrometry Laboratory.

6-(3-azidopropyl)-3-ethoxycyclohex-2-enone (2)

Method A: To a solution of compound **3** (0.96 g, 4.8 mmol, synthesized as reported in [26]) in DCM (100 ml) was added triethylamine (2.67 ml, 19.1 mmol) and followed by methanesulfonyl chloride (1.31 ml, 19.1 mmol) at 0 °C. To this was added 4-dimethylaminopyridine (0.059 g, 0.5 mmol). The reaction was stirred for 2 h and concentrated *in vacuo*. The resulting syrup was dissolved in EtOAc (50 ml) and water (75 ml). The aqueous phase was partitioned EtOAc (3 x 50 ml) and the organic phases were combined, washed with water (50 ml), and dried over Na_2SO_4. The reaction mixture was concentrated *in vacuo*. To a solution of the resulting compound in DMF (25 ml) was added sodium azide (3.1 g, 47.7 mmol) and the reaction was warmed to 85 °C and stirred for 8 h. The reaction was concentrated *in vacuo* and diluted with water (75 ml). The aqueous phase was partitioned with EtOAc (4 x 50 ml). The organic phases were combined, washed with water (2x20 ml), dried over Na_2SO_4, and concentrated. The resulting syrup was purified by silica gel chromatography eluting with 8:2 hexanes:ethyl acetate to provide the title compound **2** (0.74 g, 3.3 mmol) in 70% yield as a yellow oil. **Method B:** To a lithium diisopropylamide (LDA) solution, prepared from diisopropylamine (0.082 ml, 2.2 mmol) and *n*-BuLi (0.78 ml of a 2.5 M solution in hexanes, 2 mmol) in anhydrous tetrahydrofuran (THF) (10 ml) at –78 °C under argon, was added compound **5** (0.139 g, 1.0 mmol) in THF (10 ml), dropwise, over 30 min. The reaction was stirred for an additional 30 min at -78 °C. Then hexamethylphosphoramide (HMPA, 0.17 ml, 1.0 mmol) was added, followed by the dropwise addition of 3-iodopropyl azide (**11)** (0.25 g, 1.2 mmol) in THF (10 ml). The reaction was allowed to warm to rt and stirred for 6 h. The reaction was quenched with water (10 ml) and NH_4Cl (20 ml). The aqueous phase was partitioned with DCM (3 x 25 ml), and the organic phases were combined, washed with brine (30 ml), dried over Na_2SO_4, and concentrated. The resulting syrup

was purified by silica gel chromatography eluting with 8:2 hexanes:ethyl acetate to provide the title compound **2** (0.031 g, 0.02 mmol) in 14% yield as a yellow oil. R_f: 0.24 (8:2 hexanes:ethyl acetate). ^{1}H NMR ($CDCl_3$, 400MHz): δ □5.29 (s, 1H), 3.88 (q, *J*=6.6, 2H), 3.29 (t, *J*=6.6, 2H), 2.42 (t, *J*=6.6, 2H), 2.23-2.17 (m, 1H), 2.06-2.00 (m, 1H), 1.87-1.80 (m, 1H), 1.77-1.69 (m, 1H), 1.67-1.45 (m, 3H), 1.32 (t, *J*=6.8, 3H). ^{13}C NMR ($CDCl_3$, 100MHz): δ 202.0, 177.2, 102.1, 64.3, 62.3, 44.7, 30.0, 28.1, 26.5, 25.5, 14.1. ESI-HRMS calcd. for $C_{11}H_{17}N_3O_2$ (M + H) 224.1399, found 224.1391.

6-(3-azidopropyl)-3-hydroxycyclohex-2-enone (1)

To a solution of **2** (0.74 g, 3.3 mmol) in acetonitrile (10 ml) and water (10 ml) was added CAN (0.18 g, 0.3 mmol). The solution was heated to reflux for 3 h. The reaction mixture was then diluted with brine (40 ml), and partitioned with EtOAc (4 x 35 ml). The organic phases were combined, washed with brine (30 ml), dried over Na_2SO_3, and concentrated *in vacuo*. The resulting orange solid was purified by silica gel chromatography eluted with 1:1 hexanes:ethyl acetate to give compound **1** as a pale yellow solid (0.58 g, 3.0 mmol) in 90% yield. R_f: 0.3 (1:1 hexanes:ethyl acetate). ^{1}H NMR ($(CD_3)_2SO$, 400MHz): δ □10.97 (s, 1H), 5.17 (s, 1H), 3.32 (t, *J*=6.8, 2H), 2.31 (s, 2H), 2.12 (s, 1H), 2.00-1.93 (m, 1H), 1.78-1.70 (m, 1H), 1.58-1.51 (m, 3H) 1.32 (s, 1H). ($(CD_3)_2SO$, 100MHz): δ 103.5, 51.0, 41.9, 29.4, 26.9, 26.2, 26.0. ESI-HRMS calcd. for $C_9H_{13}N_3NaO_2$ (M + Na) 218.0905, found 218.0895.

3.6.2 Cloning, expression, and purification of Rab1a.

Rab1a, cloned in to pET14b (Novagen) without a His6-tag was expressed and purified from *Escheria coli* strain BL21 (DE3) RIPL (Stratagene) as previously described [108]. C204S C205S Rab1a was generated by site-directed PCR with the following primers: 5'-CAGTCAGGTGGAGGTTCCTCCTAATGACTCGAGG-3' and 5'-CCTCGAGTCATTAGGAGGAACCTCCACCTGACTG-3'. Rab1a C26A, Rab1a C126A, and Rab1a C26A C126A using site-directed PCR mutagenesis with the following primers: 5'CAGGGGTTGGAAAGTCTGCGCTTCTTCTTAGGTTTGC-3' and 5'-GCAAACCTAAGAAGAAGCGCAGACTTTCCAACCCCTG-3' for C26A and 5'-CAACAAATTGTTGGTAGGGAACAAAGCGGATCTGACCAC-3' and 5'-GTGGTCAGATCCGCTTTGTTCCCTACCAACAATTTGTTG-3' for C126A. Successful cloning was confirmed by DNA sequencing analysis.

3.6.3 Cloning of FLAG and HA-tagged GAPDH and PrxI

Human PrxI and GAPDH coding sequences were prepared by PCR from pDNR-LIB (ATCC) and pCMV-SPORT6 vector (ATCC) containing the respective proteins. Amplification of PrxI was performed with forward primer 5′-AGGGATCCTCTTCAGGAAATGCTAAAATTGGGC-3′ and pcDNA3-FLAG-HA-PrxI was generated by subcloning PrxI into the BamHI and EcoRI sites of pcDNA3-FLAG-HA (Addgene 10792). Amplification of GAPDH was performed with forward primer: 5′-CCGGATCCGGGAAGGTGAAGGTCGGAGTCAACG-3′ and pcDNA3-FLAG-HA-GAPDH was generated by subcloning GAPDH into the BamHI and NotI sites in pcDNA3-FLAG-HA. The C173A PrxI mutant was generated using the following primers: 5′-GACAAACATGGGGAAGTGGCTCCAGCTGGCTGGAAACCT-3′ and 5′-

AGGTTTCCAGCCAGCTGGAGCCACTTCCCCATGTTTGTC-3′. Successful cloning was confirmed by DNA sequencing and Western blot analysis to confirm protein expression.

3.6.4 Transfection of GAPDH and PrxI

HeLa cells were transfected at 80% confluency with pcDNA3-FLAG-HA PrxI, pcDNA3-FLAG-HA-GAPDH or pcDNA3-FLAG-HA (3 μg) and Lipofectamine reagent (Invitrogen, 15 μl) for 5 h according to manufacturer guidelines. After transfection, cells were cultured in DMEM supplemented with 10% fetal bovine serum (FBS), 1% penicillin-streptomycin-L-glutamine (PSG) and 1% MEM non-essential amino acids (MEM-NEAA) and allowed to recover for 18 h prior to harvest.

3.6.5 Sulfenic acid detection in HeLa cells treated with hydrogen peroxide

HeLa cells transfected with C173A PrxI were washed with sterile PBS, trypsinized, neutralized with complete media then incubated with or without H_2O_2 (200 μM) for 15 min at rt in DMEM (0.5% FBS). The cells were then treated with DAz-2 (5 mM) or DMSO (1% v/v) for 2 h at 37 °C, washed with PBS (×3) and the lysate fraction generated. Protein concentrations were determined by Bradford assay and the proteins ligated with p-biotin (200 μM) and DTT (5 mM) for 2 h at 37 °C. The proteins were precipitated with cold acetone, resuspended in 0.2% SDS PBS and analyzed by Western blot. The membrane was probed with HRP-streptavidin (1:10,000) to detect modified proteins.

3.6.6 Measuring intracellular ROS concentrations in HeLa cells

Intracellular ROS was measured in HeLa cells as previously described [109]. Briefly, HeLa cells were washed with sterile PBS, trypsinized and the cell suspension neutralized with complete media. The cells were washed in DMEM (0.5% FBS), aliquoted (6×10^5/tube) and incubated with either DMSO (1% v/v) or DAz-2 (5 mM) for 2 h at 37 °C in DMEM (0.5% FBS). Additionally, HeLa cells were treated with DAz-2 (5 mM) for 2 h at 37 °C and then exposed to H_2O_2 (400 μM). Following incubation, cells were washed with sterile PBS (×2) and 1×10^5 cells from each reaction were apportioned into a 96-well plate. In subsequent steps, cells were washed and loaded with DCF-DA (10 μM in PBS). Fluorescence emission was monitored at 525 nm after excitation at 488 nm over the course of 30 min.

3.6.7 Quantification of total, reduced, and oxidized glutathione in HeLa cells

Reduced and oxidized levels of glutathione in HeLa cells were measured as previously described [110]. Briefly, HeLa cells were treated with DAz-2 (5 mM) or DMSO (1% v/v) for 2 h at 37 °C, as described above. A cell lysate was prepared and levels of reduced and oxidized glutathione were measured using the Glutathione Assay kit (cat. no. 703002, Cayman Chemicals) according to the manufacturer's instructions. GSH and GSSG concentrations are reported as nmol/mg protein (Figure 3.6b, left panel) and are comparable to values previously reported for HeLa cells [111]. When cells were treated were DAz-2, no significant change was observed in the percentage of the total glutathione present in the reduced form, as compared to the DMSO control sample (Figure 3.6b, right panel). The percentage of reduced GSH measured in our assays (81% ±3) agrees well with previously reported values for HeLa cells [112].

3.6.8 Trypan blue evaluation of cell viability

Cells were routinely evaluated for viability before and after incubation with DAz-2 (5 mM) or DMSO (1-5%) control. Briefly, HeLa cells were trypsinized and then resuspended in media containing 10% FBS. The cells were collected by centrifugation and resuspended in PBS. The cell suspension was mixed with an equal volume of trypan blue solution (0.4% w/v). After 3 min incubation at rt, 10 μL of the mixture was loaded onto a hemocytometer and then counted under a microscope.

3.6.9 LogP determination

Equal volumes (250 μL) of 1-octanol and water were equilibrated for 18 h. Afterwards, compound (200 μg) was added and the solution was mixed vigorously for 4 h at rt. Following mixing, samples were equilibrated for 0.5 h at rt and compound concentrations in 1-octanol and water were determined using UV-Vis spectroscopy.

3.6.10 Staudinger ligation

Staudinger ligation was carried out by incubation of purified protein or cell lysate (1 mg ml^{-1}) with p-Biotin (200 μM) and DTT (5 mM) for 2 h at 37 °C with agitation. Reactions in lysate were quenched by the addition of cold acetone (1 ml), incubated at –80 °C for 20 min and collected by centrifugation at 4 °C for 20 min (17,000 *g*). The protein pellet was washed once with cold

acetone (200 µl) and then re-suspended in 0.2% sodium dodecyl sulfate in phosphate-buffered saline (SDS-PBS).

3.6.11 Western blot

Biotinylated proteins were separated by SDS-PAGE using Criterion XT 4–12% Bis-Tris gels (BioRad) or NuPAGE Novex 4-12% Bis-Tris Midi gels (Invitrogen) and transferred to a polyvinylidene difluoride (PVDF) membrane (BioRad). After transfer, the PVDF membrane was blocked with 3% BSA or 5% milk in phosphate-buffered saline Tween-20 (PBST) overnight at 4 °C or 1 h at rt. The membrane was washed with PBST (2 $\times$ 10 min) then incubated with 1:10,000 to 1:100,000 HRP-streptavidin. PVDF membrane was washed with PBST (2 $\times$ 5 min, 1 $\times$ 10 min) and then developed with ECL Plus chemiluminescence (GE Healthcare). To verify equal protein loading, GAPDH was probed with 1:1,000 anti-GAPDH (Santa-Cruz) and 1:35,000 rabbit anti-mouse-HRP (Invitrogen). To assess endogenous oxidative stress, hyperoxidized Prxs were probed with 1:2,000 anti-Prx-SO3 antibody (Abcam), which recognizes the sulfinic and sulfonic acid forms of PrxI-IV, and 1:100,000 goat anti-rabbit-HRP (Invitrogen). Membranes were routinely stained with Ponceau S to assess quality of protein transfer and loading.

3.6.12 Cell culture

HeLa cells were maintained in a humidified atmosphere of 5% CO_2 at 37 °C and cultured in DMEM media supplemented with 10% fetal bovine serum (FBS), 1% penicillin-streptomycin-L-glutamine (PSG) and 1% MEM non essential amino acids (MEM-NEAA).

3.6.13 Preparation of HeLa cell lysates

HeLa cells (~90% confluent in 10 cm dishes) were washed with sterile PBS (×3) and the plate incubated on ice for 5 min. Cells were then gently scraped with a rubber policeman and transferred to an eppendorf tube. Cold lysis buffer (100–150 μl) (50 mM Tris pH 8.0, 150 mM NaCl, 1% NP-40) containing 2× PI was added and the tube incubated on ice for 20 min with frequent mixing. The mixture was then centrifuged at 4 °C for 20 min (17,000 *g*). The supernatant was collected and used immediately or flash-frozen and stored at -80 °C. DAz-1, DAz-2, or DMSO treated cells were washed with PBS (×3) prior to addition of lysis buffer.

3.6.14 Enrichment of biotinylated proteins

NeutrAvidin-coated beads (Pierce) were incubated with biotinylated proteins for 2 h at 4 °C and washed [×3 PBS, ×1 RIPA (50 mM Tris HCl, pH 7.4, 0.5% sodium deoxycholate, 0.1% SDS, 1% NP-40), ×0.2% SDS-PBS and ×1 with PBS]. Proteins were eluted from NeutrAvidin in 40 μl elution buffer EB (50 mM Tris HCl, pH 7.4, 1% SDS, 1 mM biotin) with heating to 95 °C for 5 min.

3.6.15 Isolation of DAz-2 labeled proteins for MS analysis

HeLa cells (8 x 10 cm dishes) were grown to 90-95% confluence. Replicate samples of approximately 5×10^6 cells were resuspended in 0.5% FBS DMEM (4 ml) containing DAz-2 (5 mM) or DMSO (1% v/v). Cells were incubated for 2 h at 37 °C with frequent mixing and harvested at 1,000 *g* for 5 min. In addition, cells were routinely evaluated for viability before and after

treatment (Figure 3.4). After washing with PBS (x3), cells were incubated for an additional 1 h in complete DMEM. Lysates were generated, pre-cleared with NeutrAvidin beads (20 µl) for 25 min at 4 °C and subjected to Staudinger ligation (1 mg ml^{-1}) and quenched with cold acetone (1 ml). Protein pellets were harvested and washed with cold acetone (200 µl) before complete resuspension in PBS containing 0.2% SDS. NeutrAvidin beads (60 µl) were incubated with lysate (500 µl) for 2 h at 4 °C, collected by centrifugation at 2,500 *g* for 1 min, washed (×3 PBS, ×1 RIPA, ×1 PBS) and proteins were eluted in EB by heating at 95 °C for 10 min. Eluents were collected, concentrated by vacuum evaporation (SpeedVac), and resuspended in water (38 µl) with SDS-PAGE loading dye. Samples were boiled at 95 °C for 5 min, resolved by SDS-PAGE and visualized by staining with Colloidal Blue (Invitrogen). Proteins were digested in-gel with trypsin, extracted and the resulting peptides were subjected to LC-MS/MS analysis. MS/MS data were analyzed using the MASCOT sequence database; peptides with probability values of $P \leq 0.05$ were considered statistically significant and included in Table 3.1 and Appendix 3.6.1.

3.6.16 Detection of sulfenic acid modifications in Rab1a and calreticulin.

Sulfenic acid modification of recombinant wild-type, C26A, C126A, and C26A C126A Rab1a GTPase was verified by incubating protein (10 µM) with DAz-2 (1 mM) or DMSO (10% v/v) in PBS for 15 min at rt. Sulfenic acid modification of calreticulin was verified by incubating protein (Abcam, 1 µM) with DAz-2 (1 mM) or DMSO (10% v/v) in 50 mM Tris, 50 mM NaCl, 5 mM $CaCl_2$, pH 7.1. In some reactions, calreticulin was pre-treated with dimedone (10 mM) for 0.5 h at rt and then DAz-2 (1 mM). Alternatively, calreticulin was exposed to H_2O_2 (1 mM) for 0.5 h at rt and then DAz-2 (1 mM). Proteins were resolved by SDS-PAGE and analyzed by HRP-streptavidin Western blot.

3.7 Appendices

3.7.1 Proteins identified in proteomic study

Complete list of identified proteins with sulfenic acid modifications in HeLa cells. [a]

Protein	Location[b]	Accession Number	Reference
Cytoskeleton			
Actin, beta-like 2	C	NP_001017992.1	(*25, 46*)
Actin-like protein	C	AAX82193.1	
Actin prepeptide	C	AAA51586.1	(*44,50,52,65,115*)
Alpha 1 actin	C	NP_001091.1	(*25, 42, 46*)
Alpha actin 1 proprotein	C	NP_005150.1	
ANKRD26-like family C member 1A	C	NP_001077007.1	
ANKRD26-like family C member 1B	C	NP_001093241.1	
Beta actin	C	NP_001092.1	(*25,42,46,66,67*)
Beta-tubulin	C	AAB59507.1	(*62*)
Cofilin 1	C	NP_005498.1	(*44*)
Filamin A , alpha isoform 1	C	NP_001447.2	
Filamin A , alpha isoform CRA_e	C	EAW72748.1	
Filamin 2	C	AAF80245.1	
Flightless-I homolog	C	AAC03568.1	
Gamma actin	C	AAA51580.1	
Gamma filamin	C	AAD12245.1	
hCG1748768 isoform CRA_b	C	EAW59257.1	
Moesin	C	NP_002435.1	(*43, 116*)
Mutant beta actin	C	CAA45026.1	(*25, 46*)
Mutant desmin	C	AAN37810.1	(*25, 41, 42*)
Myosin heavy polypeptide 9	C	NP_002464.1	(*42, 46, 65*)
Myosin heavy polypepide 11, smooth muscle, isoform CRA_e	C	EAW53929.1	(*65*)
Peripherin	C	AAA60190.1	
Radixin	C	NP_002897.1	(*116, 117*)
Similar to cytoskeleton-associated protein 4	C	AAH25341.1	
Similar to tubulin beta 5	C	XP_935073.1	(*43*)
TUBB3 protein	C	AAH01678.2	(*46*)
Tubulin alpha 1B	C	NP_035784.1	(*46, 62*)
Tubulin alpha 1B chain	C	AAA91576.1	(*43, 62, 118*)
Tubulin alpha 3e	C	NP_997195.1	(*46*)
Tubulin alpha 4A chain	C	CAA30026.1	(*42, 46*)
Tubulin alpha 8	C	NP_061816.1	(*62*)
Tubulin beta	C	0805287A	(*62*)
Tubulin beta chain	C	AAH20946.1	(*62*)
Tubulin beta 2A chain	C	NP_001060.1	(*43, 46*)
Tubulin beta 2C chain	C	NP_006079.1	(*43, 46*)
Tubulin beta 3 chain	C	AAC52035.1	(*43, 46*)
Tubulin beta 4	C	NP_006078.2	(*46*)
Tubulin beta 4q chain	C	AAB48456.1	(*46*)
Tubulin beta 6	C	NP_080749.2	
Tubulin, beta 8	C	NP_817124.1	
Tubulin beta polypeptide 4 member Q	C	XP_001713916.1	

Protein	Location	Accession Number	Reference
DNA Repair			
80 kDa MCM3-associated protein	C,N	BAA25498.1	
ATP-dependent DNA helicase II subunit 2	N	BAD96323.1	
Ku80 isoform CRA_b	N	EAW70563.1	
Minichromosome maintenance complex component 6	N	NP_005906.2	
Metabolism			
Aldehyde dehydrogenase 3A2 isoform 2	ER	NP_000373.1	(*52*)
Aldolase A	C	CAA30979.1	(*44, 46*)
Alpha-enolase, lung specific	C	Q05524.1	(*44,52,115,119*)
Amino acid transporter E16	C,PM	AAC61479.1|	
ATP-citrate synthase	C	AAB60340.1	
ATP-citrate (pro-s-)-lyase	C	CAA45614.1	
ATPase, H+/K+ exchanging, alpha subunit	PM	AAA35988.1	
ATP synthase, mitochondrial F0 complex, subunit B1	M	CAA42782.1	(*25, 42, 46*)
ATP synthase, mitochondrial F1 complex, alpha subunit	M	AAH08028	(*25, 42, 46, 120*)
C1-tetrahydrofolate synthase	C	P11586.3	
Catechol-O-methyltransferase	PM	AAA68929.1	
Cytosolic iron-sulfur protein assembly 1 homolog	C	NP_004795.1	(*52*)
Enolase 1	C	AAH46928.1	(*43, 52, 120*)
Enolase 1, alpha	C,N	NP_001419.1	(*44, 46, 52,115,119*)
Enolase 2, gamma	C,M	CAA31512.1	(*52, 121*)
Enolase 3, beta	C	CAB94588.1	
FASN variant protein	PM	BAE06070	(*121*)
Fatty acid synthase (FAS)	PM	AAC50259.1	(*121*)
Glucosidase alpha	ER,G	BAA07642	
Glyceraldehyde-3-phosphate dehydrogenase	C	CAA25833.1	(*17, 41-43, 47, 52, 62*)
Glyceraldehyde-3-phosphate dehydrogenase-like 6	C	XP_001727006.1	
L-lactate dehydrogenase B	C	NP_002291.1	(*46, 65*)
L-lactate dehydrogenase A isoform 1	C	NP_005557.1	(*43, 46*)
Lysophosphatidylcholine acyltransferase 1	ER,PM	NP_079106.3	
Neutral amino acid transporter B	PM	AAC50629.1	
Phosphoglycerate dehydrogenase	C	NP_006614.2	(*47, 120*)
Pyruvate kinase	C	CAA39849.1	(*46, 52, 62, 63*)
Skeletal muscle glyceraldehyde-3-phosphate dehydrogenase	C	3GPD|R	(*46, 50, 52, 62*)
Succinate dehydrogenase complex, subunit A, flavoprotein	M	AAA20683.1	(*42, 46, 47*)
Transketolase	C	CAA47919.1	(*52, 120, 122*)
TKT protein	C	AAH02433.1	(*52, 120, 122*)
Nuclear Transport			
Exportin 1 (CRM1)	C,N	NP_003391.1	(*123*)
Exportin 2 (CRM2)	C,N	AAC50387.1	
Exportin 7	C,N	EAW63733.1	
Exportin, tRNA (Exportin t)	C,N	AAC39793.1	
Importin 5 (RanBP5)	C,N	AAH45640.1	
Importin 7 (RanBP7)	C,N	NP_006382.1	
Importin 9	C,N	NP_060555.2	
Importin beta-1 (Karyopherin beta-1)	C,N	Q14974	
Importin beta-2	C,N	Q92973	(*43*)
Ran	C,N	AAC99400.1	(*42, 113*)

Protein	Location	Accession Number	[c] Reference
Transportin 1 isoform CRA_b	C,N	EAW95715.1	(*43*)
Transportin 1	C,N	AAC50723.1	(*43*)
Transportin 2	C,N	BAE06093.1	
Other			
Albumin	S	AAH41789.1	(*23, 46*)
Alpha-2-HS-glycoprotein	S	P02765.1	
Dermcidin	S	NP_444513.1	(*46*)
Laminin receptor-like protein 5	C	AAK69721.1	
Phosphate carrier protein	ER,M	NP_002626.1	(*42*)
Possible J 56 gene segment		AAB86742.1	
PREDICTED: POTE 2		XP_933678.1	
PREDICTED: POTE 2		XP_934799.2	
Solute carrier family 25	ER,M	EAW89869.1	(*42, 65*)
Protein Homeostasis			
Aminopeptidase puromycin sensitive	C,N	XP_001173616.1	
Calnexin	ER	NP_001737.1	
Calreticulin	C,ER,N	NP_004334.1	(*43*)
Chaperonin containing TCP1, subunit 3 gamma	C	AAH08019.1	(*46*)
Endoplasmic reticulum-Golgi intermediate compartment protein 1	ER,G	BAA86495.1	
Endoplasmin	C	NP_003290.1	(*46*)
Heat shock 70 kDa protein 1L	C	AAA63228.1	(*46*)
Heat shock 70 kDa Protein 8 isoform 1 variant	C,N	BAD96505.1	
Heat shock cognate 71 kDa protein	C,N	NP_006588.1	(*61*)
Hsp60	M	AAK60261.1	(*44, 46, 52, 120*)
Hsp70-2	ER,M,N	AAD21815.1	(*52, 115, 119, 120*)
Hsp75 (TRAP1)	M	A55877	
Hsp90-Alpha	C	P07900	(*43,46, 61*)
Hsp90 B2	C	AAX38250.1	(*42, 43, 46*)
Hsp90 B1	ER,PM	AAH09195.1	(*42, 43, 46*)
p97 (Valosin-containing protein)	C,ER	NP_009057.1	(*52, 124*)
Plasminogen	S	AAH60513.1	(*46*)
PREDICTED: CCT-eta	C	XP_001727067.1	(*43*)
Tumor rejection antigen (gp96) 1 variant	ER	BAD92771.1	
Ubiquitin-activating enzyme E1	C,N	CAA40296.1	(*52, 114*)
Protein synthesis			
EEF1A1 protein	C	AAH70500.1	(*52, 120*)
Elongation factor 1 alpha 1	C	NP_001393.1	(*42, 43, 52, 120*)
Elongation factor 1 alpha 1-like 14	C	AAC09385.1	
Elongation factor 1 alpha 2	C	NP_001949.1	
Elongation factor 1 gamma	C	NP_001395.1	(*43, 46*)
Elongation factor 2	C	NP_001952.1	(*43, 46*)
Glutaminyl-tRNA synthetase	C	CAA38224.1	(*47*)
hCG2023776	C	EAW76978	
hCG2025340 isoform CRA_b	C	EAW82780.1	
hCG2010471	C	EAW56066.1	
hnRNP U protein	N,PM	CAA46472.1	

Protein	Location	Accession Number	Reference
Vesicle Transport			
Clathrin heavy chain 1	C,PM	NP_004850.1	(*125*)
Clathrin heavy chain 2	C,PM	AAC50494.1	(*125*)
Coatomer protein complex, subunit beta 1	C,G,PM	AAD41240.1	
Rab1a isoform 1	C,ER,G	P62820	
Rab1b	C,ER,G	NP_112243.1	
Rab4a isoform c	C,PM	EAW69891.1	
Rab5c	C,EE,G,PM	AAA74081.1	
Rab8a	C,G,PM	NP_005361.2	
Rab10	C,G,PM	NP_057215.2	
Rab15	C,PM	P59190.1	
Rab33b	C,G	NP_112586.1	
Rab37 isoform 2	C,PM	NP_001006639.1	
Rab39a	C,G,PM	CAA68227.1	
Reticulon 3 isoform a	ER,G	NP_006045.1	(*62*)
Reticulon 3 isoform d	ER,G	NP_958833.1	(*62*)
Reticulon 4 (Nogo-A)	ER,N	CAB99248.1	
Sec22b	ER,G	NP_035472.1	

[a] Peptides from proteins with probability values of $P \leq 0.05$ were considered statistically significant.
[b] C, cytoplasm; ER, endoplasmic reticulum; G, golgi; M, mitochondria; N, nucleus; NU, nucleolus; PM, plasma membrane; S, secreted.
[c] Previous identification as redox-active whether oxidized or S-thiolated (with corresponding references).

3.7.2 Appendix of ^{1}H and ^{13}C NMR

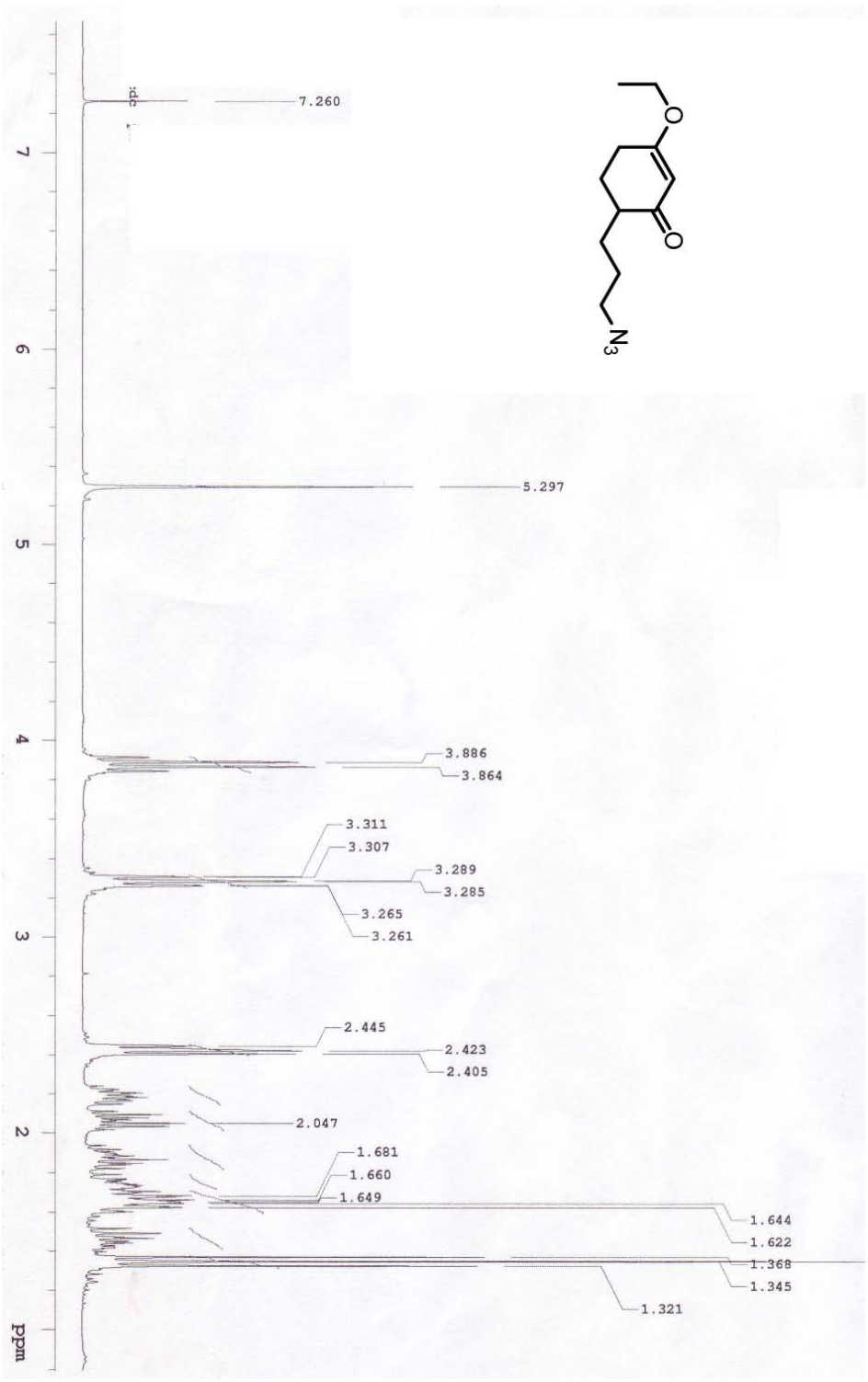
7.260
5.297
3.886
3.864
3.311
3.307
3.289
3.285
3.265
3.261
2.445
2.423
2.405
2.047
1.681
1.660
1.649
1.644
1.622
1.368
1.345
1.321
O
O
N3
ppm

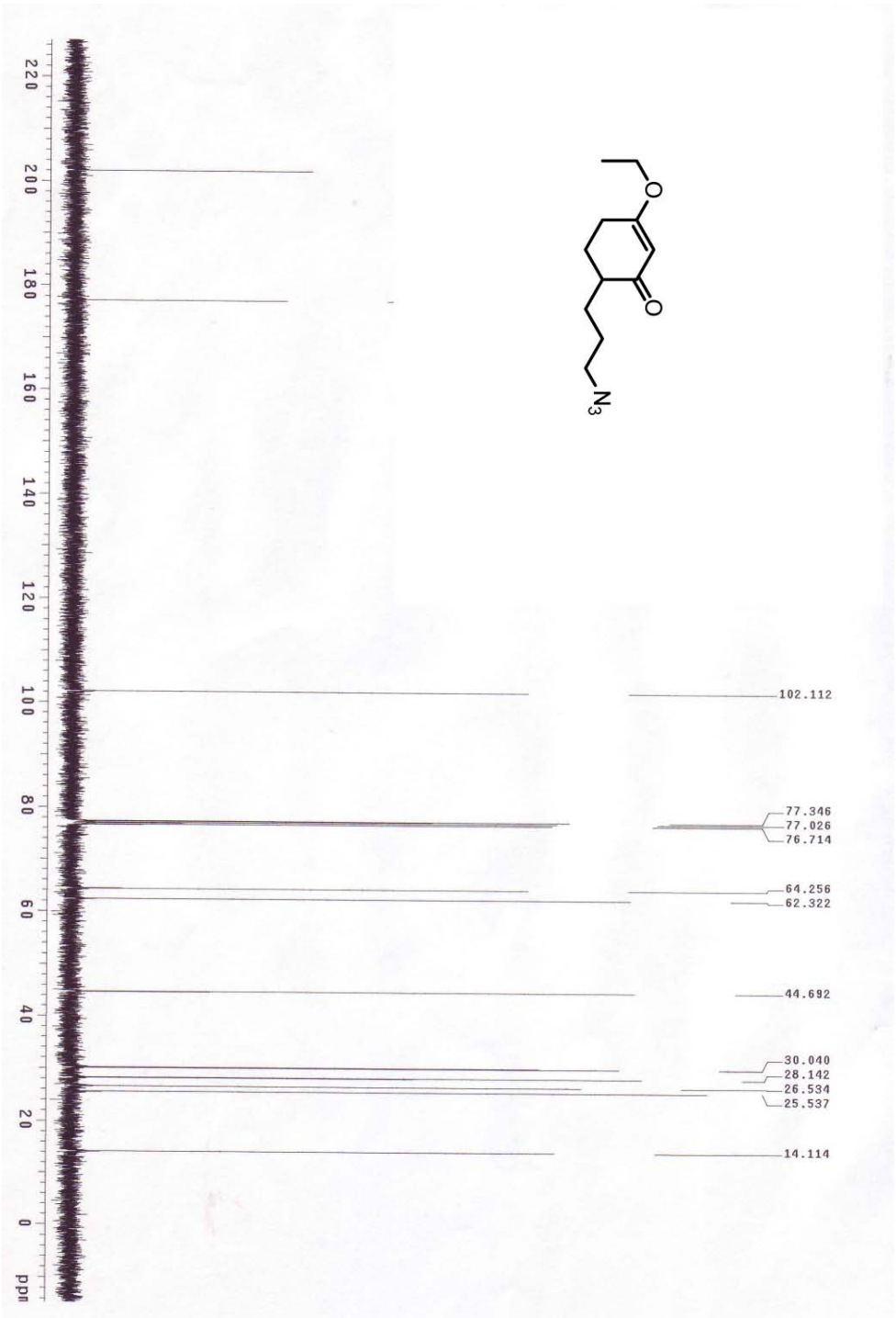
220
200
180
160
140
120
100
80
60
40
20
0
ppm
O
O
N3
102.112
77.346
77.026
76.714
64.256
62.322
44.692
30.040
28.142
26.534
25.537
14.114

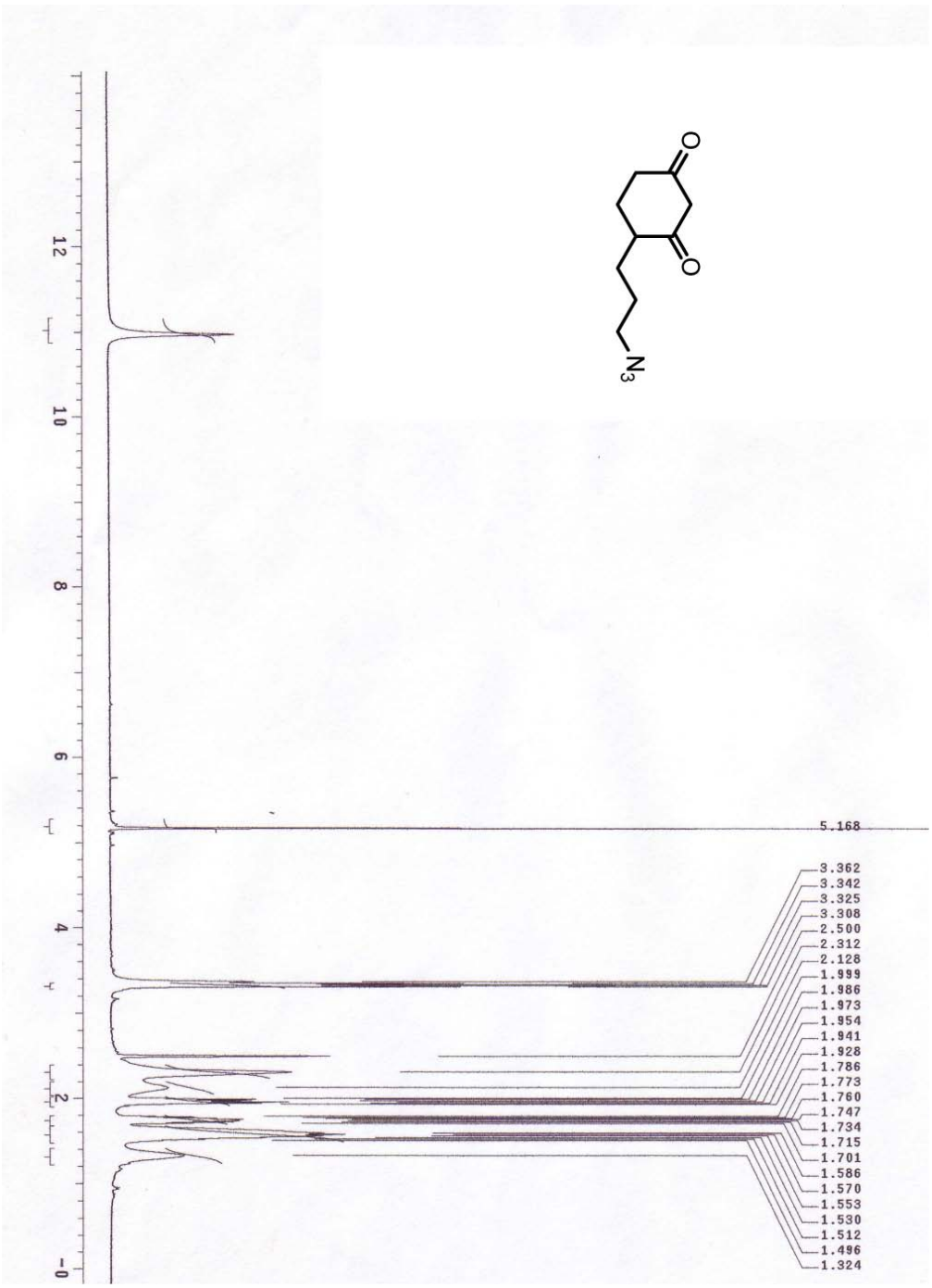
O
O
N3
5.168
3.362
3.342
3.325
3.308
2.500
2.312
2.128
1.999
1.986
1.973
1.954
1.941
1.928
1.786
1.773
1.760
1.747
1.734
1.715
1.701
1.586
1.570
1.553
1.530
1.512
1.496
1.324

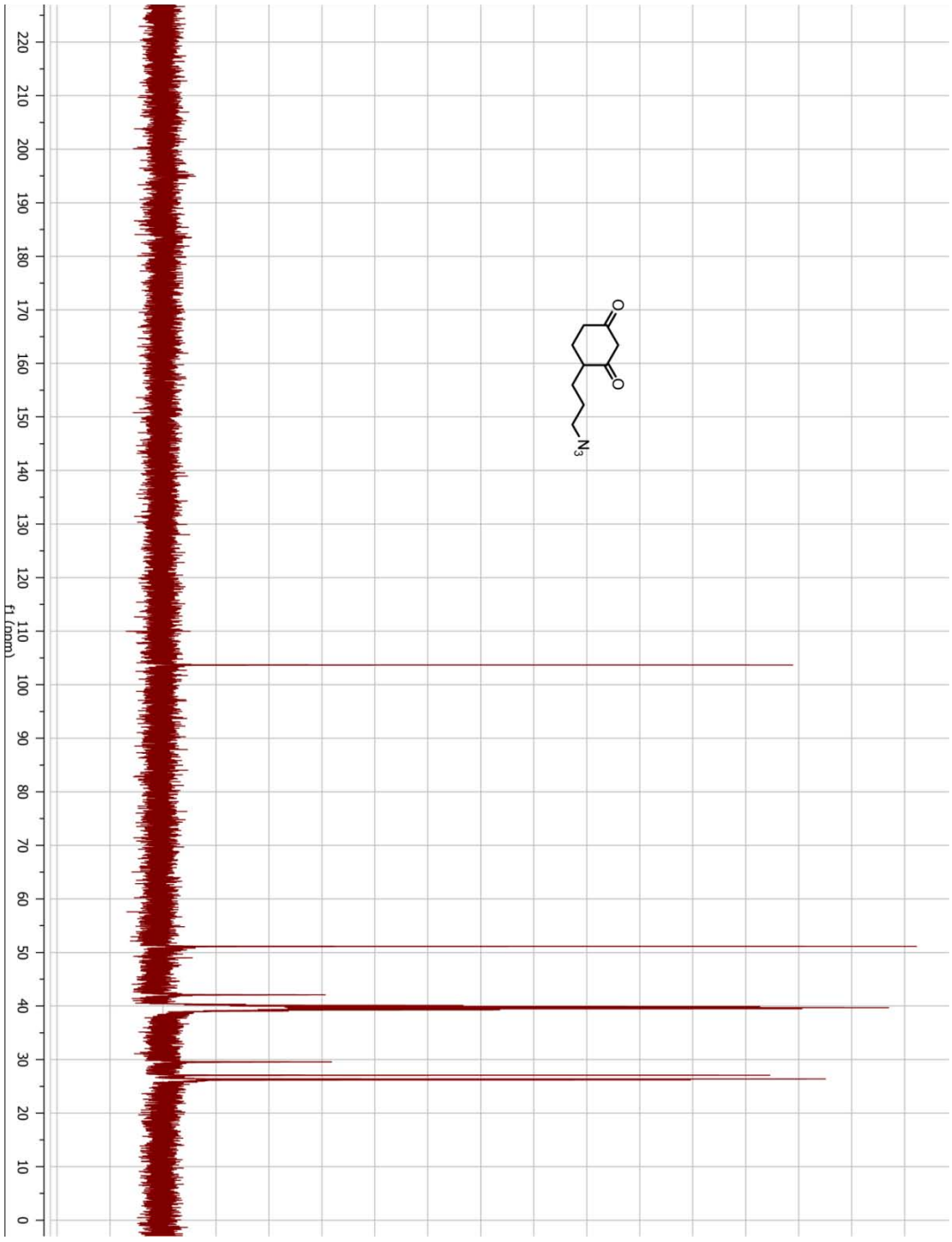
O
O
N3
f1 (ppm)
220
210
200
190
180
170
160
150
140
130
120
110
100
90
80
70
60
50
40
30
20
10
0

Notes

This work has been published as "Mining the thiol proteome for sulfenic acid modifications reveals new targets for oxidation in cells." ACS Chem Biol. **2009** Sep 18;4(9):783-99. Stephen E. Leonard, Khalilah G. Reddie, and Kate S Carroll designed the experiments. Stephen E. Leonard conducted *in vitro* experiments. Khalilah G. Reddie conducted live cell experiments. Stephen E. Leonard performed organic synthesis.

Acknowledgements

We thank the Life Sciences Institute, the Leukemia & Lymphoma Society Special Fellows Award #3100-07 and the American Heart Association Scientist Development Grant #0835419N to K.S.C. for support of this work. We also thank S. Pfeffer for the Rab1a plasmid and R. Kaufman for the calreticulin antibody.

3.8 References

1. D'Autreaux B, Toledano MB: **ROS as signalling molecules: mechanisms that generate specificity in ROS homeostasis**. *Nat. Rev. Mol. Cell. Biol.* 2007, **8**:813-824.
2. Rhee SG: **Cell signaling. H_2O_2, a necessary evil for cell signaling**. *Science* 2006, **312**:1882-1883.
3. Terada LS: **Specificity in reactive oxidant signaling: think globally, act locally**. *J Cell Biol* 2006, **174**:615-623.
4. Sundaresan M, Yu ZX, Ferrans VJ, Irani K, Finkel T: **Requirement for generation of H_2O_2 for platelet-derived growth factor signal transduction**. *Science* 1995, **270**:296-299.
5. Lee SR, Kwon KS, Kim SR, Rhee SG: **Reversible inactivation of protein-tyrosine phosphatase 1B in A431 cells stimulated with epidermal growth factor**. *J Biol Chem* 1998, **273**:15366-15372.
6. Suh YA, Arnold RS, Lassegue B, Shi J, Xu X, Sorescu D, Chung AB, Griendling KK, Lambeth JD: **Cell transformation by the superoxide-generating oxidase Mox1**. *Nature* 1999, **401**:79-82.
7. Finkel T: **Redox-dependent signal transduction**. *FEBS Lett* 2000, **476**:52-54.
8. Poole LB, Nelson KJ: **Discovering mechanisms of signaling-mediated cysteine oxidation**. *Curr. Opin. Chem. Biol.* 2008, **12**:18-24.
9. Paulsen CE, Carroll KS: **Chemical dissection of an essential redox switch in yeast**. *Chem Biol* 2009, **16**:217-225.

10. Giles NM, Watts AB, Giles GI, Fry FH, Littlechild JA, Jacob C: **Metal and redox modulation of cysteine protein function**. *Chem Biol* 2003, **10**:677-693.
11. Claiborne A, Yeh JI, Mallett TC, Luba J, Crane EJ, 3rd, Charrier V, Parsonage D: **Protein-sulfenic acids: diverse roles for an unlikely player in enzyme catalysis and redox regulation**. *Biochemistry* 1999, **38**:15407-15416.
12. Reddie KG, Carroll KS: **Expanding the functional diversity of proteins through cysteine oxidation**. *Curr Opin Chem Biol* 2008, **12**:746-754.
13. Ranaivoson FM, Antoine M, Kauffmann B, Boschi-Muller S, Aubry A, Branlant G, Favier F: **A structural analysis of the catalytic mechanism of methionine sulfoxide reductase A from Neisseria meningitidis**. *J Mol Biol* 2008, **377**:268-280.
14. van Montfort RL, Congreve M, Tisi D, Carr R, Jhoti H: **Oxidation state of the active-site cysteine in protein tyrosine phosphatase 1B**. *Nature* 2003, **423**:773-777.
15. Crane EJ, 3rd, Vervoort J, Claiborne A: **^{13}C NMR analysis of the cysteine-sulfenic acid redox center of enterococcal NADH peroxidase**. *Biochemistry* 1997, **36**:8611-8618.
16. Trivelli X, Krimm I, Ebel C, Verdoucq L, Prouzet-Mauleon V, Chartier Y, Tsan P, Lauquin G, Meyer Y, Lancelin JM: **Characterization of the yeast peroxiredoxin Ahp1 in its reduced active and overoxidized inactive forms using NMR**. *Biochemistry* 2003, **42**:14139-14149.
17. Benitez LV, Allison WS: **The inactivation of the acyl phosphatase activity catalyzed by the sulfenic acid form of glyceraldehyde 3-phosphate dehydrogenase by dimedone and olefins**. *J Biol Chem* 1974, **249**:6234-6243.
18. Claiborne A, Mallett TC, Yeh JI, Luba J, Parsonage D: **Structural, redox, and mechanistic parameters for cysteine-sulfenic acid function in catalysis and regulation**. *Adv. Protein Chem.* 2001, **58**:215-276.
19. Michalek RD, Nelson KJ, Holbrook BC, Yi JS, Stridiron D, Daniel LW, Fetrow JS, King SB, Poole LB, Grayson JM: **The requirement of reversible cysteine sulfenic acid formation for T cell activation and function**. *J Immunol* 2007, **179**:6456-6467.
20. Davis FA, Jenkins LA, Billmers RL: **Chemistry of sulfenic acids. 7. Reason for the high reactivity of sulfenic acids. Stabilization by intramolecular hydrogen bonding and electronegativity effects**. *Journal of Organic Chemistry* 1986, **51**:1033-1040.
21. Claiborne A, Miller H, Parsonage D, Ross RP: **Protein-sulfenic acid stabilization and function in enzyme catalysis and gene regulation**. *FASEB J* 1993, **7**:1483-1490.
22. Aversa MC, Barattucci A, Bonaccorsi P, Giannetto P: **Recent advances and perspectives in the chemistry of sulfenic acids**. *Curr. Org. Chem.* 2007, **11**:1034-1052.
23. Carballal S, Radi R, Kirk MC, Barnes S, Freeman BA, Alvarez B: **Sulfenic acid formation in human serum albumin by hydrogen peroxide and peroxynitrite**. *Biochemistry* 2003, **42**:9906-9914.
24. Conway ME, Poole LB, Hutson SM: **Roles for cysteine residues in the regulatory CXXC motif of human mitochondrial branched chain aminotransferase enzyme**. *Biochemistry* 2004, **43**:7356-7364.
25. Charles RL, Schroder E, May G, Free P, Gaffney PR, Wait R, Begum S, Heads RJ, Eaton P: **Protein sulfenation as a redox sensor: proteomics studies using a novel biotinylated dimedone analogue**. *Mol Cell Proteomics* 2007, **6**:1473-1484.
26. Poole LB, Klomsiri C, Knaggs SA, Furdui CM, Nelson KJ, Thomas MJ, Fetrow JS, Daniel LW, King SB: **Fluorescent and affinity-based tools to detect cysteine sulfenic acid formation in proteins**. *Bioconjug Chem* 2007, **18**:2004-2017.
27. Poole LB, Zeng BB, Knaggs SA, Yakubu M, King SB: **Synthesis of chemical probes to map sulfenic acid modifications on proteins**. *Bioconjug Chem* 2005, **16**:1624-1628.

28. Go YM, Jones DP: **Redox compartmentalization in eukaryotic cells**. *Biochim Biophys Acta* 2008.
29. Lopez-Mirabal HR, Winther JR: **Redox characteristics of the eukaryotic cytosol**. *Biochim. Biophys. Acta* 2008, **1783**:629-640.
30. Reddie KG, Seo YH, Muse III WB, Leonard SE, Carroll KS: **A chemical approach for detecting sulfenic acid-modified proteins in living cells**. *Mol Biosyst* 2008, **4**:521-531.
31. Seo YH, Carroll KS: **Facile synthesis and biological evaluation of a cell-permeable probe to detect redox-regulated proteins**. *Bioorg Med Chem Lett* 2009, **19**:356-359.
32. Agard NJ, Baskin JM, Prescher JA, Lo A, Bertozzi CR: **A comparative study of bioorthogonal reactions with azides**. *ACS Chem. Biol.* 2006, **1**:644-648.
33. Soellner MB, Nilsson BL, Raines RT: **Reaction mechanism and kinetics of the traceless Staudinger ligation**. *J Am Chem Soc* 2006, **128**:8820-8828.
34. Allison WS: **Formation and reactions of sulfenic acids in proteins**. *Acc. Chem. Res.* 1976, **9**:293-299.
35. Conrad PC, Kwiatkowski PL, Fuchs PL: **Synthesis via vinyl sulfones. 18. Rapid access to a series of highly functionalized α,β-unsaturated cyclopentenones. A caveat on aminospirocyclization**. *Journal of Organic Chemistry* 1987, **52**:586-591.
36. Cowan-Jacob SW, Kaufmann M, Anselmo AN, Stark W, Grutter MG: **Structure of rabbit-muscle glyceraldehyde-3-phosphate dehydrogenase**. *Acta Crystallogr D Biol Crystallogr* 2003, **59**:2218-2227.
37. Poole LB: **The catalytic mechanism of peroxiredoxins**. *Subcell Biochem* 2007, **44**:61-81.
38. Hiller Y, Gershoni JM, Bayer EA, Wilchek M: **Biotin binding to avidin. Oligosaccharide side chain not required for ligand association**. *Biochem. J.* 1987, **248**:167-171.
39. Woo HA, Kang SW, Kim HK, Yang KS, Chae HZ, Rhee SG: **Reversible oxidation of the active site cysteine of peroxiredoxins to cysteine sulfinic acid. Immunoblot detection with antibodies specific for the hyperoxidized cysteine-containing sequence**. *J Biol Chem* 2003, **278**:47361-47364.
40. Halliwell BaG, J. M. C.: *Free Radicals in Biology and Medicine* edn 4th. New York: Oxford; 2007.
41. Brennan JP, Miller JI, Fuller W, Wait R, Begum S, Dunn MJ, Eaton P: **The utility of N,N-biotinyl glutathione disulfide in the study of protein *S*-glutathiolation**. *Mol Cell Proteomics* 2006, **5**:215-225.
42. Brennan JP, Wait R, Begum S, Bell JR, Dunn MJ, Eaton P: **Detection and mapping of widespread intermolecular protein disulfide formation during cardiac oxidative stress using proteomics with diagonal electrophoresis**. *J Biol Chem* 2004, **279**:41352-41360.
43. Cumming RC, Andon NL, Haynes PA, Park M, Fischer WH, Schubert D: **Protein disulfide bond formation in the cytoplasm during oxidative stress**. *J Biol Chem* 2004, **279**:21749-21758.
44. Fratelli M, Demol H, Puype M, Casagrande S, Eberini I, Salmona M, Bonetto V, Mengozzi M, Duffieux F, Miclet E, et al.: **Identification by redox proteomics of glutathionylated proteins in oxidatively stressed human T lymphocytes**. *Proc Natl Acad Sci U S A* 2002, **99**:3505-3510.
45. Greco TM, Hodara R, Parastatidis I, Heijnen HF, Dennehy MK, Liebler DC, Ischiropoulos H: **Identification of *S*-nitrosylation motifs by site-specific mapping of the *S*-nitrosocysteine proteome in human vascular smooth muscle cells**. *Proc Natl Acad Sci U S A* 2006, **103**:7420-7425.
46. Lefievre L, Chen Y, Conner SJ, Scott JL, Publicover SJ, Ford WC, Barratt CL: **Human spermatozoa contain multiple targets for protein *S*-nitrosylation: an alternative**

mechanism of the modulation of sperm function by nitric oxide? *Proteomics* 2007, **7**:3066-3084.

47. Leichert LI, Jakob U: **Protein thiol modifications visualized in vivo**. *PLoS Biol* 2004, **2**:1723-1737.
48. Baty JW, Hampton MB, Winterbourn CC: **Proteomic detection of hydrogen peroxide-sensitive thiol proteins in Jurkat cells**. *Biochem J* 2005, **389**:785-795.
49. Dennehy MK, Richards KA, Wernke GR, Shyr Y, Liebler DC: **Cytosolic and nuclear protein targets of thiol-reactive electrophiles**. *Chem. Res. Toxicol.* 2006, **19**:20-29.
50. Eaton P, Byers HL, Leeds N, Ward MA, Shattock MJ: **Detection, quantitation, purification, and identification of cardiac proteins *S*-thiolated during ischemia and reperfusion**. *J Biol Chem* 2002, **277**:9806-9811.
51. Gao C, Guo H, Wei J, Mi Z, Wai PY, Kuo PC: **Identification of *S*-nitrosylated proteins in endotoxin-stimulated RAW264.7 murine macrophages**. *Nitric Oxide* 2005, **12**:121-126.
52. Le Moan N, Clement G, Le Maout S, Tacnet F, Toledano MB: **The Saccharomyces cerevisiae proteome of oxidized protein thiols: contrasted functions for the thioredoxin and glutathione pathways**. *J Biol Chem* 2006, **281**:10420-10430.
53. Pfeffer SR: **Rab GTPases: specifying and deciphering organelle identity and function**. *Trends Cell Biol* 2001, **11**:487-491.
54. Farnsworth CC, Seabra MC, Ericsson LH, Gelb MH, Glomset JA: **Rab geranylgeranyl transferase catalyzes the geranylgeranylation of adjacent cysteines in the small GTPases Rab1A, Rab3A, and Rab5A**. *Proc. Natl. Acad. Sci. U.S.A.* 1994, **91**:11963-11967.
55. Michalak M, Groenendyk J, Szabo E, Gold LI, Opas M: **Calreticulin, a multi-process calcium-buffering chaperone of the endoplasmic reticulum**. *Biochem J* 2009, **417**:651-666.
56. Schrag JD, Bergeron JJ, Li Y, Borisova S, Hahn M, Thomas DY, Cygler M: **The Structure of calnexin, an ER chaperone involved in quality control of protein folding**. *Mol. Cell.* 2001, **8**:633-644.
57. Fomenko DE, Xing W, Adair BM, Thomas DJ, Gladyshev VN: **High-throughput identification of catalytic redox-active cysteine residues**. *Science* 2007, **315**:387-389.
58. Miller EW, Chang CJ: **Fluorescent probes for nitric oxide and hydrogen peroxide in cell signaling**. *Curr Opin Chem Biol* 2007, **11**:620-625.
59. Cohen MS, Hadjivassiliou H, Taunton J: **A clickable inhibitor reveals context-dependent autoactivation of p90 RSK**. *Nat. Chem. Biol.* 2007, **3**:156-160.
60. Hang HC, Loureiro J, Spooner E, van der Velden AW, Kim YM, Pollington AM, Maehr R, Starnbach MN, Ploegh HL: **Mechanism-based probe for the analysis of cathepsin cysteine proteases in living cells**. *ACS Chem. Biol.* 2006, **1**:713-723.
61. Ghezzi P, Bonetto V, Fratelli M: **Thiol-disulfide balance: from the concept of oxidative stress to that of redox regulation**. *Antioxid. Redox Signal.* 2005, **7**:964-972.
62. Hao G, Derakhshan B, Shi L, Campagne F, Gross SS: **SNOSID, a proteomic method for identification of cysteine *S*-nitrosylation sites in complex protein mixtures**. *Proc Natl Acad Sci U S A* 2006, **103**:1012-1017.
63. Leichert LI, Gehrke F, Gudiseva HV, Blackwell T, Ilbert M, Walker AK, Strahler JR, Andrews PC, Jakob U: **Quantifying changes in the thiol redox proteome upon oxidative stress in vivo**. *Proc Natl Acad Sci U S A* 2008, **105**:8197-8202.
64. McDonagh B, Ogueta S, Lasarte G, Padilla CA, Barcena JA: **Shotgun redox proteomics identifies specifically modified cysteines in key metabolic enzymes under oxidative stress in Saccharomyces cerevisiae**. *J. Proteomics* 2009, **72**:677-689.
65. Saurin AT, Neubert H, Brennan JP, Eaton P: **Widespread sulfenic acid formation in tissues in response to hydrogen peroxide**. *Proc Natl Acad Sci U S A* 2004, **101**:17982-17987.

66. Shelton MD, Chock PB, Mieyal JJ: **Glutaredoxin: role in reversible protein *S*-glutathionylation and regulation of redox signal transduction and protein translocation**. *Antioxid. Redox Signal.* 2005, **7**:348-366.
67. Johansson M, Lundberg M: **Glutathionylation of beta-actin via a cysteinyl sulfenic acid intermediary**. *BMC Biochem* 2007, **8**:26.
68. Linke K, Jakob U: **Not every disulfide lasts forever: disulfide bond formation as a redox switch**. *Anal. Chem. Antioxid. Redox Signal.* 2003, **5**:425-434.
69. Erwin PA, Mitchell DA, Sartoretto J, Marletta MA, Michel T: **Subcellular targeting and differential *S*-nitrosylation of endothelial nitric-oxide synthase**. *J Biol Chem* 2006, **281**:151-157.
70. Hashemy SI, Holmgren A: **Regulation of the catalytic activity and structure of human thioredoxin 1 via oxidation and *S*-nitrosylation of cysteine residues**. *J Biol Chem* 2008, **283**:21890-21898.
71. Cary SP, Winger JA, Derbyshire ER, Marletta MA: **Nitric oxide signaling: no longer simply on or off**. *Trends Biochem Sci* 2006, **31**:231-239.
72. Lowenstein CJ: **Nitric oxide regulation of protein trafficking in the cardiovascular system**. *Cardiovasc Res* 2007, **75**:240-246.
73. Forman HJ, Fukuto JM, Torres M: **Redox signaling: thiol chemistry defines which reactive oxygen and nitrogen species can act as second messengers**. *Am. J. Physiol. Cell Physiol.* 2004, **287**:C246-256.
74. Kemble DJ, Sun G: **Direct and specific inactivation of protein tyrosine kinases in the Src and FGFR families by reversible cysteine oxidation**. *Proc Natl Acad Sci U S A* 2009, **106**:5070-5075.
75. Giannoni E, Buricchi F, Raugei G, Ramponi G, Chiarugi P: **Intracellular reactive oxygen species activate Src tyrosine kinase during cell adhesion and anchorage-dependent cell growth**. *Mol Cell Biol* 2005, **25**:6391-6403.
76. Ikeda S, Yamaoka-Tojo M, Hilenski L, Patrushev NA, Anwar GM, Quinn MT, Ushio-Fukai M: **IQGAP1 regulates reactive oxygen species-dependent endothelial cell migration through interacting with Nox2**. *Arterioscler. Thromb. Vasc. Biol.* 2005, **25**:2295-2300.
77. Usatyuk PV, Gorshkova IA, He D, Zhao Y, Kalari SK, Garcia JG, Natarajan V: **Phospholipase D-mediated activation of IQGAP1 through Rac1 regulates hyperoxia-induced p47phox translocation and reactive oxygen species generation in lung endothelial cells**. *J Biol Chem* 2009.
78. Ragolia L, Cherpalis B, Srinivasan M, Begum N: **Role of serine/threonine protein phosphatases in insulin regulation of Na+/K+-ATPase activity in cultured rat skeletal muscle cells**. *J Biol Chem* 1997, **272**:23653-23658.
79. Tonks NK: **Redox redux: revisiting PTPs and the control of cell signaling**. *Cell* 2005, **121**:667-670.
80. Rusnak F, Reiter T: **Sensing electrons: protein phosphatase redox regulation**. *Trends Biochem Sci* 2000, **25**:527-529.
81. Barzilai A, Yamamoto K: **DNA damage responses to oxidative stress**. *DNA Repair (Amst)* 2004, **3**:1109-1115.
82. Andrews BJ, Lehman JA, Turchi JJ: **Kinetic analysis of the Ku-DNA binding activity reveals a redox-dependent alteration in protein structure that stimulates dissociation of the Ku-DNA complex**. *J Biol Chem* 2006, **281**:13596-13603.
83. Zhang WW, Yaneva M: **Reduced sulphydryl groups are required for DNA binding of Ku protein**. *Biochem J* 1993, **293 (Pt 3)**:769-774.

84. Walker JR, Corpina RA, Goldberg J: **Structure of the Ku heterodimer bound to DNA and its implications for double-strand break repair**. *Nature* 2001, **412**:607-614.
85. Ralser M, Wamelink MM, Kowald A, Gerisch B, Heeren G, Struys EA, Klipp E, Jakobs C, Breitenbach M, Lehrach H, et al.: **Dynamic rerouting of the carbohydrate flux is key to counteracting oxidative stress**. *J Biol* 2007, **6**:10.
86. Swaminathan S, Masek T, Molin C, Pospisek M, Sunnerhagen P: **Rck2 is required for reprogramming of ribosomes during oxidative stress**. *Mol Biol Cell* 2006, **17**:1472-1482.
87. Luciani N, Hess K, Belleville F, Nabet P: **Stimulation of translation by reactive oxygen species in a cell-free system**. *Biochimie* 1995, **77**:182-189.
88. Sheehan D, Meade G, Foley VM, Dowd CA: **Structure, function and evolution of glutathione transferases: implications for classification of non-mammalian members of an ancient enzyme superfamily**. *Biochem J* 2001, **360**:1-16.
89. Adler V, Yin Z, Tew KD, Ronai Z: **Role of redox potential and reactive oxygen species in stress signaling**. *Oncogene* 1999, **18**:6104-6111.
90. Chu CT, Plowey ED, Wang Y, Patel V, Jordan-Sciutto KL: **Location, location, location: altered transcription factor trafficking in neurodegeneration**. *J Neuropathol Exp Neurol* 2007, **66**:873-883.
91. Heo J: **Redox regulation of Ran GTPase**. *Biochem Biophys Res Commun* 2008, **376**:568-572.
92. Kuge S, Toda T, Iizuka N, Nomoto A: **Crm1 (XpoI) dependent nuclear export of the budding yeast transcription factor yAP-1 is sensitive to oxidative stress**. *Genes Cells* 1998, **3**:521-532.
93. Song JY, Lim JW, Kim H, Morio T, Kim KH: **Oxidative stress induces nuclear loss of DNA repair proteins Ku70 and Ku80 and apoptosis in pancreatic acinar AR42J cells**. *J Biol Chem* 2003, **278**:36676-36687.
94. Stenmark H, Olkkonen VM: **The Rab GTPase family**. *Genome Biol* 2001, **2**:1-7.
95. Heo J, Campbell SL: **Mechanism of p21Ras *S*-nitrosylation and kinetics of nitric oxide-mediated guanine nucleotide exchange**. *Biochemistry* 2004, **43**:2314-2322.
96. Adachi T, Pimentel DR, Heibeck T, Hou X, Lee YJ, Jiang B, Ido Y, Cohen RA: ***S*-glutathiolation of Ras mediates redox-sensitive signaling by angiotensin II in vascular smooth muscle cells**. *J. Biol. Chem.* 2004, **279**:29857-29862.
97. Heo J, Campbell SL: **Mechanism of redox-mediated guanine nucleotide exchange on redox-active Rho GTPases**. *J Biol Chem* 2005, **280**:31003-31010.
98. Voloboueva LA, Duan M, Ouyang Y, Emery JF, Stoy C, Giffard RG: **Overexpression of mitochondrial Hsp70/Hsp75 protects astrocytes against ischemic injury in vitro**. *J Cereb Blood Flow Metab* 2008, **28**:1009-1016.
99. Papp E, Nardai G, Soti C, Csermely P: **Molecular chaperones, stress proteins and redox homeostasis**. *Biofactors* 2003, **17**:249-257.
100. Callahan MK, Chaillot D, Jacquin C, Clark PR, Menoret A: **Differential acquisition of antigenic peptides by Hsp70 and Hsc70 under oxidative conditions**. *J Biol Chem* 2002, **277**:33604-33609.
101. Højrup P, Roepstorff, P., Houen, G.: **Human placental calreticulin characterization of domain structure and post-translational modifications.** *European Journal of Biochemistry* 2001, **268**:2558-2565.
102. Kulp MS, Frickel EM, Ellgaard L, Weissman JS: **Domain architecture of protein-disulfide isomerase facilitates its dual role as an oxidase and an isomerase in Ero1p-mediated disulfide formation**. *J Biol Chem* 2006, **281**:876-884.
103. Frickel EM, Frei P, Bouvier M, Stafford WF, Helenius A, Glockshuber R, Ellgaard L: **ERp57 is a multifunctional thiol-disulfide oxidoreductase**. *J Biol Chem* 2004, **279**:18277-18287.

104. Kang SJ, Cresswell P: **Calnexin, calreticulin, and ERp57 cooperate in disulfide bond formation in human CD1d heavy chain**. *J Biol Chem* 2002, **277**:44838-44844.
105. Molinari M, Helenius A: **Chaperone selection during glycoprotein translocation into the endoplasmic reticulum**. *Science* 2000, **288**:331-333.
106. Kimura T, Hosoda Y, Sato Y, Kitamura Y, Ikeda T, Horibe T, Kikuchi M: **Interactions among yeast protein-disulfide isomerase proteins and endoplasmic reticulum chaperone proteins influence their activities**. *J Biol Chem* 2005, **280**:31438-31441.
107. Toft KN, Vestergaard B, Nielsen SS, Snakenborg D, Jeppesen MG, Jacobsen JK, Arleth L, Kutter JP: **High-throughput small angle X-ray scattering from proteins in solution using a microfluidic front-end**. *Anal. Chem.* 2008, **80**:3648-3654.
108. Aivazian D, Serrano RL, Pfeffer S: **TIP47 is a key effector for Rab9 localization**. *J Cell Biol* 2006, **173**:917-926.
109. Knobel Y, Glei M, Osswald K, Pool-Zobel BL: **Ferric iron increases ROS formation, modulates cell growth and enhances genotoxic damage by 4-hydroxynonenal in human colon tumor cells**. *Toxicol In Vitro* 2006, **20**:793-800.
110. Baker MA, Cerniglia GJ, Zaman A: **Microtiter plate assay for the measurement of glutathione and glutathione disulfide in large numbers of biological samples**. *Anal Biochem* 1990, **190**:360-365.
111. Hultberg B, Andersson A, Isaksson A: **Thiol and redox reactive agents exert different effects on glutathione metabolism in HeLa cell cultures**. *Clin Chim Acta* 1999, **283**:21-32.
112. Hansen RE, Roth D, Winther JR: **Quantifying the global cellular thiol-disulfide status**. *Proc Natl Acad Sci U S A* 2009, **106**:422-427.

Chapter 4

A periplasmic reducing system protects single cysteine residues from oxidation

4.1 Abstract

The thiol group of the amino acid cysteine can be modified to regulate protein activity. The *Escherichia coli* periplasm is an oxidizing environment in which most cysteine residues are involved in disulfide bonds. However, many periplasmic proteins contain single cysteine residues, which are vulnerable to oxidation to sulfenic acids and then irreversibly modified to sulfinic and sulfonic acids. We discovered that DsbG and DsbC, two thioredoxin-related proteins, control the global sulfenic acid content of the periplasm and protect single cysteine residues from oxidation. DsbG interacts with the YbiS protein and, along with DsbC, regulates oxidation of its catalytic cysteine residue. Thus, a potentially widespread mechanism controls sulfenic acid modification in the cellular environment.

4.2 Introduction

Many proteins secreted into the *E. coli* periplasm contain even numbers of cysteines, most of which form disulfide bonds important for protein stability. These disulfides are introduced by the oxidoreductase enzyme DsbA (disulfide bond A), which is reoxidized by DsbB (reviewed in [1]). When proteins require disulfides to be formed between nonconsecutive cysteines, DsbA can introduce incorrect disulfides. These non-native disulfides are corrected by the isomerase

DsbC, a V-shaped dimeric protein. Each subunit of DsbC contains a CXXC motif, located within a thioredoxin fold, which is kept reduced by DsbD, a membrane protein that transfers electrons from the cytoplasmic thioredoxin system to the periplasm.[1].

The periplasm contains another protein that could potentially serve as an isomerase, DsbG.[2] DsbG shares 26 % sequence identity with DsbC and is also a V-shaped dimeric protein, with a thioredoxin fold and a CXXC motif that is kept reduced by DsbD. The structure of DsbG resembles that of DsbC but the dimensions of the DsbG cleft are larger and its surface is less hydrophobic.[3] It has thus been predicted that DsbG preferentially interacts with proteins that are folded or partially folded.[3] However, the substrates of DsbG are not known and its function has remained obscure.

4.3 Results

4.3.1 DsbG substrate identification

We sought to clearly define the function of DsbG by identifying its substrates. We first used a global proteomics approach to compare the proteome of a *dsbG* mutant strain to that of a wild type, but did not find a single protein that was affected by the absence of DsbG (Appendix 4.5.1).

To trap DsbG bound to its substrates, we produced the $DsbG_{CXXA}$ mutant, in which an alanine replaces the second cysteine of the CXXC motif. This approach has been used to trap thioredoxin substrates.[4] $DsbG_{CXXA}$ was purified under non-reducing denaturing conditions. DsbG and slower migrating bands were present in the purified sample (Figure 4.1a). Addition of the reducing agent dithiothreitol (DTT) led to the disappearance of most of these bands and the

corresponding increase of DsbG, suggesting that the upper bands corresponded to DsbG bound to unknown proteins.

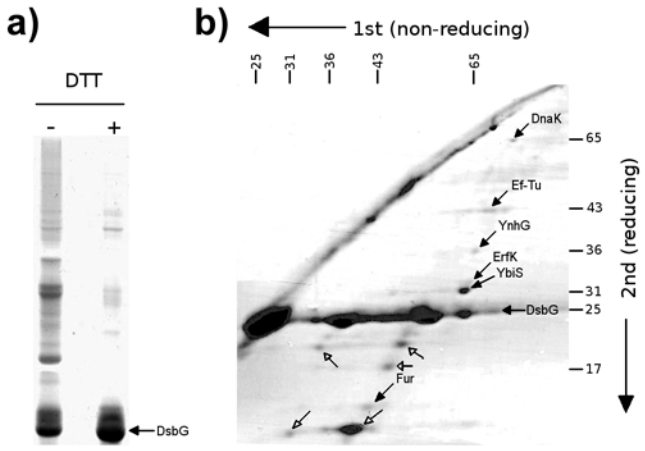

Figure 4.1 Identification of DsbG substrates. a) SDS-PAGE analysis of purified DsbGCXXA b) Separation of the complexes in a second reducing dimension. Proteins were identified by mass spectrometry. Open arrows correspond to smaller versions of DsbG that likely result from proteolysis.

The complexes were separated by two-dimensional gel electrophoresis (Figure 4.1b). Three periplasmic proteins, YbiS, ErfK and YnhG, were potential substrates of DsbG. The cytosolic proteins Ef-Tu, DnaK and Fur were also identified, but probably represent false-positives that react with DsbG during cell lysis. Indeed, Ef-Tu, has a highly reactive cysteine and has also been found in a complex with DsbA.[5]

The three periplasmic proteins were homologous proteins belonging to the same family of L,-D transpeptidases, which catalyze the cross-linking of peptidoglycan for bacterial cell wall synthesis (Figure 4.2). Because they possess a sole cysteine, essential for activity [6], these proteins are not likely in need of a disulfide isomerase but rather of a reductase to rescue their cysteine from oxidation within the oxidizing periplasm. To investigate this further, we studied the interaction between DsbG and YbiS, the most active of the three L,D-transpeptidases.[7]

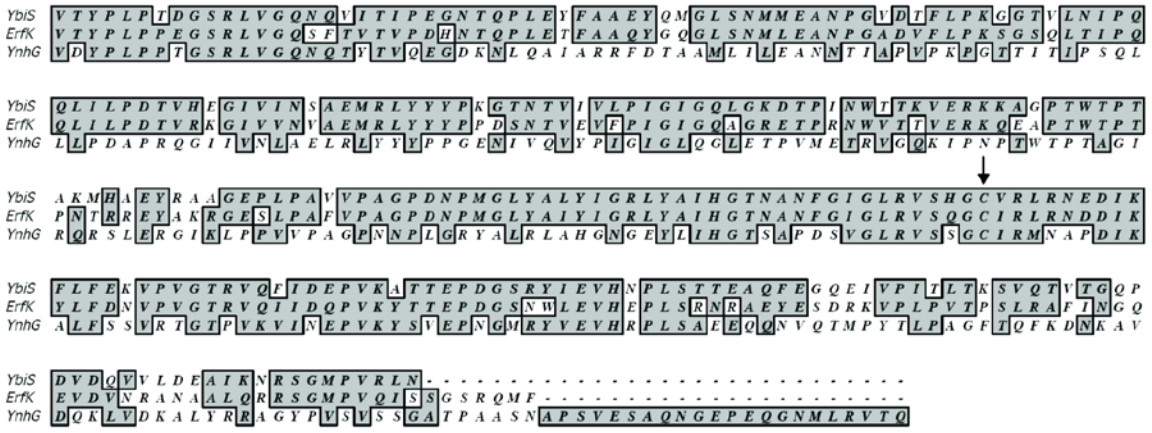

Figure 4.2 Multiple sequence alignment of ErfK, YbiS and YnhG. The identified periplasmic proteins ErfK, YbiS and YnhG belong to the same family of L,D-transpeptidases. They possess a single conserved cysteine residue, which is essential for activity (indicated by an arrow). YbiS and ErfK anchor the Braun lipoprotein to peptidoglycan, whereas YnhG synthesizes meso-DAP^3 -> meso-DAP^3 peptidoglycan cross-links.

4.3.2 DsbG reduces the oxidized cysteine of YbiS *in vitro*

We modified the cysteine of purified YbiS with 2-nitro-5-thiobenzoate (TNB) to monitor the reduction of this residue by following the release of the TNB anion (Figure 4.3a) .[8] The release of TNB was significantly faster when YbiS-TNB was incubated with reduced DsbG than with DsbC (Figure 4.3b), suggesting DsbG catalyzes the reaction more efficiently. Thus, YbiS and presumably by extension, the other homologous L,D-transpeptidases are substrates for DsbG.

4.3.3 DsbG reduces the oxidized cysteine of YbiS *in vivo*

We sought to confirm that DsbG interacts with YbiS in vivo. Expression of $DsbG_{CXXA}$ in a *dsbG* strain led to the appearance of a band of ~70 kDa, detected by both anti-YbiS and anti-DsbG antibodies (Figure 4.3c). This band migrated with the size expected for a DsbG-YbiS complex and was sensitive to DTT. In contrast, no YbiS-DsbC complex was detected when a $DsbC_{CXXS}$ mutant was expressed in a *dsbC* strain. Thus, DsbG specifically interacts with YbiS in vivo.

The fact that we trapped YbiS in complex with DsbG implied that the cysteine of YbiS oxidizes in the periplasm and suggested that YbiS requires functional DsbG to maintain its reduced, catalytically active state. To test the oxidation state of YbiS, aliquots were taken from *dsbG, dsbC, dsbCdsbG* and wild-type strains grown in stationary phase, a condition under which reactive oxygen species (ROS) accumulate. Reduced thiols were modified with mPEG, a 5-kDa molecule that covalently reacts with free thiols leading to a shift on SDS-PAGE. More oxidized YbiS was observed in *dsbG* strains (~60 %) than in wild-type (~40 %) and *dsbC* strains (~40 %) (Figure 4.3d), indicating that YbiS can be oxidized in vivo and that it preferentially depends on DsbG for reduction. The accumulation of oxidized YbiS was somewhat greater in the *dsbCdsbG* mutant (~70 %), suggesting that DsbC is able to partially replace DsbG.

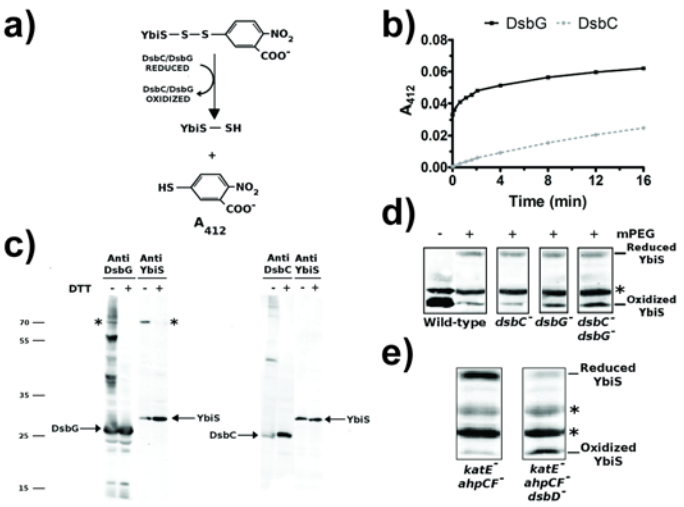

Figure 4.3 DsbG interacts with YbiS in vitro and in vivo. a) Reduction of YbiS-TNB leads to the release of the TNB anion, which can be monitored at 412 nm. b) Spectrophotometric analysis of the reaction between YbiS-TNB and DsbC or DsbG. c) Immunoblot of samples prepared from strains expressing DsbGCxxA or DsbCCxxS probed with anti-DsbG or anti-YbiS antibodies. Asterisk denotes the DsbG-YbiS complex. d) Immunoblot of samples prepared from dsbG, dsbCdsbG and e) katE ahpCF dsbD strains probed with anti-YbiS antibody (an unknown protein recognized by the YbiS antiserum is marked by an asterisk).

Both DsbG and DsbC depend on electrons provided by DsbD to stay reduced in the periplasm. [9] In the absence of DsbD, both proteins are found oxidized and are thus inactivated.[1] To confirm that inactivation of DsbG and DsbC leads to increased oxidation of YbiS by ROS, we

studied the effect of *dsbD* deletion on the oxidation state of YbiS in mutant strains in which ROS accumulate.[10] Deletion of *dsbD* caused increased oxidation of YbiS in a strain lacking the catalase KatE and the alkyl hydroperoxidase system AhpCF (Figure 4.3e). Thus, electrons flowing from the cytoplasm to DsbG and DsbC via DsbD keep the single cysteine of YbiS reduced.

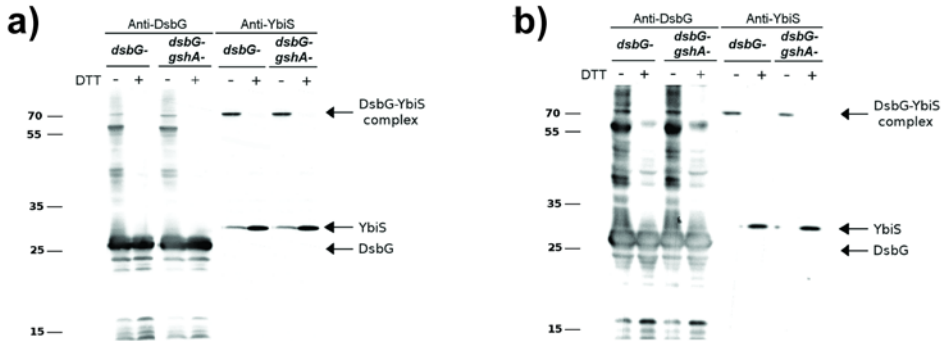

Figure 4.4 DsbG substrates are not glutathionylated. DsbG strains deficient in glutathione were grown in rich a) or MOPS minimal b) media. Regardless of the culture media, complexes between YbiS and DsbG were detected using both anti-YbiS and anti DsbG antibodies.

4.3.4 YbiS is sulfenylated *in vitro*

We next asked how the single cysteine residues of DsbG substrates are oxidized. Oxidized glutathione (GSSG), which is present in the *E. coli* periplasm [11], could potentially react with the cysteine of the transpeptidases (RSH) to form a glutathionylated adduct (RSSG). To test this hypothesis, we expressed $DsbG_{CXXA}$ in a strain lacking gamma-glutamylcysteine synthase (*gshA*), the first enzyme of the glutathione biosynthesis pathway. The formation of the YbiS-DsbG complex was still observed, even when bacteria were grown in minimal media (Figure 4.4). Thus, although we cannot rule out that a small fraction of YbiS may indeed be glutathionylated, S-glutathionylation is not the primary oxidation product in YbiS.

We next considered whether the cysteine of YbiS might be oxidized to a sulfenic acid (Cys-SOH) by oxidants present in the periplasm. Sulfenic acids are highly reactive groups that tend either to react rapidly with other cysteine residues present in the vicinity to form a disulfide bond or to be further oxidized to sulfinic or sulfonic acids.[12] Sulfenic acids can also be stabilized by electrostatic interactions within the micro-environment of certain proteins when no other cysteine is present. YbiS reacts with a genetically encoded probe based on the redox regulated domain of Yap1 [13], a yeast transcription factor that reacts with electrophilic cysteines such as sulfenic acids.[14] Thus, the active site cysteine residue of YbiS may be prone to sulfenylation.

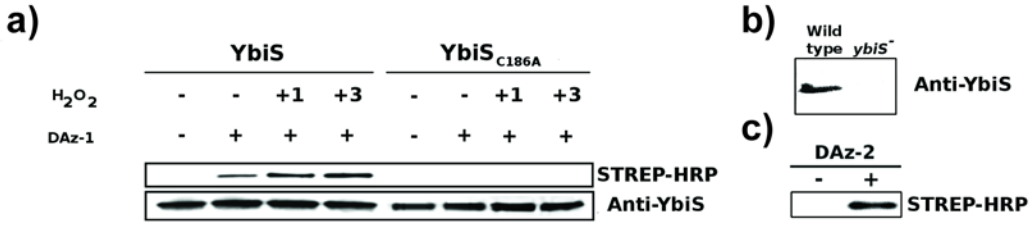

Figure 4.5 YbiS forms a stable sulfenic acid in vitro and in vivo. a) Sulfenic acid modification of YbiS or catalytically inactive YbiS CXS, untreated or exposed to H_2O_2. Sulfenylation was detected by immunoblot with Strep-HRP (upper panel). Equal protein loading was verified by reprobing with anti-YbiS antibody (lower panel). b) Detection of sulfenic acid modification of endogenous YbiS in vivo. DAz-2-labeled proteins from wild-type and ybiS cells were biotinylated, enriched on streptavidin beads, separated by SDS-PAGE, and probed with antibodies against YbiS. c) Detection of sulfenic acid modification of recombinant his-tagged YbiS in vivo. YbiS was enriched by affinity chromatography on Ni^{2+} agarose, biotinylated and DAz-2 labeling was detected by immunoblot using Strep-HRP.

Due to their high reactivity, sulfenic acids are often difficult to identify. To test whether the cysteine residue of YbiS could form a stable sulfenic acid we used DAz-1, a probe that is chemically selective for sulfenic acids.[15] In addition, DAz-1 contains an azide chemical handle that can be modified to append a biotin moiety, allowing detection of the labeled proteins by streptavidin-conjugated horseradish peroxidase (Strep-HRP) immunoblot. Purified YbiS was labeled by DAz-1, indicating that YbiS undergoes sulfenic acid formation in vitro (Figure 4.5a).

Moreover, incubation of YbiS with H_2O_2 led to an increase in protein labeling. The presence of the sulfenic acid modification was further verified by mass spectrometry analysis (Figure 4.6). By contrast, no labeling was observed for a mutant protein lacking the catalytic cysteine (Figure 4.5a). While in some proteins, such as the organic peroxide sensor OhrR [16], cysteine sulfenates condense with a backbone amide to generate a cyclic sulfenamide, this modification was not observed with YbiS.

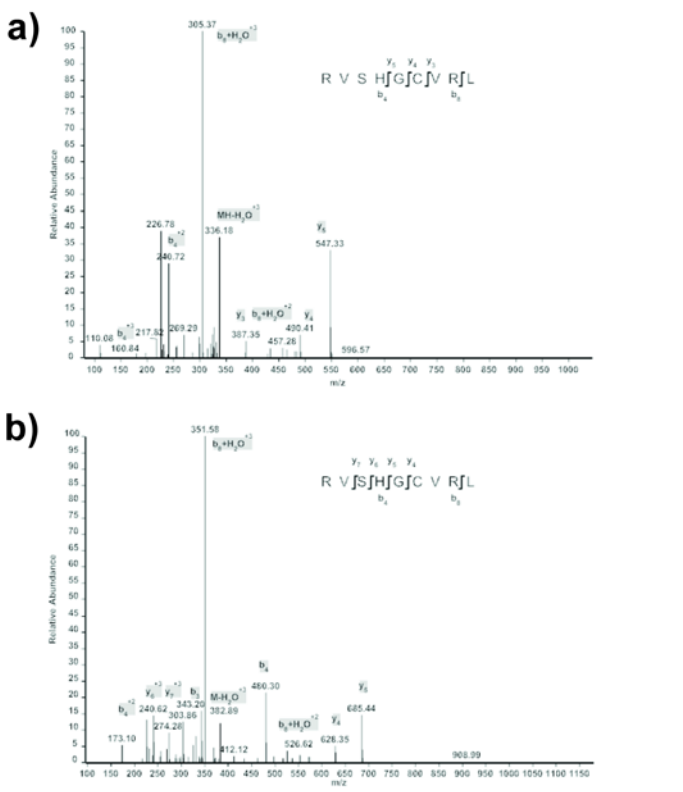

Figure 4.6 Mass spectrometry analysis of oxidized YbiS. Reduced or oxidized Ybis was digested with pepsin and analysed by LC-MS/MS. a) MS/MS spectrum of the triply charged reduced peptide RVSHGCVRL (parent ion at m/z 342.86). b) Oxidized YbiS was incubated with dimedone, a molecule that covalently reacts with sulfenic acids and produces a 138 Da mass increment. The MS/MS spectrum of the dimedone adducted peptide (parent ion at m/z 388.90) indicates that Cys186 is the adduction site.

4.3.5 YopH is sulfenylated *in vivo*

We confirmed that YbiS forms a sulfenic acid in vivo by labeling the oxidized protein directly in living cells using DAz-2, an analog of DAz-1 with improved potency.[17] After biotinylation of the probe, sulfenic acid modified proteins were captured on streptavidin beads. Immunoblot analysis with anti-YbiS antibody shows that YbiS is present in the DAz-2-labeled protein fraction (Figure 4.5b). Likewise, recombinant his-tagged YbiS could be modified in vivo by DAz-2. After enrichment on a Ni^{2+} column, YbiS was biotinylated and detected by Strep-HRP (Figure 4.5c).

Control reactions carried out in the *ybiS* strain (Figure 4.5b) or in the absence of DAz-2 (Figure 4.5c) gave no detectable protein labeling, as expected.

4.3.6 DsbG and DsbC control the level of sulfenylation in the periplasm

To determine whether DsbG and DsbC control the level of sulfenylation in the periplasm, wild-type, *dsbG*, *dsbC* and *dsbCdsbG* strains were grown in stationary phase, sulfenic acids were labeled in living cells and periplasmic extracts were prepared. After biotinylation of the probe, samples were analyzed by immunoblot using both Strep-HRP and an anti-YbiS antibody. Several periplasmic proteins were labeled by DAz-2, including a band migrating at the same position as YbiS (Figure 4.7). This in vivo snapshot of the global sulfenic acid content of a subcellular compartment reveals that sulfenic acid formation is a major posttranslational modification in the periplasm. Although the biotinylated bands were observed in periplasmic extracts prepared from all strains, the labeling was more intense in the samples prepared from *dsbCdsbG* mutants. This indicates that DsbG and DsbC are part of a periplasmic reducing system that controls the level of cysteine sulfenylation in the periplasm and provides reducing equivalents to rescue oxidatively damaged secreted proteins.

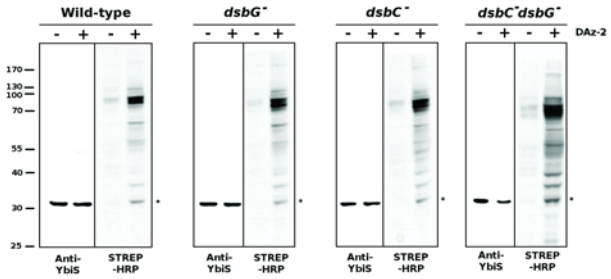

Fig. 4.7 Protein sulfenic acids accumulate in the periplasm of dsbCdsbG strains. Immunoblot of the periplasmic fraction prepared from wild-type, dsbG, dsbC and dsbCdsbG probed with anti-YbiS antibody or Strep-HRP. The asterisk denotes a band corresponding to YbiS.

4.4 Discussion

We propose the following model for the control of cysteine sulfenylation in the periplasm and the protection of single cysteines in this oxidizing compartment (Figure 4.8). In the periplasm, many proteins contain an even number of cysteines [18] that form disulfide bonds and are thus protected from further oxidation. However, some proteins, including YbiS, contain either a single cysteine or an odd number of cysteines.[18] Because they are not involved in disulfides, these cysteines would, without protection, tend to be vulnerable to oxidation and form sulfenic acids. Sulfenic acids, unless they are stabilized within the micro-environment of the protein, are susceptible to reaction with small molecule thiols to form mixed disulfides, as in the organic peroxide sensor OhrR [16], or to further oxidation to sulfinic and sulfonic acids. Oxidizing a catalytically active thiol inactivates the protein, necessitating a system in the periplasm that could rescue single cysteine residues from oxidation. DsbG, whose negatively-charged surface is better suited to interact with folded proteins, appears to be a key player in this reducing system. DsbC, whose inner surface is lined with hydrophobic residues, seems to have evolved to interact with unfolded proteins to correct non-native disulfides. In parallel to this function, DsbC could also serve as a backup for DsbG. Both DsbC and DsbG are kept reduced by DsbD. Thus, the electron flux originating from the cytoplasmic pool of NADPH provides the reducing equivalents required for both the correction of incorrect disulfides and the rescue of sulfenylated orphan cysteines.

Sulfenic acid formation is pervasive in certain eukaryotic cells [19] both as unwanted products of cysteine oxidation by ROS and in enzyme catalysis and signal transduction.[14,20] Proteins from the thioredoxin superfamily are widespread and have been identified in the majority of the genomes. Thus some of these thioredoxin superfamily members, particularly those closely

related to DsbC and DsbG, may play similar roles in controlling the global sulfenic acid content of eukaryotic cellular compartments.

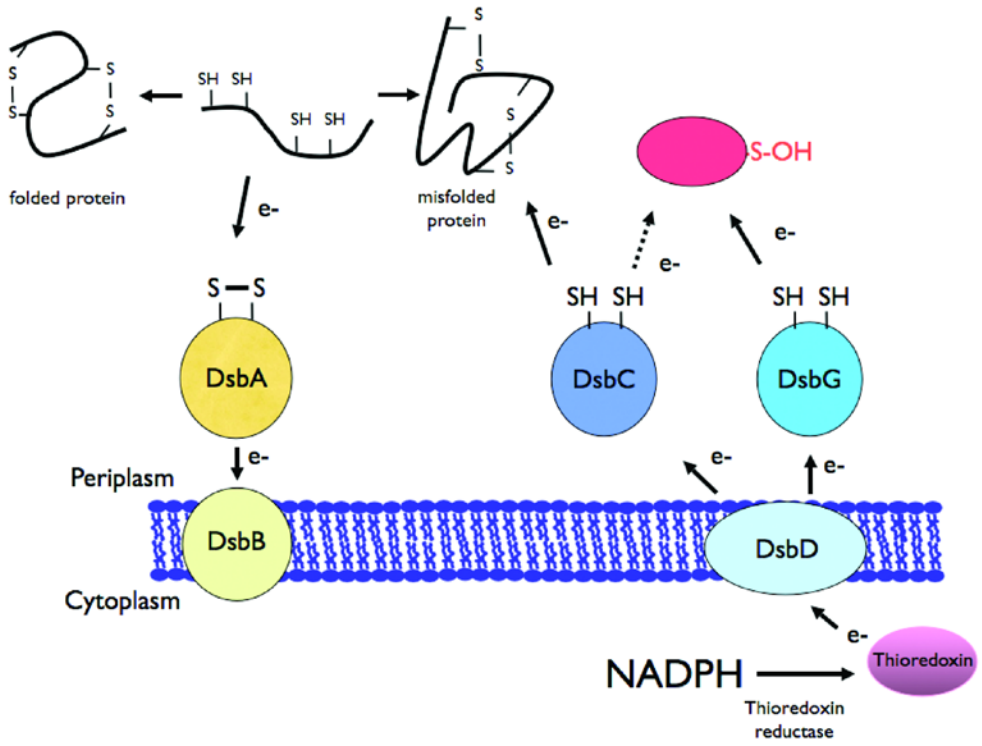

Figure 4.8 A model for sulfenic acid reduction in the periplasm. The periplasm is an oxidizing compartment in which most proteins contain an even number of cysteine residues that are oxidized to disulfide bonds by DsbA. When secreted proteins require disulfides to be formed between non-consecutive cysteines, DsbA may introduce non-native disulfides, leading to protein misfolding. The misfolded proteins, which expose hydrophobic residues on their surface, interact with the protein disulfide isomerase DsbC. DsbC catalyzes the reshuffling of the disulfide bonds, allowing the protein to fold correctly. Some periplasmic proteins possess either a single cysteine residue or an odd number of cysteine residues. Because they are not involved in the formation of a disulfide, single cysteine residues are vulnerable to oxidation and can be oxidized to sulfenic acid. Sulfenic acids are susceptible to reaction with small molecule thiols to form mixed disulfides or to further oxidation to sulfinic and sulfonic acids. Because this oxidation is likely to result in the inactivation of the protein, single cysteine residues are protected from oxidation by DsbG. Our results suggest that DsbC could serve as a backup for DsbG. DsbC could even have its own group of favorite substrates to reduce. Both DsbC and DsbG are kept reduced in the periplasm by DsbD, which transfers reducing equivalents originating from the cytoplasmic NADPH pool across the membrane.

4.5 Experimental Procedures

4.5.1 Strains and microbial techniques

Strains are listed in Appendix 4.5.2. Mutant strains were constructed by P1 transduction. MD89 was constructed by P1 transduction of the *dsbG::cm (FRT)* allele of JP514 (kindly provided by

James Bardwell, University of Michigan) into AH50. The chloramphenicol resistance gene was eliminated from the chromosome by using the pCP20 plasmid encoding the FLP recombinase.[21] The resulting strain (MD82) was transduced with the *dsbC::kan (FRT)* allele coming from the Keio collection.[22] The kanamycin resistance gene was eliminated from the chromosome in the same way, resulting in strain MD89. MD67 was constructed by P1 transduction of the *ybiS::kan (FRT)* allele from the Keio collection into AH50. MD85 was constructed by P1 transduction of the *gshA::kan (FRT)* allele from the Keio collection into MD82.

.

4.5.2 Media and growth conditions

Cultures were grown aerobically at 37°C in LB, M63 minimal medium supplemented with 0.2% glucose, vitamins (Thiamin 10 μg/ml, Biotin 1 μg/ml, Riboflavin 10 μg/ml, and Nicotinamide 10 μg/ml), 1 mM $MgSO_4$ or MOPS minimal media supplemented with 0.2 % glycerol, 0.2 % casamino acids and vitamins (Thiamin 10 μg/ml, Biotin 1 μg/ml, Riboflavin 10 μg/ml, and Nicotinamide 10 μg/ml). When necessary, media was supplemented with ampicillin (200 μg/ml), kanamycin (50 μg/ml) or chloramphenicol (25 μg/ml).

4.5.3 Plasmid constructions

The YbiS expression vector was constructed as followed: the region encoding the mature YbiS protein (without the sequence signal) was amplified from the chromosome using primers YbiScyt_Fw and YbiScyt_Rv (Appendix 4.5.4) and cloned into pET15b to yield plasmid pMD71 (Appendix 4.5.3). The sequence was verified. Plasmids pAH243 (generous gift of James Bardwell) and pMD71 were used to mutate the cysteines of DsbG and YbiS using the QuickChange Mutagenesis Protocol (Stratagene) and primers pairs $DsbG_{C112A}$_Fw/$DsbG_{C112A}$_Rv and $YbiS_{C186A}$_Fw/$YbiS_{C186A}$_Rv, respectively (Appendix 4.5.4).

To construct a plasmid expressing the full-length protein with its signal sequence, we amplified the coding DNA sequence from the chromosome using primers YbiSperi_Fw and YbiSperi_Rv (Appendix 4.5.4). The PCR product was cloned into pET3a to yield plasmid pMD50 (Appendix 4.5.3). A his-tag was fused at the C-terminus by PCR using the back-to-back primers YbiShis_Fw and YbiShis_Rv. Ligation of the linear PCR product yielded plasmid pMD52. The coding DNA sequence was then subcloned into pBAD33 using *XbaI* and *HindIII* to yield plasmid pMD53.

4.5.4 Proteomic analysis of periplasmic extracts

Cells (100 ml) were grown aerobically at 37°C in M63 minimal media to an A_{600} of 0.8 and periplasmic extracts were prepared as in.[23] Protein concentration was determined using the Bradford assay. 300 µg of periplasmic proteins were precipitated by adding trichloroacetic acid (TCA) to a final concentration of 10% w/v. The resulting pellet was successively washed with TCA and ice cold acetone, dried in a Speedvac, resuspended in 0.1 M NH_4HCO_3 pH 8.0 with 3 µg sequencing grade trypsin, and digested overnight at 30°C. Peptide samples were then acidified to pH 3.0 with formic acid and stored at 20°C. Peptides were loaded onto strong cation exchange column GROM-SIL 100 SCX (100 × 2 mm, GROM, Rottenburg, Germany) equilibrated with solvent A (5% acetonitrile v/v, 0.05% v/v formic acid pH 2.5 in water) and connected to an Agilent 1100 HPLC system. Peptides were separated using a 50 min elution gradient that consisted of 0%–50% solvent B (5% acetonitrile v/v, 1 M ammonium formate adjusted to pH 3.0 with formic acid in water) at a flow rate of 200 µl/min. Fractions were collected at 2 min intervals (20 in total) and dried using a Speedvac. Peptides were resuspended in 10 µl of solvent C (5% acetonitrile v/v, 0.01% v/v TFA in water) and analyzed by LC-MS/MS as described.[2] Raw data collection of approximately 54,000 MS/MS spectra per 2D-LC-MS/MS experiment was

followed by protein identification using the TurboSequest algorithm in the Bioworks 3.2 software package (ThermoFinnigan) against an *E. coli* protein database (SwissProt) as described.[2]

4.5.5 Overexpression and purification of DsbC, DsbG, and YbiS

DsbC and DsbG were expressed as described previously [24]. They were purified on a 5 ml HisTrap HP column (GE Healthcare) from the periplasmic extracts of BL21 (DE3) strains carrying either plasmid pMB24 or pMB23, respectively. YbiS was expressed in M63 medium supplemented with ampicillin (200 µg/ml) and chloramphenicol (25 µg/ml) in a BL21 strain harboring plasmid pMD71. Expression was induced with 0.5 mM IPTG at A_{600} ~0.6. After 12 h, cultures were centrifuged and bacteria resuspended in buffer A (50 mM sodium phosphate pH 8, 300 mM NaCl). Cells were disrupted by 2 passes through a French Press Cell at 1200 PSI. The cell lysate was then centrifuged for 1 hour at 16,000 rpm and the resulting supernatant (~25 ml) was diluted 3-fold with buffer A and applied onto a 5 ml HisTrap column. The column was washed with buffer A containing 9 mM imidazole. Proteins were eluted with an imidazole step gradient. The fractions containing YbiS were pooled, concentrated on a 5 kDa cutoff Vivaspin 15 (Sartorius) concentrator, and loaded onto a PD-10 column (GE Healthcare) equilibrated with buffer B (50 mM sodium phosphate pH 8.0, 150 mM NaCl). The protein was then diluted 10-fold in buffer C (25 mM Tris, pH 8) and loaded onto a HiTrap Q HP-Sepharose column (GE Healthcare) equilibrated with the same buffer. The column was washed with buffer C and the protein was eluted with a NaCl gradient (0–400 mM in 120 ml). The fractions containing YbiS were pooled and concentrated by ultrafiltration in an Amicon cell (YM-10 membrane), and desalted using a PD-10 column equilibrated with buffer C. The purity of the protein was >98 % as assessed by Coomassie blue gel staining. $YbiS_{C186A}$ was expressed and purified using a similar protocol.

4.5.6 Purification and separation of DsbG-substrate complexes

A one liter LB culture of JFC203 carrying pMD41 was grown at 37°C until A_{600} ~0.5. Expression was induced by addition of 0.2% L-arabinose. After 13 h, the culture was precipitated with 10% TCA and free cysteines were alkylated for two hours at 37°C in buffer A supplemented with 1% SDS and 10 mM iodoacetamide. The pH was adjusted for alkylation with 2 M Tris pH 8.8 addition. The lysate was diluted three-fold with buffer A and centrifuged at 10,000 x *g* for 30 min. The cleared lysate was loaded at 0.5 ml/min onto a 1 ml HisTrap HP column equilibrated with buffer A supplemented with 0.3% SDS. After washing with buffer A containing 0.3 % SDS and 15 mM imidazole, proteins were eluted with a step gradient from 15 mM to 300 mM imidazole. A single peak eluted at 150 mM imidazole. This fraction was concentrated by TCA precipitation. Proteins were resolved on SDS-PAGE under non-reducing conditions (first dimension). The gel lane was cut, incubated in SDS sample buffer containing 5% β-mercaptoethanol for 15 min, and placed on top of a second SDS-PAGE gel. After electrophoresis, proteins were visualized with PageBlue™ Protein Staining Solution (Fermentas).

4.5.7 Determination of the *in vivo* redox state of YbiS

To determine the *in vivo* redox state of YbiS, bacteria were grown in LB at 37°C and samples (1 ml) were taken in both exponential and stationary phases. Samples were standardized using the A_{600} values of the culture. After addition of 100 µl of 100 % ice-cold trichloroacetic acid (TCA) to the samples, free cysteines were modified using 3 mM mPEG (mPEG-MAL, Nektar Therapeutics, San Carlos, CA) as previously described.[25] YbiS was then detected by Western blot analysis using an anti-YbiS antibody produced from a rabbit immunized with the purified protein (Eurogentec, Liège, Belgium).

4.5.8 Identification of the substrates of DsbG by mass spectrometry

The stained protein band was manually excised and in-gel tryptic digestion was performed using standard protocols. Peptides were mixed with 2 mg/ml of alpha-cyano-4-hydroxycinnamic acid matrix. MS and MS/MS spectra were acquired using an Applied Biosystems 4800 MALDI TOF/TOF™ Analyzer. MS and MS/MS queries were performed using the Applied Biosystems GPS Explorer™ 3.6 software working with the Matrix Science Ltd MASCOT® Database search engine v2.1 (Boston, USA). The NCBI (The National Center for Biotechnology Information) database was used. Two hundreds ppm precursor tolerance for MS spectra and 0.1 Da fragment tolerance for MS/MS spectra were allowed. The selected charge state of + 1, one trypsin miss-cleavage and variable modifications consisting of methionine oxidation, cystein carbamidomethylation and acrylamide modified cysteine were used.

4.5.9 YbiS-TNB reduction analysis

DsbC, DsbG and YbiS were incubated first with 10 mM DTT for 1 hour at 37°C. The proteins were then loaded on a gel filtration column (NAP-5, GE Healthcare) equilibrated with 50 mM phosphate buffer pH 8, 50 mM NaCl and 1 mM EDTA and eluted with 750 µl of the same buffer. To modify the catalytic cysteine residue of YbiS, the protein was incubated 1 h at 37°C with a 3-fold excess of DTNB. Excess DTNB was removed by gel filtration using a NAP-5 column. Reduction assays were performed at room temperature using a Beckman-Coulter spectrophometer with analytical wavelength set at 412 nm and using stoichiometric concentrations of YbiS-TNB and either DsbC or DsbG. YbiS, DsbC and DsbG concentrations were determined using an extinction coefficient E_{280} of 27,390, 17,670 and 44,015 M^{-1} cm^{-1}, respectively.

4.5.10 DAz-1 labeling of purified YbiS

DAz-1 was synthesized as previously described.[15] Wild-type YbiS and $YbiS_{C186A}$ were reduced with 2 mM DTT for 15 minutes at room temperature. Reducing agent was removed by gel filtration using p-30 micro Bio-Spin columns (BioRad). Proteins were then treated with increasing concentrations of hydrogen peroxide for 15 minutes at room temperature. H_2O_2 in excess was removed by p-30 columns. Proteins were then treated with 10 mM DAz-1 (diluted in DMSO) or DMSO for 15 minutes at 37°C. The probe in excess was removed by p-30 columns and the labeled proteins were biotinylated using 250 µM p-Biotin for two hours at 37°C. The samples were loaded on a SDS-PAGE gel and the proteins transferred on a PVDF membrane. The biotinylated proteins were detected by incubating the membrane with streptavidin-HRP (GE Healthcare).

4.5.11 Identification of YbiS-dimedone adduct

YbiS (2 µM) was incubated for 5 minutes at room temperature in DMSO with or without 2 mM dimedone. Both samples were then incubated with 2 mM H_2O_2 for 15 min at room temperature before precipitation with TCA (10% vol/vol). The pellets were washed with acetone, resuspended in 0.1% TFA and digested with 1 µg pepsin (Sigma) at 30°C overnight. The digested peptide mixtures were then separated by online reversed-phase microscale capillary liquid chromatography and analysed by electrospray tandem mass spectrometry (ESI-MS/MS). The LC-MS/MS system consisted of an LCQ DECA XP Plus ion trap mass spectrometer (ThermoFisher, San José, CA, USA) equipped with a microflow electrospray ionization source and interfaced to an LCPackings Ultimate Plus Dual gradient pump, Switchos column switching device, and Famos Autosampler (Dionex, Amsterdam, Netherlands). A reverse phase peptide trap C18 Pepmap 100

Dionex (0.30 mm × 5 mm) was used in front of an analytical BioBasic-C18 column from ThermoFisher (0.18 mm × 150 mm). Samples (6.4 µl) were injected and desalted on the peptide trap equilibrated with water containing 3.5% acetonitrile, 0.1% TFA at a flow rate of 30 µl/min. After valve switching, peptides were eluted in backflush mode from the trap onto the analytical column equilibrated in solvent A (5% acetonitrile v/v, 0.05% v/v formic acid in water) and separated using a 80 min gradient from 0% to 70% solvent E (80% acetonitrile v/v, 0.05% formic acid in water) at a flow rate of 1.5 µl/min.

The mass spectrometer in positive mode was set up to acquire one full MS scan in the mass range of 300–2000 m/z, after which Zoomscan and MS2 spectra were recorded for the three most intense ions. The dynamic exclusion feature was enabled to obtain MS/MS spectra on coeluting peptides, and the exclusion time was set at 2 min. The electrospray interface was set as follows: spray voltage 3.5 kV, capillary temperature 185°C, capillary voltage 30V, tube lens offset 100V, sheath gas flow at 2. Thermo Scientific Proteome Discoverer 1.0 software with SEQUEST was used for data analysis and peptide identification. Dimedone modification of 138.00 Da was used to extract the single ion chromatogram (SIC) of m/z = 388.85 $[M+3H]^{3+}$ corresponding to the peptide RVSHGCVRL adducted with dimedone. Manual interpretation and validation of the MS/MS data was done within Xcalibur 2.0.7 (ThermoFisher).

4.5.12 Pull down experiments of biotinylated YbiS with DAz-2

The synthesis and characterization of DAz-2 has recently been described.[24] 240 ml cultures of strains AH50 (wild type) and MD67 (*ybiS*) were grown overnight at 37°C. Cells were centrifuged for 10 min at 6,000 rpm and resuspended in 3 ml of 50 mM Tris, pH 8. After addition of 3 ml of spheroplasting buffer (50 mM Tris, pH 8, 1 M sucrose, 2 mM EDTA, 0.5 mg/ml lysozyme),

samples were split up and supplemented with 2 mM DAz-2 or DMSO. Incubation was performed for 15 min at 37°C with shaking. Osmotic shock was realized by addition of 3 ml of water followed, 15 min later, by the addition of 240 µl of 1M $MgCl_2$. Samples were centrifuged for 10 min at 13,200 rpm. The supernatants were concentrated to 1 ml with Vivaspin 500 concentrators. 50 µl of Dynabeads MyOne Streptavidin T1 (Invitrogen) were prepared according to the manufacturer's protocol. 400 µl of the samples prepared from the wild-type and *ybiS* strains were then added and incubated with the beads for one hour at room temperature with constant mixing. The beads were washed five times with 400 µl of PBS + 0.1% BSA. Proteins were eluted by boiling the beads in 50 µl Laemmli buffer for 5 min and then analyzed by Western Blots using an anti-YbiS antibody.

4.5.13 *In vivo* DAz-2 labeling of periplasmic extracts

40 ml cultures of strains AH50, JFC383, JFC203 and MD89 were grown overnight at 37°C. Cells were centrifuged for 10 min at 6,000 rpm and resuspended in 500 µl of 50 mM Tris, pH 8. After addition of 500 µl of spheroplasting buffer (50 mM Tris, pH 8, 1 M sucrose, 2 mM EDTA, 0.5 mg/ml lysozyme), samples were split up and supplemented with 2 mM DAz-2 or DMSO. Incubation was performed for 15 min at 37°C with shaking. Osmotic shock was realized by addition of 500 µl of water followed, 15 min later, by the addition of 40 µl of 1M $MgCl_2$. Samples were centrifuged for 10 min at 13,200 rpm. The supernatants were concentrated to 500 µl with Vivaspin 500 concentrators and loaded on SDS-PAGE gels for Western blot analysis. Samples were standardized using the A_{600} values of the culture.

4.5.14 Purification of DAz-2 labeled YbiS on His SpinTrap columns

240 ml culture of AH50 transformed with pMD53 were grown overnight at 37°C. Expression was induced with 0.00002% of L-arabinose for one hour at 37°C, cells were centrifuged and treated with DAz-2 as described above. The sample was then concentrated to 1 ml and 400 µl were loaded on His SpinTrap columns (GE Healthcare). Equilibration, wash and elution steps were performed according to the manufacturer. Aliquots from the elution steps were loaded on SDS-PAGE gels for Western blot analysis using Strep-HRP.

4.6 Appendices

4.6.1 Periplasmic proteins identified by 2D-LC-MS/MS in WT, and *dsbG* strains

		Wild type			*dsbG*			
Protein	**Cys**	**WT 1**	**WT 2**	**average**	**dsbG 1**	**dsbG 2**	**average**	**Ratio**
RNI	8	0,06	0,07	0,07	0,13	1,46	0,80	12,23
OSTA	6	0,12	0,11	0,12	0,20	0,11	0,16	1,35
DPPA	4	1,29	1,92	1,61	1,69	1,25	1,47	0,92
DSBC	4	0,13	0,09	0,11	0,16	0,07	0,12	1,05
YEDD	3	0,13	0,11	0,12	0,27	0,25	0,26	2,17
ARGT	2	0,88	1,01	0,95	1,02	1,46	1,24	1,31
ARTI	2	4,40	4,49	4,45	4,17	4,84	4,51	1,01
ARTJ	2	5,42	5,33	5,38	5,17	4,66	4,92	0,91
CIRA	2	0,07	0,05	0,06	0,04	0,00	0,02	0,33
CN16	2	0,07	0,04	0,06	0,07	0,00	0,04	0,64
CREA	2	0,04	0,04	0,04	0,04	0,04	0,04	1,00
DSBA	2	2,63	2,08	2,36	2,14	0,96	1,55	0,66
DSBG	2	0,10	0,05	0,08	0,00	0,00	0,00	0,00
ECOT	2	0,06	0,46	0,26	0,16	0,39	0,28	1,06
HISJ	2	2,75	3,18	2,97	2,74	2,28	2,51	0,85
IVY	2	0,67	0,78	0,73	0,67	0,46	0,57	0,78
OMPA	2	2,20	2,45	2,33	1,45	2,31	1,88	0,81
OPPA	2	5,43	6,29	5,86	5,50	5,91	5,71	0,97
POTF	2	0,13	0,11	0,12	0,13	0,36	0,25	2,04
PROX	2	0,85	0,75	0,80	0,49	0,57	0,53	0,66
SODC	2	0,04	0,04	0,04	0,13	0,18	0,16	3,88
TREA	2	0,06	0,04	0,05	0,04	0,11	0,08	1,50
UGPB	2	6,96	7,69	7,33	5,73	7,94	6,84	0,93
USHA	2	0,10	0,09	0,10	0,04	0,18	0,11	1,16
YAET	2	0,13	0,41	0,27	0,40	0,46	0,43	1,59
YEBF	2	0,55	0,62	0,59	0,65	0,61	0,63	1,08
YEBY	2	0,10	0,11	0,11	0,20	0,14	0,17	1,62
YGGN	2	0,10	0,11	0,11	0,16	0,07	0,12	1,10
YHJJ	2	0,06	0,05	0,06	0,09	0,11	0,10	1,82
YTFQ	2	0,06	0,36	0,21	0,42	0,18	0,30	1,43
ZNUA	2	0,09	0,09	0,09	0,04	0,07	0,06	0,61
ECNB	1	0,06	0,37	0,22	0,27	0,18	0,23	1,05
LPP	1	0,10	0,07	0,09	0,16	0,18	0,17	2,00
NLPB	1	0,12	0,07	0,10	0,13	0,14	0,14	1,42
NLPD	1	0,06	0,05	0,06	0,09	0,11	0,10	1,82
PSPE	1	0,13	0,11	0,12	0,07	0,07	0,07	0,58
SLP	1	0,03	0,04	0,04	0,29	0,11	0,20	5,71
SLYB	1	0,12	0,11	0,12	0,13	0,14	0,14	1,17
YAJG	1	0,06	0,05	0,06	0,11	0,11	0,11	2,00
YBIS	1	0,07	0,18	0,13	0,13	0,11	0,12	0,96
YCFS	1	0,07	0,05	0,06	0,09	0,07	0,08	1,33
YFGL	1	0,07	0,07	0,07	0,07	0,07	0,07	1,00
YGDI	1	0,07	0,04	0,06	0,09	0,07	0,08	1,45
YLIB	1	0,09	0,25	0,17	0,18	0,28	0,23	1,35
YNHG	1	0,04	0,04	0,04	0,20	0,11	0,16	3,88
YNJE	1	0,84	0,07	0,46	1,14	0,07	0,61	1,33
AMIB	0	0,12	0,07	0,10	0,20	0,21	0,21	2,16
AMIC	0	0,07	0,09	0,08	0,04	0,18	0,11	1,38

		Wild type			*dsbG*			
Protein	**Cys**	**WT 1**	**WT 2**	**average**	**dsbG 1**	**dsbG 2**	**average**	**Ratio**
AMPC	0	0,10	0,05	0,08	0,20	0,04	0,12	1,60
BTUB	0	0,09	0,07	0,08	0,16	0,18	0,17	2,13
CYSP	0	2,86	2,13	2,50	1,85	3,35	2,60	1,04
DGAL	0	0,09	0,39	0,24	0,36	0,39	0,38	1,56
FKBA	0	0,40	0,41	0,41	0,62	0,36	0,49	1,21
FLGH	0	0,10	0,09	0,10	0,09	0,07	0,08	0,84
FLIC	0	5,04	3,48	4,26	3,85	1,64	2,75	0,64
FLIY	0	3,65	3,32	3,49	3,61	4,70	4,16	1,19
GLNH	0	1,42	3,23	2,33	2,65	2,42	2,54	1,09
HLPA	0	0,90	1,05	0,98	1,23	0,64	0,94	0,96
LOLA	0	0,48	0,41	0,45	0,47	0,36	0,42	0,93
MALE	0	0,94	0,57	0,76	0,71	0,25	0,48	0,64
MIPA	0	0,12	0,11	0,12	0,13	0,21	0,17	1,48
MODA	0	0,78	0,66	0,72	1,14	0,75	0,95	1,31
MPPA	0	0,10	0,12	0,11	0,20	0,21	0,21	1,86
NMPC	0	0,99	0,60	0,80	0,53	0,36	0,45	0,56
OMPC	0	6,10	4,01	5,06	5,44	3,20	4,32	0,85
OMPF	0	1,27	3,13	2,20	2,56	2,53	2,55	1,16
OMPT	0	0,58	0,66	0,62	0,60	1,32	0,96	1,55
OMPX	0	0,51	0,50	0,51	0,29	0,64	0,47	0,92
OPGG	0	0,12	0,07	0,10	0,18	0,25	0,22	2,26
OSMY	0	1,29	1,35	1,32	2,43	1,07	1,75	1,33
PHND	0	2,38	1,95	2,17	1,25	3,67	2,46	1,14
PHOE	0	1,42	1,67	1,55	1,16	0,75	0,96	0,62
POTD	0	1,20	1,30	1,25	1,05	1,17	1,11	0,89
PPIA	0	0,85	0,62	0,74	0,45	0,50	0,48	0,65
PRC	0	0,10	0,02	0,06	0,04	0,07	0,06	0,92
PSTS	0	12,12	12,92	12,52	12,50	14,31	13,41	1,07
RBSB	0	5,52	3,68	4,60	5,28	3,77	4,53	0,98
SUBI	0	0,10	0,37	0,24	0,20	0,36	0,28	1,19
SURA	0	0,79	0,80	0,80	0,53	0,78	0,66	0,82
TESA	0	0,10	0,12	0,11	0,11	0,21	0,16	1,45
TOLB	0	1,17	0,91	1,04	1,20	1,00	1,10	1,06
TOLC	0	0,12	0,07	0,10	0,13	0,04	0,09	0,89
TSX	0	0,06	0,04	0,05	0,09	0,11	0,10	2,00
YCEI	0	0,13	0,21	0,17	0,07	0,21	0,14	0,82
YDEI	0	0,10	0,11	0,11	0,36	0,18	0,27	2,57
YDGH	0	0,94	1,05	1,00	1,20	0,82	1,01	1,02
YEHZ	0	0,07	0,09	0,08	0,16	0,07	0,12	1,44
YFGC	0	0,12	0,11	0,12	0,13	0,14	0,14	1,17
YGIW	0	0,09	0,05	0,07	0,22	0,18	0,20	2,86
YNCE	0	0,46	0,37	0,42	0,47	0,61	0,54	1,30
YOHN	0	0,07	0,07	0,07	0,09	0,14	0,12	1,64
YRAP	0	0,03	0,04	0,04	0,07	0,07	0,07	2,00
YRBC	0	1,18	1,30	1,24	1,27	1,14	1,21	0,97
YTFJ	0	0,01	0,02	0,02	0,11	0,14	0,13	8,33

4.6.2 Strains used in this study

Strain	Relevant genotype	Source
AH50	MC1000 *phoR Δara714leu*$^{+}$ *phoA68*	(26)
BL21 (DE3)	F^{-} ompT gal dcm lon hsdS$_B$(r_B^- m_B^-) λ(DE3 [lacI lacUV5-T7 gene 1 ind1 sam7 nin5])	Laboratory collection
BL21 (DE3) pLysS	F^{-} ompT gal dcm lon hsdS$_B$(r_B^- m_B^-) λ(DE3) pLysS(cm^R)	Laboratory collection
JFC203	AH50 *dsbG ::kan*	Laboratory collection
JFC313	AH50 *ahpCF::kan katE :: tet*	Laboratory collection
JFC315	AH50 *ahpCF::kan katE :: tet dsbD*	Laboratory collection
JFC383	AH50 *dsbC::kan*	(27)
MD67	AH50 *ybiS::kan*	This study
MD82	AH50 *dsbG*	This study
MD85	MD82 *gshA::kan*	This study
MD89	AH50 *dsbCdsbG*	This study

4.6.3 Plasmids used in this study

Plasmid	Relevant genotype or characteristics	Source
pAH243	pBAD33a-DsbG-His_6	(28)
pET3a	IPTG inducible, Amp^R selection	Novagen
pET15b	IPTG inducible, Amp^R selection	Novagen
pET28a	IPTG inducible, Kan^R selection	Novagen
pMB23	pET28a DsbG	Received from J. Bardwell
pMB24	pET28a DsbC	Received from J. Bardwell
pMD100	Same that pMD71 but for expression of $YbiS_{C186A}$	This study
pMD35	pBAD33a $DsbC_{CXXS}$-His_6	(27)
pMD41	pBAD33a $DsbG_{CXXA}$-His_6	This study
pMD50	pET3a YbiS expressed in the periplasm	This study
pMD52	pET3a YbiS-His_6 expressed in the periplasm	This study
pMD53	pBAD33a YbiS-His_6 expressed in the periplasm	This study
pMD71	pET15b YbiS-His_6 expressed into the cytoplasm	This study

4.6.4 Primers used in this study.

Name	Sequence (5' to 3')
$DsbG_{C112A}$_Fw	GCCGATCCGTTCTGCCCATATGCTAAACAGTTCTGG
$DsbG_{C112A}$_Rv	CCAGAACTGTTTAGCATATGGGCAGAACGGATCGGC
$YbiS_{C186A}$_Fw	GTAAGTCATGGTGCTGTGCGTCTGCGTAAC
$YbiS_{C186A}$_Rv	GTTACGCAGACGCACAGCACCATGACTTAC
YbiScyt_Fw	GCGCATATGGTAACTTATCCTCTGCCAACC
YbiScyt_Rv	ATATGGATCCTTAATTCAGACGAACCGGCAT
YbiSperi_Fw	GCGCATATGAATATGAAATTGAAAACATTA
YbiSperi_Rv	ATATGGATCCATTCAGACGAACCGGCAT
YbiShis_Fw	ATGATGATGATTCAGACGAACCGGCATCCCGGA
YbiShis_Rv	CATCATCACTAAGGATCCGGCTGCTAACAAAGCCCG

Notes

This work has been published as "A periplasmic reducing system protects single cysteine residues from oxidation.." **Science.** 2009 Nov 20;326(5956):1109-11. Matthieu Depuydt purified proteins. Stephen E Leonard synthesized DAz-2. Matthieu Depuydt and Stephen E Leonard performed biochemical and *in vivo* experiments. Matthieu Depuydt, Stephen E Leonard, Kate S Carroll, and Jean-François Collet designed the experiments.

[26] [27] [28]

4.7 References

1. Messens J, Collet JF: **Pathways of disulfide bond formation in Escherichia coli**. *Int J Biochem Cell Biol* 2006, **38**:1050-1062.
2. Bessette PH, Cotto JJ, Gilbert HF, Georgiou G: **In vivo and in vitro function of the Escherichia coli periplasmic cysteine oxidoreductase DsbG**. *J Biol Chem* 1999, **274**:7784-7792.
3. Heras B, Edeling MA, Schirra HJ, Raina S, Martin JL: **Crystal structures of the DsbG disulfide isomerase reveal an unstable disulfide**. *Proc Natl Acad Sci U S A* 2004, **101**:8876-8881.
4. Balmer Y, Vensel WH, Tanaka CK, Hurkman WJ, Gelhaye E, Rouhier N, Jacquot JP, Manieri W, Schurmann P, Droux M, et al.: **Thioredoxin links redox to the regulation of fundamental processes of plant mitochondria**. *Proc Natl Acad Sci U S A* 2004, **101**:2642-2647.
5. Kadokura H, Tian H, Zander T, Bardwell JC, Beckwith J: **Snapshots of DsbA in action: detection of proteins in the process of oxidative folding**. *Science* 2004, **303**:534-537.
6. Mainardi JL, Hugonnet JE, Rusconi F, Fourgeaud M, Dubost L, Moumi AN, Delfosse V, Mayer C, Gutmann L, Rice LB, et al.: **Unexpected inhibition of peptidoglycan LD-transpeptidase from Enterococcus faecium by the beta-lactam imipenem**. *J Biol Chem* 2007, **282**:30414-30422.
7. Magnet S, Bellais S, Dubost L, Fourgeaud M, Mainardi J-L, Petit-Frere S, Marie A, Mengin-Lecreulx D, Arthur M, Gutmann L: **Identification of the L,D-Transpeptidases Responsible for Attachment of the Braun Lipoprotein to Escherichia coli Peptidoglycan**. Edited by; 2007:3927-3931. vol 189.]
8. Messens J, Van Molle I, Vanhaesebrouck P, Limbourg M, Van Belle K, Wahni K, Martins JC, Loris R, Wyns L: **How thioredoxin can reduce a buried disulphide bond**. *J Mol Biol* 2004, **339**:527-537.
9. Rietsch A, Bessette P, Georgiou G, Beckwith J: **Reduction of the periplasmic disulfide bond isomerase, DsbC, occurs by passage of electrons from cytoplasmic thioredoxin**. *J Bacteriol* 1997, **179**:6602-6608.
10. Seaver LC, Imlay JA: **Alkyl hydroperoxide reductase is the primary scavenger of endogenous hydrogen peroxide in Escherichia coli**. *J Bacteriol* 2001, **183**:7173-7181.
11. Eser M, Masip L, Kadokura H, Georgiou G, Beckwith J: **Disulfide bond formation by exported glutaredoxin indicates glutathione's presence in the E. coli periplasm**. *Proc Natl Acad Sci U S A* 2009, **106**:1572-1577.
12. Reddie KG, Carroll KS: **Expanding the functional diversity of proteins through cysteine oxidation**. *Curr Opin Chem Biol* 2008, **12**:746-754.
13. Takanishi CL, Ma LH, Wood MJ: **A genetically encoded probe for cysteine sulfenic acid protein modification in vivo**. *Biochemistry* 2007, **46**:14725-14732.
14. Paulsen CE, Carroll KS: **Chemical dissection of an essential redox switch in yeast**. *Chem Biol* 2009, **16**:217-225.
15. Reddie KG, Seo YH, Muse Iii WB, Leonard SE, Carroll KS: **A chemical approach for detecting sulfenic acid-modified proteins in living cells**. *Mol Biosyst* 2008, **4**:521-531.
16. Lee JW, Soonsanga S, Helmann JD: **A complex thiolate switch regulates the Bacillus subtilis organic peroxide sensor OhrR**. *Proc Natl Acad Sci U S A* 2007, **104**:8743-8748.
17. Leonard SE, Reddie KG, Carroll KS: **Mining the Thiol Proteome for Sulfenic Acid Modifications Reveals New Targets for Oxidation in Cells**. *ACS Chem Biol* 2009.
18. Dutton RJ, Boyd D, Berkmen M, Beckwith J: **Bacterial species exhibit diversity in their mechanisms and capacity for protein disulfide bond formation**. *Proc Natl Acad Sci U S A* 2008, **105**:11933-11938.
19. Saurin AT, Neubert H, Brennan JP, Eaton P: **Widespread sulfenic acid formation in tissues in response to hydrogen peroxide**. *Proc Natl Acad Sci U S A* 2004, **101**:17982-17987.

20. Poole LB, Nelson KJ: **Discovering mechanisms of signaling-mediated cysteine oxidation**. *Curr. Opin. Chem. Biol.* 2008, **12**:18-24.
21. Datsenko KA, Wanner BL: **One-step inactivation of chromosomal genes in Escherichia coli K-12 using PCR products**. *Proc Natl Acad Sci U S A* 2000, **97**:6640-6645.
22. Baba T, Ara T, Hasegawa M, Takai Y, Okumura Y, Baba M, Datsenko KA, Tomita M, Wanner BL, Mori H: **Construction of Escherichia coli K-12 in-frame, single-gene knockout mutants: the Keio collection**. *Mol Syst Biol* 2006, **2**:2006 0008.
23. Hiniker A, Bardwell JC: **In vivo substrate specificity of periplasmic disulfide oxidoreductases**. *J Biol Chem* 2004, **279**:12967-12973.
24. Leonard SE, Reddie KG, Carroll KS: **Mining the thiol proteome for sulfenic acid modifications reveals new targets for oxidation in cells**. *ACS Chem Biol* 2009, **4**:783-799.
25. Cho SH, Porat A, Ye J, Beckwith J: **Redox-active cysteines of a membrane electron transporter DsbD show dual compartment accessibility**. *EMBO J* 2007, **26**:3509-3520.
26. Hiniker A, Collet JF, Bardwell JC: **Copper stress causes an in vivo requirement for the Escherichia coli disulfide isomerase DsbC**. *J Biol Chem* 2005, **280**:33785-33791.
27. Vertommen D, Depuydt M, Pan J, Leverrier P, Knoops L, Szikora JP, Messens J, Bardwell JC, Collet JF: **The disulphide isomerase DsbC cooperates with the oxidase DsbA in a DsbD-independent manner**. *Mol Microbiol* 2008, **67**:336-349.
28. Hiniker A, Ren G, Heras B, Zheng Y, Laurinec S, Jobson RW, Stuckey JA, Martin JL, Bardwell JC: **Laboratory evolution of one disulfide isomerase to resemble another**. *Proc Natl Acad Sci U S A* 2007, **104**:11670-11675.

Chapter 5

Redox-Based Probes for Protein Tyrosine Phosphatases

5.1 Introduction

5.1.1 Redox signaling

Over the past two decades, it has been established that growth factors, cytokines and a host of other ligands trigger the production of hydrogen peroxide (H_2O_2) in nonphagocytic cells via their corresponding membrane receptors.[1-3] Such H_2O_2 generation has been demonstrated to regulate many basic cellular processes including growth, differentiation, adhesion, migration, senescence, and autophagy.[4-6] Once formed, H_2O_2 promotes autophosphorylation of the membrane receptor and induction of the signaling cascade.

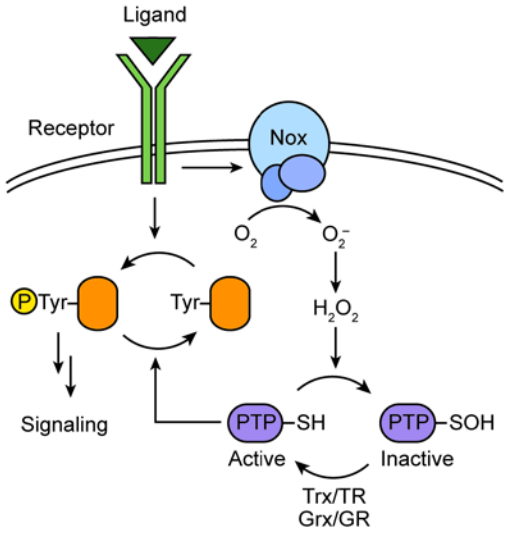

Figure 5.1 Proposed model for redox-dependent signal transduction. After ligand stimulation H_2O_2 levels increase, via the recruitment of cytosolic proteins and subsequent activation of membrane-bound NAPDH oxidase (Nox). Increased H_2O_2 production can lead to the oxidation of specific reactive Cys residues within proteins, with concomitant modulation of protein function. In PTPs, oxidation results in inactivation (and unopposed kinase action) until H_2O_2 levels decline and phosphatase activity is restored by reduction of the Cys residue.

Landmark publications from the Finkel and Rhee laboratories were the first to demonstrate an essential role for ROS growth factor receptor-mediated signal transduction.[7,8] As illustrated in Figure 5.1, ligand stimulation leads to a transient burst of H_2O_2 and a net increase in tyrosine phosphorylation of numerous

proteins, including the growth factor receptor itself.[9,10] Likewise, application of peroxide scavengers such as *N*-acetyl cysteine or catalase inhibits ligand-induced tyrosine phosphorylation. In large part, these effects are believed to arise from oxidative inhibition of protein tyrosine phosphatases (PTPs), which function as antagonists of protein tyrosine kinases and return membrane receptors to their resting state.[11,12]

5.1.2 Protein tyrosine phosphatase oxidation

There are ~80 members of the PTP superfamily, including the Tyr-specific enzymes and dual-specificity phosphatases (DSPs) that also recognize Ser/Thr.[13] The catalytic activity of PTPs depends upon an invariant active site Cys within the conserved signature motif [His-Cys-$(X)_5$-Arg-(Ser/Thr)] located at the bottom of the active site pocket.[14] Due to the nature of the active site environment, the catalytic Cys residue exhibits a remarkably low p*K*a (4.5 to 5.5) and is present as the thiolate anion at physiological pH. The low p*K*a serves to enhance the nucleophilicity of this residue, but also renders it susceptible to oxidation and enzymatic inactivation.[15] Consequently, oxidative inhibition of PTPs promotes phosphorylation-dependent signaling cascades.

Biochemical evidence indicates that upon exposure to H_2O_2, the catalytic Cys residue is converted into the sulfenic acid form and results in PTP inactivation (Figure 5.1).[16] This oxoform can react with a backbone amide to form a cyclic sulfenyl-amide for classical PTPs or an adjacent thiol in DSPs to form an intramolecular disulfide.[17] The activity of PTPs can be restored through the action of cellular antioxidants, such as the thioredoxin and glutaredoxin reducing systems.[11,12,18,19] Thus, oxidation of the catalytic Cys is reversible and represents a dynamic mechanism of PTP regulation.

Although the model presented in Figure 5.1 is supported by a number of elegant studies, it is also well known that the rate of reaction of a PTP with H_2O_2 is ~10^5 times slower than the equivalent reaction with peroxiredoxin, an antioxidant enzyme.[16,17] This raises the question of whether a nonenzymatic reaction can account for the formation of the sulfenic acid in PTPs.[20] This apparent discrepancy may reflect the possibility that enzymatic H_2O_2 generation needs to occur in close proximity to PTPs so that the oxidant concentration is high enough to make the rate of the uncatalyzed reaction physiologically relevant, or oxidation of the Cys residue may be catalyzed by another enzyme. Evidence to support or revise these proposals will require a better understanding of the mechanisms that underlie cellular compartmentalization, the extent of PTP oxidation *in situ*, and/or the discovery of a specific Cys oxidase.

5.1.3 Methods to detect protein tyrosine phosphatase oxidation

These outstanding questions, coupled with the physiological importance of PTPs, and their therapeutic relevance to diseases such as cancer and diabetes have motivated the development of methods for monitoring reversible PTP oxidation.[21,22] The majority of these approaches rely on the loss of reactivity with thiol-modifying reagents or the restoration of labeling by reducing agents. These techniques require that free thiols are completely blocked by alkylating agents prior to the reduction step and are thus, limited to enrichment from protein extracts. Methods to decrease oxidation artifacts after cell lysis have been reported[22]; however, they require specialized reagents or equipment, and other issues such as loss of labile modifications and temporal resolution are not addressed.

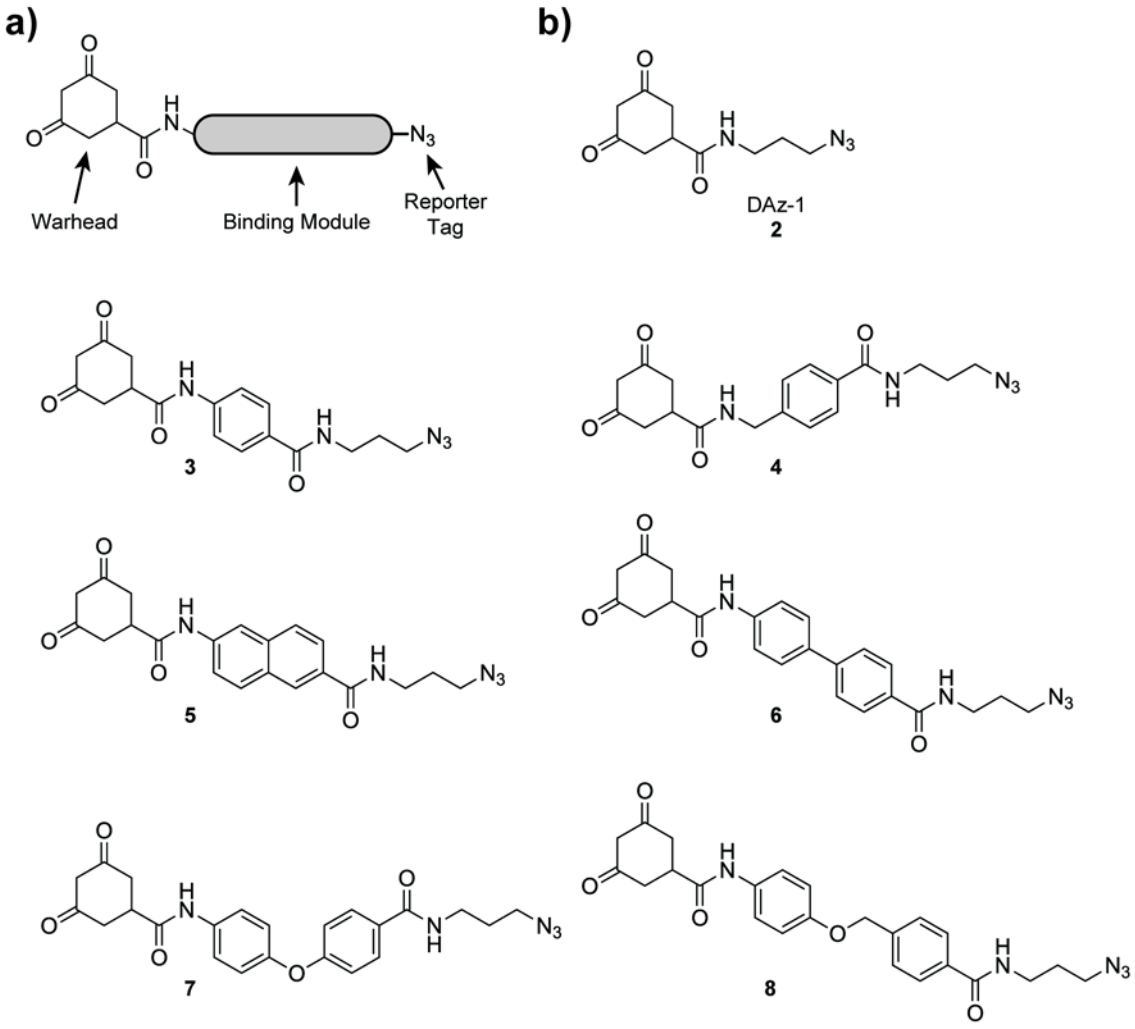

Figure 5.2 Redox-based probes (RBPs) for detecting reversible PTP oxidation. a) Design strategy for RBP includes the cyclic 1,3-diketone warhead, a synthetic module that directs binding to the PTP active site target, and an azide reporter tag for downstream analysis. b) Structures of the parent compound DAz-1 2 and the focused RBP library (3-8) synthesized and evaluated in this study.

Direct labeling methods that exploit the selective reaction of sulfenic acid and 5,5-dimethyl-1,3-cyclohexanedione (dimedone) **1** and related analogs have also been used to monitor PTP oxidation (Scheme 5.1).[23,24] Recently, we have reported the development of azide- and alkyne-based analogs of dimedone, such as DAz-1 **2** (Scheme 5.1) that enable trapping and tagging of sulfenic acid-modified proteins directly in cells.[24,25] The azide or alkyne chemical

reporter group can be used for bioorthogonal Staudinger and Huisgen [3+2] cycloaddition coupling reactions for downstream analysis of labeled proteins.

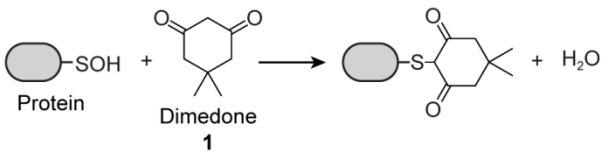

Scheme 5.1 Selective reaction between a protein sulfenic acid and dimedone 1

These reagents have been successfully deployed for global profiling of protein sulfenic acid modifications.[25,26] Although dimedone-based probes have shown wide utility for investigating Cys oxidation, the modest reaction rate and the low cellular abundance of signaling proteins has hampered the detection of oxidized PTPs.[26,27] Herein, we present a solution to this issue and report on the design of new redox-based probes (RBPs) for direct detection of PTP oxidation with significantly increased sensitivity and selectivity.

Our overall strategy for targeting reversible PTP oxidation is to create a trifunctional probe that consists of: (1) a warhead bearing the cyclic 1,3-diketone group, (2) a module that directs binding to the PTP target, and (3) a reporter tag used for the identification, purification, or direct visualization of the probe-labeled proteins (Figure 5.2a). This approach to detect PTP oxidation is inspired by the extensive use of activity-based probes to monitor phosphatase and protease activity.[28-31] We anticipated that integrating a binding module into the dimedone scaffold would provide a redox-based probe, termed RBP, designed to react only with the oxidized form of PTPs. Modification of PTP targets by such probes would provide a direct measure of oxidation and enable their purification and identification, thereby aiding in the elucidation of the biological roles of PTP oxidation in physiological and pathophysiological redox-mediated signal transduction pathways. Along these lines, we selected a series of synthetic binding modules known to target the active site of a broad range of enzymes from the PTP superfamily (Figure 5.2b). The phenyl **3** and benzyl **4** derivatives are modeled after the phosphotyrosine ring present

in the native substrate. Additional scaffolds that are common to many known PTP inhibitors include naphthalene **5,** biphenyl **6**, oxydibenzene **7**, and (benzyloxy)benzene **8**.[32-34] Accordingly, we prepared compounds **3**-**8** (Supporting Information) and evaluated their target-binding affinity and ability to monitor PTP oxidation.

5.2 Results

5.2.1 The protein tyrosine phosphatase YopH forms a sulfenic acid

To test our compounds of interest, we used recombinant *Yersinia* phosphatase (YopH). The enzyme is a representative member of the classical PTP superfamily and has been extensively characterized *in vitro*.[35-38] Like other PTPs, YopH harbors a catalytic Cys residue in its active site, Cys403 that is characterized by a low p*K*a (~5). Since sulfenic acid formation of YopH had not been previously documented, initial experiments were directed toward determining whether Cys403 was susceptible to oxidation by H_2O_2. Analogous to other redox-sensitive PTPs, we expected that oxidation of Cys403 would manifest itself as a loss of catalytic activity. We evaluated this proposal in steady-state assays using the fluorogenic substrate, 4-methylumbelliferyl phosphate (4-MUP). As shown in Figure 5.3a, YopH activity was detected as fluorescence signal owing to dephosphorylation of 4-

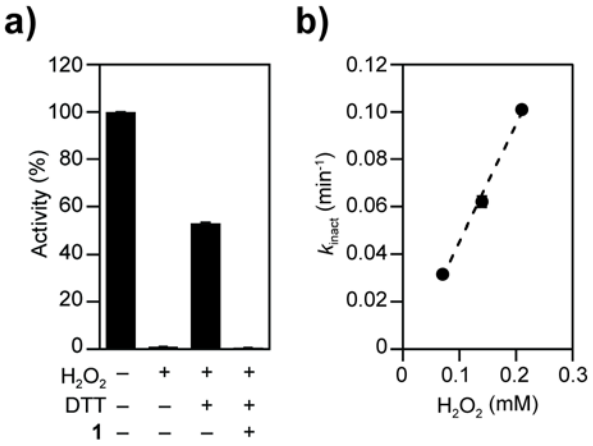

Figure 5.3 Analysis of YopH PTP oxidation by H_2O_2. a) YopH was inactivated by the addition of H2O2 in the absence of reducing agent. H_2O_2-inactivated YopH could be reactivated through DTT treatment. Dimedone 1 forms a covalent adduct with the sulfenic acid form of YopH, which prevents reactivation of YopH by DTT. b) The observed rate of YopH inactivation plotted as a function of H_2O_2 concentration. The second-order rate constant for oxidation of Cys403 by H_2O_2 was ~10 $M^{-1}s^{-1}$.

MUP. Exposure to 100 eq of H_2O_2 for 1 h abolished phosphatase activity and subsequent addition of dithiothreitol (DTT) resulted in substantial restoration of PTP function. These results are indicative of reversible sulfenic acid modification of Cys403. To verify the identity of the modification at the active site Cys, oxidized YopH was incubated with dimedone, which reacts with sulfenic acids to form a covalent adduct that is nonreducible by thiols. As expected, dimedone treatment inhibited PTP activity, which could not be restored by incubation with DTT. Mass spectrometry analysis also confirmed the adduct formation in a stoichiometry of 1:1 (Figure 5.4). Having established that YopH is susceptible to oxidation, the second-order rate constant for reaction of Cys403 with H_2O_2 was determined to be ~10 $M^{-1}s^{-1}$, consistent with values obtained for other PTPs (Figure 5.3b).[16]

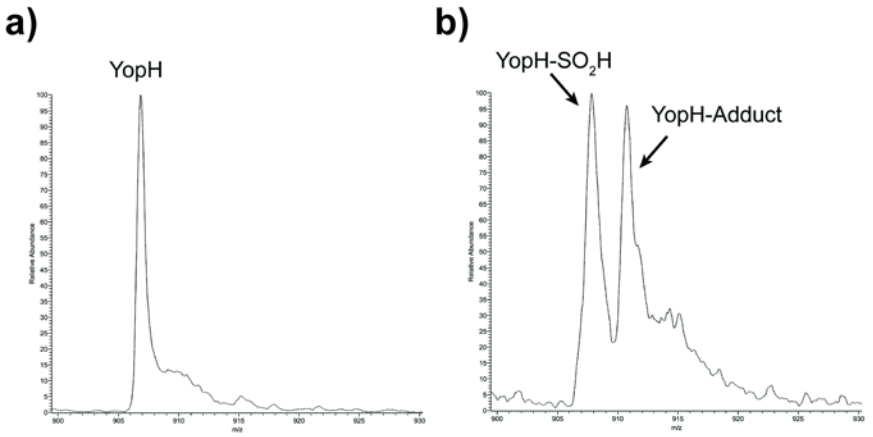

Figure 5.4 YopH forms a covalent adduct with dimedone with 1:1 stoichiometry. a) ESI mass spectra of active, unmodified YopH (33514.8 Da expected; 33514.6 Da observed). b) ESI mass spectrum of H_2O_2-treated YopH incubated with dimedone (33653.6 Da expected; 33653.2 Da observed). The signal at ~908 m/z corresponds to sulfinic acid-modified YopH (33546.8 expected; 33549.7 Da observed).

5.2.2 PTP active site is targeted by RBP binding element

Next, we examined the ability of compounds **3**-**8**, and the parent compound DAz-1, to reversibly inhibit activity of YopH. To this end, the dissociation constants (K_i) for inhibition were

determined by conducting the assays under reducing conditions, in the absence of H_2O_2. The resulting data fit well to a simple model of competitive inhibition[39] and the K_i values are summarized in Table 5.1. No significant inhibition by DAz-1 was observed at concentrations up to 12 mM,[40] consistent with the absence of an active site-targeted binding module. Phenyl **3** was moderately active, with a 130-fold increase in binding affinity relative to DAz-1. By contrast, benzyl **4** exhibited weak binding. Naphthalene **5** showed a 255-fold increase in affinity relative to DAz-1. The biphenyl derivative **6** conferred a 4,135-fold increase in binding affinity and was the most potent inhibitor of the series (K_i = 2.9 μM). Finally, oxydibenzene **7** and (benzyloxy)benzene **8** showed K_i values in the mid-micromolar range.

Table 5.1 Inhibition constants for DAz-1 **2** and compounds **3-8** with YopH[a]

Entry	K_i (μM)
DAz-1 **2**	>12,000
3	162.1
4	2,710
5	47.1
6	2.9
7	21.4[b]
8	113.3[b]

[a] K_i values represent the average of at least three independent experiments and the standard deviation was ≤25%. [b] Compounds exhibited aggregation-based inhibition.

In many cases, protein aggregation is a common mechanism of promiscuous chemical inhibitors.[41] The kinetic assays were therefore repeated with 0.02% Triton-X 100 detergent.

Inhibition by **2**-**6** was found to be independent of enzyme and detergent concentration. By contrast, compounds **7** and **8** both demonstrated a >15-fold decrease in potency when detergent was present in the assay buffer. These data are consistent with aggregation-based inhibition of YopH by **7** and **8**. Promiscuous inhibition has been observed previously in scaffolds that contain the oxydibenzene- or (benzyloxy)benzene functional groups.[41,42]

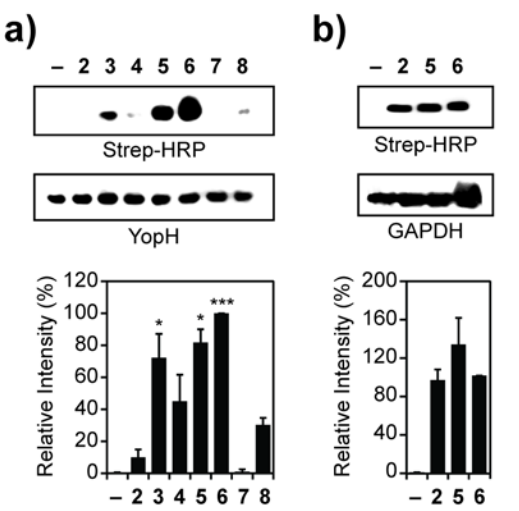

Figure 5.5 Analysis of RBP selectivity for oxidized YopH. a) RBPs detect sulfenic acid in oxidized YopH with increased sensitivity over the parent compound DAz-1 2. YopH was oxidized with H_2O_2 and incubated with compounds 2-8 or DMSO alone (–). Following p-biotin conjugation, reactions were analyzed by streptavidin-HRP western blot (top). Equal loading was verified by Ponceau S staining (bottom). b) RBPs do not increase general sulfenic acid reactivity. GAPDH was incubated with 2, 5, 6 or DMSO alone (–) followed by conjugation to p-biotin and analyzed by streptavidin-HRP western blot (top). Equal loading was verified by reprobing the blot with an antibody against GAPDH (bottom). Bar graphs summarize relative signal intensities from replicate experiments quantified via densitometry, normalized to 6, and analyzed by Student's t-test. Error bars represent s. e. m. *** indicates that $P < 0.001$ and * indicates that $P < 0.05$ when compared against detection with the parent compound, DAz-1 2.

5.2.3 RBPs detect YopH sulfenic acid

Compounds **3**-**8** were then tested for detecting sulfenic acid modification of YopH, and compared against DAz-1. For these experiments, the PTP was oxidized and then incubated for 15 min with each probe. Bioorthogonally labeled protein was detected through reaction of the azido group with phosphine-biotin (p-biotin) *via* the Staudinger ligation.[43] The products of these reactions were resolved by SDS-PAGE and analyzed by streptavidin-HRP western blot. Figure 5.5a shows that majority of compounds exhibited an increase in labeling relative to DAz-1.[44] The most significant increase in YopH sulfenic acid detection was observed for **3**, **5**, and **6**. Notably, probe **6**

exhibited the most potent K_i value and also showed the most robust detection of oxidized YopH. Naphthalene derivative **5**, which displayed the second highest binding activity, also demonstrated enhanced sulfenic acid detection. By contrast, compounds **4**, **7**, and **8** showed moderate to no reaction with the oxidized protein. The apparent lack of reactivity for compounds **7** and **8** is most likely due to the formation of promiscuous aggregates, as discussed above. Additional control experiments also verified that chemical reduction of YopH or pre-treatment of oxidized protein with dimedone inhibited azido-probe incorporation, as expected (Figure 5.6).

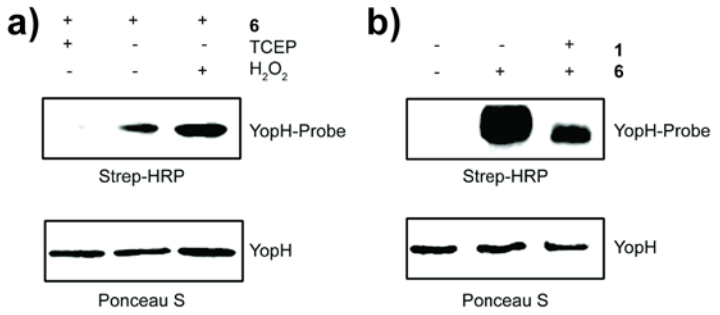

Figure 5.6 Compound 6 selectively modifies sulfenic acid-modified YopH. a) YopH labeling by compound 6 requires oxidation by H_2O_2. YopH was treated with the reducing agent TCEP, buffer alone, or H_2O_2 and then incubated with compound 6. Following Staudinger ligation, covalent modification of YopH by 6 was determined by streptavidin-HRP western blot. b) Dimedone pre-treatment blocks YopH modification by compound 6. YopH was treated with DMSO alone, compound 6, or pre-treated with dimedone 1 and then incubated with 6, as described above. Following Staudinger ligation, covalent modification of YopH by 6 was determined by streptavidin-HRP western blot.

5.2.4 RBPs demonstrate increased sensitivity for protein tyrosine phosphatase sulfenic acids

Our next goal was to assess the selectivity of probes **5** and **6**, relative to DAz-1, for detecting sulfenic acid modifications in non-PTP proteins. For this purpose, we used the metabolic enzyme glyceraldehyde 3-phosphate dehydrogenase (GAPDH). This protein forms a sulfenic acid modification at Cys149, which has been detected in previous studies by dimedone and related azido-analogs.[26,45,46] Oxidized GAPDH was incubated with DAz-1, **5**, or **6** followed by p-biotin conjugation and western blot analysis, as described above. Figure 5.5b shows that the each

azido-probe detected sulfenic acid modification of GAPDH with equal efficiency. Similar results were obtained with the thiol peroxidase, Gpx3 (data not shown). Finally, we examined the ability of compounds **5** and **6** to inhibit and detect reversible oxidation of PTP1B, another redox-sensitive tyrosine phosphatase.[8] Naphthalene **5** and biphenyl **6** inhibited PTP1B with K_i values of 0.67 ± 0.19 μM and 61.5 ± 7.0 μM, respectively. By contrast, PTP1B activity was not affected by DAz-1. Importantly, **5** and **6** showed enhanced detection of oxidized PTP1B, relative to DAz-1 (Figure 5.7). Taken together, these data establish that **5** and **6** are *bona fide* RBPs against YopH and PTP1B, thereby validating our general approach.

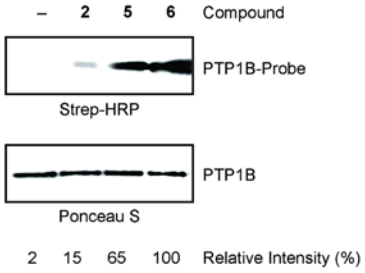

Figure 5.7 Analysis of RBP selectivity for oxidized PTP1B. RBP 5 and 6 detect sulfenic acid in oxidized PTP1B with increased sensitivity over the parent compound DAz-1 2. PTP1B was oxidized with H_2O_2 and incubated with compounds 2, 5, 6 or DMSO (–) alone. Following p-biotin conjugation, reactions were analyzed by streptavidin-HRP western blot (top). Equal loading was verified by Ponceau S staining (bottom).

5.2.5 Molecular modeling of RBP 6 in the YopH active site

To gain molecular insight into interactions between YopH and RBP **6** docking simulations were performed using AutoDock.[47] As shown in Figure 5.8, the two oxygen atoms of the cyclic diketone are predicted to form hydrogen bonds with several active site residues. In addition, the docking analysis suggests that aromatic stacking interactions can occur between the phenyl rings of RBP **6** and the side chain of Phe229. The remaining portion of the compound (*i.e.,* the chemical reporter group) appears largely exposed to solvent. Future structural studies of YopH in complex with RBP **6** should provide further insights into interactions that can facilitate active site targeting. Interestingly, the biphenyl group present in RBP **6** has been identified as a core

structure in many bioactive compounds and is considered a privileged scaffold.[48,49] Along these lines, an opportunity for future design will be to evaluate the potency of substituted biphenyls and create molecules that interact more closely with the PTP surface.

5.3 Discussion

In summary, we have developed a suite of redox-based probes that target the active site of YopH and PTP1B, which are both members of the classical PTP superfamily. Although indirect and direct methods to detect protein sulfenic acids have previously been reported,[25,45,50,51] our study provides the first example of the use of the cyclic 1,3-diketone, dimedone-like warhead to develop probes with enhanced targeting specificity. In terms of reversible inhibition, the potency of RBP **5** and **6** are comparable or exceed that of other known YopH and PTP1B inhibitors.[19] Future studies will focus on the application of RBPs to investigate PTP regulation and redox signaling in living systems. Finally, we note that the strategy employed to identify RBPs in the present manuscript may also represent an attractive starting point into the inhibitor- or tool-development cycle for other classes of proteins with redox-sensitive Cys residues.

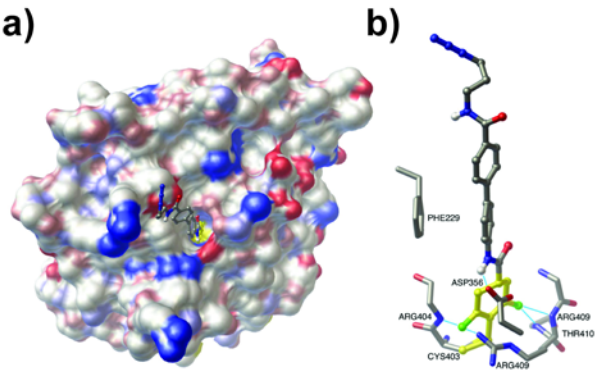

Figure 5.8 The binding conformation of RBP 6 with YopH predicted by AutoDock. a) Molecular surface representation of YopH (PDB code: 3BLT) colored by the polarity of atoms. RBP 6 is shown in balls-and-sticks. b) Detailed view of hypothetical interactions between YopH and RBP 6. The cyclic diketone is shown with carbon in yellow and oxygen in green. Hydrogen bonds are shown as thin blue lines. Images were created with the Python Molecular Viewer.[47]

5**.4 Experimental Procedures**

5.4.1 Materials

Reagents and solvents were purchased from Sigma or other commercial sources and were used without further purification. DAz-1 was synthesized as previously described.[1] YopH was expressed and purified as previously reported.[35] Recombinant PTP1b protein was purchased from Enzo Life Sciences.

5.4.2 Chemical methods

All reactions were performed under an argon atmosphere in oven-dried glassware. Analytical thin layer chromatography (TLC) was carried out using Analtech Uniplate silica gel plates and visualized using a combination of UV, potassium permanganate, and ninhydrin staining. Flash chromatography was performed using silica gel (32–63 μM, 60Å pore size) from Sorbent Technologies Incorporated. NMR spectra were obtained on a Varian Inova 400 (400 MHz for ^{1}H; 100 MHz for ^{13}C). ^{1}H and ^{13}C NMR chemical shifts are reported in parts per million (ppm) referenced to the residual solvent peak. High-resolution electrospray ionization (ESI) mass spectra were obtained with a Micromass AutoSpec Ultima Magnetic sector mass spectrometer at the University of Michigan Mass Spectrometry Laboratory. Low-resolution ESI mass spectra were obtained with a Micromass LCT Time-of-Flight mass spectrometer. Microwave reactions were performed in a Biotage Initiator Microwave Synthesizer.

5.4.3 Chemical Synthesis

Amino-N-(3-azidopropyl)benzamide (9)

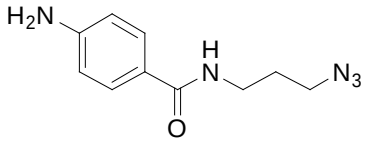

A 2-5 mL process vial flushed with argon was charged with a solution of 4-aminobenzoic acid (100 mg, 0.73 mmol), EDC (280 mg, 1.46 mmol) and DMAP (179 mg, 1.46 mmol) in dry DMF (5 mL). Subsequently 3-azidopropylamine (146 mg, 1.46 mmol) and TEA (0.204 mL, 1.46 mmol) were added to the solution. The vial was sealed, placed into the cavity of the microwave reactor and irradiated at 120 °C for 0.5 h. The DMF was removed *in vacuo* and the resulting oil was extracted with DCM/H_2O (3 x 15 mL). The organic phases were combined, dried over Na_2SO_4, filtered, and concentrated. Flash column chromatography was used for purification (EtOAc/Hexanes 6:4) to yield an oil, 4-amino-N-(3-azidopropyl)benzamide (**9**) (80 mg, 50%). ^{1}H NMR (400 MHz, $CDCl_3$) δ 7.57 (d, J = 8.5 Hz, 2H), 6.80 (s, 1H), 6.56 (d, J = 8 Hz, 2H), 4.14 (s, 2H), 3.431 – 3.383 (m, 2H), 3.30 (t, J = 6.7 Hz, 2H), 1.824 – 1.757 (m, 2H). ^{13}C NMR (100 MHz, $CDCl_3$) δ 167.7, 149.9, 128.6, 123.0, 49.3, 37.4, 28.8. ESIHRMS calcd. for $C_{10}H_{13}N_5O$ (M + Na) 242.11, found 242.1024.

N-(3-azidopropyl)-4-(3-methoxy-5-oxocyclohex-3-enecarboxamido)benzamide (10):

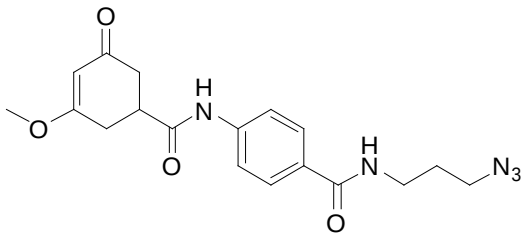

A 2-5 mL process vial flushed with argon was charged with 4-amino-N-(3-azidopropyl)benzamide (**9**) (363 mg, 1.66 mmol) and TEA (0.28 mL, 1.99 mmol)in dry DMF (2.5 mL). To this was added a solution of 3-methoxy-5-oxocyclohex-3-enecarboxylic acid (339 mg, 1.99 mmol), EDC (382 mg, 1.99 mmol), and DMAP (243 mg, 1.99 mmol) in dry DMF (2.5 mL). The vial was sealed, placed into the cavity of the microwave reactor and irradiated at 120 °C for 0.5 h. The DMF was

removed *in vacuo* and the resulting oil was extracted with DCM/H_2O (3 x 15 mL). The organic phases were combined, dried over Na_2SO_4, filtered, and concentrated. Purification was completed with flash column chromatography (EtOAc/Hexanes 1:1 to EtOAc) to yield N-(3-azidopropyl)-4-(3-methoxy-5-oxocyclohex-3-enecarboxamido)benzamide (**10**) (129 mg, 21%). ^{1}H NMR (400 MHz, $CDCl_3$) δ 8.95 (s, 1H), 7.68 (d, J = 8.4 Hz, 2H), 7.62 (d, J = 8.3 Hz, 2H), 6.73 (s, 1H), 5.37 (s, 1H), 3.70 (s, 3H), 3.55 – 3.49 (m, 2H), 3.42 (t, J = 6.5 Hz, 2H), 3.14 – 3.10 (m, 1H), 2.95 – 2.88 (m, 2H), 2.69 – 2.52 (m, 2H), 1.92 – 1.86 (m, 2H). ^{13}C NMR (100 MHz, CD_3OD) δ 198.8, 178.9, 168.2, 141.5, 129.4, 127.7, 118.9, 100.8, 55.5, 48.0, 40.8, 38.7, 37.0, 36.9, 30.9, 28.4. ESIHRMS calcd. for $C_{18}H_{21}N_5O_4$ (M + Na) 394.16, found 394.1495.

N-(3-azidopropyl)-4-(3,5-dioxocyclohex-3-enecarboxamido)benzamide (3):

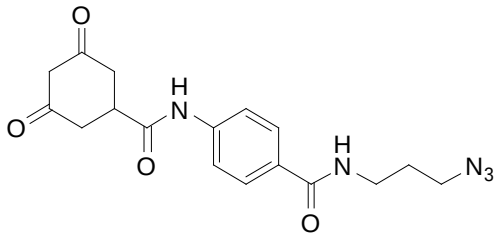

N-(3-azidopropyl)-4-(3-methoxy-5-oxocyclohex-3-enecarboxamido)benzamide (**10**) (129 mg, .348 mmol) was added to a solution of ACN/H_2O (1:1 v/v, 10 mL) with 10 mol% CAN (19 mg, .0348 mmol) and refluxed at 95 °C for 3 h. The reaction was cooled and concentrated. Flash column chromatography was used for purification (EtOAc to EtOAc/MeOH 9:1) to yield a yellow solid (**3**) (123 mg, 99%). ^{1}H NMR (400 MHz, DMSO-d_6) δ 10.22 (s, 1H), 8.41 (t, J = 5.4 Hz, 1H), 7.81 (d, J = 8.7 Hz, 2H), 7.66 (d, J = 8.7 Hz, 2H), 5.24 (s, 1H), 3.40 (t, J = 6.7 Hz, 2H), 3.32 – 3.28 (m, 2H), 3.19 – 3.10 (m, 1H), 2.57 – 2.52 (m, 2H), 2.50 – 2.42 (m, 2H), 1.80 – 1.73 (m, 2H). ^{13}C

NMR (100 MHz, DMSO-d_6) δ 171.9, 166.1, 141.9, 129.4, 128.4, 118.7, 103.7, 48.9, 39.9, 28.8. ESIHRMS calcd. for $C_{17}H_{19}N_5O_4$ (M + Na) 380.14, found 380.1325.

4-(((((9H-fluoren-9-yl)methoxy)carbonyl)amino)methyl)benzoic acid (11):

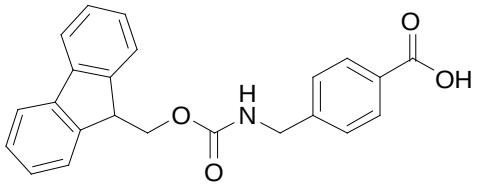

To a solution of $NaHCO_3$ (10% w/v, 10 mL) was added 4-(aminomethyl)benzoic acid (300 mg, 1.99 mmol). FMOC-OSU (805 mg, 2.98 mmol) was solubilized in THF (5 mL) and added drop wise to the reaction with vigorous stirring. The mixture was stirred at RT overnight. 1 N HCl was added to acidify the solution. The aqueous phase was then extracted with EtOAc (3 x 15 mL), the organic phases were combined, dried over Na_2SO_4, filtered, and concentrated. Purification was carried out by flash column chromatography (EtOAc/Hexanes 6:4 to EtOAc) giving the final product (**11**) (342 mg, 46%). ^{1}H NMR (400 MHz, DMSO-d_6) δ 7.95 – 7.91 (m, 2H), 7.89 (d, J = 6.9 Hz, 2H), 7.70 (d, J = 7.4 Hz, 2H), 7.42 (t, J = 7.4 Hz, 2H), 7.34 (d, J = 3.5 Hz, 2H) 7.32 (d, J = 4.8 Hz, 2H), 4.39 (d, J = 6.7 Hz, 2H), 4.24 (t, J = 7.7 Hz, 2H), 2.59 (s, 1H). ^{13}C NMR (100 MHz, DMSO-d_6) δ 173.2, 167.6, 156.8, 145.3, 144.2, 141.2, 129.7, 128.0, 127.4, 125.5, 120.5, 65.7, 47.2, 43.9, 25.6. ESIHRMS calcd. for $C_{23}H_{19}NO_4$ (M + Na) 396.1312, found 396.1212.

(9H-fluoren-9-yl)methyl 4-((3-azidopropyl)carbamoyl)benzylcarbamate (12):

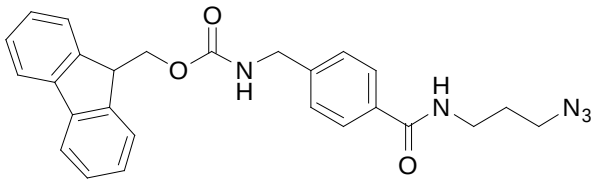

To an oven-dried flask, flushed with argon, was added a solution of 4-(((((9H-fluoren-9-yl)methoxy)carbonyl)amino)methyl)benzoic acid (**11**) (318 mg, .853 mmol) in anhydrous DMF (5 mL). TFA-Pfp was added (0.18 mL, 1.02 mmol) as well as TEA (0.143 mL, 1.02 mmol). The mixture was stirred at RT for 2 h before adding 3-azidopropylamine (103 mg, 1.02 mmol) and TEA (0.14 mL, 1.02 mmol). The reaction mixture was then left stirring overnight at RT. DMF was removed *in vacuo* and the resulting oil was extracted with DCM/H_2O (3 x 15 mL). The organic phases were combined, dried with Na_2SO_4, filtered, and concentrated. Purification was carried out by flash column chromatography (EtOAc/Hexanes 2:8 to 6:4) yielding the product (**12**) (243 mg, 63%). ^{1}H NMR (400 MHz, DMSO-d_6) δ 8.48 (t, J = 5.4 Hz, 1H), 7.89 (d, J = 7.4 Hz, 2H), 7.79 (d, J = 8.1 Hz, 2H), 7.70 (d, J = 7.4 Hz, 2H), 7.42 (t, J = 7.4 Hz, 2H), 7.33 (t, J = 7.4 Hz, 2H), 7.29 (d, J = 8.1 Hz, 2H), 4.39 – 4.35 (m, 2H), 4.24 (t, J =6.1 Hz, 2H), 3.41 (t, J = 6.7 Hz, 2H), 3.33 – 3.30 (m, 2H), 1.82 – 1.74 (m, 2H). ^{13}C NMR (100 MHz, DMSO-d_6) δ 166.5, 156.8, 144.2, 143.3, 141.1, 133.4, 128.0, 127.6, 127.4, 127.1, 125.5, 120.5, 65.7, 48.9, 47.2, 37.04, 28.8. ESIHRMS calcd. for $C_{26}H_{25}N_5O_3$ (M + Na) 478.20, found 478.1855.

4-(aminomethyl)-N-(3-azidopropyl)benzamide (13):

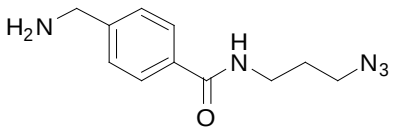

In a round bottom flask, (9H-fluoren-9-yl)methyl 4-((3-azidopropyl)carbamoyl)benzylcarbamate (**12**) (119 mg, 0.261 mmol) was added to a solution of ethanolamine in DCM (1:1 v/v, 5 mL) and

stirred for 3 h. The reaction mixture was washed with saturated $NaHCO_3$ and extracted with DCM (3 x 15 mL). The organic phases were combined, dried over Na_2SO_4, filtered, and concentrated. Flash column chromatography was used for purification (EtOAc/Hexanes 8:2 to EtOAc/MeOH 9:1) to yield 4-(aminomethyl)-N-(3-azidopropyl)benzamide (**13**) (40 mg, 66%). ^1H NMR (400 MHz, $CDCl_3$) δ 7.73 (d, J = 8.0 Hz, 2H), 7.37 (d, J = 8.0 Hz, 2H), 6.50 (s, 1H), 3.92 (s, 2H), 3.56 – 3.52 (m, 2H), 3.46 – 3.42 (m, 2H), 2.12 (s, 2H), 1.92 – 1.87 (m, 2H). ^{13}C NMR (100 MHz, $CDCl_3$) δ 167.4, 146.4, 132.9, 128.0, 126.9, 49.5, 45.8, 37.7, 28.7. ESIHRMS calcd. for $C_{26}H_{25}N_5O_3$ (M + H) 234.13, found 234.1355.

N-(3-azidopropyl)-4-((3-methoxy-5-oxocyclohex-3-enecarboxamido)methyl)benzamide (14):

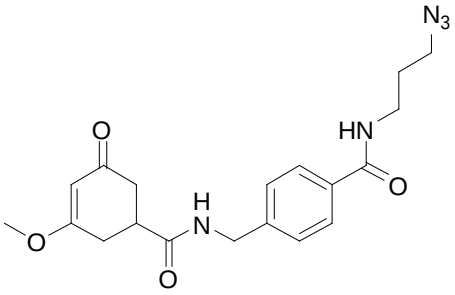

In an oven-dried round bottom flask, EDC (50 mg, .258 mmol) and DMAP (32 mg, .258 mmol) were added to a solution of 3-methoxy-5-oxocyclohex-3-enecarboxylic acid (44 mg, .2575 mmol) in anhydrous DMF (2.5 mL) under argon**.** To this was added 4-(aminomethyl)-N-(3-azidopropyl)benzamide (**13**) (40 mg, 0.172 mmol) in anhydrous DMF (2.5 mL) and TEA (0.04 mL, 0.258 mmol) and the reaction was stirred overnight at 45 °C. The DMF was removed *in vacuo* and the resulting oil was extracted using DCM/H_2O (3 x 15 mL). The organic phases were combined, dried with Na_2SO_4, filtered, and concentrated. Flash column chromatography was used to purify the product (EtOAc/Hexanes 3:7 to EtOAc/MeOH 9:1) yielding N-(3-azidopropyl)-

4-((3-methoxy-5-oxocyclohex-3-enecarboxamido)methyl)benzamide (**14**) (34 mg, 52%). ^{1}H NMR (400 MHz, $CDCl_3$) δ 7.66 (d, J = 8.3 Hz, 2H), 7.25 (d, J = 7.3 Hz, 2H), 5.35 (s, 1H), 4.46 (m, 2H), 3.70 (s, 3H), 3.56 – 3.51 (m, 2H), 3.44 (t, J = 6.5 Hz, 2H), 2.95 – 2.82 (m, 1H), 2.79 – 2.72 (m, 2H), 2.48 – 2.41 (m, 2H), 1.92 – 1.87 (m, 2H). ^{13}C NMR (100 MHz, $CDCl_3$) δ 197.6, 177.5, 172.6, 167.8, 141.8, 133.4, 127.2, 101.4, 56.0, 49.3, 42.8, 40.3, 37.6, 31.4, 29.6, 28.65. ESIHRMS calcd. for $C_{19}H_{23}N_5O_4$ (M + Na) 408.18, found 408.1648.

N-(3-azidopropyl)-4-((3,5-dioxocyclohex-3-enecarboxamido)methyl)benzamide (4):

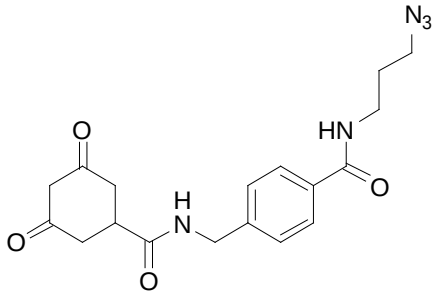

In a round bottom flask, N-(3-azidopropyl)-4-((3-methoxy-5-oxocyclohex-3-enecarboxamido)methyl)benzamide (**14**) (100 mg, 0.260 mmol) was added to a solution of ACN/H_2O (1:1 v/v, 5 mL) with 10 mol% CAN (14 mg, 0.026 mmol) and refluxed at 95 °C for 3 h. Solvent was removed *in vacuo.* Flash column chromatography was used to purify the product (EtOAc to EtOAc/MeOH 9:1) yielding (**4**) (89 mg, 92%). ^{1}H NMR (400 MHz, DMSO-d_6) δ 8.53 (t, J = 5.7 Hz, 1H), 8.48 (t, J = 5.5 Hz, 1H), 7.79 (d, J = 8.2 Hz, 2H), 7.30 (d, J = 8.1 Hz, 2H), 5.20 (s, 1H), 4.32 (d, J = 5.8 Hz, 2H), 3.40 (t, J = 6.7 Hz, 2H), 3.34 – 3.29 (m, 2H), 3.01 – 2.97 (m, 1H), 2.46 (d, J = 10.9 Hz, 2H), 2.38 – 2.32 (m, 2H), 1.82 – 1.72 (m, 2H). ^{13}C NMR (100 MHz, DMSO-d_6) δ 172.7, 166.5, 143.0, 133.4, 127.6, 127.1, 103.7, 48.9, 42.2, 37.0, 28.8. ESIHRMS calcd. for $C_{18}H_{21}N_5O_4$ (M + Na) 394.16, found 394.1491.

6-amino-N-(3-azidopropyl)-2-naphthamide (15):

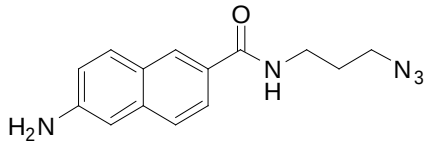

A 2-5 mL process vial flushed with argon was charged with a solution of 6-amino-2-naphthoic acid (50 mg, 0.27 mmol), EDC (58 mg, 0.30 mmol) and DMAP (52 mg, 0.30 mmol) in dry DMF (3 mL). Subsequently 3-azidopropylamine (54 mg, 0.54 mmol) and TEA (0.080 mL, 0.54 mmol) were also added to the solution. The vial was sealed, placed into the cavity of the microwave reactor and irradiated at 120 °C for 0.5 h. The DMF was removed *in vacuo* and the resulting oil was extracted with DCM/H_2O (3 x 15 mL). Flash column chromatography was used for purification (EtOAc/Hexanes 1:1) to yield an orange solid (**15)** (35 mg, 48%). ^{1}H NMR (400MHz, CD_3OD): δ 8.16 (s, 1H), 7.71 (d, *J*=8.8, 1H), 7.68 (d, *J*=9.2, 1H), 7.75 (d, *J*=8.8, 1H), 7.03 (d, *J*=8.4, 1H), 6.96 (d, *J*= 1.6, 1H), 3.47 (t, *J*=6.8, 2H), 3.40 (t, *J*= 6.8, 2H), 1.88 (q, *J*=6.4, 2H) ^{13}C NMR (100MHz, CD_3OD): δ 169.36, 147.78, 137.02, 129.75, 127.42, 126.85, 126.29, 125.31, 123.58, 118.9, 106.93, 48.84, 36.99, 28.50. ESIHRMS calcd. for $C_{11}H_{17}N_3O_2$ (M + Na) 292.1174, found 292.1175.

N-(3-azidopropyl)-6-(3-methoxy-5-oxocyclohex-3-enecarboxamido)-2-naphthamide (16):

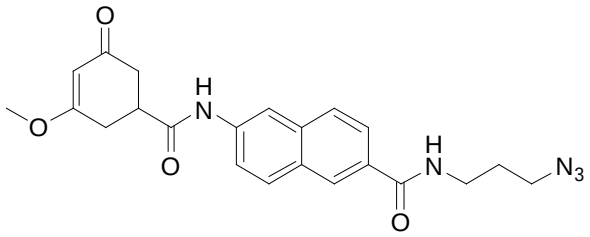

A 2-5 mL process vial flushed with argon was charged with a solution of 3-methoxy-5-oxocyclohex-3-enecarboxylic acid (22 mg, 0.13 mmol), EDC (27 mg, 0.14 mmol) and DMAP (25

mg, 0.14 mmol) in dry DMF (3 mL). 6-amino-N-(3-azidopropyl)-2-naphthamide (**15**) (35 mg, 0.13 mmol) and TEA (0.02 mL, 0.13 mmol) in dry DMF (2 mL) were then added to the solution. The vial was sealed, placed into the cavity of the microwave reactor and irradiated at 120 °C for 0.5 h. The DMF was removed *in vacuo* and the resulting oil was extracted with DCM/H_2O (3 x 15 mL). The organic phases were combined, dried over Na_2SO_4, filtered, and concentrated. Flash column chromatography was used for purification (EtOAc/Hexanes 1:1 to EtOAc) to yield an orange solid (**16**) (33 mg, 62%). ^{1}H NMR (400MHz, DMSO-d_6): δ 8.60 (t, *J*= 4.8, 1H), 8.33 (d, *J*=9.2, 2H), 8.16 (d, *J*=6.8, 1H), 7.93 (d, *J*=8.8, 1H), 7.84 (s, 1H), 7.60 (d, *J*= 7.2, 1H), 6.90 (d, *J*=6.4, 1H), 5.35 (s, 1H), 3.68 (s, 3H), 3.41 (t, *J*=6.8, 2H), 3.18 (t, *J*= 2.4, 2H), 3.13 (s, 2H), 3.12-2.56 (m, 3H), 1.78 (q, *J*=6.8, 2H). ^{13}C NMR (100MHz, DMSO-d_6): δ 196.64, 176.97, 171.89, 167.43, 166.87, 138.42, 135.13, 130.94, 130.00, 129.18, 127.74, 127.56, 125.10, 120.97, 115.31, 56.51, 49.00, 40.58, 37.15, 31.28, 28.88. ESIHRMS calcd. for $C_{22}H_{23}N_5O_4$ (M + Na) 444.1458, found 444.1649.

N-(3-azidopropyl)-6-(3,5-dioxocyclohex-3-enecarboxamido)-2-naphthamide (5):

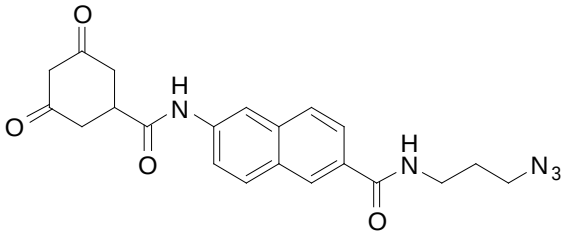

In a round bottom flask, (**16**) (33 mg, 0.08 mmol) was added to a solution of ACN/H_2O (1:1 v/v, 5 mL) with 10% CAN (4.4 mg, 0.008 mmol) and refluxed at 95 °C for 3 h. The reaction was cooled and concentrated. Flash column chromatography was used for purification (EtOAc to EtOAc/MeOH 9:1) to yield an orange solid (**5**) (30 mg, 92%). ^{1}H NMR (400MHz, DMSO-d_6): δ 8.29 (s, 2H), 7.92 (d, *J*=8.8, 1H), 7.84 (s,*2* H),7.63 (d, *J*=8.8, 1H), 5.10 (s, 1H), 3.49 (t, *J*=4.4, 2H),

3.43 (t, *J*= 6.8, 2H), 2.75-2.53 (m, 4H), 1.9 (q, *J*=7.2, 2H), 1.56 (t, *J*= 7.2, 1H). ESIHRMS calcd. for C21H21N5O4 (M + Na) 430.1491, found 430.1489.

4'-amino-N-(3-azidopropyl)-[1,1'-biphenyl]-4-carboxamide (17):

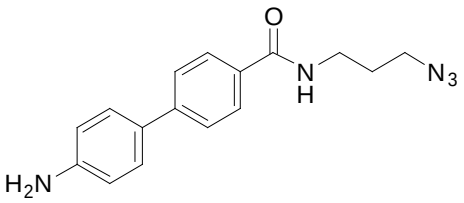

A 2-5 mL process vial flushed with argon was charged with a solution of 4'-amino-[1,1'-biphenyl]-4-carboxylic acid (125 mg, 0.587 mmol), EDC (122 mg, 0.646 mmol) and DMAP (110 mg, 0.30 mmol) in dry DMF (3 mL). Subsequently 3-azidopropylamine (88 mg, 0.88 mmol) and TEA (0.13 mL, 0.88 mmol) were also added to the solution. The vial was sealed, placed into the cavity of the microwave reactor and irradiated at 120 °C for 0.5 h. The DMF was removed *in vacuo* and the resulting oil was extracted with DCM and 10% (v/v) sodium bicarbonate (3 x 15 mL). Flash column chromatography was used for purification (EtOAc/Hexanes 4:6) to yield a white solid (**17**) (39 mg, 23%). ^{1}H NMR (400 MHz, CD_3OD) δ 7.87 – 7.79 (m, 2H), 7.73 (dd, *J* = 5.8, 3.3 Hz, 1H), 7.67 – 7.60 (m, 2H), 7.45 (d, *J* = 8.5 Hz, 2H), 6.80 (d, *J* = 8.5 Hz, 2H), 3.48 (t, *J* = 6.8 Hz, 2H), 3.43 (t, *J* = 6.7 Hz, 2H), 1.90 (dd, *J* = 13.6, 6.9 Hz, 2H). ^{13}C NMR (100 MHz, $CDCl_3$) δ 167.42, 146.56, 144.27, 131.80, 129.96, 128.08, 127.29, 126.22, 115.32, 49.59, 37.75, , 28.81. ESILRMS calcd. for $C_{16}H_{17}N_5O$ (M + H) 296, found 296.

N-(3-azidopropyl)-4'-(3-methoxy-5-oxocyclohex-3-enecarboxamido)-[1,1'-biphenyl]-4-carboxamide (18):

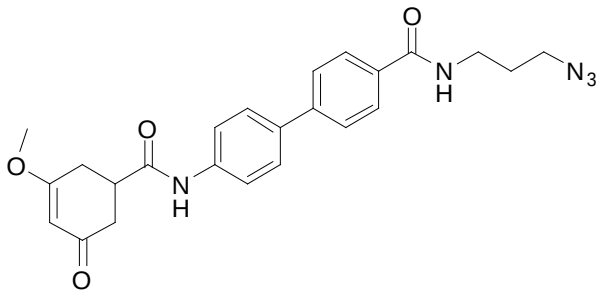

A 2-5 mL process vial flushed with argon was charged with a solution of 3-methoxy-5-oxocyclohex-3-enecarboxylic acid (23.8 mg, 0.14 mmol), EDC (26.8 mg, 0.14 mmol) and DMAP (25 mg, 0.14 mmol) in dry DMF (3 mL). 4'-amino-N-(3-azidopropyl)-[1,1'-biphenyl]-4-carboxamide (**17**) (39 mg, 0.13 mmol) and TEA (0.02 mL, 0.13 mmol) in dry DMF (2 mL) were also added to the solution. The vial was sealed, placed into the cavity of the microwave reactor and irradiated at 120 °C for 0.5 h. The DMF was removed *in vacuo* and the resulting oil was extracted with DCM/H_2O (3 x 15 mL). The organic phases were combined, dried over Na_2SO_4, filtered, and concentrated. Flash column chromatography was used for purification (EtOAc/Hexanes 6:4 to EtOAc) to yield a brown solid (**18**) (12 mg, 21%). ^{1}H NMR (400 MHz, $CDCl_3$) δ 7.81 (d, *J* = 8.4 Hz, 2H), 7.61 (d, *J* = 8.4 Hz,6H), 7.58 (s, 1H), 7.55 (d, *J* = 8.2 Hz, 1H), 6.40 (s, 1H), 5.42 (s, 1H), 3.71 (d, *J* = 12.8 Hz, 3H), 3.65 – 3.56 (m, 2H), 3.56 – 3.41 (m, 2H), 3.08 – 2.85 (m, 2H), 2.77 – 2.50 (m, 3H), 1.98 – 1.79 (m, 2H). ESIHRMS calcd. for $C_{24}H_{25}N_5O_4$ (M + Na) 470.1804, found 470.1790.

N-(3-azidopropyl)-4'-(3,5-dioxocyclohex-3-enecarboxamido)-[1,1'-biphenyl]-4-carboxamide (6):

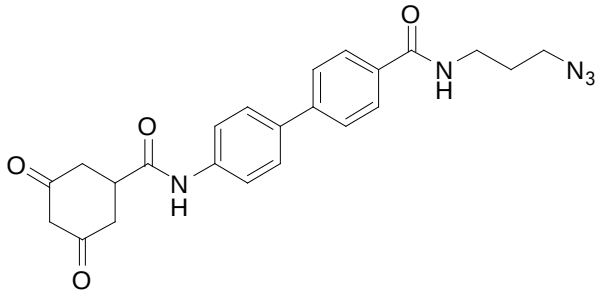

In a round bottom flask, (**18**) (12 mg, 0.027 mmol) was added to a solution of ACN/H_2O (1:1 v/v, 5 mL) with 10% CAN (1.6 mg, 0.003 mmol) and refluxed at 95 °C for 3 h. The reaction was cooled and concentrated. Flash column chromatography was used for purification (EtOAc to EtOAc/MeOH 9:1) to yield a yellow solid (**6**) (10 mg, 85%). ^{1}H NMR (400 MHz, CD_3OD) δ 8.58 (s, 1H), 7.89 (d, *J* = 8.6 Hz, 2H), 7.69 (dt, *J* = 17.3, 8.8 Hz, 6H), 5.39 (s, 1H), 3.49 (d, *J* = 5.6 Hz, 2H), 3.43 (t, *J* = 6.7 Hz, 2H), 2.66 (ddd, *J* = 40.4, 25.6, 22.0 Hz, 3H), 2.40 – 1.97 (m, 2H), 1.95 – 1.85 (m, 2H). ESILRMS calcd. for C23H23N5O4 (M + H) 434, found 434.

4-(4-aminophenoxy)-N-(3-azidopropyl)benzamide (19):

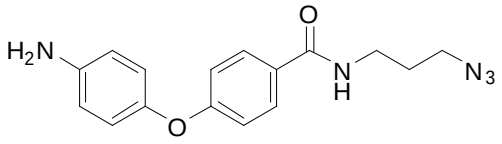

A 2-5 mL process vial flushed with argon was charged with a solution of 4-(4-aminophenoxy) benzoic acid (73.5 mg, 0.32 mmol), EDC (67 mg, 0.35 mmol) and DMAP (60.4 mg, 0.35 mmol) in dry DMF (3 mL). Subsequently 3-azidopropylamine (64 mg, 0.64 mmol) and TEA (0.09 mL, 0.64 mmol) were also added to the solution. The vial was sealed, placed into the cavity of the microwave reactor and irradiated at 120 °C for 0.5 h. The DMF was removed *in vacuo* and the resulting oil was extracted with DCM/H_2O (3 x 15 mL). Flash column chromatography was used for purification (EtOAc/Hexanes 4.5:5.5) to yield a brown solid (**19**) (31 mg, 31%). ^{1}H NMR (400 MHz, $CDCl_3$) δ 7.98 (d, *J* = 7.8 Hz, 2H), 6.89 – 6.74 (m, 4H), 6.66 – 6.56 (m, 2H), 3.21 – 3.15 (m,

2H), 3.13 – 3.06 (m, 2H), 1.79 (dt, *J* = 12.8, 6.3 Hz, 2H). ^{13}C NMR (101 MHz, $CDCl_3$) δ 128.60, 121.59,116.43,116.24, 49.61, 37.76, 28.78. ESILRMS calcd. for $C_{16}H_{17}N_5O_2$ (M + H) 312, found 312.

N-(3-azidopropyl)-4-(4-(3-methoxy-5-oxocyclohex-3-enecarboxamido)phenoxy)benzamide (20):

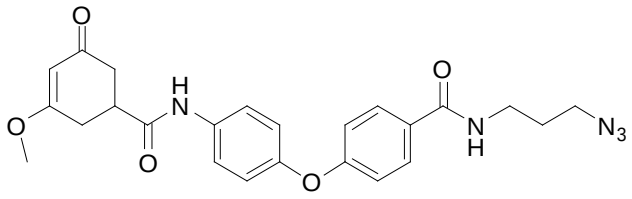

A 2-5 mL process vial flushed with argon was charged with a solution of 3-methoxy-5-oxocyclohex-3-enecarboxylic acid (19 mg, 0.11 mmol), EDC (21 mg, 0.11 mmol) and DMAP (19 mg, 0.11 mmol) in dry DMF (3 mL). Subsequently 4-(4-aminophenoxy)-N-(3-azidopropyl)benzamide (**19**) (31 mg, 0.1 mmol) and TEA (0.01 mL, 0.1 mmol) in dry DMF (2 mL) were also added to the solution. The vial was sealed, placed into the cavity of the microwave reactor and irradiated at 120 °C for 0.5 h. The DMF was removed *in vacuo* and the resulting oil was extracted with DCM/H_2O (3 x 15 mL). The organic phases were combined, dried over Na_2SO_4, filtered, and concentrated. Flash column chromatography was used for purification (EtOAc/Hexanes 1:1 to 8:2) to yield a yellow solid (**20**) (10 mg, 22%) ^{1}H NMR (400 MHz, $CDCl_3$) δ 8.19 (s, 1H), 7.68 (t, *J* = 10.9 Hz, 2H), 6.90 (dd, *J* = 19.4, 8.4 Hz, 4H), 6.72 – 6.57 (m, 2H), 6.33 (s, 1H), 5.39 (s, 1H), 3.70 (t, *J* = 12.3 Hz, 3H), 3.52 (dt, *J* = 18.2, 9.0 Hz, 2H), 3.45-3.42 (m, 2H), 3.04 (s, 1H), 2.79 – 2.45 (m, 2H), 1.93 – 1.85 (m, 2H), 1.85 – 1.74 (m, 2H). ^{13}C NMR (100 MHz, $CDCl_3$) δ 128.75, 121.76, 120.50, 117.40, 109.99, 101.84, 56.08, 49.57, 49.28, 41.63, 39.62, 37.85, 35.84, 31.34, 28.74. ESILRMS calcd. for C24H25N5O5 (M + H) 464, found 464.

N-(3-azidopropyl)-4-(4-(3,5-dioxocyclohex-3-enecarboxamido)phenoxy)benzamide (7):

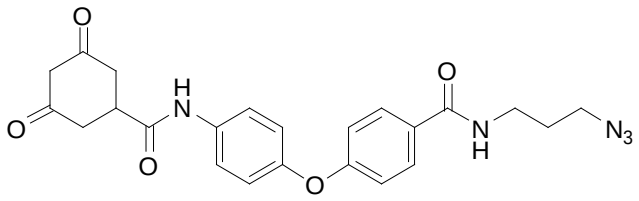

N-(3-azidopropyl)-4-(4-(3-methoxy-5-oxocyclohex-3-enecarboxamido)phenoxy)benzamide (**20**) (10 mg, 0.022 mmol) was added to a solution of ACN/H_2O (1:1 v/v, 10 mL) with 10 mol% CAN (1.2 mg, 0.002 mmol) and refluxed at 95 °C for 3 h. The reaction was cooled and concentrated. Flash column chromatography was used for purification (EtOAc to EtOAc/MeOH 9:1) to yield a white solid (**7**) (8 mg, 81%) ^{1}H NMR (400 MHz, DMSO-d_6) δ 8.21 (d, *J* = 6.9 Hz, 2H), 7.51 – 7.42 (m, 2H), 7.12 (dt, *J* = 10.8, 5.4 Hz, 2H), 6.96 (d, *J* = 7.3 Hz, 2H), 5.25 (s, 1H), 3.46 (s, 2H), 3.33 (s, 2H), 3.00 – 2.82 (m, 3H), 1.83 – 1.77 (m, 2H). ^{13}C NMR (100 MHz, DMSO-d_6) δ 128.51, 125.90, 60.20, 49.02, 46.15, 40.50, 40.29, 40.08, 21.19, 14.51, 9.04. ESILRMS calcd. for $C_{23}H_{23}N_5O_5$ (M + H) 450, found 450.

Methyl 4-((4-aminophenoxy)methyl)benzoate (21):

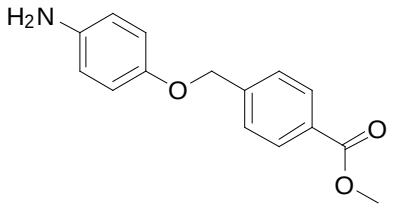

In an oven-dried round bottom flask flushed with argon NaH (60% suspension 60 mg, 1.5mM) was added to 4-aminophenol (163.5 mg, 1.5 mmol) in dry DMF (5 mL) and stirred for 1 h at 0 °C. Methyl 4-(bromomethyl)benzoate (230 mg, 0.13 mmol) in dry DMF (5 mL) was slowly added to the solution. The reaction stirred for 2 h. The DMF was removed *in vacuo* and the resulting oil was extracted with DCM/10% sodium bicarbonate (3 x 15 mL). The organic phases were

combined, dried over Na_2SO_4, filtered, and concentrated. Flash column chromatography was used for purification (EtOAc/Hexanes 1:1 to EtOAc) to yield a white solid (**21**) (265 mg, 62%). ^{1}H NMR (400 MHz, $CDCl_3$) δ 8.06 (t, *J* = 14.1 Hz, 2H), 7.47 (t, *J* = 10.1 Hz, 2H), 6.84 – 6.77 (m, 2H), 6.67 – 6.59 (m, 2H), 5.07 (d, *J* = 19.9 Hz, 2H), 3.91 (s, 3H), 3.25 (s, 2H). ^{13}C NMR (100 MHz, $CDCl_3$) δ 166.86, 151.58, 142.78, 140.45, 129.77, 129.46, 126.94, 116.32, 116.04, 70.10, 52.08. ESILRMS calcd. for $C_{15}H_{15}NO_3$ (M + H) 258, found 258.

4-((4-aminophenoxy)methyl)benzoic acid (22):

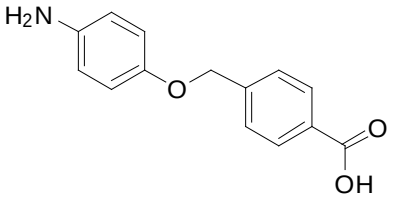

In a round bottom flask at 0 °C, potassium *tert*-butoxide (1.06 g, 11 mM) was stirred in 50 mL of ether for 15 min. H_2O (0.05 mL, 2.76 mmol) was then added to the slurry. After 5 min methyl 4-((4-aminophenoxy)methyl)benzoate (**21**) (265 mg, 0.92 mmol) was added and the reaction was stirred for 48 h. The ether was removed *in vacuo* and flash column chromatography was used for purification (EtOAc/MeOH 9:1) to yield a yellow solid (**22**) (192 mg, 86%). ^{1}H NMR (400 MHz, CD_3OD) 7.97 (t, *J* = 10.0 Hz, 2H), 7.46 (d, *J* = 8.4 Hz, 2H), 6.87 – 6.73 (m, 2H), 6.71 (dd, *J* = 6.6, 2.3 Hz, 2H). ^{13}C NMR (100 MHz, CD_3OD) δ 152.10, 141.74, 140.05, 129.22, 126.53, 116.83, 115.57, 110.12, 69.79. ESILRMS calcd. for $C_{13}H_{13}NO_3$ (M + H) 244, found 244.

4-((4-aminophenoxy)methyl)-N-(3-azidopropyl)benzamide (23):

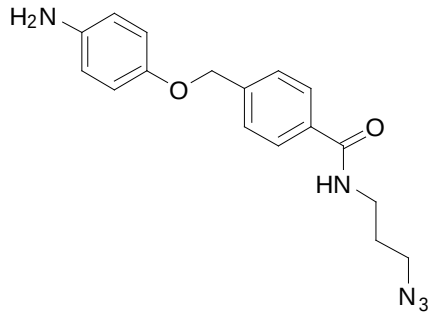

A 2-5 mL process vial flushed with argon was charged with a solution of 4-((4-aminophenoxy)methyl)benzoic acid (**22**) (100 mg, 0.41 mmol), EDC (86 mg, 0.45 mmol) and DMAP (60.4 mg, 0.45 mmol) in dry DMF (3 mL). Subsequently 3-azidopropylamine (45 mg, 0.45 mmol) and TEA (0.06 mL, 0.45 mmol) were also added to the solution. The vial was sealed, placed into the cavity of the microwave reactor and irradiated at 120 °C for 0.5 h. The DMF was removed *in vacuo* and the resulting oil was extracted with DCM/10% sodium bicarbonate (3 x 15 mL). The organic phases were combined, dried over Na_2SO_4, and concentrated. Flash column chromatography was used for purification (EtOAc/Hexanes 7:3) to yield a brown solid (**23**) (34 mg, 48**%**). ^{1}H NMR (400 MHz, $CDCl_3$) δ 8.25 – 8.13 (m, 2H), 6.81 – 6.72 (m, 2H), 6.66 – 6.58 (m, 2H), 6.54 (dd, *J* = 5.4, 1.5 Hz, 2H), 5.00 (s, 2H), 3.75 (dd, *J* = 9.3, 4.5 Hz, 2H), 3.28 (dd, *J* = 7.0, 4.4, 1.7 Hz, 2H), 1.84 – 1.74 (m, 2H). ^{13}C NMR (100 MHz, $CDCl_3$) δ 161.22, 140.77, 140.05, 127.25, 126.99, 116.31, 116.07, 70.11, 49.26, 35.85, 34.91, 29.67, 28.67, 14.88. ESILRMS calcd. for $C_{17}H_{19}N_5O_2$ (M + H) 326, found 326.

N-(3-azidopropyl)-4-((4-(3-methoxy-5-oxocyclohex-3-enecarboxamido)phenoxy)methyl)benzamide (24):

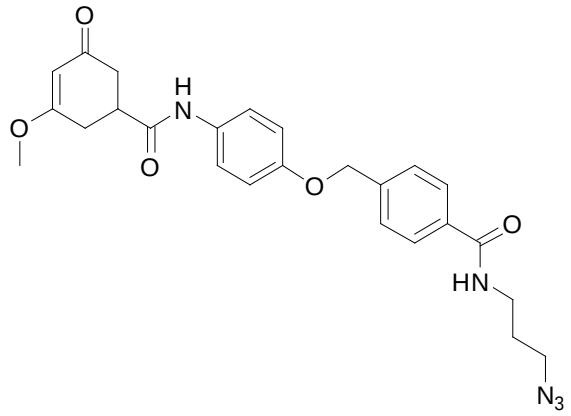

A 2-5 mL process vial flushed with argon was charged with a solution of 3-methoxy-5-oxocyclohex-3-enecarboxylic acid (17 mg, 0.10 mmol), EDC (19 mg, 0.1 mmol) and DMAP (17 mg, 0.1 mmol) in dry DMF (3 mL). Subsequently 4-((4-aminophenoxy)methyl)-N-(3-azidopropyl)benzamide (**23**) (34mg, 0.09 mmol) and TEA (0.01 mL, 0.1 mmol) in dry DMF (2 mL) were also added to the solution. The vial was sealed, placed into the cavity of the microwave reactor and irradiated at 120 °C for 0.5 h. The DMF was removed *in vacuo* and the resulting oil was extracted with DCM/H_2O (3 x 15 mL). The organic phases were combined, dried over Na_2SO_4, filtered, and concentrated. Flash column chromatography was used for purification (EtOAc/Hexanes 7:3 to EtOAc) to yield a yellow solid (**24**) (12.8 mg, 30%). ^{1}H NMR (400 MHz, $CDCl_3$) δ 7.72 – 7.67 (m, 2H), 7.44 (dd, *J* = 14.9, 8.5 Hz, 2H), 6.98 – 6.90 (m, 2H), 6.85 (d, *J* = 2.2 Hz, 1H), 5.29 – 5.25 (m, 1H), 5.05 (s, 2H), 3.85 (s, 1H), 3.50 (d, *J* = 6.0 Hz, 2H), 3.39 (t, *J* = 6.5 Hz, 2H), 2.73 – 2.44 (m, 3H), 1.89 – 1.82 (m, 2H). ESILRMS calcd. for $C_{25}H_{27}N_5O_5$ (M + Na) 500.1, found 500.2.

N-(3-azidopropyl)-4-((4-(3,5-dioxocyclohexanecarboxamido)phenoxy)methyl)benzamide (8):

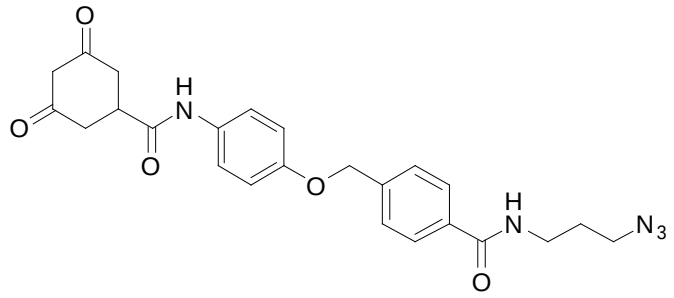

N-(3-azidopropyl)-4-((4-(3-methoxy-5-oxocyclohex-3-enecarboxamido)phenoxy)methyl)benzamide (**24**) (15 mg, 0.03 mmol) was added to a solution of ACN/H_2O (1:1 v/v, 10 mL) with 10% CAN (1.6 mg, 0.003 mmol) and refluxed at 95 °C for 3 h. The reaction was cooled and concentrated. Flash column chromatography was used for purification (EtOAc to EtOAc/MeOH 9:1) to yield a white solid (**8**) (11.8 mg, 85%) ^{1}H NMR (400 MHz, CD_3OD) δ 7.81 (s, 2H), 7.61 (s, 2H), 7.03 (s, 4H), 5.12 (s, 2H), 3.65 (s, 2H), 3.41 (s, 2H), 2.88 (s, 2H), 2.75 – 2.55 (m, 2H), 1.87 (s, 2H). ESILRMS calcd. for $C_{24}H_{25}N_5O_5$ (M + H) 464, found 464.

5.4.4 General procedure for PTP activity assay

Steady-state phosphatase assays were performed by following the enzymatic turnover of 4-methylumbelliferyl phosphate (4-MUP) by the protein tyrosine phosphatase YopH or PTP1b.[52] Briefly, to 30 µL of YopH or PTP1b (35 nM) in buffer (32 mM HEPES pH 7.2, 5 mM NaCl, 2.5 mM EDTA, 0.83% glycerol, 0.002% Brij-35) was added 5 µL of the azido-probe or DMSO control and incubated for 15 min. The assay was initiated by addition of 20 µL of 4-MUP (500 µM). The fluorescence owing to dephosphorylation of 4-MUP was measured over 15 min at 25 °C using a SpectraMax M5 plate reader (Costar 94-well plate, E_{ex} = 358 nm, 449 nm emission filter). To evaluate compounds for aggregation-based inhibition, experiments were performed as described above except that 0.02% Triton-X100 was included in the assay buffer.

5.4.5 LC/MS analysis of dimedone-tagged YopH

YopH (3 μM) was incubated with dimedone (10 mM) and H_2O_2 (30 μM) or DMSO alone in buffer (32 mM HEPES pH 7.2, 5 mM NaCl, 2.5 mM EDTA, 0.83% glycerol, 0.002% Brij-35, 0.02% Triton X-100) with rocking for 6 h at RT. The resulting samples were concentrated and exchanged into 0.1% formic acid using Amicon Ultra Centrifugal Filters (Amicon Ultra, 0.5 mL, 10k MWCO). The concentrated samples were then subjected MS analysis. An Agilent Eclipse XDB-C8 2.1mm x 15mm trap with mobile phases A (0.1% formic acid in water) and B (0.1% formic acid in acetonitrile) was used to trap, desalt and elute proteins by a linear gradient 5-90% of mobile phase B over 7 minutes at a flow rate of 200 uL/min. The desalted proteins were eluted directly on to an electrospray linear ion trap mass spectrometer (LTQ XL, Thermo Scientific) to measure protein mass.

5.4.6 Determination of the dissociation constant for inhibitor binding (K_i)

In the absence of oxidant, dimedone-based probes function as reversible inhibitors. The compound-dependence of PTP inhibition was fit to a simple model of competitive inhibition (eq 1) to yield apparent inhibitor binding constants (K_i):

$$\frac{v}{[\mathrm{YopH}]} = \frac{k_{\mathrm{cat}}[\mathrm{S}]}{[\mathrm{S}] + K_{\mathrm{m}}(1 + {[\mathrm{I}]}/{K_{\mathrm{i}}})} \qquad (1)$$

where [I] is the inhibitor concentration, [S] is the substrate (4-MUP) in excess, and K_i is the apparent inhibitor binding constant.

5.4.7 Detecting reversible PTP oxidation with azido-probes

YopH sulfenic acid was generated by oxidizing protein (30 μM) with 100 eq H_2O_2 for 1 h at RT in buffer (32 mM HEPES pH 7.2, 5 mM NaCl, 2.5 mM EDTA, 0.83% glycerol, 0.002% Brij-35, 0.02% Triton-X100). Following oxidation, catalase (100 units) was added for 15 min at RT to remove excess H_2O_2. Sulfenic acid modification of YopH was monitored by incubating protein (3 μM) with azido-probes **2**-**8** (0.5 mM) or DMSO (5% v/v) for 15 min at RT. In some reactions, YopH (30 μM) was pretreated with dimedone (50 mM) or TCEP (0.9 mM) for 0.5 h at RT and then incubated with the azido-probe. In subsequent steps, azide-tagged YopH was conjugated to phosphine-activated biotin (p-biotin; 200 μM) via the Staudinger ligation for 2 h at RT.[43] To detect PTP1B oxidation, the phosphatase was treated with H_2O_2 and probed with **2**, **5**, **6** or DMSO (5% v/v) in buffer (50 mM HEPES pH 7.2, 1 mM EDTA, 0.05% NP-40), as described above.

5.4.8 Probing sulfenic acid modification of GAPDH

Oxidized GAPDH (15 μM) in buffer (32 mM HEPES pH 7.2, 5 mM NaCl, 2.5 mM EDTA, 0.83% glycerol, 0.002% Brij-35, 0.02% Triton-X100) was incubated with DAz-1 (0.5 mM), compound **5** or **6** (0.5 mM) or DMSO (5% v/v) for 0.5 h at 37 °C. Staudinger ligation was carried out by incubation of purified protein with p-biotin (200 μM) for 2 h at 37 °C.

5.4.9 Western blot

Biotinylated proteins were separated by SDS-PAGE using Criterion XT 4–20% Bis-Tris gels (BioRad) and transferred to a polyvinylidene difluoride (PVDF) membrane (BioRad). After transfer, the PVDF membrane was blocked with 3% BSA in phosphate-buffered saline Tween-20 (PBST) for 1 h at RT. The membrane was washed with PBST (2 × 10 min) and then incubated with HRP-streptavidin (1:5,000 to 1:50,000; Pierce). PVDF membrane was washed with PBST (2

× 5 min, 1 × 10 min) and then developed with ECL Plus chemiluminescence (GE Healthcare). GAPDH was probed with anti-GAPDH (1:1,000; Santa-Cruz) and rabbit anti-mouse-HRP (1:35,000; Invitrogen). The quality of protein transfer and loading was ascertained by staining the PVDF membrane with Ponceau S.

5.4.10 Computational method for Autodock calculations

Coordinates for compounds were built with ideal geometry in InsightII (Accelrys, Inc.), including coordinates for the Cβ and Sγ positions of the cysteine adduct. The Cβ position was then overlapped on CYS403 in PDB entry 3blt. Autodock[5] was used to perform a simulated annealing conformation search, keeping the Cβ atom at the crystallographic position and searching through rotational and torsional degrees of freedom. Initial simulations revealed that the cyclic diketone formed close contacts with amino acids surrounding the active site, giving highly unfavorable interaction energies for all conformations. We then modeled induced fit by calculating a smoothed energy function. Smoothing is performed by calculating the energy potential, then scanning through the potential with a moving window, taking the minimum energy within the window at each point. This has the effect of widening the favorable basins in the potential. The default width for this smoothing window in AutoDock is 0.5 Å. In the current study, we increased this to 1.5 Å for atoms in the cyclic diketone, and kept the default values for the variable portions of the compounds.

5.5 Appendices

5.5.1 Representitive plot measuring Ki RBP 6

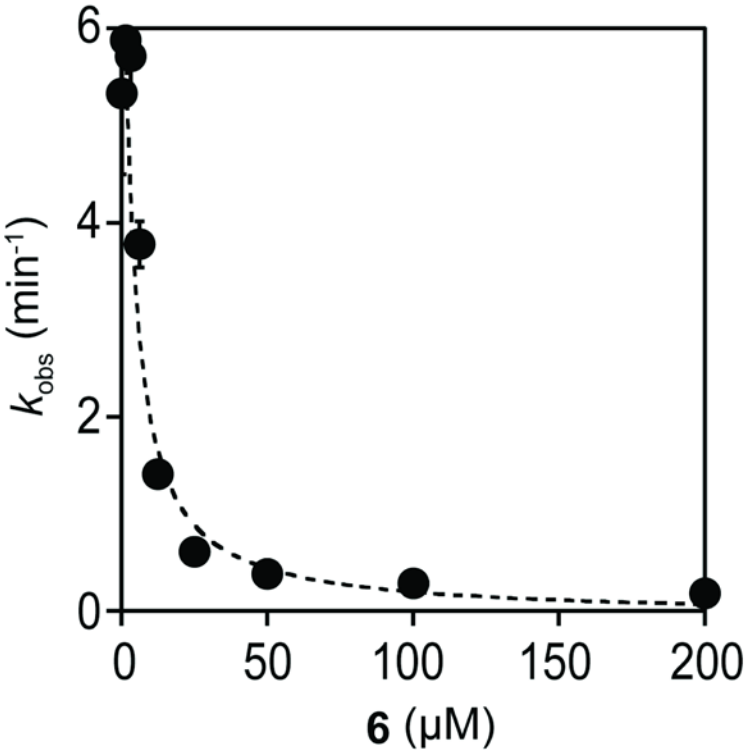

Plot of averaged initial rate versus compound 6 used to determine the averaged Ki for the inhibitor (n=3, error bars show the standard deviation). Dashed line represents fit to a simple model for competitive inhibition R^2 ≥98%.

5.5.2 Long exposure of Figure 5.5a

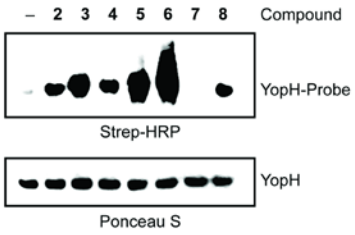

Detecting sulfenic acid modification of YopH. The phosphatase was oxidized with H2O2, incubated with compounds 2-8 or DMSO alone (–) and analyzed by streptavidin-HRP western blot as described above. Represents a longer exposure of the autoradiographic film from Figure 5.5a in the main text.

5.5.3 ^{1}H NMR and ^{13}C NMR

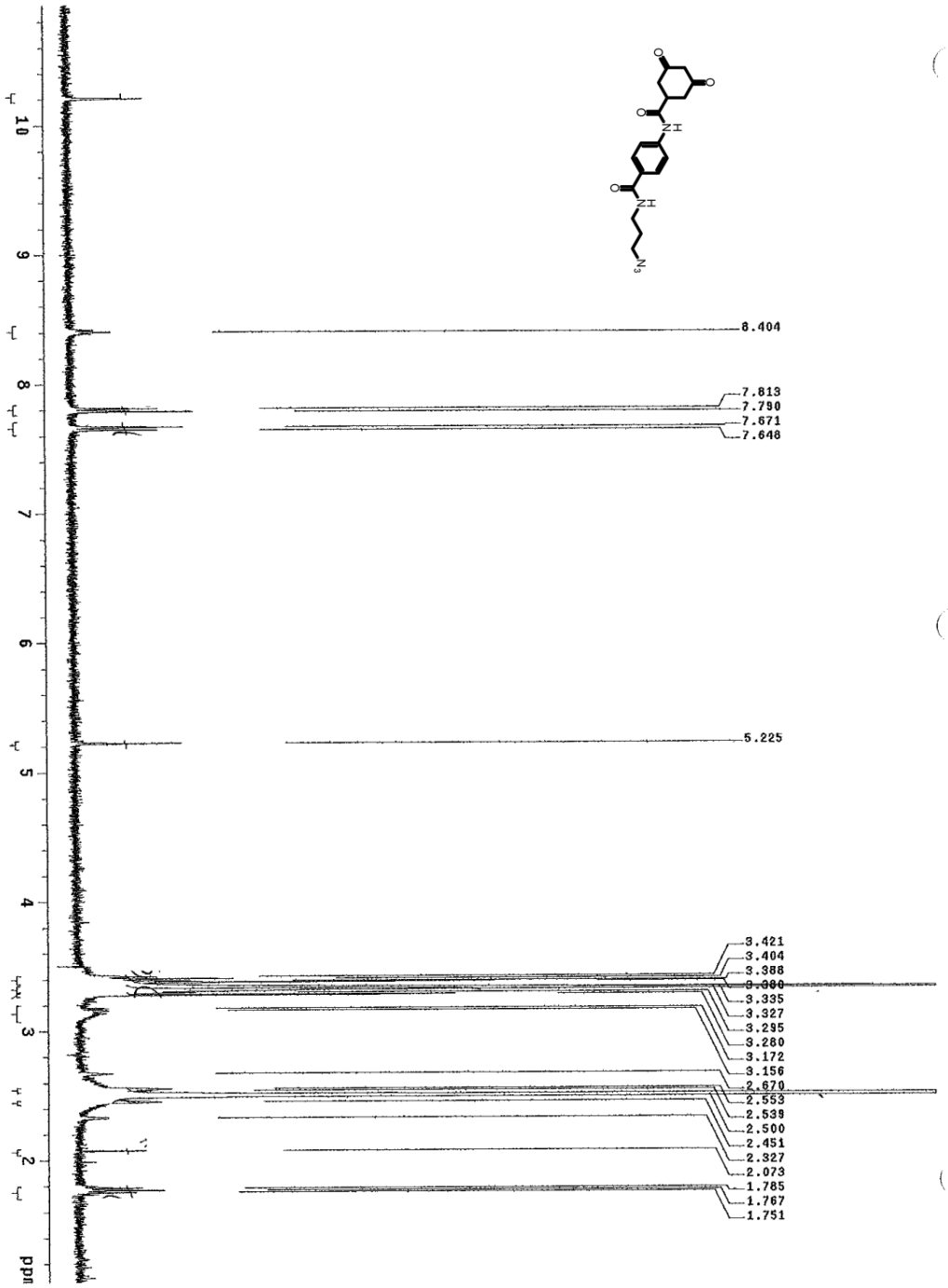

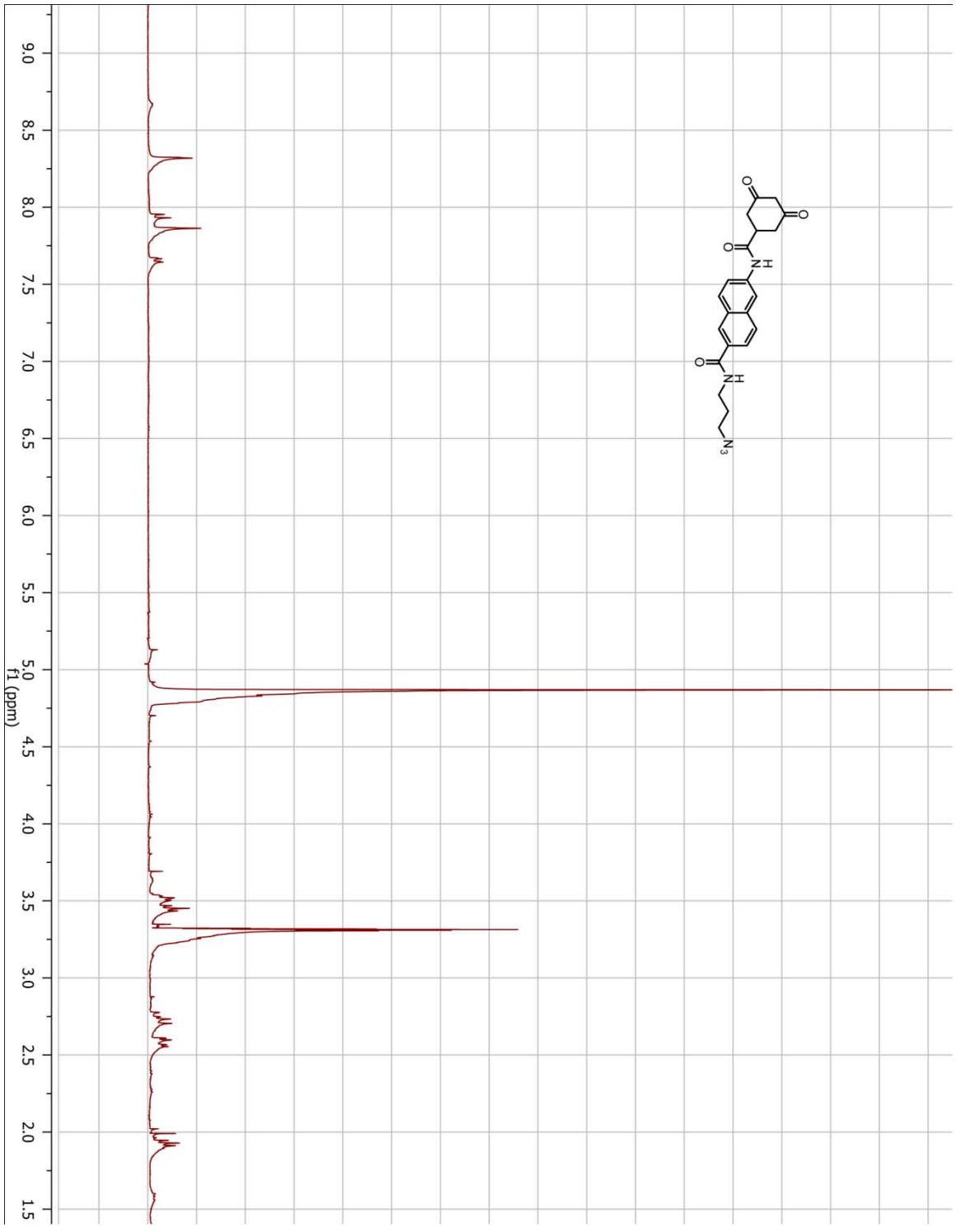
9.0
8.5
8.0
7.5
7.0
6.5
6.0
5.5
5.0
4.5
4.0
3.5
3.0
2.5
2.0
1.5
f1 (ppm)
O
O
O
H
N
O
H
N
N3

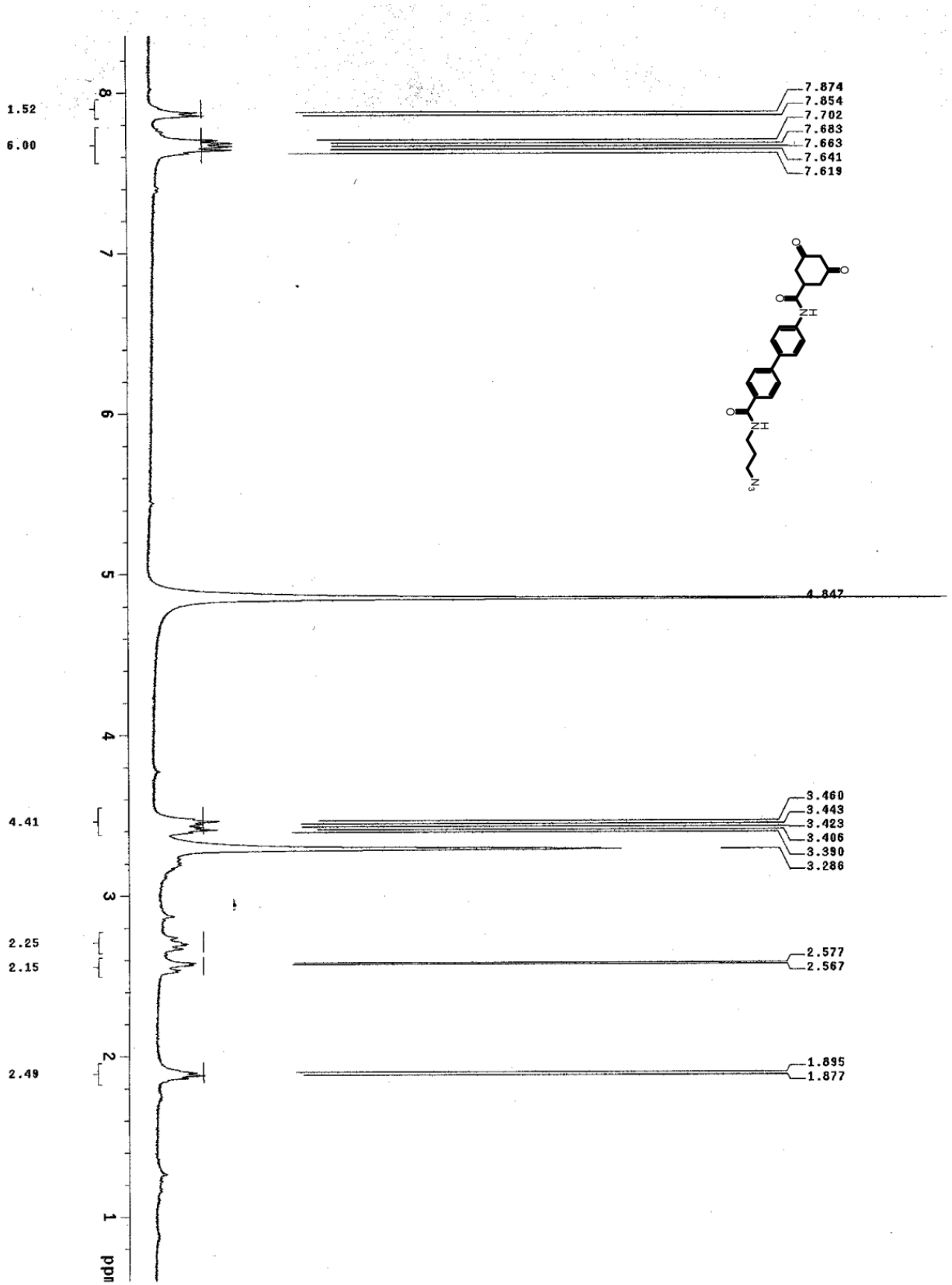
7.874
7.854
7.702
7.683
7.663
7.641
7.619
4.847
3.460
3.443
3.423
3.406
3.390
3.286
2.577
2.567
1.895
1.877
1.52
6.00
4.41
2.25
2.15
2.49
ppm

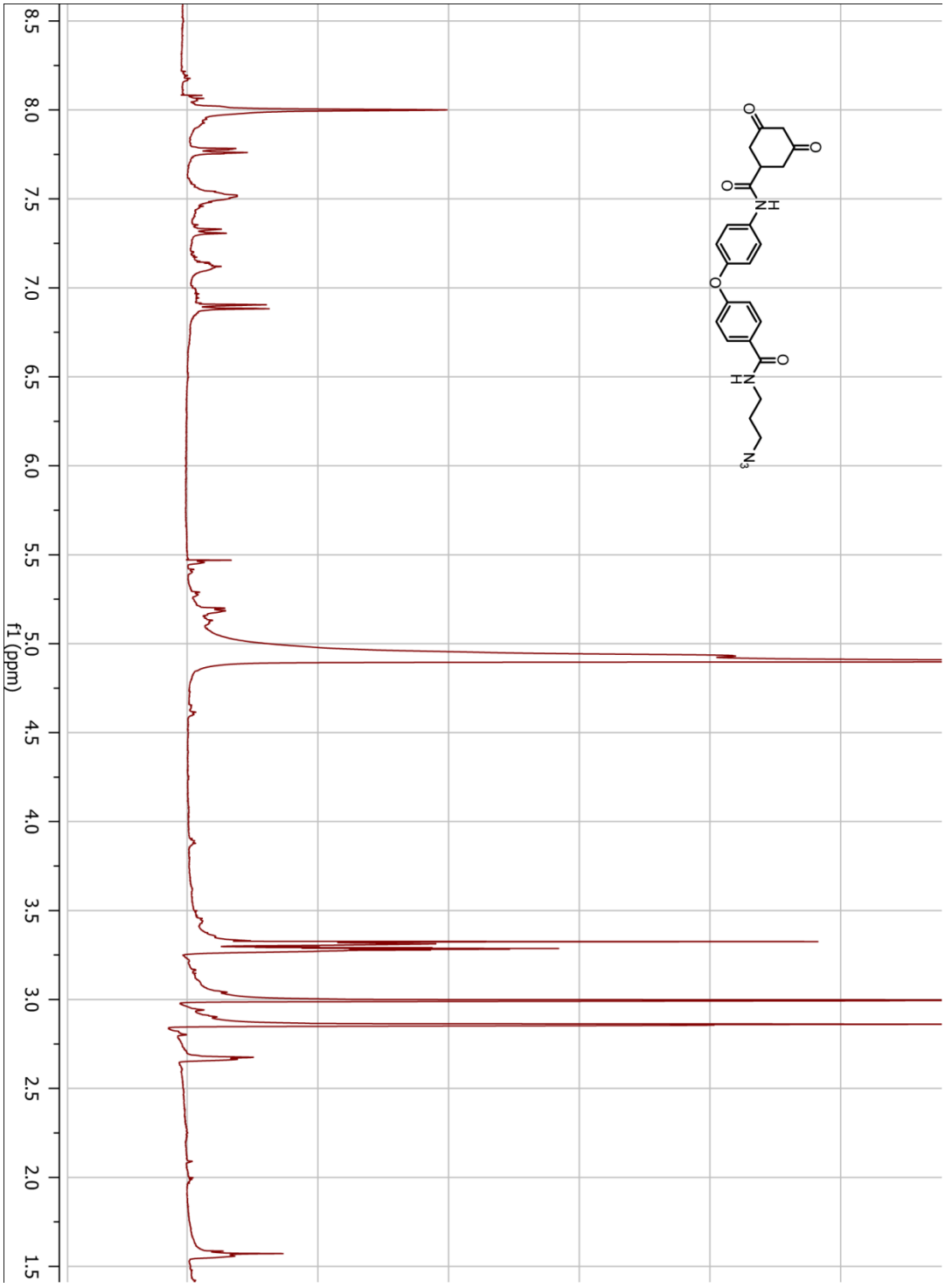
8.5
8.0
7.5
7.0
6.5
6.0
5.5
5.0
4.5
4.0
3.5
3.0
2.5
2.0
1.5
f1 (ppm)

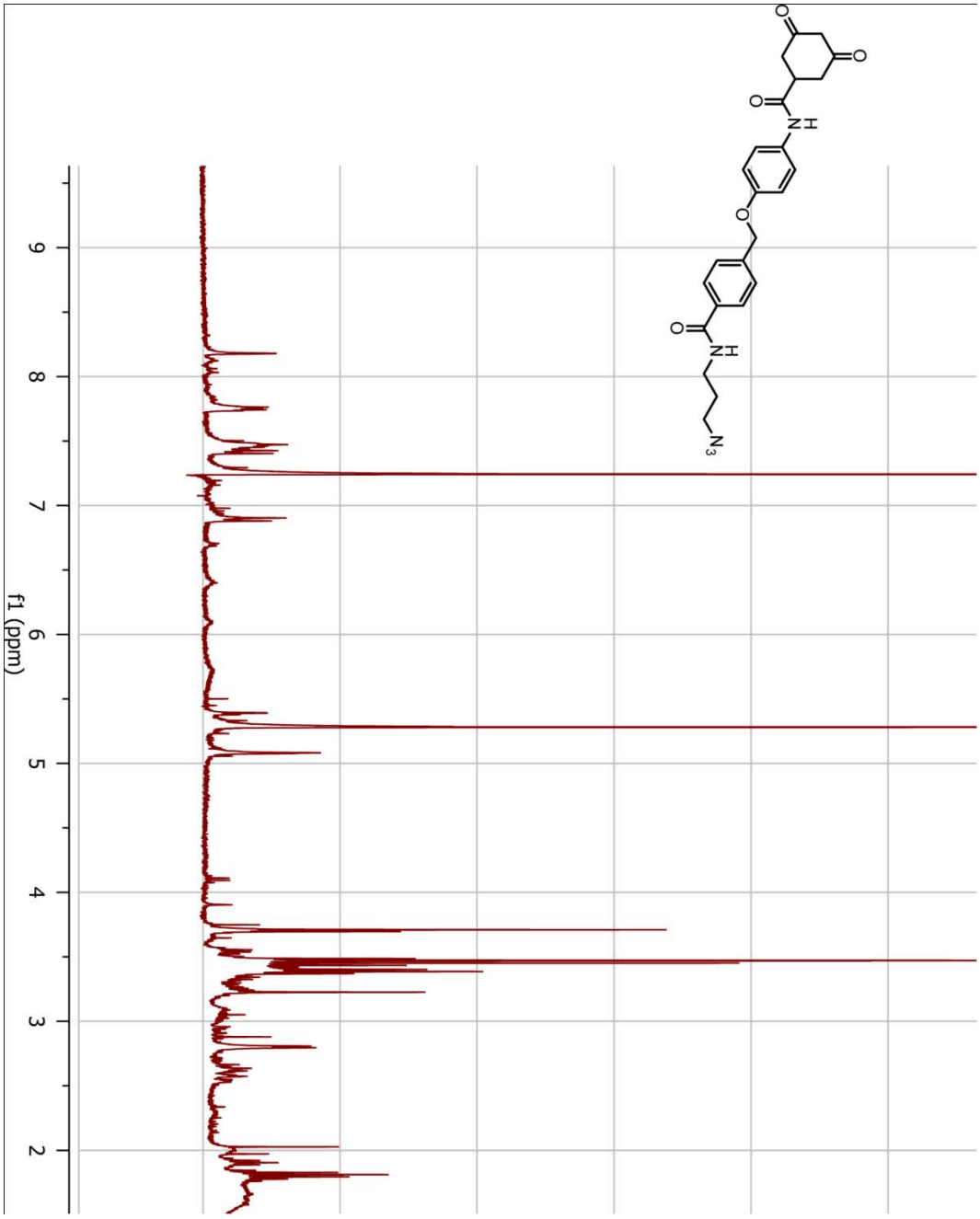
f1 (ppm)
9
8
7
6
5
4
3
2
O
O
O
H
N
O
O
H
N
N3

Notes

This work has been published as "Redox-Based Probes for Protein Tyrosine Phosphatases." Angewandte Chemie Int'l Ed. 2011 May 2;50(19):4423-7.

Stephen E. Leonard and Kate S. Carroll designed the experiments. Stephen E. Leonard and Francisco J. Garcia synthesized all compounds. Stephen E. Leonard performed the biochemistry. Jesse Song purified YopH. Francisco J. Garcia performed protein mass spectrometry. David S. Goodsell simulated the docking. We thank Prof. Mark Saper for the YopH plasmid.

5.6 References

1. Droge W: **Free radicals in the physiological control of cell function**. *Physiol Rev* 2002, **82**:47-95.
2. Finkel T: **Oxidant signals and oxidative stress**. *Curr Opin Cell Biol* 2003, **15**:247-254.
3. Lambeth JD: **NOX enzymes and the biology of reactive oxygen**. *Nat Rev Immunol* 2004, **4**:181-189.
4. Rhee SG, Bae YS, Lee SR, Kwon J: **Hydrogen peroxide: a key messenger that modulates protein phosphorylation through cysteine oxidation**. *Sci STKE* 2000, **2000**:pe1.
5. Stone JR, Yang S: **Hydrogen peroxide: a signaling messenger**. *Antioxid Redox Signal* 2006, **8**:243-270.
6. Veal EA, Day AM, Morgan BA: **Hydrogen peroxide sensing and signaling**. *Mol Cell* 2007, **26**:1-14.
7. Sundaresan M, Yu ZX, Ferrans VJ, Irani K, Finkel T: **Requirement for generation of H2O2 for platelet-derived growth factor signal transduction**. *Science* 1995, **270**:296-299.
8. Bae YS, Kang SW, Seo MS, Baines IC, Tekle E, Chock PB, Rhee SG: **Epidermal growth factor (EGF)-induced generation of hydrogen peroxide. Role in EGF receptor-mediated tyrosine phosphorylation**. *J Biol Chem* 1997, **272**:217-221.
9. Brumell JH, Burkhardt AL, Bolen JB, Grinstein S: **Endogenous reactive oxygen intermediates activate tyrosine kinases in human neutrophils**. *J Biol Chem* 1996, **271**:1455-1461.
10. Knebel A, Rahmsdorf HJ, Ullrich A, Herrlich P: **Dephosphorylation of receptor tyrosine kinases as target of regulation by radiation, oxidants or alkylating agents**. *EMBO J* 1996, **15**:5314-5325.
11. Lee SR, Kwon KS, Kim SR, Rhee SG: **Reversible inactivation of protein-tyrosine phosphatase 1B in A431 cells stimulated with epidermal growth factor**. *J Biol Chem* 1998, **273**:15366-15372.

12. Meng TC, Fukada T, Tonks NK: **Reversible oxidation and inactivation of protein tyrosine phosphatases in vivo**. *Mol Cell* 2002, **9**:387-399.
13. Alonso A, Sasin J, Bottini N, Friedberg I, Osterman A, Godzik A, Hunter T, Dixon J, Mustelin T: **Protein tyrosine phosphatases in the human genome**. *Cell* 2004, **117**:699-711.
14. Tonks NK: **Protein tyrosine phosphatases: from genes, to function, to disease**. *Nat Rev Mol Cell Biol* 2006, **7**:833-846.
15. Gates KS, Tanner JJ, Parsons ZD, Cummings AH, Zhou H: **Redox Regulation of Protein Tyrosine Phosphatases: Structural and Chemical Aspects**. *Antioxid Redox Signal* 2010.
16. Denu JM, Tanner KG: **Specific and reversible inactivation of protein tyrosine phosphatases by hydrogen peroxide: evidence for a sulfenic acid intermediate and implications for redox regulation**. *Biochemistry* 1998, **37**:5633-5642.
17. Sohn J, Rudolph J: **Catalytic and chemical competence of regulation of cdc25 phosphatase by oxidation/reduction**. *Biochemistry* 2003, **42**:10060-10070.
18. Salmeen A, Andersen JN, Myers MP, Meng TC, Hinks JA, Tonks NK, Barford D: **Redox regulation of protein tyrosine phosphatase 1B involves a sulphenyl-amide intermediate**. *Nature* 2003, **423**:769-773.
19. van Montfort RL, Congreve M, Tisi D, Carr R, Jhoti H: **Oxidation state of the active-site cysteine in protein tyrosine phosphatase 1B**. *Nature* 2003, **423**:773-777.
20. Winterbourn CC: **Reconciling the chemistry and biology of reactive oxygen species**. *Nat Chem Biol* 2008, **4**:278-286.
21. Wu RF, Terada LS: **Oxidative modification of protein tyrosine phosphatases**. *Sci STKE* 2006, **2006**:pl2.
22. Boivin B, Yang M, Tonks NK: **Targeting the reversibly oxidized protein tyrosine phosphatase superfamily**. *Sci Signal* 2010, **3**:pl2.
23. Michalek RD, Nelson KJ, Holbrook BC, Yi JS, Stridiron D, Daniel LW, Fetrow JS, King SB, Poole LB, Grayson JM: **The requirement of reversible cysteine sulfenic acid formation for T cell activation and function**. *J Immunol* 2007, **179**:6456-6467.
24. Seo YH, Carroll KS: **Facile synthesis and biological evaluation of a cell-permeable probe to detect redox-regulated proteins**. *Bioorg Med Chem Lett* 2009, **19**:356-359.
25. Reddie KG, Seo YH, Muse Iii WB, Leonard SE, Carroll KS: **A chemical approach for detecting sulfenic acid-modified proteins in living cells**. *Mol Biosyst* 2008, **4**:521-531.
26. Leonard SE, Reddie KG, Carroll KS: **Mining the thiol proteome for sulfenic acid modifications reveals new targets for oxidation in cells**. *ACS Chem Biol* 2009, **4**:783-799.
27. Charles RL, Schroder E, May G, Free P, Gaffney PR, Wait R, Begum S, Heads RJ, Eaton P: **Protein sulfenation as a redox sensor: proteomics studies using a novel biotinylated dimedone analogue**. *Mol Cell Proteomics* 2007, **6**:1473-1484.
28. Kumar S, Zhou B, Liang F, Wang WQ, Huang Z, Zhang ZY: **Activity-based probes for protein tyrosine phosphatases**. *Proc Natl Acad Sci U S A* 2004, **101**:7943-7948.
29. Kato D, Boatright KM, Berger AB, Nazif T, Blum G, Ryan C, Chehade KA, Salvesen GS, Bogyo M: **Activity-based probes that target diverse cysteine protease families**. *Nat Chem Biol* 2005, **1**:33-38.
30. Cravatt BF, Wright AT, Kozarich JW: **Activity-based protein profiling: from enzyme chemistry to proteomic chemistry**. *Annu Rev Biochem* 2008, **77**:383-414.
31. Krishnamurthy D, Barrios AM: **Profiling protein tyrosine phosphatase activity with mechanistic probes**. *Curr Opin Chem Biol* 2009, **13**:375-381.
32. Bialy L, Waldmann H: **Inhibitors of protein tyrosine phosphatases: next-generation drugs?** *Angew Chem Int Ed Engl* 2005, **44**:3814-3839.

33. Blaskovich MA: **Drug discovery and protein tyrosine phosphatases**. *Curr Med Chem* 2009, **16**:2095-2176.
34. Soellner MB, Rawls KA, Grundner C, Alber T, Ellman JA: **Fragment-based substrate activity screening method for the identification of potent inhibitors of the Mycobacterium tuberculosis phosphatase PtpB**. *J Am Chem Soc* 2007, **129**:9613-9615.
35. Zhang ZY, Clemens JC, Schubert HL, Stuckey JA, Fischer MW, Hume DM, Saper MA, Dixon JE: **Expression, purification, and physicochemical characterization of a recombinant Yersinia protein tyrosine phosphatase**. *J Biol Chem* 1992, **267**:23759-23766.
36. Zhang ZY, Dixon JE: **Active site labeling of the Yersinia protein tyrosine phosphatase: the determination of the pKa of the active site cysteine and the function of the conserved histidine 402**. *Biochemistry* 1993, **32**:9340-9345.
37. Stuckey JA, Schubert HL, Fauman EB, Zhang ZY, Dixon JE, Saper MA: **Crystal structure of Yersinia protein tyrosine phosphatase at 2.5 A and the complex with tungstate**. *Nature* 1994, **370**:571-575.
38. Schubert HL, Fauman EB, Stuckey JA, Dixon JE, Saper MA: **A ligand-induced conformational change in the Yersinia protein tyrosine phosphatase**. *Protein Sci* 1995, **4**:1904-1913.
39. See Appendix 4.5.1 for a plot of the most potent inhibitor **6.**
40. Concentrations of DAz-1 greater than 12 mM could not be tested owing to solubility issues and changes in reaction buffer pH. Thus, the K_i reported for DAz-1 in Table 1 represents a lower limit..
41. McGovern SL, Caselli E, Grigorieff N, Shoichet BK: **A common mechanism underlying promiscuous inhibitors from virtual and high-throughput screening**. *J Med Chem* 2002, **45**:1712-1722.
42. Seidler J, McGovern SL, Doman TN, Shoichet BK: **Identification and prediction of promiscuous aggregating inhibitors among known drugs**. *J Med Chem* 2003, **46**:4477-4486.
43. Saxon E, Bertozzi CR: **Cell surface engineering by a modified Staudinger reaction**. *Science* 2000, **287**:2007-2010.
44. See Appendix 4.5.2 for a longer exposure of the autoradiographic film, which shows YopH labeling by DAz-1 **2**.
45. Benitez LV, Allison WS: **The inactivation of the acyl phosphatase activity catalyzed by the sulfenic acid form of glyceraldehyde 3-phosphate dehydrogenase by dimedone and olefins**. *J Biol Chem* 1974, **249**:6234-6243.
46. Seo YH, Carroll KS: **Profiling protein thiol oxidation in tumor cells using sulfenic acid-specific antibodies**. *Proc Natl Acad Sci U S A* 2009, **106**:16163-16168.
47. Goodsell DS: **Computational docking of biomolecular complexes with AutoDock**. *Cold Spring Harb Protoc* 2009, **2009**:pdb prot5200.
48. Hajduk PJ, Bures M, Praestgaard J, Fesik SW: **Privileged molecules for protein binding identified from NMR-based screening**. *J Med Chem* 2000, **43**:3443-3447.
49. Horton DA, Bourne GT, Smythe ML: **The combinatorial synthesis of bicyclic privileged structures or privileged substructures**. *Chem Rev* 2003, **103**:893-930.
50. Ellis HR, Poole LB: **Novel application of 7-chloro-4-nitrobenzo-2-oxa-1,3-diazole to identify cysteine sulfenic acid in the AhpC component of alkyl hydroperoxide reductase**. *Biochemistry* 1997, **36**:15013-15018.
51. Saurin AT, Neubert H, Brennan JP, Eaton P: **Widespread sulfenic acid formation in tissues in response to hydrogen peroxide**. *Proc Natl Acad Sci U S A* 2004, **101**:17982-17987.
52. Hong SB, Lubben TH, Dolliver CM, Petrolonis AJ, Roy RA, Li Z, Parsons TF, Li P, Xu H, Reilly RM, et al.: **Expression, purification, and enzymatic characterization of the dual**

specificity mitogen-activated protein kinase phosphatase, MKP-4. *Bioorg Chem* 2005, **33**:34-44.

Chapter 6

Conclusions and future directions

6.1 Abstract

The data presented in the previous chapters illustrates the utility of cell-permeable small molecules that are capable of selectively detecting sulfenylated proteins. The present Chapter summarizes the key findings and significance of this work. In addition, we discuss future development and applications of these chemical tools to delineate cysteine-based redox switches in health and disease.

6.2 Conclusions: developing tools to detect cysteine sulfenylation

Over the last decade, oxidation of cysteine to sulfenic acid has emerged as a biologically relevant post-translational modification with particular importance in redox-mediated signal transduction; however, the identity of modified proteins has remained largely unknown. The overall aim of this thesis was to develop cell-permeable chemical probes that could monitor protein sulfenylation directly in cells. A broad overview of techniques used to detect reversible cysteine oxidation was described in Chapter 1. In Chapter 2, we exploited the selective reaction between a cyclic 1,3-diketone, commonly known as dimedone, with sulfenic acids to develop a cell-permeable probe for detecting cysteine oxidation in cells.

In order to expand our toolbox of sulfenic acid reactive probes, we developed a second-generation probe for sulfenic acid detection with varied connectivity between the warhead and the chemical reporter group. In Chapter 3, we described this probe, which exhibits improved potency *in vitro* and in cells. Using this more robust labeling reagent we conducted a proteomic investigation of sulfenic acid formation in HeLa cells. This study identified most known sulfenic acid-modified proteins – 14 in total, plus more than 175 new candidates, with further testing confirming oxidation in several candidate proteins.

DAz-2 was then used to study the regulation of single cysteine oxidation in the periplasm of *E. coli*. In Chapter 4 we detail the discovery of a novel system to control the global sulfenic acid content of the periplasm in which two proteins, DsbG and DsbC, protect protein cysteines from over oxidation. This study further highlights the utility of our small-molecule probes to discover new cellular redox biology.

Finally, in Chapter 5, we reported the rational design of a new generation of sulfenic acid probes, which show increased affinity for a family of enzymes, PTPs. This advance has facilitated investigation of PTP regulation and redox signaling in cell-based systems. This strategy employed to identify redox based probes (RBPs) for phosphatases may also represent an attractive starting point into the inhibitor- or tool-development cycle for other classes of proteins with redox-sensitive Cys residues.

6.3 Future directions in sulfenic acid probe development and application

6.3.1 Proteomic quantification of protein sulfenylation

As discussed in Chapter 3, prior to the first proteomic investigation of HeLa cells using DAz-2, the frequency of sulfenic acid modification was largely unknown. The aforementioned study greatly expanded the known sulfenome from approximately 20 sulfenylated proteins to almost 200.[1] However, while new protein targets of hydrogen peroxide modification have been identified, the regulatory ramifications of these modifications for the majority of these proteins remain unknown. One approach to dissect their potential functional significance is to quantify the extent of cysteine oxidation at distinct sites within a protein.

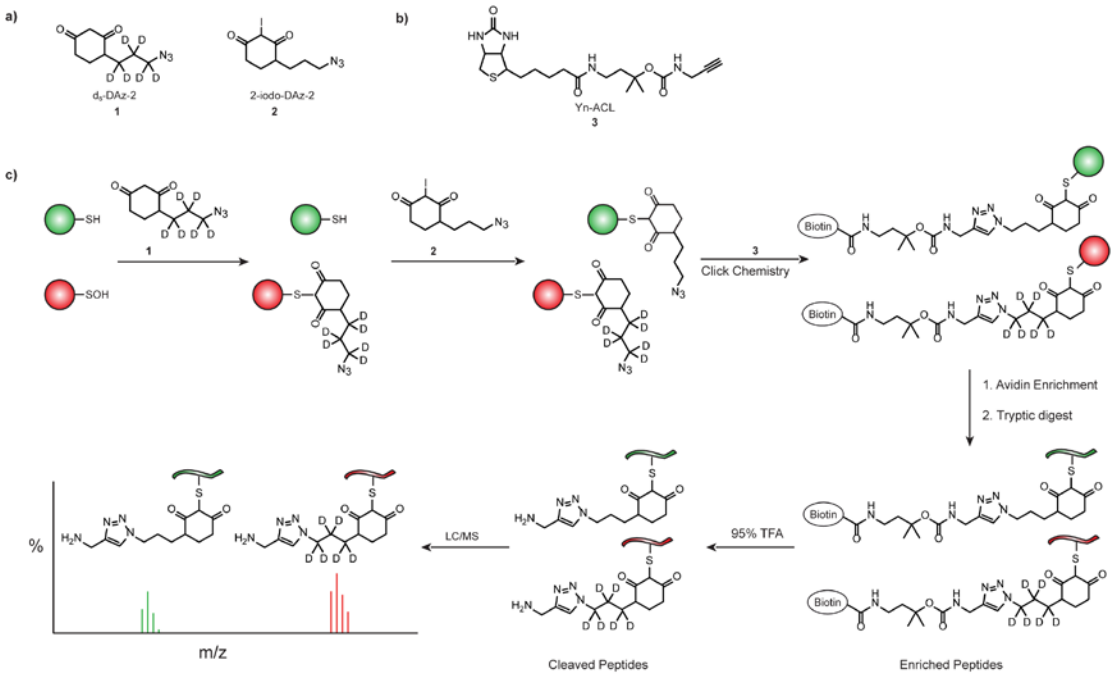

Figure 6.1 Modified ICDID to quantify sulfenic acid modification in cells. a) Isotopically heavy derivative of DAz-2 and 2-Iodo-DAz-2. b) Biotinylated acid-cleavable linker with an alkyne handle. c) Modified isotope-coded dimedone and 2-iododimedone (ICDID) allows quantitation of protein sulfenylation. Proteins are labeled with isotope-coded DAz-2 (d6-DAz-2) to covalently modify all sulfenic acids (red protein). Next, excess reagent is removed and 2-iodo-DAz-2 covalently alkylates all free thiols (green protein) resulting in a DAz-2-labeled cysteine which differs in mass by 6 Da due to incorporation of DAz-2 or d6-DAz-2. Proteins are enriched and trypsinized generating chemically identical peptides. The biotin is cleaved from the linker with TFA and analyzed by LC-MS. Relative peak intensities can determine the ratio of sulfenylation on a particular cysteine.

6.3.1.1 Isotope-coded and iodo-DAz-2

As discussed in Chapter 1, we have developed the isotope-coded dimedone and 2-iododimedone (ICDID) strategy.[2] This approach factors out protein abundance changes and enables sulfenylation site occupancy to be determined. ICDID consists of two key tagging steps: (1) deuterium-labeled dimedone (d6-dimedone) selectively labels sites of sulfenic acid modification; and (2) free thiols are alkylated with 2-iododimedone. The products of these reactions are chemically identical, but differ in mass by 6 Da. Accordingly, the extent of sulfenic acid modification at any given cysteine residue can be determined from the ratio of heavy/light isotope-labeled peak intensities in the mass spectrum.

Although ICDID represents a significant advance forward, a remaining issue is the lack of chemical handle to facilitate protein enrichment and identification. Thus, the next step is to generate heavy and light derivatives of DAz-2 **1** and its 2-iodo derivative. In this way, the ICDID strategy can be broadly applied for global profiling and quantification of cysteine oxidation in cells. The addition of a chemical reporter group allows for conjugation of a biotin affinity tag for protein enrichment and identification. However, the biotin moiety can also complicate MS analysis and subsequent database searching, especially for small peptides.[3,4] A carbamate-based acid-cleavable linker has been reported for removal of the biotin tag after protein or peptide enrichment.[5-7] Inspired by these approaches, we have synthesized an acid-cleavable linker containing an alkyne chemical handle and a biotin moiety, Yn-ACL **3** (Figure 6.1b).[8] Use of these reagents should permit identification and quantification of protein cysteine oxidation (Figure 6.2c). Quantification of sulfenic acid formation should provide insight into the physiological and pathological significance of the modification and help prioritize proteins for future analysis.

6.3.1.2 Alkyne-functionalized probes for sulfenic acid detection

The Staudinger ligation between phosphines and azides was first reported in 2000.[9] This bioorthogonal reaction selectively and covalently couples two reagents with functional groups that are not found in common biology, using mild reaction conditions (aqueous solutions at room temperature). It has been successfully used in many studies to develop probes to examine protein modification. [9-13] However, there are limitations of this reaction including sensitivity to air oxidation and slow rates of reaction. An alternative to the Staudinger ligation is the copper catalyzed [3+2] Huisgen cycloaddition reaction, which covalently couples an azide and a terminal alkyne. This reaction is not compatible with living systems due to the toxicity of copper, but does occur in aqueous environments with much faster reaction rates. Previous reports have indicated that having an alkyne on the primary probe yields higher signal to noise in detection experiments.[14] Therefore, DYn-2 **5** which is an alkyne version of DAz-2 **4**, has been synthesized (Figure 6.2). This compound is compatible with all azide-based commercially available detection reagents and will be tested for sulfenic acid reactivity.

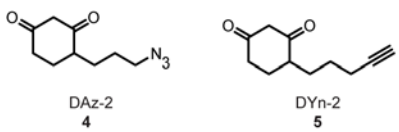

Figure 6.2 DAz-2 and alkyne derivative, DYn-2

6.3.2 Investigating the relevant oxidation targets that mediate ROS-dependent endothelial cell migration

As mentioned in Chapter 5, it is well established that growth factor stimulation of cells results in the production of hydrogen peroxide (H_2O_2) via the corresponding membrane receptor.[15-18]

Indeed, H_2O_2 generation is critical for basic cellular functions such as cell growth, differentiation, and autophagy.[19,20] Directional migration of endothelial cells is a process that occurs through receptor tyrosine kinase (RTK) signaling and is well-known to be sensitive to cellular redox changes.

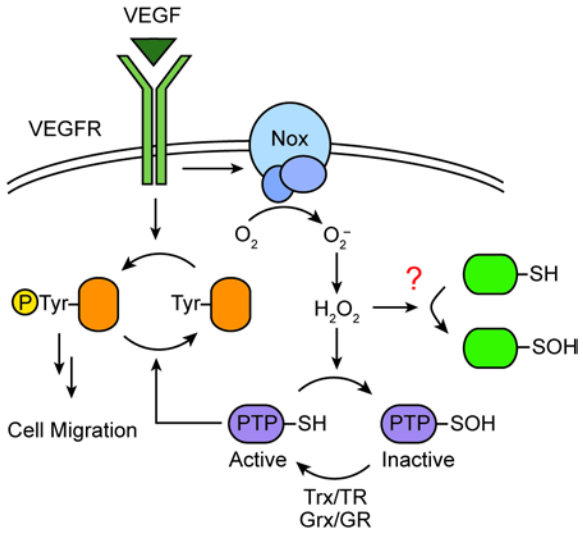

Figure 6.3 Proposed model for redox-dependent signal transduction in cell migration. After ligand stimulation H_2O_2 levels increase, via the recruitment of cytosolic proteins and subsequent activation of membrane-bound NAPDH oxidase 2 (Nox2). Increased H_2O_2 production can lead to the oxidation of specific reactive Cys residues within localized proteins, with concomitant modulation of protein function. PTP-PEST is proposed to be inactivated in response to H_2O_2 production. Additional proteins such as kinases may be oxidized as well.

PTP-PEST is a negative regulator of focal adhesion turnover, a remodeling event that is required for cell migration (Figure 6.3).[21] The phosphatase localizes to focal adhesions through interactions with the scaffold protein Paxillin.[22] This subcellular localization allows PTP-PEST to modulate phosphotyrosine levels of proteins, which regulates formation and maturation of focal adhesions. Targeted ROS production from the NADPH oxidase, Nox2, which is specifically recruited to focal adhesions, may serve to transiently inactivate PTP-PEST via oxidation of its catalytic cysteine (Figure 6.3). In addition, other key signaling proteins in the pathway are believed to be redox regulated during signaling events. Src and Pyk2 are tyrosine kinases that localize to the focal complex, which may also contain ROS-sensitive cysteine residues.[23,24] However, the nature and effect of this oxidation are not well understood. The GTPase Rac1 is a

central activator of Nox2 during RTK stimulation. Rac1 oxidation has been demonstrated to cause increased GTP hydrolysis resulting in inactivation of the Nox complex.[25] This could act as a negative feedback loop, terminating ROS production to modulate signaling events. We hypothesize that PTP-PEST and other signaling molecules including kinases Src and Pyk2 and GTPases such as Rac1 are reversibly oxidized by controlled local production of hydrogen peroxide in response to RTK activation.

To test this hypothesis, the redox-based probes described in Chapter 5 can be used to investigate sulfenic acid modification of PTP-PEST. As envisioned, an increase in PTP sulfenic acid formation would be observed in response to RTK stimulation. If multiple protein targets of hydrogen peroxide exist, an increase in the ratio of oxidized/reduced cysteines for these proteins is expected when a signaling event occurs. Comparison of stimulated and resting cells using the modified ICDID strategy described in Figure 6.2 should identify specific proteins that become oxidized in response to RTK activation. This will identify candidates of redox regulation, but will not determine the biological function of the modification. Further biochemical and genetic testing will be required to decipher the roles of cysteine oxidation. Of particular interest will be the use of point mutants in proteins with oxidized non-catalytic cysteines. Removal of these residues should modify the regulation of these proteins resulting in an altered phenotype for the signaling event. Potential targets include the Src family kinases and Rac1 which are known to have redox sensitive cysteines that are not necessary for enzyme activity.

In total, such experiments would be the first to probe the functional role of PTP oxidation in a cellular context and directly address the relevance of sulfenic acid modifications in RTK signaling.

Identifying new protein targets of hydrogen peroxide and the residues sensitive to oxidation will help elucidate the mechanism of cross-talk between redox and protein tyrosine phosphorylation. Inappropriate levels of ROS are implicated in numerous diseases including diabetes, many cancers and neurodegenerative diseases such as Alzheimer's and Parkinson's disease.[15,26-29] Delineating ROS targets involved in healthy cell processes and disease states will be critical in understanding and treating imbalances in ROS levels. This work should reveal new regulatory mechanisms in signaling pathways and advance novel therapeutic approaches to combating inappropriate oxidation in disease.

6.4 Concluding remarks

Before this work began, the extent and even existence of sulfenic acid modifications in a cellular context were uncertain. The development of tools to detect sulfenic acid modifications has revealed the widespread prevalence of these oxoforms in cells and highlights the need for future research in this fertile area. Use of these molecules in conjunction with the ratiometric techniques developed in our lab will lay the groundwork for understanding redox-based regulation of protein function and its cross-talk with protein phosphorylation in vital signaling pathways. Reversible cysteine oxidation is emerging as a central mechanism for dynamic posttranslational regulation of all major protein classes. We envision that the tools we develop will identify key redox switches in signaling networks, help elucidate the functions of reversibly oxidized cysteines and lead to novel therapeutic targets and better understanding of cellular processes in normal and disease states.

6.5 References

1. Leonard SE, Reddie KG, Carroll KS: **Mining the thiol proteome for sulfenic acid modifications reveals new targets for oxidation in cells**. *ACS Chem Biol* 2009, **4**:783-799.
2. Seo YH, Carroll KS: **Quantification of protein sulfenic acid modifications using isotope-coded dimedone and iododimedone**. *Angew Chem Int Ed Engl* 2011, **50**:1342-1345.
3. Borisov OV, Goshe MB, Conrads TP, Rakov VS, Veenstra TD, Smith RD: **Low-energy collision-induced dissociation fragmentation analysis of cysteinyl-modified peptides**. *Anal Chem* 2002, **74**:2284-2292.
4. Qiu Y, Sousa EA, Hewick RM, Wang JH: **Acid-labile isotope-coded extractants: a class of reagents for quantitative mass spectrometric analysis of complex protein mixtures**. *Anal Chem* 2002, **74**:4969-4979.
5. Fauq AH, Kache R, Khan MA, Vega IE: **Synthesis of acid-cleavable light isotope-coded affinity tags (ICAT-L) for potential use in proteomic expression profiling analysis**. *Bioconjug Chem* 2006, **17**:248-254.
6. Szychowski J, Mahdavi A, Hodas JJ, Bagert JD, Ngo JT, Landgraf P, Dieterich DC, Schuman EM, Tirrell DA: **Cleavable biotin probes for labeling of biomolecules via azide-alkyne cycloaddition**. *J Am Chem Soc* 2010, **132**:18351-18360.
7. Yang YY, Grammel M, Raghavan AS, Charron G, Hang HC: **Comparative analysis of cleavable azobenzene-based affinity tags for bioorthogonal chemical proteomics**. *Chem Biol* 2010, **17**:1212-1222.
8. Truong TH, Garcia FJ, Seo YH, Carroll KS: **Isotope-coded chemical reporter and acid-cleavable affinity reagents for monitoring protein sulfenic acids**. *Bioorganic & Medicinal Chemistry Letters* **In Press, Accepted Manuscript**.
9. Saxon E, Bertozzi CR: **Cell surface engineering by a modified Staudinger reaction**. *Science* 2000, **287**:2007-2010.
10. Hang HC, Loureiro J, Spooner E, van der Velden AW, Kim YM, Pollington AM, Maehr R, Starnbach MN, Ploegh HL: **Mechanism-based probe for the analysis of cathepsin cysteine proteases in living cells**. *ACS Chem Biol* 2006, **1**:713-723.
11. Hangauer MJ, Bertozzi CR: **A FRET-based fluorogenic phosphine for live-cell imaging with the Staudinger ligation**. *Angew Chem Int Ed Engl* 2008, **47**:2394-2397.
12. Reddie KG, Seo YH, Muse Iii WB, Leonard SE, Carroll KS: **A chemical approach for detecting sulfenic acid-modified proteins in living cells**. *Mol Biosyst* 2008, **4**:521-531.
13. Vocadlo DJ, Hang HC, Kim EJ, Hanover JA, Bertozzi CR: **A chemical approach for identifying O-GlcNAc-modified proteins in cells**. *Proc Natl Acad Sci U S A* 2003, **100**:9116-9121.
14. Hsu TL, Hanson SR, Kishikawa K, Wang SK, Sawa M, Wong CH: **Alkynyl sugar analogs for the labeling and visualization of glycoconjugates in cells**. *Proc Natl Acad Sci U S A* 2007, **104**:2614-2619.
15. Finkel T: **Oxidant signals and oxidative stress**. *Curr Opin Cell Biol* 2003, **15**:247-254.
16. Lambeth JD: **NOX enzymes and the biology of reactive oxygen**. *Nat Rev Immunol* 2004, **4**:181-189.
17. Rhee SG, Bae YS, Lee SR, Kwon J: **Hydrogen peroxide: a key messenger that modulates protein phosphorylation through cysteine oxidation**. *Sci STKE* 2000, **2000**:pe1.
18. Sundaresan M, Yu ZX, Ferrans VJ, Irani K, Finkel T: **Requirement for generation of H2O2 for platelet-derived growth factor signal transduction**. *Science* 1995, **270**:296-299.
19. Stone JR, Yang S: **Hydrogen peroxide: a signaling messenger**. *Antioxid Redox Signal* 2006, **8**:243-270.

20. Veal EA, Day AM, Morgan BA: **Hydrogen peroxide sensing and signaling**. *Mol Cell* 2007, **26**:1-14.
21. Sallee JL, Wittchen ES, Burridge K: **Regulation of cell adhesion by protein-tyrosine phosphatases: II. Cell-cell adhesion**. *J Biol Chem* 2006, **281**:16189-16192.
22. Shen Y, Schneider G, Cloutier JF, Veillette A, Schaller MD: **Direct association of protein-tyrosine phosphatase PTP-PEST with paxillin**. *J Biol Chem* 1998, **273**:6474-6481.
23. Frank GD, Motley ED, Inagami T, Eguchi S: **PYK2/CAKbeta represents a redox-sensitive tyrosine kinase in vascular smooth muscle cells**. *Biochem Biophys Res Commun* 2000, **270**:761-765.
24. Wu RF, Xu YC, Ma Z, Nwariaku FE, Sarosi GA, Jr., Terada LS: **Subcellular targeting of oxidants during endothelial cell migration**. *J Cell Biol* 2005, **171**:893-904.
25. Harraz MM, Marden JJ, Zhou W, Zhang Y, Williams A, Sharov VS, Nelson K, Luo M, Paulson H, Schoneich C, et al.: **SOD1 mutations disrupt redox-sensitive Rac regulation of NADPH oxidase in a familial ALS model**. *J Clin Invest* 2008, **118**:659-670.
26. Evans JL, Goldfine ID, Maddux BA, Grodsky GM: **Are oxidative stress-activated signaling pathways mediators of insulin resistance and beta-cell dysfunction?** *Diabetes* 2003, **52**:1-8.
27. Adams JD, Jr., Klaidman LK, Odunze IN, Shen HC, Miller CA: **Alzheimer's and Parkinson's disease. Brain levels of glutathione, glutathione disulfide, and vitamin E**. *Mol Chem Neuropathol* 1991, **14**:213-226.
28. Baldeiras I, Santana I, Proenca MT, Garrucho MH, Pascoal R, Rodrigues A, Duro D, Oliveira CR: **Oxidative Damage and Progression to Alzheimer's Disease in Patients with Mild Cognitive Impairment**. *J Alzheimers Dis* 2010.
29. Benzi G, Moretti A: **Are reactive oxygen species involved in Alzheimer's disease?** *Neurobiol Aging* 1995, **16**:661-674.

Appendix A. Experimental procedures for the synthesis of DYn-2

All reactions were performed under an argon atmosphere in oven-dried glassware. Reagents and solvents were purchased from Sigma or other commercial sources and were used without further purification. Analytical thin layer chromatography (TLC) was carried out using Analtech Uniplate silica gel plates and visualized using a combination of UV and potassium permanganate staining. Flash chromatography was performed using silica gel (32-63 μM, 60Å pore size) from Sorbent Technologies Incorporated. NMR spectra were obtained on a Varian Inova 400 (400 MHz for ^{1}H; 100 MHz for ^{13}C). ^{1}H and ^{13}C NMR chemical shifts are reported in parts per million (ppm) referenced to the residual solvent peak.

(5-Iodopent-1-yn-1-yl)trimethylsilane (1)

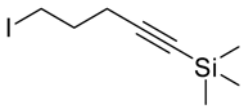

(5-Chloropent-1-yn-1-yl)trimethylsilane (1.02 mL, 5.72 mmol) was dissolved in acetone (30 mL). To this was added sodium iodide (4.29 g, 28.6 mmol) and the solution was refluxed for 21 h. Upon cooling the reaction was diluted with DCM (25 mL) and washed with water (3x15 mL). The organic phases were combined, washed with brine (15 mL), dried over Na_2SO_4, and concentrated to give a yellow oil **1** (1.37 g, 5.15 mmol) in 90% yield. ^{1}H NMR (400 MHz, $CDCl_3$) δ 3.28 (t, *J* = 6.8 Hz, 2H), 2.35 (t, *J* = 6.8 Hz, 2H), 1.99 (t, *J* = 6.8 Hz, 2H), 0.19 – 0.06 (m, 9H).

3-Ethoxy-6-(5-(trimethylsilyl)pent-4-yn-1-yl)cyclohex-2-enone (2)

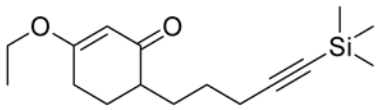

To a lithium diisopropylamide (LDA) solution, prepared from diisopropylamine (0.24 mL, 1.71 mmol) and *n*BuLi (0.69 mL of a 2.5 M solution in hexanes, 1.72 mmol) in anhydrous THF (15 mL) at -78 °C under argon, was added 3-ethoxycyclohex-2-enone (0.21 mL, 1.43 mmol) in THF (10 mL), dropwise over 30 min. The reaction was stirred for an additional 2 h at -78 °C. Then hexamethylphosphoramide (HMPA, 0.3 mL, 1.71 mmol) was added, followed by the dropwise addition of compound **1** (0.46 g, 1.71 mmol) in THF (10 mL). The reaction was allowed to warm to rt and stirred for 8 h. The reaction was quenched with water (15 mL) and sat. NH_4Cl (15 mL). The aqueous phase was extracted with DCM (3x15 mL), and the organic phases were combined, washed with brine (20 mL), dried over Na_2SO_4, and concentrated. The resulting syrup was purified with silica column using 7:3 Hexanes:EtOAc resulting in a yellow oil **2** (0.099 g, 0.36 mmol) in 26% yield. R_f: 0.2 (7:3 hexanes: ethyl acetate). ^{1}H NMR (400 MHz, $CDCl_3$) δ 5.28 (s, 1H), 3.85 (q, *J* = 7.0 Hz, 2H), 2.39 (t, *J* = 6.2 Hz, 2H), 2.23 – 2.10 (m, 2H), 2.09 – 1.97 (m, 2H), 1.95 – 1.80 (m, 2H), 1.75 – 1.64 (m, 1H), 1.62 – 1.50 (m, 2H), 1.50 – 1.38 (m, 1H), 1.38 – 1.26 (m, 3H), 0.19 – 0.06 (m, 9H).

3-Ethoxy-6-(pent-4-yn-1-yl)cyclohex-2-enone (3)

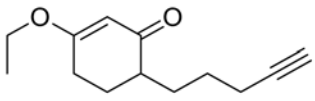

To a solution of **2** (0.09 g, 0.315 mmol) in THF (5 mL) was added TBAF solution (0.95 mL of a 1 M solution in THF, 0.95 mmol) and triethylamine (0.13 mL, 0.95 mmol). After stirring at rt for 2.5 h the reaction was quenched by adding water (5 mL) and sat. NH_4Cl (5 mL). The mixture was

extracted with DCM (3x10 mL), and the organic phases were combined, dried over Na_2SO_4, and concentrated. The resulting brown oil was purified by silica gel using 8:2 Hexanes:EtOAc to yield **3** (0.05 g, 0.243 mmol) in 77% yield. R_f: 0.2 (8:2 Hexanes:EtOAc). ^{1}H NMR (400 MHz, $CDCl_3$) δ 5.28 (s, 1H), 3.85 (q, *J* = 7.0 Hz, 2H), 2.39 (t, *J* = 6.2 Hz, 2H), 2.23 – 2.10 (m, 3H), 2.09 – 1.97 (m, 2H), 1.95 – 1.80 (m, 2H), 1.75 – 1.64 (m, 1H), 1.62 – 1.50 (m, 2H), 1.50 – 1.38 (m, 1H), 1.38 – 1.26 (m, 3H). ^{13}C NMR (100 MHz, $CDCl_3$) δ 201.18, 176.68, 102.10, 84.24, 68.37, 64.13, 44.68, 28.77, 27.94, 26.28, 26.09, 18.52, 14.09.

4-(pent-4-yn-1-yl)cyclohexane-1,3-dione (4)

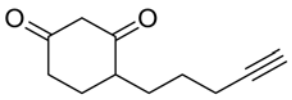

To a solution of **3** (0.04 g, 0.19 mmol) in acetonitrile (2 mL) and water (2 mL) was added CAN (0.011 g, 0.02 mmol). The solution was heated to reflux for 2.5 h. The reaction mixture was then diluted with brine (10 mL), and extracted with EtOAc (3x10 mL). The organic phases were combined, washed with brine (30 mL), dried over Na_2SO_3, and concentrated *in vacuo*. The resulting orange solid was purified by silica gel column chromatography using 1:1 Hexanes:EtOAc to give compound **4** as a pale yellow solid (0.033 g, .18 mmol) in 95% yield. R_f: 0.4 (1:1 Hexanes:EtOAc). ^{1}H NMR (400 MHz, $CDCl_3$) δ 3.52 – 3.32 (dd, *J* = 12.1, 9.0 Hz, 2H), 2.78 – 2.66 (m, 1H), 2.65 – 2.45 (m, 2H), 2.33 – 2.11 (m, 3H), 2.06 – 1.90 (m, 2H), 1.73 – 1.45 (m, 4H). ^{13}C NMR (100 MHz, $CDCl_3$) δ 204.38, 203.85, 83.79, 68.80, 58.20, 48.86, 39.59, 28.24, 25.83, 24.46, 18.45.

Appendix B. ^{1}H and ^{13}C NMR for the synthesis of DYn-2

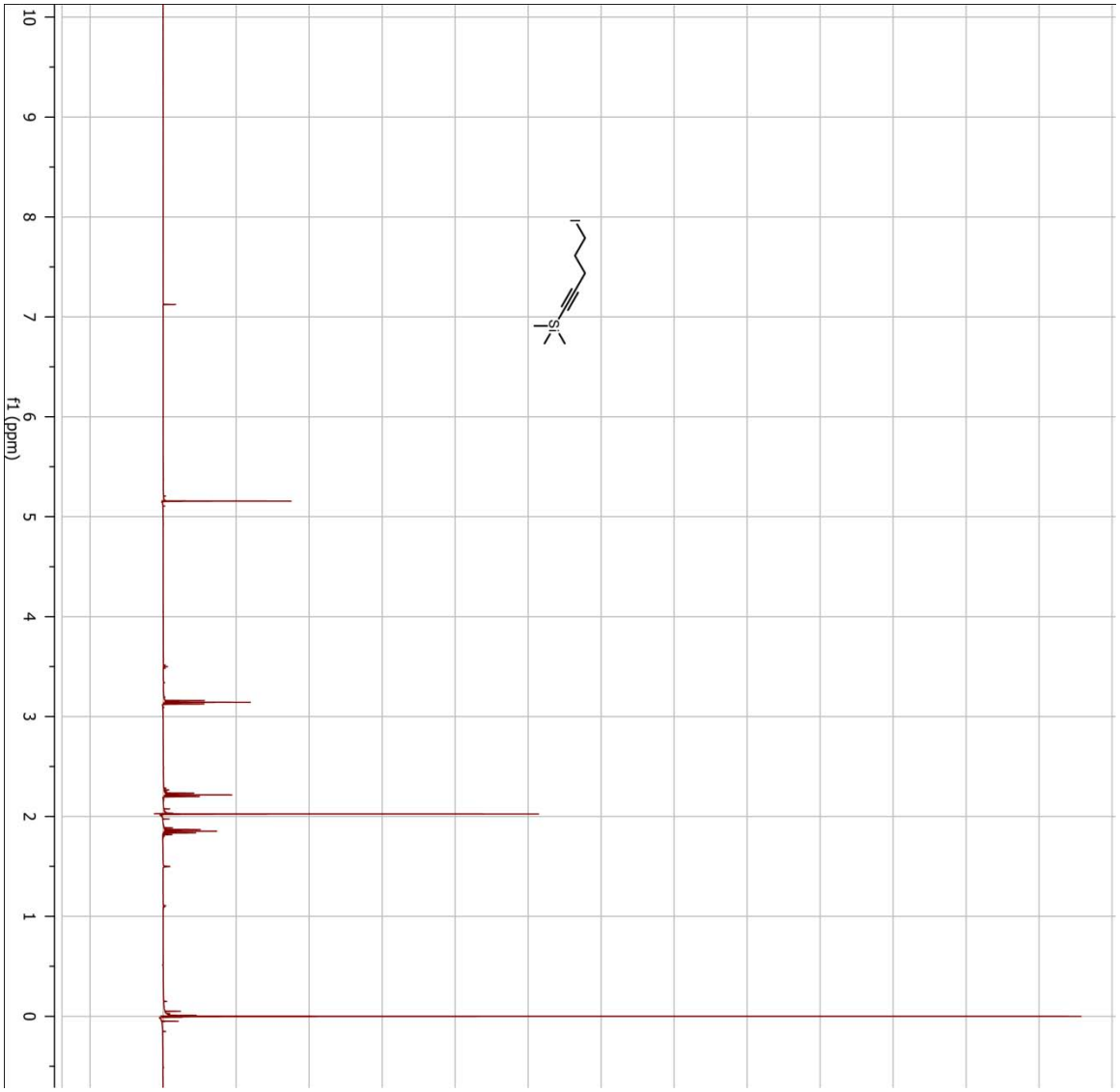

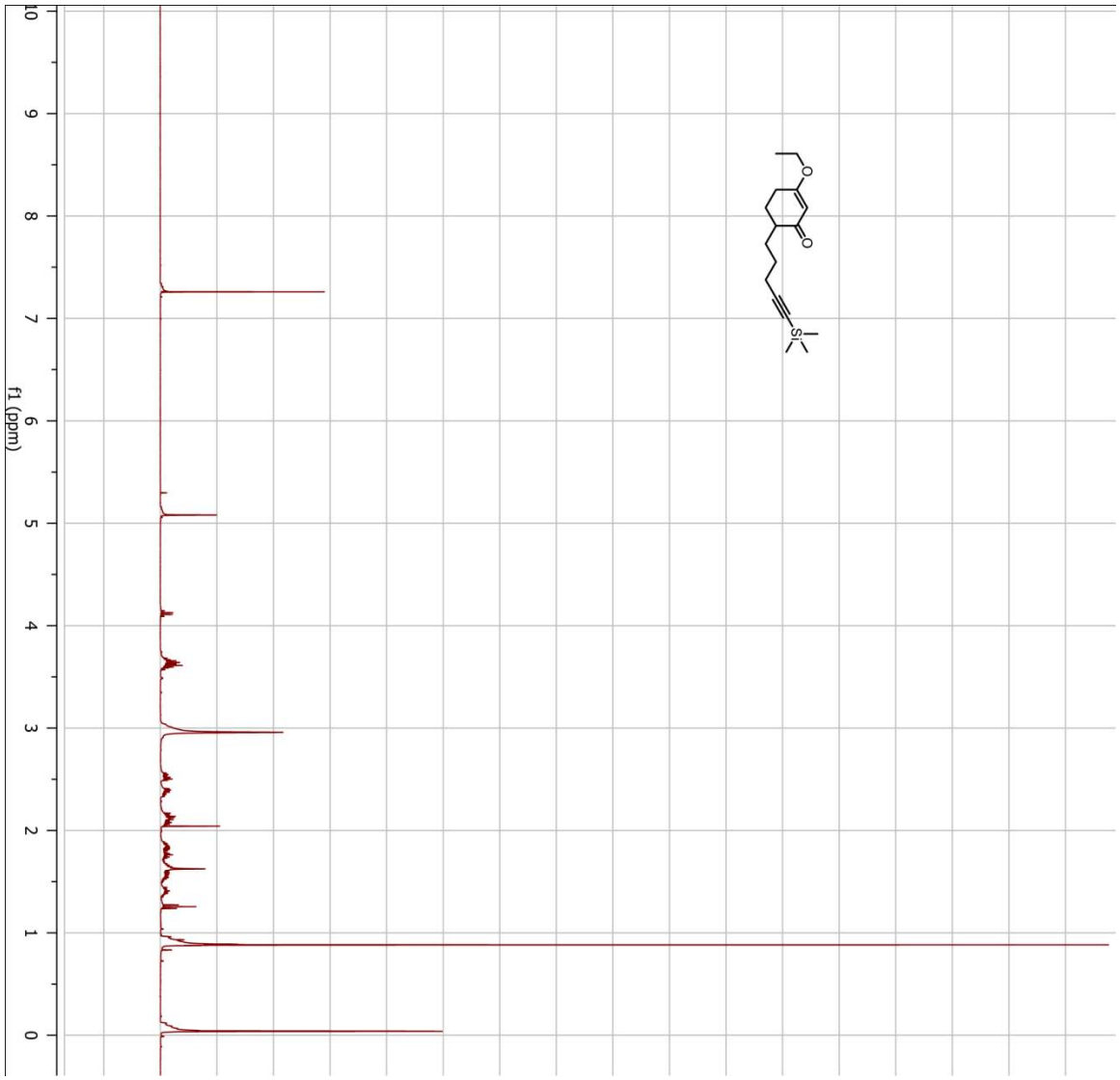
f1 (ppm)
10
9
8
7
6
5
4
3
2
1
0
O
O
Si

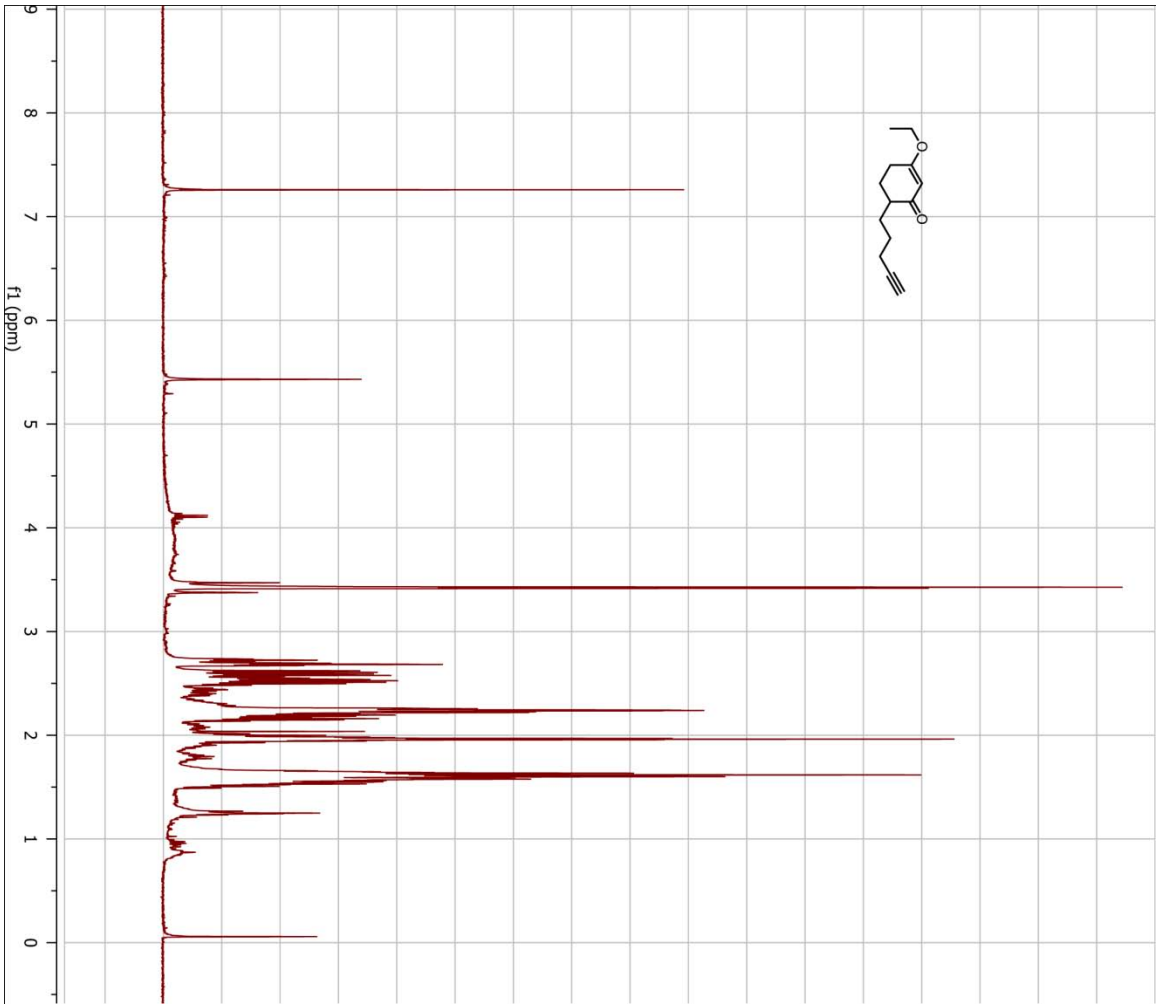
f1 (ppm)
9
8
7
6
5
4
3
2
1
0

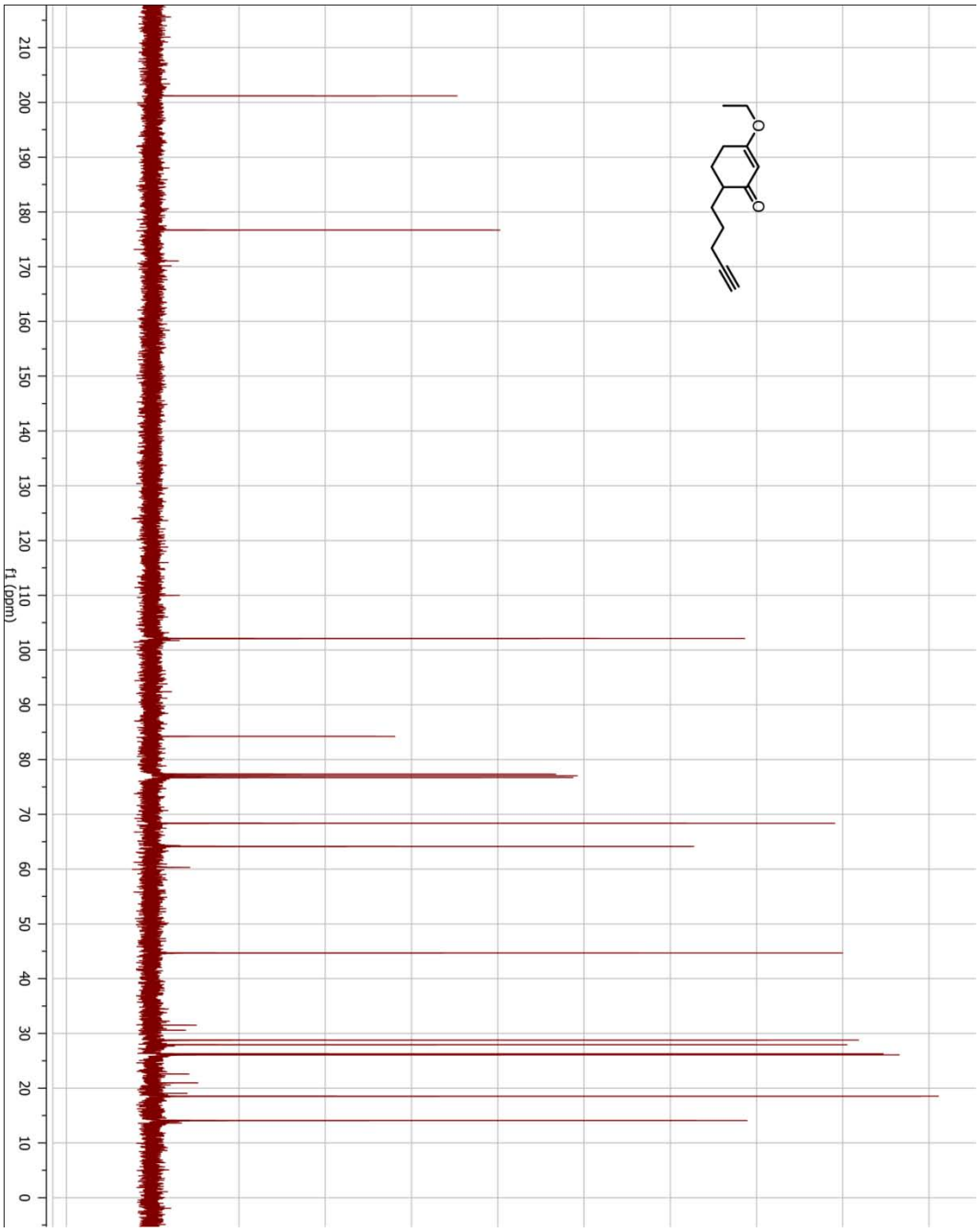
f1 (ppm)
210
200
190
180
170
160
150
140
130
120
110
100
90
80
70
60
50
40
30
20
10
0
O
O

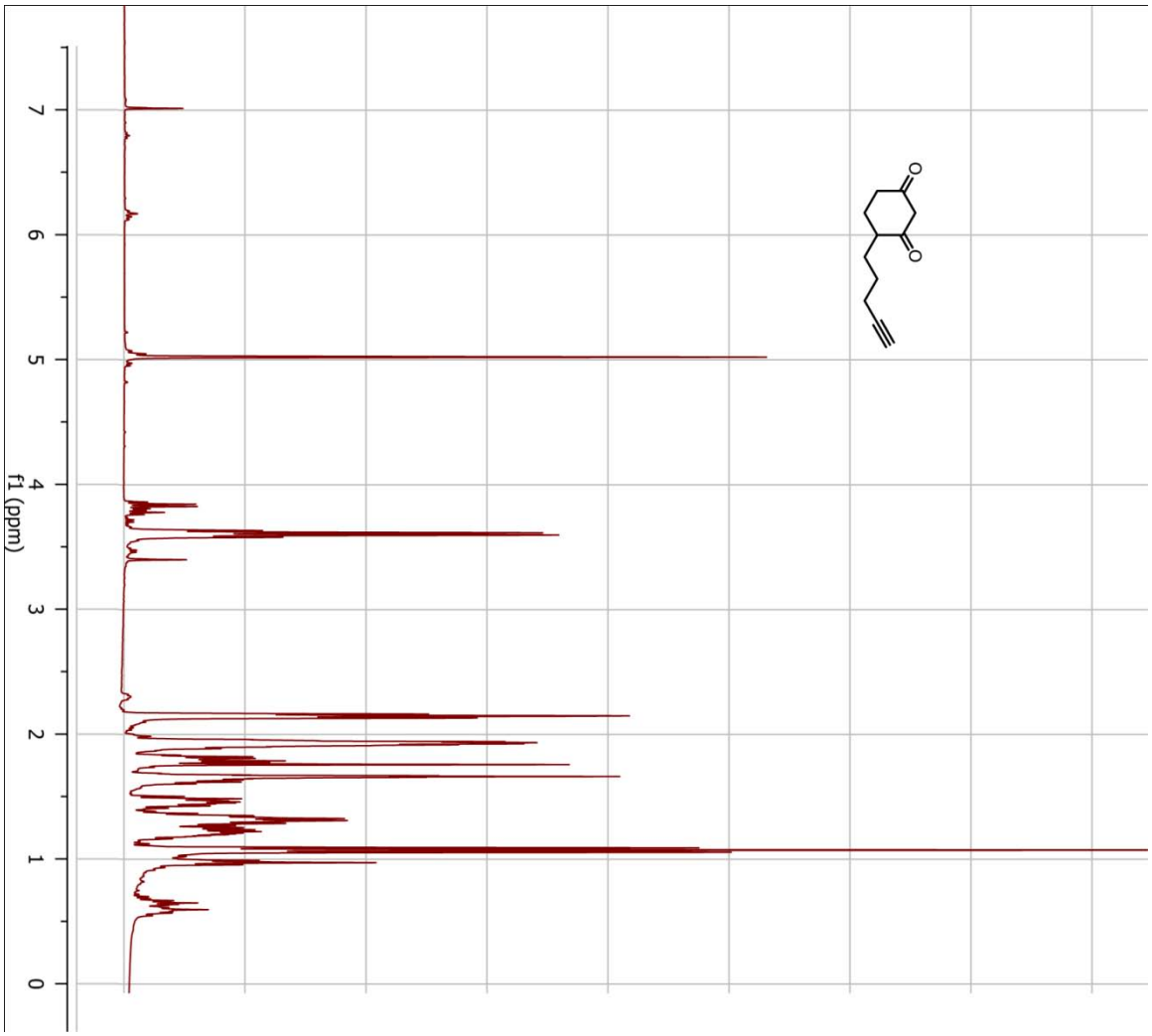
f1 (ppm)
7
6
5
4
3
2
1
0
O
O

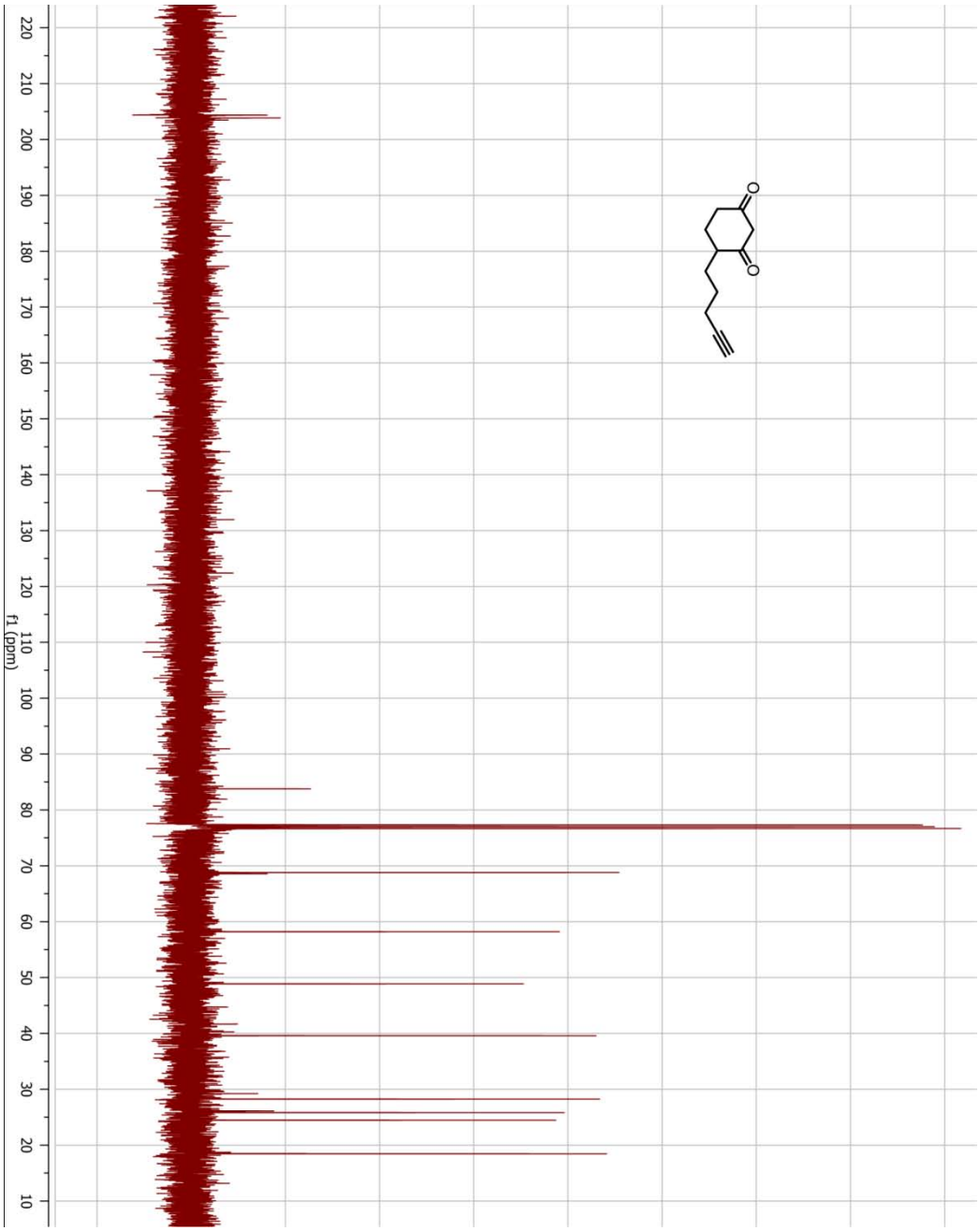
f1 (ppm)
220
210
200
190
180
170
160
150
140
130
120
110
100
90
80
70
60
50
40
30
20
10